

Durham E-Theses

M2-branes and instantons

JAMES PATRICK ALLEN

How to cite:

ALLEN, JAMES PATRICK (2013) M2-branes and instantons. Doctoral thesis, Durham University.

Use policy

The full-text may be used and/or reproduced, and given to third parties in any format or medium, without prior permission or charge, for personal research or study, educational, or not-for-profit purposes provided that:

- a full bibliographic reference is made to the original source
- a <https://etheses.durham.ac.uk/id/eprint/6959/> is made to the metadata record in Durham E-Theses
- the full-text is not changed in any way

The full-text must not be sold in any format or medium without the formal permission of the copyright holders.

Please consult the [full Durham E-Theses policy](#) for further details.

M2-branes and instantons

Coupling M2-branes to background fields, and the low-energy dynamics and symmetries of instantons

James P. Allen

A thesis presented for the degree of
Doctor of Philosophy



Department of Mathematical Sciences
University of Durham
England
April 2013

M2-branes and instantons

Coupling M2-branes to background fields, and the low-energy dynamics
and symmetries of instantons

James P. Allen

Abstract

In the first part of this thesis we discuss some of the issues arising in extending the ABJM action of multiple M2-branes to include couplings to the background 3-form field. These couplings are analogous to the Myers-Chern-Simons terms of the multiple D2-brane action. We review and extend previous results to include terms which are quadratic in the background 3-form. These are fixed by requiring that we recover the correct terms after using the novel Higgs mechanism to reduce the ABJM action to the multiple D2-brane action. We also discuss the problem of constructing a gauge invariant pull-back in the ABJM action.

In the second part of this thesis, we begin by exploring the low energy dynamics of charge two instantons in $SU(2)$ five dimensional Yang-Mills via the moduli space approximation of Manton. We also investigate dyonic instantons which have an excited scalar field and create a potential on the moduli space. In Chapter 5 we explicitly calculate the moduli space metric and potential for charge two (dyonic) instantons. These calculations are performed by using the ADHM construction.

In Chapter 6 we perform a numerical study of the low-energy dynamics of instantons and dyonic instantons. We see that instantons undergo right-angled scattering and understand this analytically in terms of symmetries of the underlying ADHM data. We also present a comprehensive study of the scattering behaviour of instantons and dyonic instantons under various initial conditions. Finally we exhibit some examples of closed geodesics on the moduli space of dyonic instantons, and geodesics which hit the moduli space singularities in finite time.

In Chapter 7 we investigate instantons with a large amount of symmetry. We first understand how the action of a symmetry on an instanton is lifted to the underlying ADHM data. The transformation of the ADHM data must be undoable by a transformation which leaves the instanton invariant, and we search for symmetric instantons by finding such transformation matrices that are representations of the symmetry group. With this method we are able to find solutions to the ADHM constraints that describe instantons with the symmetries of the 5-cell, 16-cell and 24-cell, with charge 4, 7, and 23 respectively. Finally, we see that these solutions correspond to solutions which can be constructed from the JNR ansatz.

To mum and dad

Declaration

The work in this thesis is based on research carried out at the Centre for Particle Theory, Department of Mathematical Sciences, Durham, England. No part of this thesis has been submitted elsewhere for any other degree or qualification and it is all my own work unless referenced to the contrary in the text.

The material in Chapters 1, 2 and 4, and Section 7.1 is a review of the existing literature. The material in the remaining chapters is based on original research in collaboration with my supervisor, Dr Douglas J. Smith, and Prof. Paul Sutcliffe [1, 2, 3].

Copyright © 2013 by James P. Allen

The copyright of this thesis rests with the author. No quotation from it should be published without the author's prior written consent and information derived from it should be acknowledged.

Acknowledgements

I would like to thank my supervisor, Dr Douglas J. Smith, for his guidance and availability throughout my PhD. In particular I am thankful for his immediate agreement and support when I approached him about taking my PhD in a different direction, and for always having my interests first. I would also like to thank Prof. Paul Sutcliffe for his receptiveness when I approached him looking for a suitable research topic. Both Douglas and Paul have made this PhD a pleasure to work on, thank you.

On the personal side of things, I am grateful to Sarah for her support and encouragement during the harder times of my PhD. Our regular tea shop trips and weekends away were a most enjoyable way to escape for a while, thank you.

I am also grateful to my parents, Lynn and Steve, for their support in pursuing my education. If there is anyone without whom this PhD would not have happened, it is them. Thank you.

My time in Durham has been made more enjoyable by a number of people in the maths department, Ustinov college, and further afield. Each of the people below has had a hand in this thesis one way or another. Thank you Barry, Dan, Gurdeep, Harry, Joey, Johan, John, Josh, Luke, Maddy, Matthew G, Matthew Y, Mel, Nick, Rafa, Simon, Steven and Tom.

Finally, my special thanks go to Douglas, Rafa, Sarah, and my dad, Steve, for proof reading early drafts of this thesis.

Contents

Abstract	1
Declaration	3
Acknowledgements	4
1 Introduction	7
I D-branes, M-branes and background fields	14
2 D-branes and M-branes	15
2.1 Multiple D-branes	17
2.2 Multiple M2-branes	19
2.3 Reduction of multiple M2-branes to D2-branes	23
2.4 Background fields	26
3 Higher order background field couplings	33
3.1 Quadratic couplings to background fields	34
3.2 Pull-backs with $U(N) \times U(N)$ gauge invariance	47
3.3 Discussion and conclusions	50
II Instantons	52
4 Instantons and dyonic instantons	53
4.1 Instantons in five dimensional Yang-Mills	55
4.2 Instantons as D0-branes	59
4.3 The ADHM construction	60
4.4 The moduli space of instantons	64
4.5 Dyonic instantons	74
5 The moduli space	80
5.1 The ADHM data of charge two instantons	80

5.2	The moduli space metric	84
5.3	The moduli space potential	87
5.4	Singularities in the metric	88
5.5	Geodesic submanifolds	90
6	Low energy dynamics	94
6.1	Instanton scattering	95
6.2	Dynamics of a single dyonic instanton	106
6.3	Dyonic instanton scattering	107
6.4	Geodesic completeness of the moduli space	112
6.5	Localised charge two instantons	113
6.6	Discussion and conclusions	116
7	Regular polytope symmetry	118
7.1	Symmetric instantons and other soliton systems	119
7.2	Regular polytopes	125
7.3	Group actions on the ADHM data	129
7.4	The 5-cell	131
7.5	Independent left and right actions	132
7.6	Finding invariant ADHM data	135
7.7	The 16-cell	136
7.8	The 24-cell	141
7.9	A charge 23 solution	150
7.10	Equivalence to JNR ansatz	153
7.11	Discussion and conclusions	157
8	Conclusions and outlook	160

Chapter 1

Introduction

The aim of this first chapter is to show how the research in this thesis fits into our current understanding of M-theory, string theory and topological solitons. The material is purposefully presented at a high level and will be revisited in later chapters where the details will be examined more closely and the appropriate references provided. Any background information which is not further developed can be found in the texts by Polchinski [4, 5], Johnson [6], and Manton and Sutcliffe [7].

M-theory and string theory

The first part of this thesis concerns the relationship between M-theory and string theory. We are able to understand everything in string theory in terms of the fundamental string, but we do not have a similar fundamental description of M-theory. However, we know that whatever the full M-theory turns out to be, it must reduce to eleven dimensional supergravity and the five string theories in the appropriate limits. This information gives us concrete evidence about the objects that must therefore appear in M-theory, despite our lack of a fundamental description. By understanding the links between these objects in M-theory and string theory we hope to be able to further reveal the complete M-theory picture.

String theory is our most promising theory of quantum gravity and so has been considered seriously by physicists in recent decades. The rich spectrum of space-time states in string theory arises from the quantisation of a superconformal theory on the world-sheet of the one dimensional fundamental string. Pleasingly for a fundamental theory, the string length, l_s , is the only external parameter in string theory. Upon quantising the string, there is an infinite tower of states with masses growing proportional to l_s^{-1} . We expect the string length, l_s , to be on the order of the Planck scale so that only the massless states are accessible to current experiments and for the foreseeable future.

There are five different unique supersymmetric string theories, which depend on

the possible choices we make about the topology and field content of the fundamental string. If the string is open, so that it has a boundary, then the left- and right-moving fields must be identified due to the boundary conditions. There is only one possibility for a theory with open strings, which is known as type I string theory. The bosonic space-time states arising from the open string can be grouped into a space-time vector, A_μ , with an $\text{SO}(32)$ gauge group.

If the string is closed then the left and right moving fields are independent and there are two possible closed string theories known as type IIA and type IIB, which differ in the chirality of the left and right moving fields. The type IIA and type IIB string theories share one sector where the massless space-time states are a scalar dilaton, Φ , the Kalb-Ramond 2-form, B_{mn} and the graviton, G_{mn} . It is the graviton that gives string theory its title as a quantum theory of gravity. The massless states in the remaining bosonic sector differ between type IIA and type IIB, with type IIA containing a 1-form and a 3-form field, and type IIB containing a 0-form, a 2-form and self-dual 4-form field.

The interaction of open strings in type I string theory will create closed strings. These closed strings are in fact those of type IIB theory projected so that they are unoriented, and they give rise to a space-time dilaton, graviton and 2-form field in the type I theory.

The remaining two string theories come from taking the left moving fields to be purely bosonic while the right moving fields are supersymmetric. This gives an inconsistency in the number of dimensions seen by the two sets of fields, but this can be fixed by compactifying the bosonic fields on a 16-dimensional manifold. There are two consistent choices for this compactification, giving rise to the $E_8 \times E_8$ and $\text{SO}(32)$ heterotic string theories.

In the low energy limit, the type IIA string theory reduces to type IIA supergravity, while the type IIB string theory reduces to type IIB supergravity. Type I string theory and the heterotic string theories reduce to $\mathcal{N} = 1$ supergravity in different parameterisations, at strong and weak coupling respectively.

String theory also contains a variety of extended objects known as branes. D-branes arise as the end points of open strings, and must be dynamical objects to avoid breaking Lorentz invariance. In type IIA string theory, there exist stable D0-, D2-, D4-, D6- and D8-branes, while in type IIB string theory there exist stable D1-, D3-, D5-, D7- and D9-branes. These are charged under the space-time forms, and also have corresponding solutions in type IIA and type IIB supergravity.

If string theory is to be our theory of everything then it is a little unsatisfactory that there are five consistent string theories, rather than a single unique one. However, the five string theories can all be related by a web of dualities, which is suggestive of some more fundamental underlying theory. The type IIA and type IIB theories are

related under T-duality, where the theories are equivalent when compactified on a circle of radius R and l_s^2/R respectively. The heterotic string theories are also related under T-duality. Type I string theory at small string coupling is also related to the SO(32) heterotic string theory at large coupling. This is known as S-duality and is also evident in the supergravity regime as mentioned above.

The conjectured theory that links these five string theories has been dubbed M-theory and is an eleven dimensional theory. In the low energy limit, M-theory should reduce to the unique supergravity in eleven dimensions, which further reduces to type IIA supergravity upon compactification. We do not yet have a fundamental description of M-theory as we do with string theory in terms of the fundamental string. However, we can infer a lot about the objects that must arise in M-theory by the knowledge that it must contain the five string theories and eleven dimensional supergravity. For example, from examining the field content of eleven dimensional supergravity, we know that the massless bosonic fields in M-theory must be a graviton and a 3-form. Eleven dimensional supergravity also contains stable 2-brane and 5-brane solutions, suggesting that M-theory contains appropriate M2-branes and M5-branes.

Evidence for the eleven dimensional nature of M-theory can be seen directly from type IIA string theory. The mass of the D0-brane is

$$T_0 = \frac{1}{g_s l_s}, \quad (1.0.1)$$

where g_s is the string coupling. As the string coupling grows large the mass therefore becomes light. The mass of the bound state of n D0-branes is nT_0 , so we have tower of massive states which become light as $g_s \rightarrow \infty$. This is reminiscent of the momentum states that appear in a Kaluza-Klein compactification. The D0-brane can therefore be interpreted as eleven dimensional momentum, on a circle with radius $R = g_s l_s$. The appearance of this extra dimension can also be seen in the strong coupling limit of the D2-brane action where an appropriate rewriting of the fields reveals an extra transverse dimension and the action now describes an M2-brane.

Until a few years ago, only the action of a single M2-brane was known. The action for multiple D2-branes is well known and whatever the multiple M2-brane action turns out to be, it should be the strong coupling limit of the multiple D2-brane action. Recent progress has been made towards a Lagrangian description of this theory by Bagger, Lambert and Gustavsson (BLG) with the introduction of a novel three-algebra to replace the usual Lie algebra as the gauge group generators. The number of branes is determined by the structure of the three-algebra, but there is only a single suitable three-algebra which describes two M2-branes. This theory of two M2-branes can also be formulated as an $SU(2) \times SU(2)$ gauge theory. Shortly afterwards, Aharony, Bergman, Jafferis and Maldacena (ABJM) proposed a $U(N) \times U(N)$ Chern-Simons theory which

describes N M2-branes in an orbifold background with reduced supersymmetry. Both of these theories can be reduced to the multiple D2-brane action using a novel Higgs mechanism which we will review in more detail in Chapter 2.

Recall that in type IIA string theory the space-time background contains a dilaton, a graviton and a Kalb-Ramond 2-form, as well as a 1-form and 3-form. The action for multiple D2-branes can be generalised to include couplings to all of these fields and describe the branes in a non-flat background. Both the BLG and ABJM action describe multiple M2-branes in a flat background and it is still not clear how to extend these actions to also include couplings to the background M-theory fields, the graviton and the 3-form. However, possible extensions can be tested by comparison to the known D2-brane action in the compactification limit, and this is our main focus in the next two chapters. The research in Chapter 3 concerns extending the ABJM action to contain couplings to the background 3-form of M-theory.

The other extended object in M-theory is the M5-brane and this still remains a mystery. It is hard to write down even the single M5-brane action, and while there has been some progress towards a multiple M5-brane action in recent years, it is still an open question. There is a conjecture that the M5-brane theory on a circle is dual to the five dimensional super-Yang-Mills theory that is the low energy action of multiple D4-branes. Certainly this should be true in the limit of small radius, but the claim is that five dimensional super-Yang-Mills is UV complete and the duality holds at all sizes of the compactification radius. Instantons play an important role in this correspondence, as they correspond to D0-branes in the string theory picture and to momentum modes in the compactified M-theory picture. This interplay between M-theory, string theory and instantons leads us to the second part of this thesis, where we study instantons in more detail.

Instantons

Instantons are topological solitons in four dimensional Euclidean Yang-Mills which are characterised by having a self-dual field strength. They were first discovered 35 years ago and have played an important role in understanding quantum tunnelling in four dimensional Yang-Mills, and in understanding supersymmetric gauge theories. Our interest in instantons is as dynamical solitons in five dimensional Yang-Mills on the world-volume of a stack of D4-branes, although the string theory setting is largely incidental. In this context, instantons are solutions in the four spatial dimensions, and can evolve in the time direction. Instantons sit at the head of the family of topological solitons in Yang-Mills theories, which include vortices and monopoles in three and four dimensional Yang-Mills respectively. These vortices and monopoles can be recovered from instantons via dimensional reduction. The dynamics and interactions of vortices and monopoles is well understood but relatively little is known about the

equivalent dynamics of instantons, perhaps due to them only appearing dynamically in five dimensions, outside the realm of everyday physics.

Topological solitons in different theories generally share qualitatively similar properties. The theories all split into different sectors based on a topological characteristic of the solutions, which can be indexed by an integer known as the topological charge. This topological charge arises from how many times the space-time fields ‘wrap’ the gauge group or target space of the fields. Topological solitons are non-perturbative objects in field theories since they cannot be reached by a continuous perturbation away from the vacuum due to a non-trivial ‘wrapping’. They appear as the lowest energy configurations in each topological sector and are important in understanding the full field theory.

Soliton field configurations generally resemble isolated lumps which behave like point particles when they are well separated, but take on a richer and more complicated structure when close together. Right angled scattering of two individual solitons is a common feature, which can be argued on symmetry principles alone, and there often exist interesting examples of scattering of multiple solitons which pass through a configuration of increased symmetry before scattering. For example, monopoles coming in along the points of a tetrahedron have their symmetry group promoted to that of a cube before scattering with the symmetry of the dual tetrahedron.

Instantons are qualitatively similar in behaviour to sigma model lumps which arise in a three dimensional model with a scalar that takes values on a unit sphere. Sigma model lumps are often used as a toy model for studying instantons. A common property of both, which is not shared by monopoles and vortices, is a slow roll instability in the soliton size. If the static soliton is given a small perturbation then it will either shrink or expand at constant velocity until it hits zero size or expands indefinitely. However, both instantons and sigma model lumps can be stabilised with the addition of a potential. In the case of sigma model lumps this is added in by hand, but for instantons on D4-branes this arises naturally when the D4-branes are separated by giving a scalar field a non-zero vacuum expectation value (VEV) in the Yang-Mills theory. The solitons must also be given an appropriate rotation to stabilise against collapse from the potential, and in doing so they gain an electric charge. These charged solitons, known as dyonic instantons in five dimensional Yang-Mills, are stable to perturbations.

The space of all physically different instanton solutions is known as the moduli space. As with other related soliton systems, the instanton moduli space has many nice mathematical properties and is a hyper-Kähler manifold. There has been a significant amount of study of the instanton moduli space and it has led to a deeper understanding of the mathematics of the underlying manifolds. This thesis will make use of some of these results, but our main focus is on the study of the dynamics of instantons so we will not attempt to give a rigorous treatment.

The low energy dynamics of topological solitons can generally be approximated by geodesic motion through the moduli space. Intuitively, the static solitons are the lowest energy configurations in each topological sector, and giving them a small velocity will only increase their energy slightly. These configurations will then always stay close to the minimum energy configurations by energy conservation. The moduli space can be thought of as the floor of a potential valley in the space of all solutions to the Yang-Mills equations of motion, and the evolution of slow moving solitons must stay near the bottom of this potential valley. So long as the evolution does not ascend too far up the valley, the motion can be approximated by motion exactly along the valley floor, or as the evolution through snapshots of the static solitons in the moduli space. For dyonic instantons, each solution has a different electric charge, which induces a potential on the moduli space. So long as this potential is shallow compared to the surrounding valley, the moduli space approximation is still valid. We will make this precise in Chapter 4.

Instanton solutions can be found using a technique known as the ADHM construction which recasts the problem of solving the self-dual field equation into a set of non-linear algebraic equations. This technique is used repeatedly in calculations involving instantons, as it generally allows us to turn all expressions involving derivatives and integrals into purely algebraic expressions. The ADHM construction also provides a natural coordinate system on the moduli space of instantons, at least when an explicit parameterisation of the ADHM data is known.

One of the goals of this thesis is to understand the moduli space and low energy dynamics of charge two instantons. In Chapter 5, we make use of the ADHM construction to parameterise the moduli space, and understand the physical meaning of the parameters. From here we calculate the metric on the moduli space, and in the case of dyonic instantons we also calculate the potential. This allows us to approximate the low energy dynamics of instantons and dyonic instantons via geodesic motion in this metric (for lack of a better term, we also describe motion in the presence of a potential as geodesic motion.) In Chapter 6 we present a numerical study of this motion, with algebraic insights where possible.

As well as their relationship to monopoles, vortices and sigma model lumps, instantons are also connected to Skyrmions. Every instanton solution can be transformed into a solution of the Skyrme model, and this technique can be used to produce Skyrme solutions which deviate from the true lowest energy Skyrmions by only a few percent. Symmetric instantons are particularly relevant in this context. The simplest example of a charge one instanton has spherical symmetry and gives an approximate solution to the charge one Skyrme model, also with spherical symmetry. At charge four, there exists an instanton with cubic symmetry which fits into a family with overall tetrahedral symmetry. This family describes the approximate scattering of four Skyrmions, with

the same symmetries. At charge seven there is an icosahedrally symmetric instanton which fits into a similar one parameter family with overall tetrahedral symmetry and approximately describes seven Skyrmion scattering. The utility of these symmetric instantons is not limited to Skyrmions, since each of these symmetric instanton families have also recently been found to give rise to hyperbolic monopole solutions.

Motivated by the utility of instantons which are symmetric under platonic symmetries, our aim in Chapter 7 is to find instantons which are symmetric under the symmetries of regular polytopes. Regular polytopes are the generalisation of Platonic solids to four dimensions, so that their symmetry group is a subgroup of $SO(4)$. The icosahedrally symmetric instanton was found by taking the real representations of the icosahedral group and looking for ADHM data which could be invariant under each representation. Due to the way the symmetry acts on the ADHM data, it is possible to choose a basis in which the representations split into irreducible blocks, making the search straightforward. However, when the symmetry group is a subgroup of $SO(4)$, there are two independent actions on the ADHM data, related to the fact that the double cover of $SO(4)$ is $SU(2) \times SU(2)$. This removes the freedom to put everything in a suitable basis and overcoming this problem is our main challenge in Chapter 7.

Finally, in Chapter 8 we will present a summary of our important findings and provide an outlook on how the research in this thesis may lead to other interesting work.

Part I

D-branes, M-branes and background fields

Chapter 2

D-branes and M-branes

String theory is based on the quantisation of a superconformal action on the world sheet of a string, but our current understanding of string theory includes a rich set of extended objects beyond just this fundamental string. In the type II string theories, D-branes are one such class of objects. D-branes provide a hyper-surface for the end points of open strings and are themselves dynamical objects [8]. In the modern view of string theory, open strings end on a space filling D9-brane and lower dimensional D-branes can be constructed from T-duality [6].

Due to the complexity of string theory, we must be content to explore the theory in different regimes and by understanding the behaviour of the individual objects within the theory, such as the fundamental string, D-branes and the NS5-brane. One important regime is the low energy limit of type IIA or IIB string theory, where the effective theory is either type IIA or IIB supergravity [9, 10, 11]. Quantisation of the string produces a spectrum of massless states that become the supergravity fields. The derivation of the massless states in the various string theories is given in detail in the canonical texts by Polchinski [4, 5] and Johnson [6]. Both type IIA and type IIB string theories have the same states in the Neveu-Schwarz–Neveu-Schwarz (NS-NS) sector, which arises when the left and right moving fields are taken to be anti-periodic. The massless states arising from the NS-NS sector are the graviton, $G_{\mu\nu}$, the Kalb-Ramond 2-form, $B_{\mu\nu}$, and the dilaton, ϕ . The Ramond-Ramond (RR) sector of the type II string theories arises when the world sheet fields are periodic. The RR sector of type IIA string theory contains a 1-form, and a 3-form, $C^{(1)}$ and $C^{(3)}$. The RR sector of type IIB string theory instead contains a 0-form, a 2-form and a 4-form, $C^{(0)}$, $C^{(2)}$ and $C^{(4)}$.

In type IIA and type IIB supergravity, D-branes are 1/2-BPS solitonic objects which are charged under the RR fields. In type IIB string theory and type IIB supergravity there are stable D-branes with an even number of spatial dimensions, while in the type IIA theories there exist D-branes with an odd number of spatial dimensions. These dimensions are consistent with the degree of the RR forms that they are charged under.

A comprehensive review of different brane configurations in supergravity is given in reference [12].

From a more stringy point of view, D-branes support the end points of open strings. The massless states of the open string correspond to a gauge field, A_μ , in the directions that lie on the D-brane, and scalar fields X^I , that lie transverse to the D-brane. D-branes are dynamical objects themselves and the scalars have a natural interpretation as the transverse fluctuations in the position of the D-brane.

Conceptually a similar picture exists for M-theory, although understanding the behaviour of the M-branes turns out to be significantly harder. In eleven dimensions there is a unique supergravity theory [13] and whatever complete picture of M-theory eventually emerges should be the UV completion of this supergravity theory. From eleven dimensional supergravity we can infer that the massless fields in M-theory are a metric, G , a 3-form, C , and a gravitino. In addition, M-theory contains stable M2-branes and M5-branes which are electrically and magnetically charged respectively under the 3-form [12, 14, 15].

Type IIA supergravity is the dimensional reduction of eleven dimensional supergravity on a circle [16, 17, 18]. The 1-form, $C^{(1)}$, in type IIA supergravity arises from the usual Kaluza-Klein procedure, while the 3-form, $C^{(3)}$, and the Kalb-Ramond 2-form, B , arise from the dimensional reduction of the 3-form in eleven dimensional supergravity. It is natural to expect that M-theory and type IIA string theory are also related via a dimensional reduction in the same way, or alternatively that M-theory is the strong coupling limit of type IIA string theory [19, 20, 21]. Indeed, the action of a single M2-brane can be found from the strong coupling limit of a single D2-brane, corresponding to the opening out of the compactification circle in a direction transverse to the brane [22, 23]. When M2-branes are wrapped around the compactified direction, they instead reduce to fundamental strings [24]. Similarly, the M5-brane reduces to give the NS5-brane and D4-brane of type IIA string theory [12].

It is still unknown if there is an analogue in M-theory to the fundamental string, from which the entire theory can be built. It is suspected that the M2-brane plays this role as it reduces to the fundamental string upon compactification, but we do not have the necessary understanding of the quantisation and scattering of M2-branes as we do with fundamental strings.

In this chapter we will review the world-volume actions of the D-branes and M-branes we have discussed above. The action of a single D-brane and M2-brane is well understood and the generalisation to a stack of multiple D-branes is possible, at least in the low energy limit. We will review D-branes first in Section 2.1. The action of multiple M2-branes is less well understood, although there has been significant progress towards an understanding in the past five years. In Section 2.2 we will review the recent proposals for the actions of multiple M2-branes. Finally in Section 2.3 we will look at

how the multiple D2-brane action can be recovered from the multiple M2-brane action via a novel use of the Higgs mechanism. This is a further consistency check of the M2-brane theory.

In this introductory chapter we will only be able to review a small amount of the known physics of D-branes and M-branes, but along with the references already pointed out, the reviews in references [25, 26] provide a thorough discourse of our current understanding of multiple M2-branes.

2.1 Multiple D-branes

The dynamics of single D p -brane in a flat background are governed by the Dirac-Born-Infeld (DBI) action [27, 28],

$$S_{DBI} = -T_p \int d^{p+1}x \sqrt{-\det(\gamma_{\mu\nu} + \lambda F_{\mu\nu})}, \quad (2.1.1)$$

where $\lambda = 2\pi\alpha'$, $\alpha' = l_s^2$, and $\gamma_{\mu\nu}$ is the pull-back of the flat space-time metric onto the world-volume in static gauge,

$$\gamma_{\mu\nu} = \eta_{\mu\nu} + \partial_\mu X^I \partial_\nu X^I. \quad (2.1.2)$$

This can be derived via T-duality from the space-filling D9-brane, or directly from the beta functions of the open string [29].

In the limit of small field strength, $F_{\mu\nu}$, and small derivatives of the fluctuations, $\partial_\mu X^I$, the DBI action can be expanded to leading order. We recover U(1) Yang-Mills with free massless scalar fields,

$$S = -\lambda^2 T_p \int d^{p+1}x \left(\frac{1}{4} F_{\mu\nu} F^{\mu\nu} + \frac{1}{2} \partial_\mu X^I \partial^\mu X^I \right). \quad (2.1.3)$$

We have rescaled the scalar fields by $X^I \rightarrow X^I/(2\pi\alpha')$. The Yang-Mills coupling is given by

$$\frac{1}{g_{\text{YM}}^2} = (2\pi\alpha')^2 T_p, \quad (2.1.4)$$

and we have neglected terms that are of order $(\alpha')^4$ and higher.

The DBI action describes the dynamics of a D-brane in a flat background without any of the supergravity fields turned on. To understand how a D-brane behaves if it moves in a background of these closed string fields, G_{mn} , B_{mn} , ϕ , and the RR forms, $C^{(n)}$, we must couple these fields into the action.

The background fields in the NS-NS sector are coupled to the single D-brane by

the following modification to the DBI action [6]:

$$S_{DBI} = -T_p \int d^{p+1}x e^{-\phi} \sqrt{-\det(\gamma_{\mu\nu} + \lambda F_{\mu\nu} + B_{\mu\nu})}. \quad (2.1.5)$$

The pull back of the space-time metric is now the pull-back of G , rather than of the flat metric,

$$\gamma_{\mu\nu} = P[G]_{\mu\nu} = G_{\mu\nu} + 2G_{I(\mu}\partial_{\nu)}X^I + G_{IJ}\partial_\mu X^I\partial_\nu X^J. \quad (2.1.6)$$

The dilaton contribution can be viewed as a local variation in the tension of the D-brane due to the dependence of the string coupling on the dilaton. The B field appearing in the action is the pull-back of the space-time B field,

$$B_{\mu\nu} = P[B]_{\mu\nu} = B_{\mu\nu} + 2B_{I[\mu}\partial_{\nu]}X^I + B_{IJ}\partial_\mu X^I\partial_\nu X^J. \quad (2.1.7)$$

It must be included in this way due to the presence of a boundary term on the open string in the space-time gauge transformation of B . This is compensated by a transformation in A_μ , so that the true gauge invariant quantity is $B + \lambda F$.

D-branes also carry an RR charge through couplings to the RR forms [30],

$$S_{CS} = T_p \int P \left[\sum C^{(n)} e^B \right] e^{\lambda F}. \quad (2.1.8)$$

The expression in the integral should be interpreted as only containing the terms in the expansion of the exponentials which are of degree $(p+1)$ and so can be integrated. Note that while a Dp -brane is naturally charged under $C^{(p+1)}$, it is also charged under the RR forms with a lower degree through couplings involving B and F in the exponential.

Let us now consider multiple D-branes. As N D-branes become coincident, the strings stretching between them become massless and the $U(1)^N$ gauge symmetry is enhanced to $U(N)$ [31]. The gauge field, A_μ , becomes non-abelian and the scalars lie in the adjoint representation of $U(N)$. Extending the above action to multiple D-branes is non-trivial, but in the appropriate limit the action should reduce to super-Yang-Mills theory. This theory has a scalar potential proportional to $\text{Tr}[X^I, X^J]^2$ but the naive extension of the above action by tracing over the gauge indices will not recover such terms. There are suggestions that the appropriate action can be found by T-duality from the D9-brane action [32], but it is not clear that such an action is well defined to all orders in the field strength.

In this thesis we are only concerned with the low energy limit of multiple D-branes, in which case the theory reduces to $U(N)$ super-Yang-Mills [6],

$$S = -\lambda^2 T_p \int d^{p+1}x \text{Tr} \left(\frac{1}{4} F_{\mu\nu} F^{\mu\nu} + \frac{1}{2} D_\mu X^I D^\mu X^I - \frac{1}{4} [X^I, X^J]^2 \right). \quad (2.1.9)$$

For a single D-brane the coupling to the background fields, $C^{(n)}$, is consistent with T-duality, but for multiple D-branes with a non-abelian gauge group it must be modified to the Myers-Chern-Simons [32] action with the inclusion of higher degree RR forms,

$$S_{MCS} = T_p \int \text{STr} \left(P \left[e^{i\lambda \mathbf{i}_X \mathbf{i}_X} \sum C^{(n)} e^B \right] e^{\lambda F} \right). \quad (2.1.10)$$

Here \mathbf{i}_X is the interior product and lowers the degree of a form,

$$\mathbf{i}_X \mathbf{i}_X C = \frac{1}{6} C_{mnp} [X^m, X^n] dx^p. \quad (2.1.11)$$

Multiple D-branes are therefore also charged under higher degree RR forms.

The field strength is naturally matrix valued, but the background forms, $C^{(n)}$, and Kalb-Ramond 2-form, B , must be promoted to functionals of the transverse coordinates, X^I , via their Taylor expansion,

$$C_{mnp}^{(3)}(x^\mu; X^I) = \sum_{n=0}^{\infty} \frac{1}{n!} X^{I_1} \dots X^{I_n} (\partial_{I_1} \dots \partial_{I_n}) C_{mnp}^{(3)}(x^\mu; x^I) \Big|_{x^I=0}. \quad (2.1.12)$$

This may seem unusual for the background fields, but recall that the D-brane positions are described by $N \times N$ matrices, and so we are not considering the value of the 3-form at individual points any more, but rather the value it takes on each of the N branes simultaneously. For example, consider the case of N separated branes where the gauge group is broken to $U(1)^N$ and the X s become diagonal matrices. Then the matrix valued 3-form also becomes diagonal with the diagonal entries describing the value it takes at the position of each of the N D2-branes.

The trace in the Myers-Chern-Simons term is the symmetrised trace, STr , where the terms inside the trace are taken to be symmetrised. All of the F , $[X, X]$, DX and X terms are symmetrised, including those inside the Taylor expansion of C and B .

2.2 Multiple M2-branes

It has proved much harder to find a world-volume description of multiple M-branes, but some recent developments have shown that it is not impossible. In this thesis we will be concerned mainly with the action of multiple M2-branes, although there have also been recent developments in understanding M5-branes [33, 34, 35, 36, 37].

From our understanding of M2-branes as solitons in eleven-dimensional supergravity we know that the M2-branes preserve 16 supercharges and must therefore have a world-volume theory with $\mathcal{N} = 8$ supersymmetry. Since the M2-brane is embedded in eleven dimensions, we expect there to be eight scalar degrees of freedom describing its embedding. We also expect eight fermionic degrees of freedom and no other dynamical

degrees of freedom. In particular there will be no dynamical gauge field, although this does not exclude the possibility of a non-dynamical gauge field, such as would arise from a Chern-Simons theory. The theory of M2-branes must also be conformal because it arises as the strong coupling limit of supersymmetric $U(N)$ Yang-Mills in three dimensions. The Yang-Mills coupling g_{YM} increases in the infrared and so the M2-brane theory must lie at a conformally invariant fixed point.

2.2.1 The BLG action

The first suitable proposal for a theory of multiple M2-branes was from Bagger and Lambert [38, 39], and independently from Gustavsson [40]. The novel feature of this theory is a three-bracket, which is a generalisation of the Lie bracket,

$$[T^a, T^b, T^c] = f^{abc} T^d. \quad (2.2.1)$$

Here the generators, T^a , lie in a vector space which is a three-algebra and the three-bracket must satisfy a generalised Jacobi identity. We will address the question of whether such a space exists later, but for now let us take it as a given.

The Bagger-Lambert-Gustavsson (BLG) theory contains 8 scalars, X^I , and 16 fermions arranged in a 32 component real spinor, Ψ , satisfying

$$\Gamma_{012}\Psi = -\Psi, \quad (2.2.2)$$

and a gauge field \tilde{A}_μ . This representation of the fermions is used to make contact with the supersymmetries of the eleven dimensional space-time. The supersymmetries preserved by the M2-brane are taken to satisfy

$$\Gamma_{012}\epsilon = \epsilon. \quad (2.2.3)$$

The scalars and fermions take values in the three-algebra,

$$X^I = X_a^I T^a, \quad (2.2.4)$$

$$\Psi = \Psi_a T^a. \quad (2.2.5)$$

The gauge field, \tilde{A}_μ , should map a member of the three-algebra to another member of the three-algebra and so must have two gauge indices. The gauge symmetry is

$$\delta X_a^I = \Lambda^b{}_a X_b^I, \quad (2.2.6)$$

$$\delta \tilde{A}_\mu{}^a{}_b = \partial_\mu \Lambda^a{}_b + \tilde{A}_\mu{}^a{}_c \Lambda^c{}_b - \Lambda^a{}_c \tilde{A}_\mu{}^c{}_b. \quad (2.2.7)$$

The covariant derivative is

$$D_\mu X_a^I = \partial_\mu X_a^I - \tilde{A}_\mu^b{}_a X_b^I, \quad (2.2.8)$$

which transforms covariantly under the above gauge symmetry.

To define a Lagrangian for these fields, there must be an inner product, h , on the three-algebra that can be used to raise and lower the gauge indices,

$$\langle X, Y \rangle = h^{ab} X_a Y_b. \quad (2.2.9)$$

When the structure constants have all their indices raised they must be fully anti-symmetric so that gauge transformations leave the inner product invariant,

$$f^{abcd} = f^{[abcd]} = f^{abc} h^{ed}. \quad (2.2.10)$$

The Lagrangian of the BLG theory is

$$\mathcal{L} = \frac{1}{2} D_\mu X^{Ia} D^\mu X_a^I + \frac{i}{2} \Psi^a \Gamma^\mu D_\mu \Psi_a + \frac{i}{4} \Psi_b \Gamma_{IJ} X_c^I X_d^J \Psi_a f^{abcd} - V + \mathcal{L}_{CS}, \quad (2.2.11)$$

where the potential is

$$V = \frac{1}{12} X_a^i X_b^j X_c^k X_e^l X_f^m X_g^n f^{abcd} f^{efg}{}_d, \quad (2.2.12)$$

and there is a Chern-Simons like term,

$$\mathcal{L}_{CS} = \frac{1}{2} \varepsilon^{\mu\nu\rho} \left(f^{abcd} A_{\mu ab} \partial_\nu A_{\rho cd} + \frac{2}{3} f^{cda}{}_g f^{efgb} A_{\mu ab} A_{\nu cd} A_{\rho ef} \right). \quad (2.2.13)$$

The gauge field in this Chern-Simons term is defined in terms of \tilde{A}_μ by

$$\tilde{A}_\mu^c{}_d = A_{\mu ab} f^{abc}{}_d. \quad (2.2.14)$$

This Lagrangian is invariant under the following supersymmetry transformations,

$$\delta X_a^I = i\epsilon \Gamma^I \Psi_a, \quad (2.2.15)$$

$$\delta \Psi_a = D_\mu X_a^I \Gamma^\mu \Gamma^I \epsilon - \frac{1}{6} X_b^I X_c^J X_d^K f^{bcd}{}_a \Gamma^{IJK} \epsilon, \quad (2.2.16)$$

$$\delta \tilde{A}_\mu^b{}_a = i\epsilon \Gamma_\mu \Gamma_I X_c^I \Psi_d f^{cdb}{}_a. \quad (2.2.17)$$

To recap, this theory is invariant under 16 supersymmetries and an SO(8) R-symmetry, and is conformally invariant, as expected for multiple M2-branes. From our understanding of D-branes, we would expect the size of the three-algebra to be related to the number of M2-branes. Unfortunately, it turns out that there is only a single finite

three-algebra with Euclidean signature [41, 42]. This three-algebra has the structure constants and inner product given by

$$f^{abcd} = \frac{2\pi}{k} \varepsilon^{abcd}, \quad h^{ab} = \delta^{ab}, \quad (2.2.18)$$

and describes two M2-branes in the background of an $\mathbb{R}^8/\mathbb{Z}_{2k}$ orbifold [43, 44]. While the BLG theory is unable to describe arbitrary stacks of M2-branes, it is still remarkable in giving the first plausible description of non-abelian M2-branes.

2.2.2 The ABJM action

Shortly after the construction of the BLG model, a class of models with a $U(N) \times U(N)$ gauge group but only $\mathcal{N} = 6$ supersymmetry were proposed by Aharony, Bergman, Jafferis and Maldacena (ABJM) to describe arbitrary numbers of M2-branes [45]. The ABJM theory contains four complex scalars, Z^A ($A = 1, 2, 3, 4$) and fermions, ψ_A , which are in the bi-fundamental representation, (N, \bar{N}) , of the gauge group. There are also non-dynamical gauge fields, A_μ^L and A_μ^R , which transform under each $U(N)$ respectively.

The Lagrangian for the ABJM theory is

$$\mathcal{L} = -\text{Tr} \left(D_\mu Y_A^\dagger D^\mu Y^A \right) + i \text{Tr} \left(\psi^{A\dagger} \gamma^\mu D_\mu \psi_A \right) - V_{\text{bos}} - V_{\text{ferm}} - \mathcal{L}_{\text{CS}}, \quad (2.2.19)$$

where the sextic bosonic potential is

$$V_{\text{bos}} = \frac{4\pi^2}{3k^2} \text{Tr} \left(4Z^A Z_A^\dagger Z^B Z_C^\dagger Z^C Z_B^\dagger - 4Z^A Z_B^\dagger Z^C Z_A^\dagger Z^B Z_C^\dagger - Z^A Z_A^\dagger Z^B Z_B^\dagger Z^C Z_C^\dagger - Z_A^\dagger Z^A Z_B^\dagger Z^B Z_C^\dagger Z^C \right), \quad (2.2.20)$$

and the Yukawa-like terms are

$$V_{\text{ferm}} = \frac{2\pi i}{k} \text{Tr} \left(Z_A^\dagger Z^A \psi^{B\dagger} \psi_B - Z^A Z_A^\dagger \psi_B \psi^{B\dagger} + 2Z^A Z_B^\dagger \psi_A \psi^{B\dagger} - 2Z_A^\dagger Z^B \psi^{A\dagger} \psi_B + \varepsilon^{ABCD} Z_A^\dagger \psi_B Z_C^\dagger \psi_D - \varepsilon_{ABCD} Z^A \psi^{B\dagger} Z^C \psi^{D\dagger} \right). \quad (2.2.21)$$

The covariant derivative acts as

$$D_\mu Z^A = \partial_\mu Z^A + iA_\mu^L Z^A - iZ^A A_\mu^R, \quad (2.2.22)$$

and the final piece in the ABJM Lagrangian contains the Chern-Simons terms for the gauge fields,

$$\mathcal{L}_{\text{CS}} = \frac{k}{4\pi} \varepsilon^{\mu\nu\rho} \text{Tr} \left(A_\mu^L \partial_\nu A_\rho^L + \frac{2i}{3} A_\mu^L A_\nu^L A_\rho^L - A_\mu^R \partial_\nu A_\rho^R - \frac{2i}{3} A_\mu^R A_\nu^R A_\rho^R \right). \quad (2.2.23)$$

The ABJM action is invariant under the following supersymmetry transformations:

$$\delta Z^A = -\epsilon^{AB}\psi_B. \quad (2.2.24)$$

$$\begin{aligned} \delta\psi_B = & \gamma^\mu\epsilon_{AB}D_\mu Z^A + \frac{2\pi}{k}\left(Z^C Z_B^\dagger Z^D - Z^D Z_B^\dagger Z^C\right)\epsilon_{CD} \\ & - \frac{2\pi}{k}\left(Z^A Z_C^\dagger Z^C - Z^C Z_C^\dagger Z^A\right)\epsilon_{AB}, \end{aligned} \quad (2.2.25)$$

$$\delta A_\mu^L = \frac{2\pi i}{k}\left(\epsilon_{AB}\gamma_\mu Z^B\psi^{\dagger A} - \epsilon^{AB}\gamma_\mu\psi_A Z_B^\dagger\right), \quad (2.2.26)$$

$$\delta A_\mu^R = \frac{2\pi i}{k}\left(\epsilon_{AB}\gamma_\mu\psi^{\dagger A} Z^B - \epsilon^{AB}\gamma_\mu Z_B^\dagger\psi_A\right). \quad (2.2.27)$$

The ABJM theory describes N M2-branes in the background of a $\mathbb{C}^4/\mathbb{Z}_k$ orbifold. This can be seen from the vacuum moduli space, or from the brane construction where a configuration of NS5-, D5- and D3-branes is T-dualised and lifted to M-theory to describe the background geometry [45, 26].

2.3 Reduction of multiple M2-branes to D2-branes

M-theory reduces to type IIA string theory upon compactification of one of the spatial dimensions. In this limit, M2-branes which do not wrap the compactified direction should reduce to D2-branes in the type IIA theory. This reduction was first understood for multiple M2-branes in the BLG theory when one of the scalar fields is given a large expectation value [46]. After integrating out one half of the gauge potential the theory reduces to the multiple D2-brane action. This novel Higgs mechanism can also be applied to the ABJM theory where the $U(N) \times U(N)$ theory reduces to super-Yang-Mills with a $U(N)$ gauge group [47, 48] describing multiple D2-branes. In this section we will review this reduction for the ABJM theory.

2.3.1 The novel Higgs mechanism

We can understand the relation between the ABJM theory and multiple D2-branes if we consider the background $\mathbb{C}^4/\mathbb{Z}_k$ orbifold as a cone over S^7/\mathbb{Z}_k . The angle of the cone is proportional to k^{-1} and the expectation value of the scalar, $\langle X^8 \rangle = v$, is proportional to how far away the branes are sitting from the tip of the cone. If we keep the ratio of k and v fixed then the radius of the cross section of the cone around where the branes are located will remain constant. In the limit of $k \rightarrow \infty$ and $v \rightarrow \infty$ where the ratio is kept constant, the local space looks like a flat cylinder, $\mathbb{R}^7 \times S^1$. The M2-branes are therefore in a compactified flat background where they should behave like D2-branes in type IIA string theory. This is illustrated in Figure 2.1.

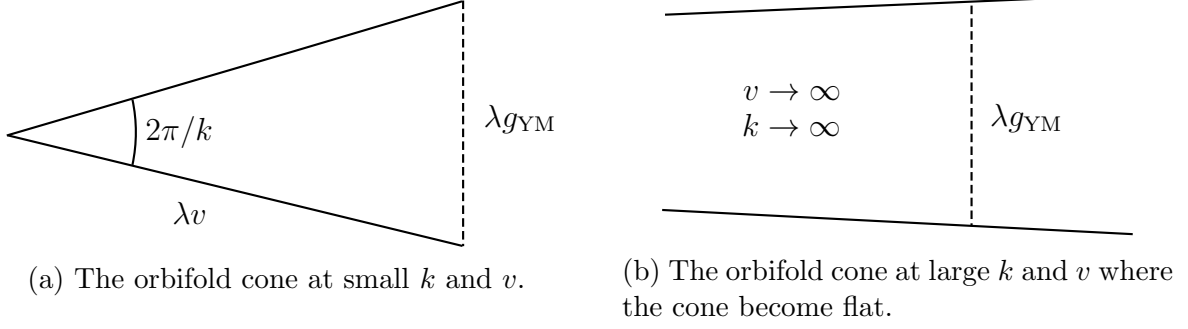


Figure 2.1: As k and v go to infinity with their ratio fixed, the cross section at v remains at a constant radius. However, the cone becomes flatter as v gets larger, and in the limit $k, v \rightarrow \infty$ the cross section around v looks like a cylinder.

To understand this procedure in detail, let us begin by rewriting the gauge fields as

$$A_\mu^\pm = \frac{1}{2} \left(A_\mu^L \pm A_\mu^R \right). \quad (2.3.1)$$

In this notation the covariant derivative becomes

$$D_\mu Y^A = \tilde{D}_\mu Y^A + i\{A_\mu^-, Y^A\}, \quad (2.3.2)$$

where

$$\tilde{D}_\mu Y^A = \partial_\mu Y^A + i[A_\mu^+, Y^A]. \quad (2.3.3)$$

The Chern-Simons term becomes

$$\mathcal{L}_{\text{CS}} = \frac{k}{2\pi} \epsilon^{\mu\nu\lambda} \text{Tr} \left(A_\mu^- F_{\nu\lambda}^+ + \frac{2}{3} i A_\mu^- A_\nu^- A_\lambda^- \right), \quad (2.3.4)$$

where

$$F_{\mu\nu}^+ = \partial_\mu A_\nu^+ - \partial_\nu A_\mu^+ + i[A_\mu^+, A_\nu^+]. \quad (2.3.5)$$

To make contact with the 8 transverse directions to the M2-branes, and eventually the 7 transverse directions to the D2-branes, we will write the complex scalar fields, Z^A , as

$$Z^A = X^A + iX^{A+4}. \quad (2.3.6)$$

Here the X^I fields ($I = 1, \dots, 8$) are Hermitian matrices which can be expanded in a basis of the identity matrix and the Hermitian generators of $\mathfrak{su}(N)$.

To reduce the ABJM action to that of multiple D2-branes, we take one of the scalar fields to have a vacuum expectation value (VEV),

$$\langle Z^4 \rangle = \frac{v}{2} T^0, \quad (2.3.7)$$

or equivalently,

$$\langle X^4 \rangle = \frac{v}{2} T^0. \quad (2.3.8)$$

In giving X^4 a VEV, we have broken the $U(N) \times U(N)$ gauge symmetry to its diagonal subgroup $U(N)$ where the left and right groups are identified.

In the D2-brane action that we will recover, the Yang-Mills coupling will be given by

$$g_{\text{YM}} = \frac{2\pi v}{k}. \quad (2.3.9)$$

As discussed at beginning of this section, the appropriate limit is $v \rightarrow \infty$ and $k \rightarrow \infty$ while keeping g_{YM} fixed.

In the action above, A_μ^- is an auxiliary field and can be integrated out. We will find its equation of motion shortly, but for now we note that it is of order v^{-1} . We can now expand the action around the VEV of Z^4 , neglecting terms of higher order in v^{-1} . The covariant derivatives become

$$D_\mu Z^a \rightarrow \tilde{D}_\mu X^a + i\tilde{D}_\mu X^{a+4}, \quad a = 1, 2, 3 \quad (2.3.10)$$

$$D_\mu Z^4 \rightarrow \tilde{D}_\mu X^4 + i\tilde{D}_\mu X^8 + ivA_\mu^-. \quad (2.3.11)$$

We can shift the auxiliary gauge field,

$$A_\mu^- \rightarrow A_\mu^- - \frac{1}{v} \tilde{D}_\mu X^8, \quad (2.3.12)$$

so that the covariant derivatives are

$$D_\mu Z^a \rightarrow \tilde{D}_\mu X^a + i\tilde{D}_\mu X^{a+4}, \quad (2.3.13)$$

$$D_\mu Z^4 \rightarrow \tilde{D}_\mu X^4 + ivA_\mu^-. \quad (2.3.14)$$

This shift will also introduce a term into the action proportional to $\varepsilon^{\mu\nu\rho} \tilde{D}_\mu X^8 F_{\nu\rho}^+$ from the Chern-Simons term. However this can be written as a total derivative by use of the Bianchi identity for $F_{\nu\rho}^+$.

Neglecting higher order terms in v^{-1} , the bosonic part of the action becomes

$$S = \int d^3x \text{Tr} \left(-\tilde{D}_\mu X^i \tilde{D}^\mu X^i - v^2 A_\mu^- A^{-\mu} + \frac{k}{2\pi} \varepsilon^{\mu\nu\lambda} A_\mu^- F_{\nu\lambda}^+ \right) - V_{\text{bos}}, \quad (2.3.15)$$

where $i = 1, \dots, 7$. The bosonic potential reduces to

$$V_{\text{bos}} = \frac{2\pi^2 v^2}{k^2} \text{Tr}[X^i, X^j]^2. \quad (2.3.16)$$

We can eliminate A_μ^- from the action by solving for its equation of motion. In doing so, we find the equation of motion is

$$A^{-\mu} = \frac{k}{4\pi v^2} \varepsilon^{\mu\nu\rho} F_{\nu\rho}^+. \quad (2.3.17)$$

There are higher order terms in v^{-1} that we have ignored. Substituting this back into the action we have

$$S = \int d^3x \operatorname{Tr} \left(-\tilde{D}_\mu X^i \tilde{D}^\mu X^i - \frac{1}{2g_{\text{YM}}^2} F_{\mu\nu}^+ F^{+\mu\nu} \right) - V_{\text{bos}}, \quad (2.3.18)$$

where we have used the identification of g_{YM} in equation (2.3.9). After rescaling $\tilde{X} = X g_{\text{YM}}$, the action becomes that of Yang-Mills gauge theory,

$$S = \frac{1}{g_{\text{YM}}^2} \int d^3x \operatorname{Tr} \left(-\tilde{D}_\mu \tilde{X}^i \tilde{D}^\mu \tilde{X}^i - \frac{1}{2} F_{\mu\nu}^+ F^{+\mu\nu} - \frac{1}{2} [\tilde{X}^i, \tilde{X}^j]^2 \right). \quad (2.3.19)$$

We have only shown the bosonic terms here, but the fermionic terms also reduce in the appropriate way to recover supersymmetric $\mathcal{N} = 8$ Yang-Mills. Note that there are no terms involving X^8 at first order in this action. The degree of freedom that we have lost has been absorbed by A_μ^+ to give it the one degree of freedom of a dynamical gauge field in three dimensions. The Chern-Simons terms of the M2-branes have given rise to a Yang-Mills kinetic term for A_μ^+ .

2.4 Background fields

So far we have only considered the action of multiple M2-branes in the limit of a flat background, where the metric is flat and the 3-form is zero. In this section, and in the next chapter we will be concerned with extending the multiple M2-brane action to include couplings to the background 3-form.

For a single M2-brane the full non-linear world-volume action is understood, and the bosonic part is [49]

$$S = -T_{\text{M2}} \int d^3x \left(\sqrt{-\det \gamma} + \frac{1}{3!} \varepsilon^{\mu\nu\rho} \partial_\mu X^m \partial_\nu X^n \partial_\rho X^p C_{mnp} \right), \quad (2.4.1)$$

where $\gamma_{\mu\nu}$ is the pull back of the space-time metric,

$$\gamma_{\mu\nu} = \partial_\mu X^m \partial_\nu X^n G_{mn}. \quad (2.4.2)$$

The BLG and ABJM theories provide a non-abelian generalisation of the first term in this action, but so far we have not commented on the possible generalisation of the

second term.

One possible approach to find a non-abelian generalisation of the coupling to the background 3-form is to consider all possible couplings which preserve a modified supersymmetry. In the limit $T_{\text{M2}} \rightarrow \infty$, the extension to the BLG action in a specific supersymmetric background is argued to be [50],

$$\begin{aligned} \mathcal{L} = & 2\tilde{G}_{IJKL} \text{Tr} \left(X^I, [X^J, X^K, X^L] \right) - \frac{1}{2}m^2 \text{Tr} \left(X^I, X^I \right) \\ & - \frac{i}{8} \text{Tr} \left(\Psi \Gamma^{IJKL}, \Psi \right) \tilde{G}_{IJKL}, \end{aligned} \quad (2.4.3)$$

where

$$\begin{aligned} \tilde{G}_{IJKL} = & -\frac{1}{3!} \varepsilon^{\mu\nu\rho} \left(G_7 + \frac{1}{2} C_3 \wedge G_4 \right)_{\mu\nu\rho IJKL} \\ = & \frac{1}{4!} \varepsilon_{IJKLMNPQ} G^{MNPQ}, \end{aligned} \quad (2.4.4)$$

and G_{IJKL} is taken to be constant. The mass introduced for X^I is proportional to $G^2 = G_{IJKL} G^{IJKL}$.

An approach to find a more general construction is to use our knowledge of the Myers-Chern-Simons action for the non-abelian coupling of background fields to a stack of multiple D2-branes. The terms that may be present in the multiple M2-brane action can be fixed upon reduction to the D2-brane theory. Using this approach a gauge invariant extension of the BLG action can be written down [51],

$$\begin{aligned} S_{\text{MCS}} = & \int d^3x \left(\lambda_1 \varepsilon^{\mu\nu\rho} g^{abc} C_{IJK} D_\mu X_a^I D_\nu X_b^J D_\rho X_c^K \right. \\ & \left. + \lambda_2 \varepsilon^{\mu\nu\rho} d^{gabc} f^{def}{}_g C_{IJKLMN} X_d^I X_e^J X_f^K D_\mu X_a^L D_\nu X_b^M D_\rho X_c^N \right). \end{aligned} \quad (2.4.5)$$

The 6-form that we have introduced here is the dual of the 3-form. The constants g^{abc} and d^{abcd} encode our lack of understanding of how to define a symmetric trace over the three-algebra generators since the inner product does not extend to multiple generators,

$$g^{abc} = \text{STr} \left(T^a T^b T^c \right), \quad (2.4.6)$$

$$d^{abcd} = \text{STr} \left(T^a T^b T^c T^d \right). \quad (2.4.7)$$

Gauge invariance of this action imposes the conditions

$$g^{d(abfc)fe}{}_d = 0, \quad (2.4.8)$$

$$d^{gabc} f^{ji[d}{}_h f^{ef]h}{}_g + d^{gh(abfc)ji}{}_d f^{def}{}_g = 0. \quad (2.4.9)$$

For the three-algebra, \mathcal{A}_4 , these can be fixed uniquely by comparing the action obtained in the reduction to D2-branes with the expected couplings in the Myers-Chern-Simons terms.

A similar argument can be made about the extension of the ABJM action [52], where the $U(N) \times U(N)$ gauge group allows for a more concrete understanding of the nature of the coupling to the background 3-form and 6-form.

First one needs to understand how to pull back the space-time fields so that they can be coupled into the ABJM action. This is well understood for D2-branes in the background of the type IIA 3-form. The pullback in static gauge is given by

$$\begin{aligned}
 P[\tilde{C}]_{\mu\nu\rho} &= \tilde{C}_{\mu\nu\rho} + 3\tilde{\lambda}\tilde{C}_{\mu\nu I}D_\rho\tilde{X}^I + 3\tilde{\lambda}^2\tilde{C}_{\mu IJ}D_\nu\tilde{X}^I D_\rho\tilde{X}^J \\
 &\quad + \tilde{\lambda}^3\tilde{C}_{IJK}D_\mu\tilde{X}^I D_\nu\tilde{X}^J D_\rho\tilde{X}^K.
 \end{aligned}
 \tag{2.4.10}$$

Note that from now on we will label fields in the type IIA theory with tildes to distinguish them from the M-theory fields. The type IIA 3-form can be extended to a matrix valued functional of \tilde{X}^I by replacing the transverse coordinates in its Taylor expansion with \tilde{X}^I as explained in Section 2.1.

In the ABJM action, the fields are in the bifundamental representation of $U(N) \times U(N)$ and it is not clear how to pull back the space-time 3-form to the world-volume. A naive attempt might be to take the pullback to be

$$\begin{aligned}
 P[C]_{\mu\nu\rho} &= C_{\mu\nu\rho} + 3\lambda C_{\mu\nu A}D_\rho Z^A + 3\lambda^2 C_{\mu A\bar{B}}D_\nu Z^A D_\rho Z^{\dagger}_{\bar{B}} \\
 &\quad + \lambda^3 C_{A\bar{B}C}D_\mu Z^A D_\nu Z^{\dagger}_{\bar{B}} D_\rho Z^C + (\text{c.c.}).
 \end{aligned}
 \tag{2.4.11}$$

The different components of C are chosen so that the terms shown above transform in the left $U(N)$ while the complex conjugate transforms in the right. In the dimensional reduction to type IIA string theory, the M-theory 3-form should reduce to the RR 3-form, \tilde{C} , and the Kalb-Ramond 2-form, \tilde{B} . However, there are not enough components in the 3-form coefficients in the above pullback to recover all of the independent components of the IIA 3-form and Kalb-Ramond field.

It is possible to take the components of C to have a more general gauge index structure and therefore couple to terms which would not be gauge invariant under normal matrix multiplication such as $\text{Tr}(C_{\mu AB}D_\nu Z^A D_\rho Z^B)$. We will discuss this further in the next chapter, but for now we will jump ahead to an easier problem where the $U(N) \times U(N)$ gauge group has been broken to its diagonal subgroup by giving one of the scalar fields a large expectation value. In this case the most general combination

of terms that may arise is [52]:

$$\begin{aligned}
 S_C = T_{\text{M2}} \int d^3x \varepsilon^{\mu\nu\rho} \text{Tr} & \left(C_{\mu\nu\rho} + 3\lambda C_{\mu\nu A} D_\rho Z^A \right. \\
 & + 3\lambda^2 \left(C_{\mu A \bar{B}}^{(1)} D_\nu Z^A D_\rho Z^{\dagger \bar{B}} - C_{\mu A \bar{B}}^{(2)} D_\nu Z^{\dagger \bar{B}} D_\rho Z^A \right. \\
 & \quad \left. \left. + C_{\mu AB}^{(3)} D_\nu Z^A D_\rho Z^B \right) \right. \\
 & + \lambda^3 \left(C_{ABC}^{(1)} D_\mu Z^A D_\nu Z^B D_\rho Z^C + C_{ABC}^{(2)} D_\mu Z^A D_\nu Z^B D_\rho Z^{\dagger \bar{C}} \right. \\
 & \quad \left. - C_{AC\bar{B}}^{(3)} D_\mu Z^A D_\nu Z^{\dagger \bar{B}} D_\rho Z^C + C_{BC\bar{A}}^{(4)} D_\mu Z^{\dagger \bar{A}} D_\nu Z^B D_\rho Z^C \right) \\
 & + (\text{c.c.}),
 \end{aligned} \tag{2.4.12}$$

where $T_{\text{M2}} = \lambda^{-2}$ is the M2-brane tension and $\lambda = 2\pi l_p^{3/2}$. Note that the upper indices on the 3-form coefficients should not be confused with the indices that label the different type IIA RR forms with different degrees. The C field coefficients are anti-symmetric in any groups of identical types of indices. For example,

$$C_{ABC}^{(1)} = C_{[ABC]}^{(1)}, \quad C_{AB\bar{C}}^{(2)} = C_{[AB]\bar{C}}^{(2)}, \quad C_{\mu AB}^{(3)} = C_{\mu[AB]}^{(3)}. \tag{2.4.13}$$

We perform the Higgsing procedure as above: expand around the expectation value, consider only leading order terms, and rescale $\tilde{X} = X g_{\text{YM}}$. After doing so and using equations (2.3.13) and (2.3.14) the action can be written as

$$S_C = T_{\text{M2}} \int d^3x \varepsilon^{\mu\nu\rho} \text{Tr} \left(P[\tilde{C}]_{\mu\nu\rho} + \lambda v A_\mu^- P[\tilde{B}]_{\nu\rho} \right). \tag{2.4.14}$$

The fields marked with tildes correspond to the type IIA background fields and are related to the 3-form coefficients in the ABJM action. For example, the world-volume components of the Kalb-Ramond field, $\tilde{B}_{\mu\nu}$, are given by

$$\tilde{B}_{\mu\nu} = 3i \left(C_{\mu\nu 4} - C_{\mu\nu 4}^\dagger \right). \tag{2.4.15}$$

The identifications of the rest of the components of \tilde{B} and \tilde{C} with the coefficients of the 3-form in the ABJM action are given at the end of this section. The pullbacks of the type IIA fields are given by

$$\begin{aligned}
 P[\tilde{C}]_{\mu\nu\rho} = \tilde{C}_{\mu\nu\rho} + 3\tilde{\lambda} \tilde{C}_{\mu\nu i} \tilde{D}_\rho \tilde{X}^i + 3\tilde{\lambda}^2 \tilde{C}_{\mu ij} \tilde{D}_\nu \tilde{X}^i \tilde{D}_\rho \tilde{X}^j \\
 + \tilde{\lambda}^3 \tilde{C}_{ijk} \tilde{D}_\mu \tilde{X}^i \tilde{D}_\nu \tilde{X}^j \tilde{D}_\rho \tilde{X}^k,
 \end{aligned} \tag{2.4.16}$$

and

$$P[\tilde{B}]_{\mu\nu} = \tilde{B}_{\mu\nu} + 2\tilde{\lambda}\langle\langle\tilde{B}_{\mu i}\tilde{D}_\nu\tilde{X}^i\rangle\rangle + \tilde{\lambda}^2\langle\langle\tilde{B}_{ij}\tilde{D}_\nu\tilde{X}^i\tilde{D}_\rho\tilde{X}^j\rangle\rangle, \quad (2.4.17)$$

where \tilde{D} is the covariant derivative in the recovered Yang-Mills theory, as in equation (2.3.2). We have defined $\tilde{\lambda} = \lambda/g_{\text{YM}}$ and $\langle\langle\dots\rangle\rangle$ denotes the symmetric product. In order to remove some undesirable terms that arise from this reduction but are not present in the D2-brane action, we must identify the following 3-form coefficients:

$$C_{\mu AB}^{(2)} = C_{\mu AB}^{(3)}, \quad (2.4.18)$$

and

$$C_{ABC}^{(2)} = C_{ABC}^{(3)} = C_{ABC}^{(4)}. \quad (2.4.19)$$

When integrating out A_μ^- the equation of motion now becomes

$$\begin{aligned} A^{-\mu} &= \frac{k}{4\pi v^2}\varepsilon^{\mu\nu\rho}F_{\nu\rho}^+ + \frac{T_{\text{M2}}\lambda}{2v}\varepsilon^{\mu\nu\rho}P[\tilde{B}_{\nu\rho}] \\ &= \frac{k}{4\pi v^2}\varepsilon^{\mu\nu\rho}\left(F_{\nu\rho}^+ + T_{\text{M2}}\tilde{\lambda}g_{\text{YM}}^2P[\tilde{B}_{\nu\rho}]\right) \\ &= \frac{k}{4\pi v^2}\varepsilon^{\mu\nu\rho}\left(F_{\nu\rho}^+ + \frac{1}{\tilde{\lambda}}P[\tilde{B}_{\nu\rho}]\right), \end{aligned} \quad (2.4.20)$$

where we have used

$$T_{\text{M2}} = \frac{1}{\lambda^2} = \frac{1}{g_{\text{YM}}^2\tilde{\lambda}^2}. \quad (2.4.21)$$

Substituting back into the action gives

$$S = \frac{1}{g_{\text{YM}}^2}\int d^3x \text{Tr}\left(-\tilde{D}_\mu\tilde{X}_i\tilde{D}^\mu\tilde{X}^i - \frac{1}{2}\left(F_{\mu\nu}^+ + \tilde{\lambda}^{-1}P[\tilde{B}_{\mu\nu}]\right)^2\right) - V_{\text{bos}}. \quad (2.4.22)$$

This is the extension of the low energy action for multiple D2-branes in equation (2.1.9) to include the background Kalb-Ramond field, where \tilde{F} replaced by the gauge invariant quantity $\tilde{F} + (2\pi\alpha')^{-1}\tilde{B}$. The tension of the D2-brane is identified with the tension of the M2-brane, $T_{\text{M2}} = T_{\text{D2}}$, and we saw in Section 2.1 that in the low energy limit, the D2-brane action is Yang-Mills theory with coupling constant,

$$\frac{1}{g_{\text{YM}}^2} = (2\pi\alpha')^2 T_{\text{D2}}. \quad (2.4.23)$$

The quantity $\tilde{\lambda}$ should therefore be identified with $2\pi\alpha'$. The expected coupling to $\tilde{C}_{(3)}$

is also included, via its pull-back,

$$S_{\text{MCS}} = T_{\text{D2}} \int d^3x \varepsilon^{\mu\nu\rho} \text{Tr} \left(P[\tilde{C}]_{\mu\nu\rho} \right). \quad (2.4.24)$$

Identification of $SU(4)$ fields with $SO(7)$ fields

We present here a list of the identifications made in [52] between the components of the $SU(4)$ and $SO(7)$ fields. In this thesis we have scaled $\tilde{B}_{\mu\nu} \rightarrow 3\tilde{B}_{\mu\nu}$ and $\tilde{B}_{\mu i} \rightarrow \frac{3}{2}\tilde{B}_{\mu i}$ compared to the original paper. This gives the pullback of \tilde{B} a more natural form:

$$P[\tilde{B}_{\mu\nu}] = \tilde{B}_{\mu\nu} + 2\lambda \langle\langle \tilde{B}_{\mu i} \tilde{D}_\nu \tilde{X}^i \rangle\rangle + \lambda^2 \langle\langle \tilde{B}_{ij} \tilde{D}_\nu \tilde{X}^i \tilde{D}_\rho \tilde{X}^j \rangle\rangle. \quad (2.4.25)$$

The identifications used in this thesis are then:

$$\tilde{C}_{\mu\nu\rho} = C_{\mu\nu\rho} + C_{\mu\nu\rho}^\dagger, \quad (2.4.26)$$

$$\tilde{B}_{\mu\nu} = 3i \left(C_{\mu\nu 4} - C_{\mu\nu 4}^\dagger \right), \quad (2.4.27)$$

$$\tilde{C}_{\mu\nu a} = C_{\mu\nu a} + C_{\mu\nu a}^\dagger, \quad (2.4.28)$$

$$\tilde{C}_{\mu\nu a+4} = i \left(C_{\mu\nu a} - C_{\mu\nu a}^\dagger \right), \quad (2.4.29)$$

$$\tilde{C}_{\mu\nu 4} = C_{\mu\nu 4} + C_{\mu\nu 4}^\dagger, \quad (2.4.30)$$

$$\tilde{B}_{\mu 4} = 6i \left(C_{\mu 4\bar{4}}^{(1)} - C_{\mu 4\bar{4}}^{(1)\dagger} \right), \quad (2.4.31)$$

$$\tilde{B}_{\mu a} = 3i \left(C_{\mu 4\bar{a}}^{(1)} - C_{\mu 4\bar{a}}^{(1)\dagger} + C_{\mu a\bar{4}}^{(1)} - C_{\mu a\bar{4}}^{(1)\dagger} + C_{\mu 4a}^{(3)} - C_{\mu 4a}^{(3)\dagger} \right), \quad (2.4.32)$$

$$\tilde{B}_{\mu a+4} = 3 \left(C_{\mu 4\bar{a}}^{(1)} + C_{\mu 4\bar{a}}^{(1)\dagger} - C_{\mu a\bar{4}}^{(1)} - C_{\mu a\bar{4}}^{(1)\dagger} - C_{\mu 4a}^{(3)} - C_{\mu 4a}^{(3)\dagger} \right), \quad (2.4.33)$$

$$\tilde{C}_{\mu 4a} = C_{\mu 4\bar{a}}^{(1)} + C_{\mu 4\bar{a}}^{(1)\dagger} - C_{\mu a\bar{4}}^{(1)} - C_{\mu a\bar{4}}^{(1)\dagger} + C_{\mu 4a}^{(3)} + C_{\mu 4a}^{(3)\dagger}, \quad (2.4.34)$$

$$\tilde{C}_{\mu 4a+4} = -i \left(C_{\mu 4\bar{a}}^{(1)} - C_{\mu 4\bar{a}}^{(1)\dagger} + C_{\mu a\bar{4}}^{(1)} - C_{\mu a\bar{4}}^{(1)\dagger} - C_{\mu 4a}^{(3)} + C_{\mu 4a}^{(3)\dagger} \right), \quad (2.4.35)$$

$$\tilde{C}_{\mu ab} = C_{\mu a\bar{b}}^{(1)} - C_{\mu b\bar{a}}^{(1)\dagger} - C_{\mu b\bar{a}}^{(1)} + C_{\mu a\bar{b}}^{(1)\dagger} + C_{\mu ab}^{(3)\dagger} + C_{\mu ab}^{(3)}, \quad (2.4.36)$$

$$\tilde{C}_{\mu ab+4} = i \left(C_{\mu a\bar{b}}^{(1)\dagger} - C_{\mu b\bar{a}}^{(1)} - C_{\mu ab}^{(1)} + C_{\mu b\bar{a}}^{(1)\dagger} - C_{\mu ab}^{(3)\dagger} + C_{\mu ab}^{(3)} \right), \quad (2.4.37)$$

$$\tilde{C}_{\mu a+4b} = i \left(C_{\mu b\bar{a}}^{(1)} - C_{\mu a\bar{b}}^{(1)\dagger} + C_{\mu ab}^{(1)} - C_{\mu b\bar{a}}^{(1)\dagger} + C_{\mu ab}^{(3)} \right) - C_{\mu ab}^{(3)\dagger}, \quad (2.4.38)$$

$$\tilde{C}_{\mu a+4b+4} = C_{\mu a\bar{b}}^{(1)\dagger} - C_{\mu b\bar{a}}^{(1)} + C_{\mu ab}^{(1)} - C_{\mu b\bar{a}}^{(1)\dagger} - C_{\mu ab}^{(3)\dagger} - C_{\mu ab}^{(3)}. \quad (2.4.39)$$

and

$$\tilde{B}_{a4} = -6i(C_{a4\bar{4}}^{(2)} - C_{a4\bar{4}}^{(2)\dagger}), \quad (2.4.40)$$

$$\tilde{B}_{4a+4} = -6(C_{a4\bar{4}}^{(2)} + C_{a4\bar{4}}^{(2)\dagger}), \quad (2.4.41)$$

$$\tilde{B}_{ab} = 3i(C_{ab4}^{(1)} - C_{ab4}^{(1)\dagger} - C_{ab\bar{4}}^{(2)} + C_{ab\bar{4}}^{(2)\dagger} + C_{b4\bar{a}}^{(2)} - C_{b4\bar{a}}^{(2)\dagger} - C_{a4\bar{b}}^{(2)} + C_{a4\bar{b}}^{(2)\dagger}), \quad (2.4.42)$$

$$\tilde{B}_{ab+4} = -3(C_{ab4}^{(1)} + C_{ab4}^{(1)\dagger} - C_{ab\bar{4}}^{(2)} - C_{ab\bar{4}}^{(2)\dagger} + C_{b4\bar{a}}^{(2)} + C_{b4\bar{a}}^{(2)\dagger} + C_{a4\bar{b}}^{(2)} + C_{a4\bar{b}}^{(2)\dagger}), \quad (2.4.43)$$

$$\tilde{B}_{a+4b} = -3(C_{ab4}^{(1)} + C_{ab4}^{(1)\dagger} - C_{ab\bar{4}}^{(2)} - C_{ab\bar{4}}^{(2)\dagger} - C_{b4\bar{a}}^{(2)} - C_{b4\bar{a}}^{(2)\dagger} - C_{a4\bar{b}}^{(2)} - C_{a4\bar{b}}^{(2)\dagger}), \quad (2.4.44)$$

$$\tilde{B}_{a+4b+4} = -3i(C_{ab4}^{(1)} - C_{ab4}^{(1)\dagger} - C_{ab\bar{4}}^{(2)} + C_{ab\bar{4}}^{(2)\dagger} - C_{b4\bar{a}}^{(2)} + C_{b4\bar{a}}^{(2)\dagger} + C_{a4\bar{b}}^{(2)} - C_{a4\bar{b}}^{(2)\dagger}), \quad (2.4.45)$$

$$\tilde{C}_{ab4} = (C_{ab4}^{(1)} + C_{ab4}^{(1)\dagger} + C_{ab\bar{4}}^{(2)} + C_{ab\bar{4}}^{(2)\dagger} + C_{b4\bar{a}}^{(2)} + C_{b4\bar{a}}^{(2)\dagger} - C_{a4\bar{b}}^{(2)} - C_{a4\bar{b}}^{(2)\dagger}), \quad (2.4.46)$$

$$\tilde{C}_{a4b+4} = -(C_{ab4}^{(1)} - C_{ab4}^{(1)\dagger} + C_{ab\bar{4}}^{(2)} - C_{ab\bar{4}}^{(2)\dagger} + C_{b4\bar{a}}^{(2)} - C_{b4\bar{a}}^{(2)\dagger} + C_{a4\bar{b}}^{(2)} - C_{a4\bar{b}}^{(2)\dagger}), \quad (2.4.47)$$

$$\tilde{C}_{4a+4b+4} = -(C_{ab4}^{(1)} + C_{ab4}^{(1)\dagger} + C_{ab\bar{4}}^{(2)} + C_{ab\bar{4}}^{(2)\dagger} - C_{b4\bar{a}}^{(2)} - C_{b4\bar{a}}^{(2)\dagger} + C_{a4\bar{b}}^{(2)} + C_{a4\bar{b}}^{(2)\dagger}), \quad (2.4.48)$$

$$\tilde{C}_{abc} = C_{abc}^{(1)} + C_{abc}^{(1)\dagger} + C_{ab\bar{c}}^{(2)} + C_{ab\bar{c}}^{(2)\dagger} - C_{ac\bar{b}}^{(2)} - C_{ac\bar{b}}^{(2)\dagger} + C_{bc\bar{a}}^{(2)} + C_{bc\bar{a}}^{(2)\dagger}, \quad (2.4.49)$$

$$\tilde{C}_{abc+4} = i(C_{abc}^{(1)} - C_{abc}^{(1)\dagger} - C_{ab\bar{c}}^{(2)} + C_{ab\bar{c}}^{(2)\dagger} - C_{ac\bar{b}}^{(2)} + C_{ac\bar{b}}^{(2)\dagger} + C_{bc\bar{a}}^{(2)} - C_{bc\bar{a}}^{(2)\dagger}), \quad (2.4.50)$$

$$\tilde{C}_{ab+4c+4} = -(C_{abc}^{(1)} + C_{abc}^{(1)\dagger} - C_{ab\bar{c}}^{(2)} - C_{ab\bar{c}}^{(2)\dagger} + C_{ac\bar{b}}^{(2)} + C_{ac\bar{b}}^{(2)\dagger} + C_{bc\bar{a}}^{(2)} + C_{bc\bar{a}}^{(2)\dagger}), \quad (2.4.51)$$

$$\tilde{C}_{a+4b+4c+4} = -i(C_{abc}^{(1)} - C_{abc}^{(1)\dagger} - C_{ab\bar{c}}^{(2)} + C_{ab\bar{c}}^{(2)\dagger} + C_{ac\bar{b}}^{(2)} - C_{ac\bar{b}}^{(2)\dagger} - C_{bc\bar{a}}^{(2)} + C_{bc\bar{a}}^{(2)\dagger}). \quad (2.4.52)$$

Note that there is also a factor of 2 difference in the expressions for \tilde{B}_{a4} and \tilde{B}_{a+44} and a difference of sign of the $C^{(3)\dagger}$ parts of $C_{\mu ij}$. These appear to be mistakes in the original paper.

Chapter 3

Higher order background field couplings

In the previous chapter we have seen a prescription for extending the ABJM action to including a coupling to the background 3-form of M-theory. This was derived by assumptions of gauge invariance, at least in the action with partially broken gauge symmetry, and by requiring that the action reduce to the action of multiple D2-branes after performing the novel Higgs mechanism. Our goal in this chapter is to extend this construction to include quadratic couplings to the background 3-form. Recall that the full action of multiple D2-branes contains the Myers-Chern-Simons terms [32],

$$S_{\text{MCS}} = T_{\text{D2}} \int \text{STr} \left(P \left[e^{\frac{i}{2} \tilde{\lambda} [\tilde{X}, \tilde{X}]} \left(\sum \tilde{C}_n e^{\tilde{B}} \right) \right] e^{\tilde{\lambda} \tilde{F}} \right). \quad (3.0.1)$$

This contains terms which include both the type IIA 3-form, \tilde{C} , and the Kalb-Ramond 2-form, \tilde{B} . Since both the type IIA 3-form and the Kalb-Ramond 2-form are recovered from the M-theory 3-form, these can only arise from terms in the ABJM action which are quadratic in the M-theory 3-form.

In the D-brane action, the trace must be taken to be the symmetric trace. One of the aims of this chapter is to understand the appropriate prescription for contracting the matrix structure of the terms in the ABJM action, which we will continue to refer to as a trace, even though it may be more general. This trace must maintain gauge invariance with the unbroken $U(N) \times U(N)$ gauge group and reduce to the linear couplings shown in the previous chapter when the gauge group is broken to its diagonal subgroup. A possible prescription has been given previously when considering the linear couplings [52], and we will comment on this further in this chapter. However, there are some subtleties in this prescription that have not been previously considered and we hope to address these more fully. Having an understanding of the higher order couplings to the 3-form will be useful in further understanding this point.

In Section 3.1 we will deduce the form of the quadratic couplings of the 3-form in the ABJM action, after the $U(N) \times U(N)$ gauge group has been broken to its diagonal subgroup. Beginning at this intermediate step allows us to concretely determine the terms which must be present by matching with the terms in the D2-brane action. In Section 3.2 we will comment on the form of the coupling to the 3-form in the ABJM action with the unbroken gauge symmetry.

3.1 Quadratic couplings to background fields

Before we can construct the possible quadratic terms in the ABJM action we note that the fields in the D2- and M2-brane actions are matrix valued and so their ordering is important. In the Myers-Chern-Simons term of the D2-brane action the usual trace is replaced by the symmetrised trace, STr . All of the terms in this should be appropriately symmetrised, with commutators treated as a single term to avoid setting everything to zero. In particular,

$$\text{STr} \left(\tilde{C} \tilde{B} [\tilde{X}, \tilde{X}] \right) = \frac{1}{2} \text{STr} \left(\tilde{C} \tilde{B} [\tilde{X}, \tilde{X}] + \tilde{B} \tilde{C} [\tilde{X}, \tilde{X}] \right). \quad (3.1.1)$$

This prescription does not make sense for the wedge product of two identical 3-forms since symmetrizing the non-abelian structure would set everything to zero. Instead this product should be naturally anti-symmetric:

$$C_{ijk} C_{lmo} = -C_{lmo} C_{ijk}, \quad \text{by anti-symmetry of contracted indices} \quad (3.1.2)$$

$$= C_{ijk} C_{lmo}, \quad \text{by anti-symmetry of non-abelian product.} \quad (3.1.3)$$

This argument is perhaps too simple since the world-volume and tranverse indices are not treated equally in the ABJM action. However, we will see later that this property is also required to match with the sign of certain terms in the reduction to the D2-brane action.

To conserve notation as much as possible, we will not explicitly show the anti-symmetrization of the quadratic terms in the coefficients of the 3-form, but this should always be taken as implicit. For example, we will only write $C_{\mu\nu\rho} C_{ABC}^{(1)}$ where we also mean to include $-C_{ABC}^{(1)} C_{\mu\nu\rho}$.

Our procedure is straightforward. We will begin by writing all possible terms which are quadratic in the coefficients of the M-theory 3-form, C . The coefficients of C have been given previously in the linear action in equation (2.4.12). We will fix the coefficients of the quadratic terms by reducing to the D2-brane action and comparing to the known terms there. In the identification of the linear terms between the ABJM action and the D-brane action we had the freedom to identify the correct components

to ensure the actions matched. With these identifications already fixed we no longer have this freedom and it is not clear *a priori* whether such an identification will be possible at quadratic order.

The terms we would like to recover in the D2-brane action come from the $\tilde{C} \wedge \tilde{B}$ piece of the Myers-Chern-Simons action in equation (3.0.1),

$$\begin{aligned}
 \tilde{\mathcal{L}} &= \frac{1}{2} \mu_2 \tilde{\lambda} i \text{STr} \left(P \left[[\tilde{X}, \tilde{X}] \tilde{C}_3 \wedge \tilde{B} \right] \right) \\
 &= \frac{1}{2} \mu_2 \tilde{\lambda} i \varepsilon^{\mu\nu\rho} \text{STr} \left(\tilde{C}_{[\mu\nu\rho} \tilde{B}_{ij]} [\tilde{X}^i, \tilde{X}^j] + 3 \tilde{\lambda} \tilde{C}_{[\mu\nu i} \tilde{B}_{jk]} [\tilde{X}^i, \tilde{X}^j] \tilde{D}_\rho \tilde{X}^k \right. \\
 &\quad + 3 \tilde{\lambda}^2 \tilde{C}_{[\mu ij} \tilde{B}_{kl]} [\tilde{X}^i, \tilde{X}^j] \tilde{D}_\nu \tilde{X}^k \tilde{D}_\rho \tilde{X}^l \\
 &\quad \left. + \tilde{\lambda}^3 \tilde{C}_{[ijk} \tilde{B}_{lm]} [\tilde{X}^i, \tilde{X}^j] \tilde{D}_\mu \tilde{X}^k \tilde{D}_\nu \tilde{X}^l \tilde{D}_\rho \tilde{X}^m \right). \tag{3.1.4}
 \end{aligned}$$

In the following sections we will look at which terms we must add in to the M2-brane action to be able to recover each of the terms above. Nothing in the reduction procedure will remove or add derivatives so we can match the theories term by term based on the number of derivatives.

The rest of this section is a presentation of some rather lengthy algebra in matching the terms in the two actions. Little will be missed by jumping ahead to the final result, which we present at the end of this section.

3.1.1 No derivatives

Let us look first at the quadratic terms in the M2- and D2-brane actions that have no derivatives, coming from the coefficients in the pullback with three world-volume indices. We know what these terms in the D2-brane action are and we can use this information to construct the appropriate terms in the ABJM action with broken gauge symmetry. The term in the D2-brane action with no derivatives is given by the first term of equation (3.1.4) and after expanding out the antisymmetry in the indices of \tilde{C} and \tilde{B} this is

$$\tilde{\mathcal{L}}_0 = \frac{\mu_2 \tilde{\lambda}}{20} i \varepsilon^{\mu\nu\rho} \text{Tr} \left(\tilde{C}_{\mu\nu\rho} \tilde{B}_{ij} [\tilde{X}^i, \tilde{X}^j] - 6 \tilde{C}_{\mu\nu i} \tilde{B}_{\rho j} [\tilde{X}^i, \tilde{X}^j] + 3 \tilde{C}_{\mu ij} \tilde{B}_{\nu\rho} [\tilde{X}^i, \tilde{X}^j] \right). \tag{3.1.5}$$

To find the appropriate terms in the M2-brane action which reduce to the above expression, we should consider all possible quadratic couplings, as dictated by R-symmetry and gauge invariance, with arbitrary coefficients. The coefficients can then be fixed by comparison to the D2-brane action. For clarity, we will only present the final result here and then demonstrate that it does indeed reduce to the required D2-brane action.

The quadratic terms in the ABJM action with no derivatives are,

$$S_0 = \int \mathcal{L}_1 + \mathcal{L}_2 + \mathcal{L}_3 + \mathcal{L}_4 + (\text{c.c.}), \quad (3.1.6)$$

where

$$\mathcal{L}_1 = -\frac{6}{5} \frac{\pi \mu_2 \lambda}{k} \varepsilon^{\mu\nu\rho} \text{Tr} \left(C_{\mu\nu\rho} C_{ABC}^{(1)} \gamma^{ABC} - C_{\mu\nu\rho} C_{ABC}^{(2)} \beta_C^{AB} \right), \quad (3.1.7)$$

$$\mathcal{L}_2 = -\frac{6}{5} \frac{\pi \mu_2 \lambda}{k} \varepsilon^{\mu\nu\rho} \text{Tr} \left(C_{\mu\nu\rho} C_{ABC}^{(1)\dagger} \gamma^{ABC\dagger} - C_{\mu\nu\rho} C_{ABC}^{(2)\dagger} \beta_C^{AB\dagger} \right), \quad (3.1.8)$$

$$\mathcal{L}_3 = +\frac{36}{5} \frac{\pi \mu_2 \lambda}{k} \varepsilon^{\mu\nu\rho} \text{Tr} \left(C_{\mu\nu A} C_{\rho BC}^{(1)} \beta_C^{AB} - \frac{3}{2} C_{\mu\nu A} C_{\rho BC}^{(3)} \gamma^{ABC} \right), \quad (3.1.9)$$

$$\mathcal{L}_4 = -\frac{36}{5} \frac{\pi \mu_2 \lambda}{k} \varepsilon^{\mu\nu\rho} \text{Tr} \left(C_{\mu\nu A} C_{\rho C\bar{B}}^{(1)\dagger} \beta_C^{AB} - \frac{1}{2} C_{\mu\nu A} C_{\rho BC}^{(3)\dagger} \beta_A^{BC\dagger} \right), \quad (3.1.10)$$

and

$$\beta_C^{AB} = Z^{[A} Z_C^\dagger Z^{B]} = \frac{1}{2} \left(Z^A Z_C^\dagger Z^B - Z^B Z_C^\dagger Z^A \right), \quad (3.1.11)$$

$$\gamma^{ABC} = Z^{[A} Z^B Z^C]. \quad (3.1.12)$$

Recall that the products of components of the 3-form, C , are implicitly anti-symmetric. Note that complex conjugation also affects the indices, for example, $C_{\rho C\bar{B}}^{(1)\dagger} = (C^{(1)\dagger})_{\rho C\bar{B}}$.

The Kalb-Ramond field is recovered from the components of the M-theory 3-form where one of the SU(4) indices is 4, so we can see that the first term in the D2-brane action in equation (3.1.5) should be recovered from \mathcal{L}_1 , \mathcal{L}_2 and their conjugates, while the second and third term in the D2-brane action should be recovered from \mathcal{L}_3 , \mathcal{L}_4 and their conjugates. Let us now do this identification in detail.

When one of the scalar fields in the ABJM action, Z^4 , acquires a large vacuum expectation value, $\langle Z^4 \rangle = \frac{v}{2} T^0$, the only components of (3.1.11) and (3.1.12) which will remain in the limit $v \rightarrow \infty$ are

$$\beta_4^{a4} = \frac{v}{2} \left([X^a, X^4] + i[X^{a+4}, X^4] \right), \quad (3.1.13)$$

$$\beta_4^{ab} = \frac{v}{4} \left([X^a, X^b] + i[X^{a+4}, X^b] + i[X^a, X^{b+4}] - [X^{a+4}, X^{b+4}] \right), \quad (3.1.14)$$

$$\beta_b^{a4} = \frac{v}{4} \left([X^a, X^b] + i[X^{a+4}, X^b] - i[X^a, X^{b+4}] + [X^{a+4}, X^{b+4}] \right), \quad (3.1.15)$$

$$\gamma^{ab4} = \frac{v}{12} \left([X^a, X^b] + i[X^{a+4}, X^b] + i[X^a, X^{b+4}] - [X^{a+4}, X^{b+4}] \right). \quad (3.1.16)$$

In this limit and after rescaling $\tilde{X} = X g_{\text{YM}}$, the expression \mathcal{L}_1 becomes

$$\begin{aligned}
 \mathcal{L}_1 = & -\frac{3}{20}\mu_2\tilde{\lambda}\varepsilon^{\mu\nu\rho}\text{Tr}\left(C_{\mu\nu\rho}\left(C_{ab4}^{(1)} - C_{ab\bar{4}}^{(2)} - C_{a\bar{4}b}^{(2)} + C_{b\bar{4}a}^{(2)}\right)[\tilde{X}^a, \tilde{X}^b]\right. \\
 & + 2iC_{\mu\nu\rho}\left(C_{ab4}^{(1)} - C_{ab\bar{4}}^{(2)} + C_{a\bar{4}b}^{(2)} + C_{b\bar{4}a}^{(2)}\right)[\tilde{X}^a, \tilde{X}^{b+4}] \\
 & - C_{\mu\nu\rho}\left(C_{ab4}^{(1)} - C_{ab\bar{4}}^{(2)} + C_{a\bar{4}b}^{(2)} - C_{b\bar{4}a}^{(2)}\right)[\tilde{X}^{a+4}, \tilde{X}^{b+4}] \\
 & \left. - 4C_{\mu\nu\rho}C_{a\bar{4}\bar{4}}^{(2)}[\tilde{X}^a, \tilde{X}^4] - 4iC_{\mu\nu\rho}C_{a\bar{4}\bar{4}}^{(2)}[\tilde{X}^{a+4}, \tilde{X}^4]\right).
 \end{aligned} \tag{3.1.17}$$

Similarly, \mathcal{L}_2 becomes

$$\begin{aligned}
 \mathcal{L}_2 = & \frac{3}{20}\mu_2\tilde{\lambda}\varepsilon^{\mu\nu\rho}\text{Tr}\left(C_{\mu\nu\rho}\left(C_{ab4}^{(1)\dagger} - C_{ab\bar{4}}^{(2)\dagger} - C_{a\bar{4}b}^{(2)\dagger} + C_{b\bar{4}a}^{(2)\dagger}\right)[\tilde{X}^a, \tilde{X}^b]\right. \\
 & - 2iC_{\mu\nu\rho}\left(C_{ab4}^{(1)\dagger} - C_{ab\bar{4}}^{(2)\dagger} + C_{a\bar{4}b}^{(2)\dagger} + C_{b\bar{4}a}^{(2)\dagger}\right)[\tilde{X}^a, \tilde{X}^{b+4}] \\
 & - C_{\mu\nu\rho}\left(C_{ab4}^{(1)\dagger} - C_{ab\bar{4}}^{(2)\dagger} + C_{a\bar{4}b}^{(2)\dagger} - C_{b\bar{4}a}^{(2)\dagger}\right)[\tilde{X}^{a+4}, \tilde{X}^{b+4}] \\
 & \left. - 4C_{\mu\nu\rho}C_{a\bar{4}\bar{4}}^{(2)\dagger}[\tilde{X}^a, \tilde{X}^4] + 4iC_{\mu\nu\rho}C_{a\bar{4}\bar{4}}^{(2)\dagger}[\tilde{X}^{a+4}, \tilde{X}^4]\right).
 \end{aligned} \tag{3.1.18}$$

Recall that the type IIA fields, \tilde{C} and \tilde{B} are a combination of the components of the M-theory 3-form, as given at the end of Section 2.4. To see that \mathcal{L}_1 and \mathcal{L}_2 have indeed reduced to the correct terms in the D2-brane action, we can expand the terms in the D2-brane action in terms of the indices a , 4 and $a+4$ where $a = 1, \dots, 3$, and then expand the type IIA fields in terms of the M-theory 3-form components. The algebra is lengthy but straightforward, and the result is that the corresponding terms in the D2-brane action can be written as:

$$\begin{aligned}
 & \frac{\mu_2\tilde{\lambda}}{20}i\varepsilon^{\mu\nu\rho}\text{Tr}\left(\tilde{C}_{\mu\nu\rho}\tilde{B}_{ij}[\tilde{X}^i, \tilde{X}^j]\right) \\
 & = \frac{\mu_2\tilde{\lambda}}{20}i\varepsilon^{\mu\nu\rho}\text{Tr}\left(\tilde{C}_{\mu\nu\rho}\left(\tilde{B}_{ab}[\tilde{X}^a, \tilde{X}^b] + 2\tilde{B}_{a4}[\tilde{X}^a, \tilde{X}^4] + 2\tilde{B}_{ab+4}[\tilde{X}^a, \tilde{X}^{b+4}] \right.\right. \\
 & \quad \left. - 2\tilde{B}_{4a+4}[\tilde{X}^{a+4}, \tilde{X}^4] + \tilde{B}_{a+4b+4}[\tilde{X}^{a+4}, \tilde{X}^{b+4}]\right) \\
 & = -\frac{3}{20}\mu_2\tilde{\lambda}\varepsilon^{\mu\nu\rho}\text{Tr} \\
 & \quad \left(C_{\mu\nu\rho}\left(C_{ab4}^{(1)} - C_{ab\bar{4}}^{(2)} - C_{a\bar{4}b}^{(2)} + C_{b\bar{4}a}^{(2)} - C_{ab4}^{(1)\dagger} + C_{ab\bar{4}}^{(2)\dagger} + C_{a\bar{4}b}^{(2)\dagger} - C_{b\bar{4}a}^{(2)\dagger}\right)[\tilde{X}^a, \tilde{X}^b]\right. \\
 & \quad + 2iC_{\mu\nu\rho}\left(C_{ab4}^{(1)} - C_{ab\bar{4}}^{(2)} + C_{a\bar{4}b}^{(2)} + C_{b\bar{4}a}^{(2)} + C_{ab4}^{(1)\dagger} - C_{ab\bar{4}}^{(2)\dagger} + C_{a\bar{4}b}^{(2)\dagger} + C_{b\bar{4}a}^{(2)\dagger}\right)[\tilde{X}^a, \tilde{X}^{b+4}] \\
 & \quad - C_{\mu\nu\rho}\left(C_{ab4}^{(1)} - C_{ab\bar{4}}^{(2)} + C_{a\bar{4}b}^{(2)} - C_{b\bar{4}a}^{(2)} - C_{ab4}^{(1)\dagger} + C_{ab\bar{4}}^{(2)\dagger} - C_{a\bar{4}b}^{(2)\dagger} + C_{b\bar{4}a}^{(2)\dagger}\right)[\tilde{X}^{a+4}, \tilde{X}^{b+4}] \\
 & \quad \left. - 4C_{\mu\nu\rho}\left(C_{a\bar{4}\bar{4}}^{(2)} - C_{a\bar{4}\bar{4}}^{(2)\dagger}\right)[\tilde{X}^a, \tilde{X}^4] - 4iC_{\mu\nu\rho}\left(C_{a\bar{4}\bar{4}}^{(2)} + C_{a\bar{4}\bar{4}}^{(2)\dagger}\right)[\tilde{X}^{a+4}, \tilde{X}^4] + (\text{c.c.})\right).
 \end{aligned} \tag{3.1.19}$$

The expansion in the final line has used the expressions at the end of Section 2.4. These terms are indeed equal to $\mathcal{L}_1 + \mathcal{L}_2 + (\text{c.c.})$.

Next we will consider the \mathcal{L}_3 and \mathcal{L}_4 terms in the proposed M2-brane action. These mix the worldvolume and SU(4) indices across the components of C . The first of these, \mathcal{L}_3 , reduces as follows:

$$\begin{aligned}
 & \frac{9}{10}\mu_2\tilde{\lambda}\varepsilon^{\mu\nu\rho}\text{Tr} \tag{3.1.20} \\
 & \left(C_{\mu\nu a} \left(C_{\rho 4\bar{b}}^{(1)} + C_{\rho b\bar{4}}^{(1)} - C_{\rho b4}^{(3)} \right) [\tilde{X}^a, \tilde{X}^b] + C_{\mu\nu a} \left(C_{\rho 4\bar{b}}^{(1)} - C_{\rho b\bar{4}}^{(1)} + C_{\rho b4}^{(3)} \right) [\tilde{X}^{a+4}, \tilde{X}^{b+4}] \right. \\
 & + i \left(C_{\mu\nu a} C_{\rho b\bar{4}}^{(1)} - C_{\mu\nu b} C_{\rho a\bar{4}}^{(1)} - C_{\mu\nu a} C_{\rho 4\bar{b}}^{(1)} - C_{\mu\nu b} C_{\rho 4\bar{a}}^{(1)} - C_{\mu\nu a} C_{\rho b4}^{(3)} + C_{\mu\nu b} C_{\rho a4}^{(3)} \right) [\tilde{X}^a, \tilde{X}^{b+4}] \\
 & + 2C_{\mu\nu a} C_{\rho 4\bar{4}}^{(1)} [\tilde{X}^a, \tilde{X}^4] + 2iC_{\mu\nu a} C_{\rho 4\bar{4}}^{(1)} [\tilde{X}^{a+4}, \tilde{X}^4] \\
 & - C_{\mu\nu 4} \left(C_{\rho a\bar{b}}^{(1)} + \frac{1}{2}C_{\rho ab}^{(3)} \right) [\tilde{X}^a, \tilde{X}^b] - iC_{\mu\nu 4} \left(-C_{\rho a\bar{b}}^{(1)} - C_{\rho b\bar{a}}^{(1)} + C_{\rho ab}^{(3)} \right) [\tilde{X}^a, \tilde{X}^{b+4}] \\
 & - C_{\mu\nu 4} \left(C_{\rho a\bar{b}}^{(1)} - \frac{1}{2}C_{\rho ab}^{(3)} \right) [\tilde{X}^{a+4}, \tilde{X}^{b+4}] - 2C_{\mu\nu 4} C_{\rho a\bar{4}}^{(1)} [\tilde{X}^a, \tilde{X}^4] \\
 & \left. - 2iC_{\mu\nu 4} C_{\rho a\bar{4}}^{(1)} [\tilde{X}^{a+4}, \tilde{X}^4] \right).
 \end{aligned}$$

This recovers half of the remaining terms in the D2-brane action, and we will see shortly that \mathcal{L}_4 recovers the other half. The remaining terms in the D2-brane action with no derivatives in equation (3.1.5) are

$$-\frac{3}{10}\mu_2\tilde{\lambda}i\varepsilon^{\mu\nu\rho}\text{Tr}\left(\tilde{C}_{\mu\nu i}\tilde{B}_{\rho j}[\tilde{X}^i, \tilde{X}^j]\right), \tag{3.1.21}$$

and

$$\frac{3}{20}\mu_2\tilde{\lambda}i\varepsilon^{\mu\nu\rho}\text{Tr}\left(\tilde{B}_{\mu\nu}\tilde{C}_{\rho ij}[\tilde{X}^i, \tilde{X}^j]\right). \tag{3.1.22}$$

We can again expand these in terms of the M-theory 3-form components, although we will ignore conjugated coefficients for now. The expansion of these terms is respectively,

$$\begin{aligned}
 & \frac{9}{10}\mu_2\tilde{\lambda}\varepsilon^{\mu\nu\rho}\text{Tr} \tag{3.1.23} \\
 & \left(C_{\mu\nu a} \left(C_{\rho 4\bar{b}}^{(1)} + C_{\rho b\bar{4}}^{(1)} - C_{\rho b4}^{(3)} \right) [\tilde{X}^a, \tilde{X}^b] + C_{\mu\nu a} \left(C_{\rho 4\bar{b}}^{(1)} - C_{\rho b\bar{4}}^{(1)} + C_{\rho b4}^{(3)} \right) [\tilde{X}^{a+4}, \tilde{X}^{b+4}] \right. \\
 & - i \left(C_{\mu\nu a} C_{\rho 4\bar{b}}^{(1)} - C_{\mu\nu a} C_{\rho b\bar{4}}^{(1)} + C_{\mu\nu a} C_{\rho b4}^{(3)} + C_{\mu\nu b} C_{\rho 4\bar{a}}^{(1)} + C_{\mu\nu b} C_{\rho a\bar{4}}^{(1)} - C_{\mu\nu b} C_{\rho a4}^{(3)} \right) [\tilde{X}^a, \tilde{X}^{b+4}] \\
 & + 2C_{\mu\nu a} C_{\rho 4\bar{4}}^{(1)} [\tilde{X}^a, \tilde{X}^4] + 2iC_{\mu\nu a} C_{\rho 4\bar{4}}^{(1)} [\tilde{X}^{a+4}, \tilde{X}^4] \\
 & \left. - C_{\mu\nu 4} \left(C_{\rho 4\bar{a}}^{(1)} + C_{\rho a\bar{4}}^{(1)} - C_{\rho a4}^{(3)} \right) [\tilde{X}^a, \tilde{X}^4] - iC_{\mu\nu 4} \left(-C_{\rho 4\bar{a}}^{(1)} + C_{\rho a\bar{4}}^{(1)} - C_{\rho a4}^{(3)} \right) [\tilde{X}^{a+4}, \tilde{X}^4] \right),
 \end{aligned}$$

and

$$\begin{aligned}
 & \frac{9}{10} \mu_2 \tilde{\lambda} \varepsilon^{\mu\nu\rho} \text{Tr} \tag{3.1.24} \\
 & \left(\frac{1}{2} C_{\mu\nu 4} \left(C_{\rho b \bar{a}}^{(1)} - C_{\rho a \bar{b}}^{(1)} - C_{\rho ab}^{(3)} \right) [\tilde{X}^a, \tilde{X}^b] + i C_{\mu\nu 4} \left(C_{\rho b \bar{a}}^{(1)} + C_{\rho a \bar{b}}^{(1)} - C_{\rho ab}^{(3)} \right) [\tilde{X}^a, \tilde{X}^{b+4}] \right. \\
 & + \frac{1}{2} C_{\mu\nu 4} \left(C_{\rho b \bar{a}}^{(1)} - C_{\rho a \bar{b}}^{(1)} + C_{\rho ab}^{(3)} \right) [\tilde{X}^{a+4}, \tilde{X}^{b+4}] - C_{\mu\nu 4} \left(-C_{\rho 4 \bar{a}}^{(1)} + C_{\rho a \bar{4}}^{(1)} + C_{\rho a 4}^{(3)} \right) [\tilde{X}^a, \tilde{X}^4] \\
 & \left. - i C_{\mu\nu 4} \left(C_{\rho 4 \bar{a}}^{(1)} + C_{\rho a \bar{4}}^{(1)} + C_{\rho a 4}^{(3)} \right) [\tilde{X}^{a+4}, \tilde{X}^4] \right).
 \end{aligned}$$

The terms $C_{\mu\nu 4} \left(C_{\rho 4 \bar{a}}^{(1)} + C_{\rho a \bar{4}}^{(3)} \right) [\tilde{X}^{a+4}, \tilde{X}^4]$ and $C_{\mu\nu 4} \left(C_{\rho 4 \bar{a}}^{(1)} - C_{\rho a \bar{4}}^{(3)} \right) [\tilde{X}^a, \tilde{X}^4]$ cancel and do not appear in the overall action. This is appropriate as they are the only terms which cannot be recovered from the possible couplings in the M2-brane action. Every other term can be matched exactly with \mathcal{L}_3 .

The conjugated terms which we ignored are recovered from \mathcal{L}_4 . The terms in \mathcal{L}_4 are similar to \mathcal{L}_3 , but instead contain one component of C which is conjugated and one which is not. These recover the appropriate terms in the D2-brane action with a similar mixed conjugation structure. We begin by looking at the second term in \mathcal{L}_4 , from equation (3.1.10),

$$\frac{18}{5} \frac{\pi \mu_2 \lambda}{k} \text{Tr} \left(C_{\mu\nu A} C_{\rho BC}^{(3)\dagger} \beta_A^{BC\dagger} \right). \tag{3.1.25}$$

In the reduction this gives the terms

$$\begin{aligned}
 & \frac{9}{10} \mu_2 \tilde{\lambda} \text{Tr} \left(C_{\mu\nu a} C_{\rho b 4}^{(3)\dagger} [\tilde{X}^a, \tilde{X}^b] + C_{\mu\nu a} C_{\rho b 4}^{(3)\dagger} [\tilde{X}^{a+4}, \tilde{X}^{b+4}] \right. \\
 & - i \left(C_{\mu\nu a} C_{\rho b 4}^{(3)\dagger} + C_{\mu\nu b} C_{\rho a 4}^{(3)\dagger} \right) [\tilde{X}^a, \tilde{X}^{b+4}] - \frac{1}{2} C_{\mu\nu 4} C_{\rho ab}^{(3)\dagger} [\tilde{X}^a, \tilde{X}^b] \\
 & + i C_{\mu\nu 4} C_{\rho ab}^{(3)\dagger} [\tilde{X}^a, \tilde{X}^{b+4}] + \frac{1}{2} C_{\mu\nu 4} C_{\rho ab}^{(3)\dagger} [\tilde{X}^{a+4}, \tilde{X}^{b+4}] \\
 & \left. - 2 C_{\mu\nu 4} C_{\rho a 4}^{(3)\dagger} [\tilde{X}^a, \tilde{X}^4] + 2 i C_{\mu\nu 4} C_{\rho a 4}^{(3)\dagger} [\tilde{X}^{a+4}, \tilde{X}^4] \right). \tag{3.1.26}
 \end{aligned}$$

It is straightforward to see that these are exactly the terms that would have appeared in equation (3.1.23) and equation (3.1.24) if we had included the $C^{(3)\dagger}$ from $\tilde{C}_{\mu ij}$ and $\tilde{B}_{\mu i}$.

The remaining term in \mathcal{L}_4 is

$$-\frac{36}{5} \frac{\pi \mu_2 \lambda}{k} \text{Tr} \left(C_{\mu\nu A} C_{\rho C \bar{B}}^{(1)\dagger} \beta_C^{AB} \right). \tag{3.1.27}$$

Whenever $C_{\mu a \bar{b}}^{(1)}$ appears in $\tilde{C}_{\mu ij}$ and $\tilde{B}_{\mu i}$ it always appears alongside its conjugate in the form $-C_{\mu b \bar{a}}^{(1)\dagger}$. Comparing this with the first term of equation (3.1.9) we see that its inclusion in the M2 action will automatically give the correct $C^{(1)\dagger}$ terms in the D2 action.

We have successfully matched all of the terms in the reduction of our proposed extension of the ABJM action to the expected terms in the D2-brane action at the no-derivative level. Mostly this was a straightforward matching of coefficients but we note that it is a non-trivial result that it was possible to match these actions. The relationship between the type IIA fields and the M-theory 3-form was fixed at the linear coupling level but they also appear to be consistent with our extension to quadratic couplings so far. The matching includes the appropriate coefficients and signs of the cross terms, and also leads to a cancellation of the only terms which cannot be recovered from the M2-brane action. We will see similar consistency at the next level, with one derivative, in the next section.

3.1.2 One derivative

Conceptually we will follow the same procedure as before to identify the appropriate quadratic 3-form terms with one derivative in the M2-brane action. However the algebra quickly gets more complicated since we now have an extra SU(4) or SO(7) index in the product of C fields which will triple the number of ways we can split these terms into components with the indices, a , 4, and $a + 4$. There are now also some terms where both of the components of the type IIA fields, \tilde{C} and \tilde{B} , are sums of more than one of the M-theory components, and so give many more cross terms when they are expanded out.

The terms that we must recover in the D2-brane action with one derivative are

$$\begin{aligned} & \frac{3}{2}\mu_2\tilde{\lambda}^2{}_i \text{Tr} \left(\tilde{C}_{[\mu\nu i}\tilde{B}_{jk]}[\tilde{X}^i, \tilde{X}^j]\tilde{D}_\rho\tilde{X}^k \right) \\ &= \frac{3}{20}\mu_2\tilde{\lambda}^2{}_i \text{Tr} \left(\left(2\tilde{C}_{\mu\nu i}\tilde{B}_{jk} + \tilde{C}_{\mu\nu k}\tilde{B}_{ij} + 2\tilde{C}_{\mu ij}\tilde{B}_{\nu k} \right. \right. \\ & \quad \left. \left. - 4\tilde{C}_{\mu ik}\tilde{B}_{\nu j} + \tilde{C}_{ijk}\tilde{B}_{\mu\nu} \right) [\tilde{X}^i, \tilde{X}^j]\tilde{D}_\rho\tilde{X}^k \right). \end{aligned} \quad (3.1.28)$$

To begin with we will consider the terms in the M2-action with the index structure (μ, ν, A) and (B, C, D) ,

$$\begin{aligned} & \frac{54}{5} \frac{\pi\mu_2\lambda^2}{k} \text{Tr} \left(\left(C_{\mu\nu A}C_{BCD}^{(1)} - \frac{1}{3}C_{\mu\nu D}C_{ABC}^{(1)} \right) \gamma^{ABC} D_\rho Z^D \right. \\ & \quad \left. + C_{\mu\nu A}C_{BC\bar{D}}^{(2)} \gamma^{ABC} D_\rho Z^{\dagger\bar{D}} + \left(\frac{2}{3}C_{\mu\nu A}C_{BC\bar{D}}^{(2)} + \frac{1}{3}C_{\mu\nu C}C_{AB\bar{D}}^{(2)} \right) \beta_D^{AB} D_\rho Z^C \right). \end{aligned} \quad (3.1.29)$$

Looking at the index structure, the terms in this piece of the M2-brane action should reduce to the first, second and fifth terms in the D2-brane action in equation (3.1.28).

After the reduction via the novel Higgs mechanism this becomes

$$\begin{aligned}
 & \frac{9}{10}\mu_2\tilde{\lambda}^2 \text{Tr} \left(\left(\frac{1}{2}C_{\mu\nu 4}C_{abc}^{(1)} - C_{\mu\nu a}C_{4bc}^{(1)} - \frac{1}{2}C_{\mu\nu c}C_{ab4}^{(1)} \right) \right. \\
 & \quad \times \left([\tilde{X}^a, \tilde{X}^b] + i[\tilde{X}^{a+4}, \tilde{X}^b] + i[\tilde{X}^a, \tilde{X}^{b+4}] - [\tilde{X}^{a+4}, \tilde{X}^{b+4}] \right) \left(D_\rho\tilde{X}^c + iD_\rho\tilde{X}^{c+4} \right) \\
 & + \left(C_{\mu\nu a}C_{b4\bar{c}}^{(2)} + \frac{1}{2}C_{\mu\nu 4}C_{ab\bar{c}}^{(2)} \right) \\
 & \quad \times \left([\tilde{X}^a, \tilde{X}^b] + i[\tilde{X}^{a+4}, \tilde{X}^b] + i[\tilde{X}^a, \tilde{X}^{b+4}] - [\tilde{X}^{a+4}, \tilde{X}^{b+4}] \right) \left(D_\rho\tilde{X}^c - iD_\rho\tilde{X}^{c+4} \right) \\
 & + \left(C_{\mu\nu a}C_{bc\bar{4}}^{(2)} + \frac{1}{2}C_{\mu\nu c}C_{ab\bar{4}}^{(2)} \right) \\
 & \quad \times \left([\tilde{X}^a, \tilde{X}^b] + i[\tilde{X}^{a+4}, \tilde{X}^b] + i[\tilde{X}^a, \tilde{X}^{b+4}] - [\tilde{X}^{a+4}, \tilde{X}^{b+4}] \right) \left(D_\rho\tilde{X}^c + iD_\rho\tilde{X}^{c+4} \right) \\
 & + \left(C_{\mu\nu a}C_{4c\bar{b}}^{(2)} - C_{\mu\nu 4}C_{ac\bar{b}}^{(2)} + C_{\mu\nu c}C_{a4\bar{b}}^{(2)} \right) \\
 & \quad \times \left([\tilde{X}^a, \tilde{X}^b] + i[\tilde{X}^{a+4}, \tilde{X}^b] - i[\tilde{X}^a, \tilde{X}^{b+4}] + [\tilde{X}^{a+4}, \tilde{X}^{b+4}] \right) \left(D_\rho\tilde{X}^c + iD_\rho\tilde{X}^{c+4} \right) \\
 & + \left(C_{\mu\nu a}C_{4c\bar{4}}^{(2)} - C_{\mu\nu 4}C_{ac\bar{4}}^{(2)} + C_{\mu\nu c}C_{a4\bar{4}}^{(2)} \right) \\
 & \quad \times \left([\tilde{X}^a, \tilde{X}^b] + i[\tilde{X}^{a+4}, \tilde{X}^b] - i[\tilde{X}^a, \tilde{X}^{b+4}] + [\tilde{X}^{a+4}, \tilde{X}^{b+4}] \right) \left(D_\rho\tilde{X}^c + iD_\rho\tilde{X}^{c+4} \right) \\
 & \quad \left. \times \left([\tilde{X}^a, \tilde{X}^4] + i[\tilde{X}^{a+4}, \tilde{X}^4] \right) \left(D_\rho\tilde{X}^c + iD_\rho\tilde{X}^{c+4} \right) \right).
 \end{aligned} \tag{3.1.30}$$

Note that we have ignored the $D_\rho Z^4$ pieces for now.

The quadratic components no longer factorize nicely and comparing this to the expected D2-brane action is harder. We can still proceed by inspection though, and evaluate each term in the D2-brane action in turn. In the lists below, we list the index structure of a term in the D2-brane action and then show its contribution when it is expanded in terms of M-theory 3-form coefficients. These can all then be checked to match with the terms above from the M2-brane action. We won't show the matching of every term explicitly, but we will present enough to hopefully convince the reader that it is possible. The first term in the D2-brane action in equation (3.1.28) has contributions from

$$\tilde{C}_{\mu\nu a}\tilde{B}_{bc} : -\frac{9}{10}\mu_2\tilde{\lambda}^2 C_{\mu\nu a} \left(C_{bc4}^{(1)} - C_{bc\bar{4}}^{(2)} + C_{c4\bar{b}}^{(2)} - C_{b4\bar{c}}^{(2)} \right) [\tilde{X}^a, \tilde{X}^b] \tilde{D}_\rho\tilde{X}^c, \tag{3.1.31}$$

$$\tilde{C}_{\mu\nu a+4}\tilde{B}_{b+4c} : \frac{9}{10}\mu_2\tilde{\lambda}^2 C_{\mu\nu a} \left(C_{bc4}^{(1)} - C_{bc\bar{4}}^{(2)} - C_{c4\bar{b}}^{(2)} - C_{b4\bar{c}}^{(2)} \right) [\tilde{X}^{a+4}, \tilde{X}^{b+4}] \tilde{D}_\rho\tilde{X}^c, \tag{3.1.32}$$

$$\tilde{C}_{\mu\nu a}\tilde{B}_{b+4c} : -\frac{9}{10}i\mu_2\tilde{\lambda}^2 C_{\mu\nu a} \left(C_{bc4}^{(1)} - C_{bc\bar{4}}^{(2)} - C_{c4\bar{b}}^{(2)} - C_{b4\bar{c}}^{(2)} \right) [\tilde{X}^a, \tilde{X}^{b+4}] \tilde{D}_\rho\tilde{X}^c, \tag{3.1.33}$$

$$\tilde{C}_{\mu\nu a+4}\tilde{B}_{bc} : -\frac{9}{10}i\mu_2\tilde{\lambda}^2 C_{\mu\nu a} \left(C_{bc4}^{(1)} - C_{bc\bar{4}}^{(2)} + C_{c4\bar{b}}^{(2)} - C_{b4\bar{c}}^{(2)} \right) [\tilde{X}^{a+4}, \tilde{X}^b] \tilde{D}_\rho\tilde{X}^c, \tag{3.1.34}$$

$$\tilde{C}_{\mu\nu a}\tilde{B}_{bc+4} : -\frac{9}{10}i\mu_2\tilde{\lambda}^2 C_{\mu\nu a} \left(C_{bc4}^{(1)} - C_{bc\bar{4}}^{(2)} + C_{c4\bar{b}}^{(2)} + C_{b4\bar{c}}^{(2)} \right) [\tilde{X}^a, \tilde{X}^b] \tilde{D}_\rho\tilde{X}^{c+4}. \tag{3.1.35}$$

We have not written down $\tilde{C}_{\mu\nu a}\tilde{B}_{b+4c+4}$, $\tilde{C}_{\mu\nu a+4}\tilde{B}_{bc+4}$ or $\tilde{C}_{\mu\nu a+4}\tilde{B}_{b+4c+4}$ here. The second

term has contributions from

$$\tilde{C}_{\mu\nu c}\tilde{B}_{ab}: -\frac{9}{20}\mu_2\tilde{\lambda}^2 C_{\mu\nu c}\left(C_{ab4}^{(1)}-C_{ab\bar{4}}^{(2)}+C_{b4\bar{a}}^{(2)}-C_{a4\bar{b}}^{(2)}\right)[\tilde{X}^a,\tilde{X}^b]\tilde{D}_\rho\tilde{X}^c, \quad (3.1.36)$$

$$\tilde{C}_{\mu\nu c}\tilde{B}_{ab+4}: -\frac{9}{20}i\mu_2\tilde{\lambda}^2 C_{\mu\nu c}\left(C_{ab4}^{(1)}-C_{ab\bar{4}}^{(2)}+C_{b4\bar{a}}^{(2)}+C_{a4\bar{b}}^{(2)}\right)[\tilde{X}^a,\tilde{X}^{b+4}]\tilde{D}_\rho\tilde{X}^c, \quad (3.1.37)$$

$$\tilde{C}_{\mu\nu c}\tilde{B}_{a+4b}: -\frac{9}{20}i\mu_2\tilde{\lambda}^2 C_{\mu\nu c}\left(C_{ab4}^{(1)}-C_{ab\bar{4}}^{(2)}-C_{b4\bar{a}}^{(2)}-C_{a4\bar{b}}^{(2)}\right)[\tilde{X}^{a+4},\tilde{X}^b]\tilde{D}_\rho\tilde{X}^c, \quad (3.1.38)$$

$$\tilde{C}_{\mu\nu c+4}\tilde{B}_{a+4b}: \frac{9}{20}\mu_2\tilde{\lambda}^2 C_{\mu\nu c}\left(C_{ab4}^{(1)}-C_{ab\bar{4}}^{(2)}-C_{b4\bar{a}}^{(2)}-C_{a4\bar{b}}^{(2)}\right)[\tilde{X}^{a+4},\tilde{X}^b]\tilde{D}_\rho\tilde{X}^{c+4}. \quad (3.1.39)$$

The fifth term has contributions from

$$\tilde{C}_{abc}\tilde{B}_{\mu\nu}: -\frac{9}{20}\mu_2\tilde{\lambda}^2\left(C_{abc}^{(1)}+C_{ab\bar{c}}^{(2)}-C_{a\bar{c}b}^{(2)}+C_{b\bar{c}a}^{(2)}\right)C_{\mu\nu 4}[\tilde{X}^a,\tilde{X}^b]\tilde{D}_\rho\tilde{X}^c, \quad (3.1.40)$$

$$\tilde{C}_{a+4bc}\tilde{B}_{\mu\nu}: -\frac{9}{20}i\mu_2\tilde{\lambda}^2\left(C_{abc}^{(1)}+C_{ab\bar{c}}^{(2)}-C_{b\bar{c}a}^{(2)}-C_{a\bar{c}b}^{(2)}\right)C_{\mu\nu 4}[\tilde{X}^{a+4},\tilde{X}^b]\tilde{D}_\rho\tilde{X}^c, \quad (3.1.41)$$

$$\tilde{C}_{ab+4c}\tilde{B}_{\mu\nu}: -\frac{9}{20}i\mu_2\tilde{\lambda}^2\left(C_{abc}^{(1)}+C_{ab\bar{c}}^{(2)}+C_{b\bar{c}a}^{(2)}+C_{a\bar{c}b}^{(2)}\right)C_{\mu\nu 4}[\tilde{X}^a,\tilde{X}^{b+4}]\tilde{D}_\rho\tilde{X}^c, \quad (3.1.42)$$

$$\tilde{C}_{a+4b+4c}\tilde{B}_{\mu\nu}: \frac{9}{20}\mu_2\tilde{\lambda}^2\left(C_{abc}^{(1)}+C_{ab\bar{c}}^{(2)}-C_{b\bar{c}a}^{(2)}+C_{a\bar{c}b}^{(2)}\right)C_{\mu\nu 4}[\tilde{X}^{a+4},\tilde{X}^{b+4}]\tilde{D}_\rho\tilde{X}^c. \quad (3.1.43)$$

These can indeed be identified with the terms in the M2-brane action in equation (3.1.30) if we take into account the anti-symmetrised product between the components of C .

In the reduced M2-brane action in equation (3.1.30) we have ignored contributions from terms involving $D_\rho Z^4$ but we will demonstrate with a few examples that these also match. Consider the following terms which should also be included:

$$\begin{aligned} & \frac{9}{10}\mu_2\tilde{\lambda}^2 \text{Tr} \left(\left(2C_{\mu\nu a}C_{b44}^{(2)} + C_{\mu\nu 4}C_{ab4}^{(2)} \right) \right. \\ & \left. \times \left([\tilde{X}^a, \tilde{X}^b] + i[\tilde{X}^{a+4}, \tilde{X}^b] + i[\tilde{X}^a, \tilde{X}^{b+4}] - [\tilde{X}^{a+4}, \tilde{X}^{b+4}] \right) \tilde{D}_\rho\tilde{X}^4 \right). \end{aligned} \quad (3.1.44)$$

If we expand out the terms in the D2-brane action in equation (3.1.28) where one of the indices is 4 we see that they are indeed recovered from these terms in the reduced M2-brane action. For example, we have the following terms with only one 4 index in the D2-brane action:

$$\tilde{C}_{\mu\nu a}\tilde{B}_{b4}: \frac{9}{5}\mu_2\tilde{\lambda}^2 C_{\mu\nu a}C_{b44}^{(2)}[\tilde{X}^a,\tilde{X}^b]\tilde{D}_\rho\tilde{X}^4, \quad (3.1.45)$$

$$\tilde{C}_{\mu\nu a}\tilde{B}_{b+44}: \frac{9}{5}\mu_2\tilde{\lambda}^2 iC_{\mu\nu a}C_{b44}^{(2)}[\tilde{X}^a,\tilde{X}^{b+4}]\tilde{D}_\rho\tilde{X}^4, \quad (3.1.46)$$

$$\tilde{C}_{\mu\nu a+4}\tilde{B}_{b4}: \frac{9}{5}\mu_2\tilde{\lambda}^2 iC_{\mu\nu a}C_{b44}^{(2)}[\tilde{X}^{a+4},\tilde{X}^b]\tilde{D}_\rho\tilde{X}^4, \quad (3.1.47)$$

$$\tilde{C}_{\mu\nu a+4}\tilde{B}_{b+44}: -\frac{9}{5}\mu_2\tilde{\lambda}^2 C_{\mu\nu a}C_{b44}^{(2)}[\tilde{X}^{a+4},\tilde{X}^{b+4}]\tilde{D}_\rho\tilde{X}^4, \quad (3.1.48)$$

which are all recovered in the reduced M2-brane action terms in equation (3.1.44).

From the second and fifth term in the D2-brane action in equation (3.1.28) we once

again have some appropriate cancellations that remove fields which cannot appear in the reduction of our M2-brane action,

$$\begin{aligned}
 & \tilde{C}_{\mu\nu 4} \tilde{B}_{ab} + \tilde{C}_{ab 4} \tilde{B}_{\mu\nu} : \\
 & - \frac{9}{20} \mu_2 \tilde{\lambda}^2 \left(C_{\mu\nu 4} \left(C_{ab4}^{(1)} - C_{ab4}^{(2)} + C_{b4a}^{(2)} - C_{a4b}^{(2)} \right) [\tilde{X}^a, \tilde{X}^b] \tilde{D}_\rho \tilde{X}^4 \right. \\
 & \quad \left. + \left(C_{ab4}^{(1)} + C_{ab4}^{(2)} + C_{b4a}^{(2)} - C_{a4b}^{(2)} \right) C_{\mu\nu 4} [X^a, X^b] \tilde{D}_\rho X^4 \right) \\
 & = \frac{9}{10} \mu_2 \tilde{\lambda}^2 C_{\mu\nu 4} C_{ab4}^{(2)} [\tilde{X}^a, \tilde{X}^b] \tilde{D}_\rho \tilde{X}^4.
 \end{aligned} \tag{3.1.49}$$

The remaining term is expected in the reduced M2-brane action terms in equation (3.1.44).

There are no $C_{\mu\nu 4} C_{i44}^{(2)}$ terms remaining in equation (3.1.44) from the $D_\rho Z^4$ terms in the M2-brane action. This is appropriate since we see that the corresponding terms involving $C_{\mu\nu 4} \tilde{B}_{i4}$ in the D2-brane action will also cancel with each other. Explicitly, the terms of this form which arise from

$$\left(2\tilde{C}_{\mu\nu i} \tilde{B}_{jk} + \tilde{C}_{\mu\nu k} \tilde{B}_{ij} \right) [\tilde{X}^i, \tilde{X}^j] \tilde{D}_\rho \tilde{X}^k \tag{3.1.50}$$

are

$$\left(-2\tilde{C}_{\mu\nu 4} \tilde{B}_{i4} + 2\tilde{C}_{\mu\nu 4} \tilde{B}_{i4} \right) [\tilde{X}^i, \tilde{X}^4] \tilde{D}_\rho \tilde{X}^4 = 0. \tag{3.1.51}$$

So far we have shown that our proposed M2-brane couplings in equation (3.1.29) will recover the first, second and fifth term of the D2-brane action at the one-derivative level, as in equation (3.1.28). Next we will look at how to recover the third and fourth terms in the D2-brane action. These are more complicated because both the \tilde{C} and \tilde{B} fields are a sum of multiple components of the M-theory 3-form and their expansion introduces many cross terms. Considering only a few of the total components, these terms give us the following expression, where the daggered terms (d.t.) are either

identical or come with a sign change compared to their equivalent undaggered terms:

$$\begin{aligned}
 & \frac{3}{20}\mu_2\tilde{\lambda}^2 i \operatorname{Tr} \left(\left(2\tilde{C}_{\mu ij}\tilde{B}_{\mu k} - 4\tilde{C}_{\mu ik}\tilde{B}_{\nu j} \right) [\tilde{X}^i, \tilde{X}^j]\tilde{D}_\rho\tilde{X}^k \right) \\
 & = -\frac{9}{10}\mu_2\tilde{\lambda}^2 \operatorname{Tr} \\
 & \quad \left[\left(\left(C_{\mu a\bar{b}}^{(1)} - C_{\mu\bar{b}a}^{(1)} + C_{\mu ab}^{(3)} + (\text{d.t.}) \right) \left(C_{\nu 4\bar{c}}^{(1)} + C_{\nu c\bar{4}}^{(1)} - C_{\nu c4}^{(3)} - (\text{d.t.}) \right) \right. \right. \\
 & \quad \left. \left. - 2 \left(C_{\mu a\bar{c}}^{(1)} - C_{\mu\bar{c}a}^{(1)} + C_{\mu ac}^{(3)} + (\text{d.t.}) \right) \left(C_{\nu 4\bar{b}}^{(1)} + C_{\nu b\bar{4}}^{(1)} - C_{\nu b4}^{(3)} - (\text{d.t.}) \right) \right) \right. \\
 & \quad \left. \times [\tilde{X}^a, \tilde{X}^b]\tilde{D}_\rho\tilde{X}^c \right. \\
 & \quad + \left(2 \left(-C_{\mu a\bar{b}}^{(1)} - C_{\mu\bar{b}a}^{(1)} + C_{\mu ab}^{(3)} - (\text{d.t.}) \right) \left(C_{\nu 4\bar{c}}^{(1)} + C_{\nu c\bar{4}}^{(1)} - C_{\nu c4}^{(3)} - (\text{d.t.}) \right) \right. \\
 & \quad + 2 \left(C_{\mu a\bar{c}}^{(1)} - C_{\mu\bar{c}a}^{(1)} + C_{\mu ac}^{(3)} + (\text{d.t.}) \right) \left(C_{\nu 4\bar{b}}^{(1)} - C_{\nu b\bar{4}}^{(1)} + C_{\nu b4}^{(3)} + (\text{d.t.}) \right) \\
 & \quad \left. + 2 \left(C_{\mu b\bar{c}}^{(1)} + C_{\mu\bar{c}b}^{(1)} + C_{\mu bc}^{(3)} - (\text{d.t.}) \right) \left(C_{\mu 4\bar{a}}^{(1)} + C_{\mu a\bar{4}}^{(1)} - C_{\mu a4}^{(3)} - (\text{d.t.}) \right) \right) \\
 & \quad \left. \times i[\tilde{X}^a, \tilde{X}^{b+4}]\tilde{D}_\rho\tilde{X}^c \right] + \dots
 \end{aligned} \tag{3.1.52}$$

We have not expanded this expression fully, but we have gone far enough to fix the coefficients of the appropriate terms in the M2-brane action. The pieces mixing $C^{(1)}$ and $C^{(3)}$ can be recovered from the following M2-brane action couplings:

$$-\frac{108}{5} \frac{\pi\mu_2\lambda^2}{k} \operatorname{Tr} \left(C_{\mu[AB]}^{(3)} C_{\nu|C|\bar{D}}^{(1)} \beta_D^{BC} D_\rho Z^A \right), \tag{3.1.53}$$

and

$$-\frac{108}{5} \frac{\pi\mu_2\lambda^2}{k} \operatorname{Tr} \left(C_{\mu AB}^{(3)} C_{\nu C\bar{D}}^{(1)} \gamma^{ABC} D_\rho Z_D^\dagger \right). \tag{3.1.54}$$

In the reduction, these become respectively

$$\begin{aligned}
 & -\frac{9}{5}\mu_2\tilde{\lambda}^2 \operatorname{Tr} \left(\left(-C_{\mu a\bar{b}}^{(1)} C_{\nu c4}^{(3)} - C_{\mu ac}^{(3)} C_{\nu 4\bar{b}}^{(1)} + C_{\mu c\bar{b}}^{(1)} C_{\nu a4}^{(3)} \right) \right. \\
 & \quad \times \left([\tilde{X}^a, \tilde{X}^b] + i[\tilde{X}^{a+4}, \tilde{X}^b] - i[\tilde{X}^a, \tilde{X}^{b+4}] + [\tilde{X}^{a+4}, \tilde{X}^{b+4}] \right) \left(\tilde{D}_\rho\tilde{X}^c + i\tilde{D}_\rho\tilde{X}^{c+4} \right) \\
 & \quad + \left(-C_{\mu ac}^{(3)} C_{\nu b\bar{4}}^{(1)} + \frac{1}{2} C_{\mu ab}^{(3)} C_{\nu c\bar{4}}^{(1)} \right) \\
 & \quad \times \left([\tilde{X}^a, \tilde{X}^b] + i[\tilde{X}^{a+4}, \tilde{X}^b] + i[\tilde{X}^a, \tilde{X}^{b+4}] - [\tilde{X}^{a+4}, \tilde{X}^{b+4}] \right) \left(\tilde{D}_\rho\tilde{X}^c + i\tilde{D}_\rho\tilde{X}^{c+4} \right) \\
 & \quad + 2 \left(-C_{\mu c4}^{(3)} C_{\nu a\bar{4}}^{(1)} - C_{\mu ac}^{(3)} C_{\nu 4\bar{4}}^{(1)} + C_{\mu a4}^{(3)} C_{\nu c\bar{4}}^{(1)} \right) \\
 & \quad \left. \times \left([\tilde{X}^a, \tilde{X}^4] + i[\tilde{X}^{a+4}, \tilde{X}^4] \right) \left(\tilde{D}_\rho\tilde{X}^c + i\tilde{D}_\rho\tilde{X}^{c+4} \right) \right),
 \end{aligned} \tag{3.1.55}$$

and

$$\begin{aligned}
 & -\frac{9}{10}\mu_2\tilde{\lambda}^2 \text{Tr} \left(\left(-2C_{\mu\bar{b}\bar{c}}^{(1)}C_{\nu a\bar{4}}^{(3)} + C_{\mu\bar{a}\bar{b}}^{(3)}C_{\nu\bar{4}\bar{c}}^{(1)} \right) \right. \\
 & \quad \left. \times \left([\tilde{X}^a, \tilde{X}^b] + i[\tilde{X}^{a+4}, \tilde{X}^b] + i[\tilde{X}^a, \tilde{X}^{b+4}] - [\tilde{X}^{a+4}, \tilde{X}^{b+4}] \right) \left(\tilde{D}_\rho\tilde{X}^c - i\tilde{D}_\rho\tilde{X}^{c+4} \right) \right). \tag{3.1.56}
 \end{aligned}$$

These can be identified with the appropriate terms in the D2-brane action in equation (3.1.52) assuming once again that the product of the M-theory 3-form components is anti-symmetric.

The quadratic $C^{(1)}$ pieces can be recovered from the following terms in the M2 action:

$$-\frac{72}{5}\frac{\pi\mu_2\lambda^2}{k} \text{Tr} \left(C_{\mu\bar{A}\bar{B}}^{(1)}C_{\nu\bar{C}\bar{D}}^{(1)}\beta_B^{AC}D_\rho Z_D^\dagger + C_{\mu\bar{A}\bar{B}}^{(1)}C_{\nu\bar{C}\bar{D}}^{(1)}\beta_A^{BD\dagger}D_\rho Z^C \right), \tag{3.1.57}$$

which in the reduction becomes

$$\begin{aligned}
 & -\frac{9}{5}\mu_2\tilde{\lambda}^2 \text{Tr} \left(\left(C_{\mu\bar{a}\bar{b}}^{(1)}C_{\nu\bar{4}\bar{c}}^{(1)} - C_{\mu\bar{a}\bar{c}}^{(1)}C_{\nu\bar{4}\bar{b}}^{(1)} \right) \right. \\
 & \quad \times \left([\tilde{X}^a, \tilde{X}^b] + i[\tilde{X}^{a+4}, \tilde{X}^b] - i[\tilde{X}^a, \tilde{X}^{b+4}] + [\tilde{X}^{a+4}, \tilde{X}^{b+4}] \right) \left(\tilde{D}_\rho\tilde{X}^c - i\tilde{D}_\rho\tilde{X}^{c+4} \right) \\
 & \quad + C_{\mu\bar{b}\bar{c}}^{(1)}C_{\nu\bar{a}\bar{4}}^{(1)} \\
 & \quad \times \left([\tilde{X}^a, \tilde{X}^b] + i[\tilde{X}^{a+4}, \tilde{X}^b] + i[\tilde{X}^a, \tilde{X}^{b+4}] - [\tilde{X}^{a+4}, \tilde{X}^{b+4}] \right) \left(\tilde{D}_\rho\tilde{X}^c - i\tilde{D}_\rho\tilde{X}^{c+4} \right) \\
 & \quad - \left(C_{\mu\bar{b}\bar{a}}^{(1)}C_{\nu\bar{c}\bar{4}}^{(1)} - C_{\mu\bar{c}\bar{a}}^{(1)}C_{\nu\bar{b}\bar{4}}^{(1)} \right) \\
 & \quad \times \left([\tilde{X}^a, \tilde{X}^b] - i[\tilde{X}^{a+4}, \tilde{X}^b] + i[\tilde{X}^a, \tilde{X}^{b+4}] + [\tilde{X}^{a+4}, \tilde{X}^{b+4}] \right) \left(\tilde{D}_\rho\tilde{X}^c + i\tilde{D}_\rho\tilde{X}^{c+4} \right) \\
 & \quad - C_{\mu\bar{c}\bar{b}}^{(1)}C_{\nu\bar{4}\bar{a}}^{(1)} \\
 & \quad \times \left([\tilde{X}^a, \tilde{X}^b] - i[\tilde{X}^{a+4}, \tilde{X}^b] - i[\tilde{X}^a, \tilde{X}^{b+4}] - [\tilde{X}^{a+4}, \tilde{X}^{b+4}] \right) \left(\tilde{D}_\rho\tilde{X}^c + i\tilde{D}_\rho\tilde{X}^{c+4} \right). \tag{3.1.58}
 \end{aligned}$$

The terms involving multiple $C^{(3)}$ terms can be recovered from the following extension to the M2-brane action:

$$\frac{108}{5}\frac{\pi\mu_2\lambda^2}{k} \text{Tr} \left(C_{\mu\bar{A}\bar{B}}^{(3)}C_{\nu\bar{C}\bar{D}}^{(3)}\gamma^{ABC}D_\rho Z^D \right), \tag{3.1.59}$$

which reduces to

$$\begin{aligned}
 & -\frac{9}{10}\mu_2\tilde{\lambda}^2 \text{Tr} \left(\left(C_{\mu\bar{a}\bar{b}}^{(3)}C_{\nu\bar{c}\bar{4}}^{(3)} + 2C_{\mu\bar{b}\bar{c}}^{(3)}C_{\nu\bar{a}\bar{4}}^{(3)} \right) \right. \\
 & \quad \left. \times \left([\tilde{X}^a, \tilde{X}^b] + i[\tilde{X}^{a+4}, \tilde{X}^b] + i[\tilde{X}^a, \tilde{X}^{b+4}] - [\tilde{X}^{a+4}, \tilde{X}^{b+4}] \right) \left(\tilde{D}_\rho\tilde{X}^c + i\tilde{D}_\rho\tilde{X}^{c+4} \right) \right). \tag{3.1.60}
 \end{aligned}$$

Finally, to obtain the terms with mixed conjugation, we must include the following

terms in the M2-brane action:

$$\frac{108}{5} \frac{\pi \mu_2 \lambda^2}{k} \text{Tr} \left(C_{\mu AB}^{(3)\dagger} C_{\nu CD}^{(1)} \gamma^{ABD\dagger} D_\rho Z^C \right), \quad (3.1.61)$$

$$\frac{36}{5} \frac{\pi \mu_2 \lambda^2}{k} \text{Tr} \left(C_{\mu AB}^{(3)\dagger} C_{\nu CD}^{(1)} \beta_C^{AB\dagger} D_\rho Z^D \right), \quad (3.1.62)$$

and

$$\frac{36}{5} \frac{\pi \mu_2 \lambda^2}{k} \text{Tr} \left(C_{\mu AB}^{(3)\dagger} C_{\nu CD}^{(3)} \beta_A^{CD} D_\rho Z_B^\dagger \right). \quad (3.1.63)$$

These reduce respectively to

$$\begin{aligned} & \frac{9}{10} \mu_2 \tilde{\lambda}^2 \text{Tr} \left(\left(2C_{\mu\bar{c}b}^{(1)} C_{\nu a4}^{(3)\dagger} - C_{\mu ab}^{(3)\dagger} C_{\nu\bar{c}4}^{(1)} \right) \right. \\ & \quad \left. \times \left([\tilde{X}^a, \tilde{X}^b] - i[\tilde{X}^{a+4}, \tilde{X}^b] - i[\tilde{X}^a, \tilde{X}^{b+4}] - [\tilde{X}^{a+4}, \tilde{X}^{b+4}] \right) \left(\tilde{D}_\rho \tilde{X}^c + i\tilde{D}_\rho \tilde{X}^{c+4} \right) \right), \end{aligned} \quad (3.1.64)$$

and

$$\begin{aligned} & \frac{9}{10} \mu_2 \tilde{\lambda}^2 \text{Tr} \left(-C_{\mu ab}^{(3)\dagger} C_{\nu 4\bar{c}}^{(1)} \right. \\ & \quad \times \left([\tilde{X}^a, \tilde{X}^b] - i[\tilde{X}^{a+4}, \tilde{X}^b] - i[\tilde{X}^a, \tilde{X}^{b+4}] - [\tilde{X}^{a+4}, \tilde{X}^{b+4}] \right) \left(\tilde{D}_\rho \tilde{X}^c + i\tilde{D}_\rho \tilde{X}^{c+4} \right) \\ & \quad - 2C_{\mu\bar{b}c}^{(1)} C_{\nu a4}^{(3)\dagger} \\ & \quad \left. \times \left([\tilde{X}^a, \tilde{X}^b] - i[\tilde{X}^{a+4}, \tilde{X}^b] + i[\tilde{X}^a, \tilde{X}^{b+4}] + [\tilde{X}^{a+4}, \tilde{X}^{b+4}] \right) \left(\tilde{D}_\rho \tilde{X}^c + i\tilde{D}_\rho \tilde{X}^{c+4} \right) \right), \end{aligned} \quad (3.1.65)$$

and

$$\begin{aligned} & \frac{9}{10} \mu_2 \tilde{\lambda}^2 \text{Tr} \left(2C_{\mu\bar{b}c}^{(3)\dagger} C_{\nu a4}^{(3)} \right. \\ & \quad \times \left([\tilde{X}^a, \tilde{X}^b] + i[\tilde{X}^{a+4}, \tilde{X}^b] - i[\tilde{X}^a, \tilde{X}^{b+4}] + [\tilde{X}^{a+4}, \tilde{X}^{b+4}] \right) \left(\tilde{D}_\rho \tilde{X}^c + i\tilde{D}_\rho \tilde{X}^{c+4} \right) \\ & \quad + C_{\mu ab}^{(3)} C_{\nu 4\bar{c}}^{(3)\dagger} \\ & \quad \left. \times \left([\tilde{X}^a, \tilde{X}^b] + i[\tilde{X}^{a+4}, \tilde{X}^b] + i[\tilde{X}^a, \tilde{X}^{b+4}] - [\tilde{X}^{a+4}, \tilde{X}^{b+4}] \right) \left(\tilde{D}_\rho \tilde{X}^c + i\tilde{D}_\rho \tilde{X}^{c+4} \right) \right). \end{aligned} \quad (3.1.66)$$

These can all be identified with the known terms in the D2-brane action given in equation (3.1.52).

Combining all of the terms considered so far with no derivatives and one derivative, we have identified the following additional couplings at quadratic order in the

background fields:

$$\begin{aligned}
 S = \frac{6}{5} \frac{\pi \mu_2 \lambda}{k} \int \varepsilon^{\mu\nu\rho} \text{Tr} & \left(-C_{\mu\nu\rho} C_{ABC}^{(1)} \gamma^{ABC} + C_{\mu\nu\rho} C_{ABC}^{(2)} \beta_C^{AB} \right. \\
 & - C_{\mu\nu\rho} C_{ABC}^{(1)\dagger} \gamma^{ABC\dagger} + C_{\mu\nu\rho} C_{ABC}^{(2)\dagger} \beta_C^{AB\dagger} \\
 & + 3 \left(2C_{\mu\nu A} C_{\rho BC}^{(1)} \beta_C^{AB} + 3C_{\mu\nu A} C_{\rho BC}^{(3)} \gamma^{ABC} - 2C_{\mu\nu A} C_{\rho C\bar{B}}^{(1)\dagger} \beta_C^{AB} + C_{\mu\nu A} C_{\rho BC}^{(3)\dagger} \beta_A^{BC\dagger} \right) \\
 & + 3\lambda \left(3C_{\mu\nu A} C_{BCD}^{(1)} \gamma^{ABC} D_\rho Z^D - C_{\mu\nu D} C_{ABC}^{(1)} \gamma^{ABC} D_\rho Z^D \right. \\
 & \quad + 3C_{\mu\nu A} C_{BC\bar{D}}^{(2)} \gamma^{ABC} D_\rho Z_D^\dagger + 2C_{\mu\nu A} C_{BC\bar{D}}^{(2)} \beta_D^{AB} D_\rho Z^C + C_{\mu\nu C} C_{AB\bar{D}}^{(2)} \beta_D^{AB} D_\rho Z^C \Big) \\
 & + 6\lambda \left(-2C_{\mu\bar{A}B}^{(1)} C_{\nu C\bar{D}}^{(1)} \beta_B^{AC} D_\rho Z_D^\dagger - 2C_{\mu\bar{A}B}^{(1)} C_{\nu C\bar{D}}^{(1)} \beta_A^{BD\dagger} D_\rho Z^C \right. \\
 & \quad - 2C_{\mu\bar{A}B}^{(3)} C_{\nu C\bar{D}}^{(1)} \beta_D^{BC} D_\rho Z^A - C_{\mu\bar{B}C}^{(3)} C_{\nu A\bar{D}}^{(1)} \beta_D^{BC} D_\rho Z^A - 3C_{\mu\bar{A}B}^{(3)} C_{\nu C\bar{D}}^{(1)} \gamma^{ABC} D_\rho Z_D^\dagger \\
 & \quad + 3C_{\mu\bar{A}B}^{(3)} C_{\nu C\bar{D}}^{(3)} \gamma^{ABC} D_\rho Z^D + 3C_{\mu\bar{A}B}^{(3)\dagger} C_{\nu C\bar{D}}^{(1)} \gamma^{ABD\dagger} D_\rho Z^C \\
 & \quad \left. \left. + C_{\mu\bar{A}B}^{(3)\dagger} C_{\nu C\bar{D}}^{(1)} \beta_C^{AB\dagger} D_\rho Z^D + C_{\mu\bar{A}B}^{(3)\dagger} C_{\nu C\bar{D}}^{(3)} \beta_A^{CD} D_\rho Z_B^\dagger \right) \right). \tag{3.1.67}
 \end{aligned}$$

Unfortunately the algebra has grown too complex to continue this identification to the two- and three-derivative terms, however we have shown evidence that this matching would be possible if we could fix the correct coefficients.

3.2 Pull-backs with $U(N) \times U(N)$ gauge invariance

In this section we will see how the extensions to the ABJM action with a broken gauge symmetry may be lifted to the full action with an unbroken $U(N) \times U(N)$ symmetry.

We have seen in Chapter 2 that the trace of the usual matrix product does not provide enough degrees of freedom in the 3-form to recover all of the independent components of the type IIA 3-form and the Kalb-Ramond field. To recover all of the necessary components, we must include couplings which are not gauge invariant with the usual trace, such as $\text{Tr}(C_{\mu AB} D_\nu Z^A D_\rho Z^B)$. These can be included in a gauge invariant way by using a generalised trace, $\{\text{Tr}\}$, in which the coefficients of the 3-form are taken to have a more general index structure than $N \times N$ matrices, so that they couple in the most general gauge invariant way possible [52],

$$\{\text{Tr}\}(C_{\mu\nu A} D_\rho Z^A) = (C_{\mu\nu A})_{\hat{a}}^{\hat{a}} (D_\rho Z^A)_{\hat{a}}^{\hat{a}}, \tag{3.2.1}$$

$$\{\text{Tr}\}(C_{\mu AB} D_\nu Z^A D_\rho Z^B) = (C_{\mu AB})_{ab}^{\hat{a}\hat{b}} (D_\nu Z^A)_{\hat{a}}^{\hat{a}} (D_\rho Z^B)_{\hat{b}}^{\hat{b}}, \tag{3.2.2}$$

$$\{\text{Tr}\}(C_{\mu A\bar{B}} D_\nu Z^A D_\rho Z_B^\dagger) = (C_{\mu A\bar{B}})_{\hat{a}\hat{b}}^{\hat{a}\hat{b}} (D_\nu Z^A)_{\hat{a}}^{\hat{a}} (D_\rho Z_B^\dagger)_{\hat{b}}^{\hat{b}}, \tag{3.2.3}$$

$$\{\text{Tr}\}(C_{ABC} D_\nu Z^A D_\mu Z^B D_\rho Z^C) = (C_{ABC})_{abc}^{\hat{a}\hat{b}\hat{c}} (D_\mu Z^A)_{\hat{a}}^{\hat{a}} (D_\nu Z^B)_{\hat{b}}^{\hat{b}} (D_\rho Z^C)_{\hat{c}}^{\hat{c}}, \tag{3.2.4}$$

$$\{\text{Tr}\}(C_{A\bar{B}\bar{C}} D_\nu Z^A D_\mu Z^B D_\rho Z_C^\dagger) = (C_{A\bar{B}\bar{C}})_{\hat{a}\hat{b}\hat{c}}^{\hat{a}\hat{b}\hat{c}} (D_\mu Z^A)_{\hat{a}}^{\hat{a}} (D_\nu Z^B)_{\hat{b}}^{\hat{b}} (D_\rho Z_C^\dagger)_{\hat{c}}^{\hat{c}}. \tag{3.2.5}$$

The 3-form coefficients must be functionals of the transverse matrix coordinates, $Z^A(x)$ and $Z_A^\dagger(x)$, as well as having a dependence on the world-volume coordinates, x^μ . They can be defined by a Taylor expansion in the transverse directions, although only certain products of the matrix coordinates are permissible due to the gauge index structure, for example,

$$(C_{\mu A \bar{B}})_{\hat{a} \hat{b}} = \delta_a^b \delta_{\hat{b}}^{\hat{a}} C_{\mu A \bar{B}}^{(0)} + (Z_C^\dagger Z^D)_{\hat{b}}^{\hat{a}} \delta_a^b C_{\mu A \bar{B}, \bar{C} D}^{(2,1)} + (Z^C Z_D^\dagger)_{\hat{b}}^{\hat{a}} \delta_a^b C_{\mu A \bar{B}, \bar{C} D}^{(2,2)} + \dots \quad (3.2.6)$$

and

$$(C_{\mu AB})_{\hat{a} \hat{b}} = (Z_C^\dagger)_{\hat{b}}^{\hat{a}} (Z_D^\dagger)_{\hat{a}}^{\hat{b}} C_{\mu AB, \bar{C} \bar{D}}^{(2)} + \dots \quad (3.2.7)$$

Each of the terms in these Taylor expansions will expand into a product of regular traces upon substitution into $\{\text{Tr}\}$. The reduction to D2-branes preserves the trace structure, but the D-brane action must only contain single trace terms [53, 54], not products of traces. This greatly restricts the possible terms, and terms like the following are disallowed as they would split into two traces:

$$(Z^A)_{\hat{a}}^{\hat{a}} (Z_B^\dagger)_{\hat{b}}^{\hat{b}} C_{\mu A \bar{B}, \bar{C} \bar{D}}^{(2,3)}. \quad (3.2.8)$$

The fact that these expansions have no terms which are linear in Z^A or Z_A^\dagger is consistent with a background of a $\mathbb{C}^4/\mathbb{Z}_k$ orbifold. The orbifold action is

$$z^A \rightarrow e^{2\pi i/k} z^A, \quad \bar{z}^A \rightarrow e^{-2\pi i/k} \bar{z}^A, \quad (3.2.9)$$

with the indices A and \bar{A} of the space-time 3-form transforming appropriately. If the 3-form is to be invariant under this orbifold action then the orders of the allowed terms in its expansion in terms of z^A and \bar{z}^A are identical to the orders of the allowed terms in the world-volume pullback of the components of the 3-form in terms of Z^A and Z_A^\dagger .

In this chapter and the previous chapter we found the couplings of the 3-form to the ABJM action that must be recovered from this generalised trace when the gauge symmetry is broken to the diagonal $U(N)$. However, there are some previously unmentioned subtleties which we would now like to address. In the linear 3-form couplings with broken symmetry, in equation (2.4.12), the following terms are included,

$$\text{Tr} \left(C_{\mu AB}^{(3)} D_\nu Z^A D_\rho Z^B \right), \quad (3.2.10)$$

and

$$\text{Tr} \left(C_{ABC}^{(3)} D_\mu Z^A D_\nu Z^B D_\nu Z^B \right). \quad (3.2.11)$$

However, there is no way that these terms could appear with this ordering in the

unbroken action with $U(N) \times U(N)$ gauge symmetry and still be gauge invariant. Instead, the individual Z and Z^\dagger terms in the Taylor series of $C_{\mu AB}$ and C_{ABC} must be interspersed with the derivative terms rather than being grouped together at the front. This is best illustrated with an example, so let us consider the Taylor expansion of the generalised trace of $C_{\mu AB}$. This is

$$\begin{aligned} & \{\text{Tr}\} \left(C_{\mu AB} D_\nu Z^A D_\rho Z^B \right) \\ &= \text{Tr} \left(C_{\mu AB, \bar{C}\bar{D}}^{(2)} D_\nu Z^A Z_C^\dagger D_\rho Z^B Z_D^\dagger \right. \\ & \quad \left. + C_{\mu AB, \bar{C}\bar{D}\bar{E}\bar{F}}^{(4)} D_\nu Z^A Z_C^\dagger Z^D Z_E^\dagger D_\rho Z^B Z_F^\dagger + \dots \right), \end{aligned} \quad (3.2.12)$$

and we see that the definition of the C field in terms of its Taylor expansion cannot be considered as a single term in the trace which can be grouped at the front.

This does not significantly affect our analysis of these two chapters since the coefficients are still identical and the reduction procedure happens in the same way. The difference is that the ordered trace must be replaced with the appropriate generalised trace where the 3-form expansion is mixed with the other terms in a gauge invariant manner.

Recall that in the Myers-Chern-Simons term in the D2-brane action, the trace is the symmetrised trace, where all X , $[X, X]$ and F terms are symmetrised. Due to this symmetrised trace, there are many mixed terms, as in the extended ABJM action. However, not all of the orderings of the symmetrised terms are recovered from the ABJM action. For example, in the ABJM action, the terms at quadratic order in Z in the Taylor expansion of the 3-form with transverse indices are:

$$\begin{aligned} & \text{Tr} \left(C_{\mu AB, \bar{C}\bar{D}}^{(2,1)} Z^C Z_D^\dagger (D_\nu Z^A) (D_\rho Z_B^\dagger) + C_{\mu AB, \bar{C}\bar{D}}^{(2,2)} (D_\nu Z^A) Z_C^\dagger Z^D (D_\rho Z_B^\dagger) \right. \\ & \quad \left. + C_{\mu AB, \bar{C}\bar{D}}^{(2)} (D_\nu Z^A) Z_C^\dagger (D_\rho Z^B) Z_D^\dagger \right), \end{aligned} \quad (3.2.13)$$

which reduces to

$$\begin{aligned} & \text{Tr} \left(C_{\mu ab, \bar{c}\bar{d}}^{(2,1)} X^c X^d (D_\nu X^a) (D_\rho X^b) + C_{\mu ab, \bar{c}\bar{d}}^{(2,2)} (D_\nu X^a) X^c X^d (D_\rho X^b) \right. \\ & \quad \left. + C_{\mu ab, \bar{c}\bar{d}}^{(2)} (D_\nu X^a) X^c (D_\rho X^b) X^d + \dots \right). \end{aligned} \quad (3.2.14)$$

If the trace were symmetrised then we could pull out the 3-form coefficients from the expansion of $C_{\mu AB}$ and $C_{\mu A\bar{B}}$ into an overall factor which we identified with $\tilde{C}_{\mu ab}$ as before. However, it is not clear how to impose the required symmetrised trace in the ABJM action that would reduce to the symmetrised trace on the D2-brane.

3.3 Discussion and conclusions

In this chapter we have identified couplings in the M2-brane action which partially recover the terms making up the full $\tilde{C} \wedge \tilde{B}$ part of the D2-brane action. Due to the growth in the number of terms with each additional derivative it is infeasible to match the two actions fully at quadratic order using the brute force method of expanding and comparing that we have used above. However, there is significant evidence that it is in principle possible to recover all of the terms in the $\tilde{C} \wedge \tilde{B}$ piece of the D2-brane action via a similar extension to two- and three-derivative terms, once the coefficients have been fixed by comparison to the D2-brane action.

The explicit identifications shown above have required a number of unexpected and non-trivial simplifications and we have qualitatively seen all of the features which will be involved in the full identification process. For example, terms which naively seem to appear in the D2-brane action but have no way to be recovered from the M2-brane action have naturally cancelled within the D2-brane action itself. It is reassuring that the introduction of terms which mix daggered and undaggered components of the M-theory 3-form was both natural in the M2-brane action and was required to produce the D2-brane action. We have been free to choose the coefficients in the M2-brane action to obtain the correct factors in the D2-brane action. However, many of the terms in the D2-brane action are recovered from a mixture of more than one term in the M2-brane action and it was not guaranteed that it would be possible to make this consistent. Fortunately the coefficients we fixed came with the correct ratios to make this possible, which is further evidence that it should be possible to extend the action to all orders in C .

It is still an open question how to construct an extension to the ABJM action that preserves the full $U(N) \times U(N)$ gauge symmetry. The difficulty lies in recovering all of the expected orderings in the symmetrised trace of the pullback, $P[C]$, rather than only those that can be constructed out of gauge invariant orderings of alternate bifundamental and anti-bifundamental fields. An answer to this will hopefully also provide some indication of the form of the full coupling, which may be constructed directly from the wedge product $P[C] \wedge P[C]$ rather than having to match every coefficient by hand. Certainly our identification of the necessary coefficients will provide a suitable test for any such proposal.

For further work, examining the gauge invariance of the ABJM action under background gauge transformations of the 3-form may provide useful insights into how to construct the necessary pull-back. The abelian pullback of C involving partial derivatives will transform as a total derivative under the background gauge transformation $C \rightarrow C + d\Lambda$ and thus leave the action invariant. However, the generalised pullback involving covariant derivatives no longer transforms as an overall total derivative and

we should instead view the pull-back as an object with its own transformation under background field transformations [55].

We also note that the above procedure only recovers $\tilde{C} \wedge \tilde{B}$ terms but the D2-brane action also contains $\tilde{C} \wedge F$ terms. It is not clear how the novel way in which the Yang-Mills term appears in reduction can be extended to produce a term which couples the field strength to the background fields.

Ultimately the results of this chapter will be useful in furthering our understanding of the couplings between the background 3-form and the ABJM action, but they are not completely satisfactory. We have only been able to provide partial answers, but we are hopefully one step closer to understanding how to construct a fully gauge invariant coupling of the background 3-form to the ABJM action that meets all of the requirements to reduce to the Myers-Chern-Simons term in the D2-brane action, with a symmetrised trace and correct quadratic combinations of the type IIA 3-form and Kalb-Ramond field.

Part II

Instantons

Chapter 4

Instantons and dyonic instantons

In the rest of this thesis we will be concerned with the study of instantons. These are relevant to multiple M5-branes and their relation to D4-branes, but most of our attention is given to the instanton solutions themselves rather than the brane interpretation.

An instanton is a gauge field with four spatial components whose field strength is self-dual [56],

$$F_{ij} = \frac{1}{2}\varepsilon_{ijkl}F_{kl}. \quad (4.0.1)$$

Solutions to this equation appear in a number of different contexts in theoretical physics. In QCD they are relevant in understanding quantum tunnelling between different vacua, and instantons play an important role in describing non-perturbative effects in supersymmetric gauge theories. For comprehensive reviews on the role of instantons in these two areas, see [57] and [58].

In the following chapters we are interested in instanton solutions as solitons in higher dimensional theories. Since the instantons occupy four spatial dimensions themselves, we need at least a five dimensional theory for them to appear as solitons. Instantons in this context have not seen as much study as lower dimensional solitons such as monopoles, vortices and skyrmions. Instantons have mostly likely been neglected due to the clear lack of four spatial dimensions in everyday physics. However, in the context of string theory, higher dimensional Yang-Mills theories are natural candidates for study since they appear as the low energy world-volume theory of Dp -branes for $p > 4$.

For a review of monopoles, vortices and instantons, as well as solitons in general, see the book by Manton and Sutcliffe [7] as well as the lecture notes by Tong [59]. The comprehensive review of monopoles and dyons by Weinberg and Yi [60] is also an appropriate background which will help put our instanton results into context.

The low energy world-volume theory of multiple D4-branes is described by maximally supersymmetric Yang-Mills theory, as discussed in the previous part of this thesis. Instantons appear in this theory as 1/2-BPS objects with a static gauge field,

a self-dual field strength and no non-zero scalar fields or fermions. In the global string theory picture, these instantons are D0-branes dissolved in the D4-branes, as can be seen by matching the charge and the supersymmetries that they break [61, 62, 30, 63].

The world-volume theory also admits 1/4-BPS dyonic instanton solutions, where a single scalar field has a non-zero expectation value in the background of an instanton [64]. Monopoles also have a 1/4-BPS dyonic counterpart [65, 66, 67] with an additional scalar field excited. These dyonic solutions have a constant rotation in the unbroken global gauge and are electrically charged [68]. In the BPS configuration, the repulsive electric charge is exactly balanced by the attractive force of the scalar field. From the string theory point of view dyonic instantons are a bound state of fundamental strings and D0-branes between the D4-branes [64, 69] and can be interpreted as supertubes [70, 71].

There have been recent compelling arguments that instantons in the super-Yang-Mills world-volume theory of D4-branes may have a deeper connection than previously thought to multiple M5-branes [72, 73]. In the dimensional reduction of M5-branes, instantons arise as states carrying Kaluza-Klein momentum along the compactification circle [74, 75]. Any theory describing multiple M5-branes must therefore recover instantons in the compactification limit and this has been important in exploring the validity of proposed theories [76, 77]. It may be possible to understand more about the theory of multiple M5-branes by considering the degrees of freedom and bound states of instantons in five dimensional Yang-Mills [78]. This is an active topic of research that originally motivated the work presented in this thesis. However we found that our approach led us to consider the dynamics of instantons in the classical regime instead. The results in this thesis do not directly relate to M-theory, although future work may be able to complete the circle and return to this original goal.

There are many solutions to the self-dual field equation and so many possible configurations of instantons with a given topological charge. The space of solutions is known as the moduli space and has a rich geometry. A strong mathematical treatment of instantons and their moduli space is beyond the scope of this thesis, but the book by Donaldson and Kronheimer [79] is a suitable place to find such a treatment. Our main interest in the moduli space is through the moduli space approximation of Manton [80], where the low-energy dynamics of instantons can be approximated by geodesic motion on the moduli space. Instantons are the minimal energy solutions with a given topological charge and so a slight perturbation will still remain close to the minimal energy. The evolution of the perturbation will necessarily remain close to the moduli space in the full space of solutions due to energy conservation. This motion can then be approximated by motion on the moduli space with any small radiative modes ignored. The motion of dyonic instantons can be approximated in a similar way although the motion on the moduli space now takes place in the presence of a potential which arises

from the electric charge. Much of our understanding is based on the similar behaviour of monopole dyons where the concept of a potential on the moduli space was first understood [81, 82, 83].

In this introductory chapter we will review some properties of instanton and dyonic instanton solutions. In Section 4.1 we begin with an overview of how instantons arise as the minimal energy solutions in each topological sector of Yang-Mills. In Section 4.3 we will review the ADHM construction which provides a powerful method for constructing instantons in a purely algebraic manner without needing to solve the first-order self-dual field equation directly. Throughout the next few chapters of this thesis we will make use of the ability to express the gauge field in terms of the ADHM data to reduce complicated expressions involving derivatives and integrals to purely algebraic expressions. This technique is immediately useful in Section 4.4 where we review the derivation of an expression for the metric on the moduli space in terms of the ADHM data. In Section 4.5 we will see how the presence of a scalar field with non-zero expectation value leads to dyonic instantons and how the underlying instanton is undistorted. We also see how the scalar field induces a potential on the moduli space.

In Chapter 5 we will use the ADHM construction for charge two instantons to explicitly calculate the metric and potential on the moduli space. The symmetries of the ADHM construction allow us to understand some of the topology of the moduli space, and the symmetries of the metric allow us to understand its geodesic structure. In Chapter 6 we will use the explicit moduli space metric and potential to explore the low energy dynamics of charge two (dyonic) instantons via the moduli space approximation. We will present a numerical study of the range of possible scatterings of two (dyonic) instantons, and also understand how some of the generic behaviour, such as a right angled scattering and the varying strength of their interaction, can be understood analytically from the underlying ADHM construction and metric.

4.1 Instantons in five dimensional Yang-Mills

Let us start with the simplest theory in which instantons appear, four dimensional Euclidean Yang-Mills with an $SU(N)$ gauge group. The Yang-Mills action is

$$S = -\frac{1}{4} \int d^4x \operatorname{Tr} (F_{ij} F_{ij}). \quad (4.1.1)$$

We have set the coupling constant to one since it will not play a role in our discussion. In our conventions the gauge field, A_i , is Hermitian and the field strength is

$$F_{ij} = \partial_i A_j - \partial_j A_i - i[A_i, A_j]. \quad (4.1.2)$$

This theory splits into an infinite number of topological sectors labelled by an integer, k . Each solution to the equations of motion must lie in one of these topological sectors and instantons are the solutions with the least energy in each sector.

We are concerned with fields which have a finite energy and so the field strength must tend to zero as we head towards the boundary at spatial infinity,

$$\lim_{|x| \rightarrow \infty} F_{ij} = 0. \tag{4.1.3}$$

At spatial infinity the gauge field is therefore pure gauge,

$$A_i \Big|_{|x|=\infty} = ig^{-1} \partial_i g, \tag{4.1.4}$$

where $g(x) \in \text{SU}(N)$. Every finite action field configuration therefore contains a map,

$$g : S_\infty^3 \rightarrow \text{SU}(N). \tag{4.1.5}$$

Such maps fall into distinct homotopy classes depending on how the map wraps S^3 around the non-trivial structure of $\text{SU}(N)$. The third homotopy group of $\text{SU}(N)$ is \mathbb{Z} so the homotopy class of g can be labelled by an integer, k . Any two maps with the same k lie in the same homotopy class and can be continuously deformed into each other. When two such maps lie in different homotopy classes there is no continuous deformation between them. Depending on the context, the integer k is known as the Pontryagin number, the second Chern class or simply the topological degree. We will generally refer to it as the instanton number or topological charge.

The degree of the map g can be calculated by

$$k = \frac{1}{24\pi^2} \int_{S_\infty^3} \text{Tr} \left((g dg^{-1}) \wedge (g dg^{-1}) \wedge (g dg^{-1}) \right). \tag{4.1.6}$$

The integrand is the normalised volume form on $\text{SU}(N)$ so that each wrap of $\text{SU}(N)$ by g contributes one to the integral. This degree can also be calculated in terms of the field strength directly as

$$k = \frac{1}{8\pi^2} \int \text{Tr} (F \wedge F) = \frac{1}{8\pi^2} \int d^4x \text{Tr} \left(\frac{1}{2} \varepsilon_{ijkl} F_{ij} F_{kl} \right). \tag{4.1.7}$$

To see this we note that

$$\text{Tr} (F \wedge F) = d \text{Tr} \left(F \wedge A + \frac{1}{3} i A \wedge A \wedge A \right), \tag{4.1.8}$$

so k can be written as

$$k = \frac{1}{8\pi^2} \int_{S_\infty^3} \text{Tr} (F \wedge A + \frac{1}{3} i A \wedge A \wedge A). \quad (4.1.9)$$

The first term vanishes since F vanishes at infinity and the final term is the volume form of $SU(N)$ as above.

Every solution to the Yang-Mills equations of motion can therefore be classified by its topological charge, k , and each topological sector will have solutions with minimum energy. When $k = 0$ this is the vacuum solution, but with non-zero k , the minimum energy solutions in that sector have non-zero energy. To see this we can use a technique which was introduced by Bogomol'nyi in the Russian paper [84], and is well known. It was also used in the original paper on instantons [56] without special mention. We complete the square in the expression for the energy density and in doing so pull out a term which is proportional to the topological charge,

$$\begin{aligned} E &= \frac{1}{4} \int d^4x \text{Tr} (F_{ij} F_{ij}) \\ &= \frac{1}{4} \int d^4x \text{Tr} \left(\frac{1}{2} (F_{ij} \pm \frac{1}{2} \varepsilon_{ijkl} F_{kl})^2 \mp \frac{1}{2} \varepsilon_{ijkl} F_{ij} F_{kl} \right). \end{aligned} \quad (4.1.10)$$

The first term is a total square and so must be non-negative. The energy is therefore bounded below by

$$E \geq 2\pi^2 |k|, \quad (4.1.11)$$

where k is the topological charge.

This energy bound is only attained when the squared quantity is zero and the fields are self-dual or anti-self-dual,

$$F_{ij} = \pm \frac{1}{2} \varepsilon_{ijkl} F_{kl}. \quad (4.1.12)$$

Solutions to the (anti-)self-dual field equation are called (anti-)instantons and they are the global minima of the energy within each topological sector. These fields automatically satisfy the Yang-Mills equations of motion due to the Bianchi identity.

From now on we will consider only instantons with non-negative topological degree. The treatment of anti-instantons would be identical but with the appropriate signs reversed. The topological charge can be interpreted as the number of instantons and we will use it synonymously with the term 'instanton number'. Solutions to the self-dual field equation with instanton number k will typically have their energy density localised around k points. When these points are far apart the solutions are approximately the superposition of k charge one instantons. However, when these points are close together, this approximation no longer holds and there is a rich structure within the solutions.

Instantons naturally appear within higher dimensional Yang-Mills theories where they are embedded in four of the spatial dimensions. The focus of this thesis will be on five dimensional Yang-Mills, where the added time dimension allows instantons to be studied as dynamical solitons, like monopoles in four dimensional theories.

The action of five dimensional Yang-Mills is

$$S = -\frac{1}{4} \int d^5x \operatorname{Tr} (F_{\mu\nu} F^{\mu\nu}), \quad (4.1.13)$$

and the energy is

$$E = \int d^4x \operatorname{Tr} \left(\frac{1}{2} F_{i0} F_{i0} + \frac{1}{4} F_{ij} F_{ij} \right). \quad (4.1.14)$$

The interesting topology from wrapping $SU(N)$ at spatial infinity remains and the BPS equations are now

$$F_{ij} = \frac{1}{2} \varepsilon_{ijkl} F_{kl}, \quad (4.1.15)$$

$$F_{i0} = 0. \quad (4.1.16)$$

The solutions to these equations are static instantons in the spatial direction, A_i , and have $A_0 = 0$.

The general solution for a charge one instanton is given by the 't Hooft ansatz [85],

$$A_i = -\frac{1}{2} \eta_{ij}^a \sigma^a \partial_j \log \rho, \quad (4.1.17)$$

where η_{ij}^a is the 't Hooft symbol, and ρ is

$$\rho = 1 + \frac{\lambda^2}{|x - a|^2}. \quad (4.1.18)$$

There are 5 free parameters in this solution: a is a four vector and describes the position of the instanton, and λ describes its size. Up to gauge transformations, the 't Hooft solution describes all charge one instantons. This solution can also be generalised to general instanton number, k , by taking,

$$\rho = 1 + \sum_{i=1}^k \frac{\lambda_i^2}{|x - a_i|^2}, \quad (4.1.19)$$

which describes k instantons at positions a_i , with sizes λ_i .

The Jackiw-Nohl-Rebbi (JNR) ansatz [86] is a generalisation of the 't Hooft ansatz, and it describes the most general charge two instanton. For general charge k , it is given

by

$$\rho = \sum_{i=0}^k \frac{\lambda_i^2}{|x - a_i|^2}. \quad (4.1.20)$$

The interpretation of the parameters is less clear here, but the 't Hooft ansatz is recovered in the limit $\lambda_0^2 = a_0^2 \rightarrow \infty$.

The number of parameters in the 't Hooft ansatz scales as $5k + 3$, with the 3 coming from overall global gauge transformations. The number of parameters in the JNR ansatz scales as $5k + 8$ and when $k = 1$ or 2 , the JNR ansatz contains redundant parameters. In general, the number of parameters in the instanton solutions should scale as $8k$ [87, 88, 89], and the missing $3k$ are related to the relative gauge orientation of the instantons, which are not captured by either the 't Hooft or the JNR ansatz. In Section 4.3 we will review the ADHM construction which provides an implicit method for constructing general solutions to the instanton BPS equations and captures all $8k$ degrees of freedom.

4.2 Instantons as D0-branes

In the second part of this thesis we are mostly concerned with the treatment of instantons as classical solitons, and how they compare to other soliton systems of a similar nature. However, we have seen that instantons also play an important role in string theory, and possibly M-theory, so in this section we will briefly review the brane interpretation of instantons.

The five dimensional $SU(N)$ Yang-Mills theory considered previously is the low energy bosonic action of N D4-branes. Instantons appear as solutions to the field equation on the world-volume, but from the space-time picture, they are D0-branes. The first clue to this identification is the coupling of the D4-brane to the background 1-form as in equation (2.1.10):

$$S_{C^{(1)}} = T_4 \lambda^2 \int \text{Tr} \left(C^{(1)} \wedge F \wedge F \right). \quad (4.2.1)$$

In the presence of an instanton the $F \wedge F$ term is proportional to the instanton number, k , and the coupling of $C^{(1)}$ to the D4-branes is identical to the coupling of $C^{(1)}$ to k D0-branes:

$$S_{C^{(1)}} = k T_0 \int \text{Tr} C^{(1)}. \quad (4.2.2)$$

The supersymmetries broken by the instanton are also identical to those broken by the D0-branes.

The world-volume description of instantons has a dual description in term of a D4-D0-brane system [61, 62, 30, 63]. The moduli space of the D0-brane has two branches.

The Coulomb branch describes the D0-branes when they are separated from the D4-branes, and the moduli describe the D0-branes' positions transverse to the D4-branes. The Higgs branch describes the the D0-branes when they are confined within the D4-branes, and can be identified with the moduli space of instantons in the Yang-Mills world-volume theory. These two branches are connected via small instantons, with the limit of instantons going to zero size corresponding to the transition between the Higgs branch and the Coulomb branch.

4.3 The ADHM construction

To find solutions which are instantons we need to solve the BPS equation for a self-dual field strength. This a first-order differential equation for the gauge field, A_i , so is easier to solve than the full second-order equations of motion. However, the BPS equation is still too complicated to solve directly in general. Solving the BPS equation can be reduced to an algebraic problem by using the construction of Atiyah, Drinfel'd, Hitchin and Manin (ADHM) [90], based on previous work by Ward [91]. The ADHM construction only involves solving a set of non-linear algebraic constraints to find solutions of the BPS equations. It is still difficult to solve these constraints in general but the problem is at least tractable for low instanton number, k , and for a small gauge group.

In this thesis we will only be concerned with instantons in the $SU(2)$ gauge group. Rather than giving a description of the ADHM construction for arbitrary N , we will assume from now on that $N = 2$. The advantage of this is that for $SU(2)$ the ADHM construction can be written in terms of quaternions, and the notation and algebra is simpler than in the general case. The space of quaternions is denoted by \mathbb{H} , and we will use a representation of the quaternions in terms of 2×2 complex matrices,

$$\begin{aligned} e_a &= i\sigma_a, \quad (a = 1, 2, 3), \\ e_4 &= \mathbb{1}_2, \end{aligned} \tag{4.3.1}$$

where σ_a are the Pauli matrices. These satisfy the quaternion algebra

$$e_1^2 = e_2^2 = e_3^2 = e_1e_2e_3 = -1. \tag{4.3.2}$$

We will prefer the notation e_i rather than $\{1, i, j, k\}$ since being able to index the four components is useful. If $p = p^i e_i$ is a quaternion in this representation then its conjugate is given by p^\dagger . Unit quaternions therefore satisfy $p^\dagger p = \mathbb{1}_2$ and can be identified with $SU(2)$. The purely imaginary quaternions form the Lie algebra $\mathfrak{su}(2)$

with e_1, e_2 and e_3 acting as generators,

$$[e_a, e_b] = 2\varepsilon_{abc}e_c. \quad (4.3.3)$$

The spatial coordinate x can also be written as a quaternion with the four spatial components becoming the four quaternion components, $x = x^i e_i$.

The starting point of the ADHM construction is a $(k+1) \times k$ quaternion valued matrix, $\Delta(x)$, which is linear in x and is known as the ADHM data. This can always be put in the canonical form [92, 93],

$$\Delta(x) = a - bx, \quad (4.3.4)$$

where

$$a = \begin{pmatrix} L \\ M \end{pmatrix}, \quad b = \begin{pmatrix} 0 \\ \mathbb{1}_k \end{pmatrix}. \quad (4.3.5)$$

In this block form, L is a length k row vector and M is a $k \times k$ matrix. In general the form of $\Delta(x)$ can be less constrained, but it can always be brought into this form by using transformations which leave the resulting gauge field invariant.

The entries of L and M are arbitrary, except for the requirement that Δ satisfy the ADHM constraint,

$$\Delta^\dagger \Delta = f^{-1}, \quad (4.3.6)$$

where f is real and invertible. If f is not invertible then the ADHM data corresponds to a singular instanton configuration. In terms of L and M this constraint is

$$L^\dagger L + M^\dagger M - M^\dagger x - \bar{x} M + |x|^2 = f^{-1}. \quad (4.3.7)$$

The quadratic term in x is automatically real. If we write the linear term in x with the quaternionic components of M made explicit,

$$- ((M^i)^\dagger \bar{e}_i x + M^i \bar{x} e_i), \quad (4.3.8)$$

then we see that this will be real if and only if M is symmetric,

$$M^\dagger = M. \quad (4.3.9)$$

The term that is constant with respect to x remains as a non-linear constraint on a ,

$$a^\dagger a = L^\dagger L + M^\dagger M = \mu^{-1}, \quad (4.3.10)$$

for some real matrix μ .

Given ADHM data, Δ , which satisfies this constraint, a self-dual gauge field can be constructed by finding a quaternionic column vector, U , of length $k + 1$ in the null space of Δ^\dagger ,

$$\Delta^\dagger U = 0. \quad (4.3.11)$$

This column vector should be normalised to have unit norm,

$$U^\dagger U = 1. \quad (4.3.12)$$

The gauge field is then constructed from U in the following manner:

$$A_i = iU^\dagger \partial_i U. \quad (4.3.13)$$

The normalisation of U ensures that A_i is Hermitian.

To see that the resulting F_{ij} is indeed self-dual we can directly evaluate F_{ij} using this ansatz for A_i . At the end of this section we will present a collection of useful identities and results for manipulating quantities arising from the ADHM construction, and we use many of these in the following without comment:

$$\begin{aligned} F_{ij} &= i\partial_i U^\dagger \partial_j U - i\partial_j U^\dagger \partial_i U + iU^\dagger \partial_i U U^\dagger \partial_j U - iU^\dagger \partial_j U U^\dagger \partial_i U \\ &= i\partial_i U^\dagger (\mathbb{1} - U U^\dagger) \partial_j U - i\partial_j U^\dagger (\mathbb{1} - U U^\dagger) \partial_i U \\ &= i\partial_i U^\dagger \Delta f \Delta^\dagger \partial_j U - i\partial_j U^\dagger \Delta f \Delta^\dagger \partial_i U \\ &= iU^\dagger \partial_i \Delta f \partial_j \Delta^\dagger U - iU^\dagger \partial_j \Delta f \partial_i \Delta^\dagger U \\ &= -iU^\dagger b f (e_i \bar{e}_j - e_j \bar{e}_i) b^\dagger U. \end{aligned} \quad (4.3.14)$$

The only appearance of the indices is in the term $(e_i \bar{e}_j - e_j \bar{e}_i)$ which can easily be checked to be self-dual.

Note that the choice of U in the ADHM construction is far from unique. If $U(x)$ satisfies the conditions in equations (4.3.11) and (4.3.12) then so will $U(x) \rightarrow U(x)\Omega(x)$ for any unit quaternion $\Omega(x)$. The resulting gauge field is then

$$A_i(x) \rightarrow \Omega(x)^\dagger A_i(x) \Omega(x) + i\Omega(x)^\dagger \partial_i \Omega(x), \quad (4.3.15)$$

which is a gauge transformation of A_i by Ω^\dagger . For a given initial set of ADHM data, the gauge field is therefore only specified up to a gauge transformation. In practice, any method of finding an explicit solution for U will pick some canonical gauge.

There is some redundancy present in the ADHM data since the gauge field is invariant under a transformation of the ADHM data of the following form:

$$\Delta \rightarrow Q\Delta R^{-1}, \quad \text{where } Q = \begin{pmatrix} p & 0 \\ 0 & R \end{pmatrix}. \quad (4.3.16)$$

Here R is a real and orthogonal $k \times k$ matrix, and p is a unit quaternion. This transformation preserves the ADHM constraints and it transforms U as

$$U \rightarrow QU. \quad (4.3.17)$$

Since Q is independent of x this leaves A_i unchanged. This symmetry is of crucial importance in much of the work we will present later in this thesis. In Chapter 5 we will use this symmetry to project out variations of the zero-modes on the moduli space that are proportional to gauge transformations and therefore find the metric through purely algebraic means. The quotient structure of the moduli space of instantons also arises from the action of these symmetries. In Chapter 7 we will construct symmetric instantons by finding ADHM data that is invariant under matrices, p and R , that form a representation of the symmetry group.

As a method to construct instanton solutions the ADHM construction is a useful tool. In fact, once the redundancy in equation (4.3.16) is taken into account, solutions to the ADHM constraint are in one-to-one correspondence with solutions to the self-dual field equation. That is, every instanton has some underlying ADHM data which can be used to construct it, as can be seen by counting the number of independent parameters in the ADHM construction. Naively we count $4k$ real parameters in L and $2k(k+1)$ real parameters in M . These must satisfy the ADHM constraints which remove $\frac{3}{2}k(k-1)$ degrees of freedom. The transformation in equation (4.3.16) has $\frac{1}{2}k(k-1)$ parameters in R and 3 in p . These are redundancies in the parameterisation of the ADHM data which we should discount. Altogether there are therefore $8k-3$ degrees of freedom in the ADHM data. It is conventional to include global gauge transformations in our counting of degrees of freedom which brings the total to $8k$, the expected dimension of the moduli space. Note that for general gauge group, $SU(N)$, the moduli space has dimension $4kN$.

If we can find an appropriate parameterisation of the ADHM data that satisfies the ADHM constraints and breaks the symmetry in equation (4.3.16) then this will also provide us with a coordinate system on the space of instantons of a given charge. We will see that we can do this explicitly for $k=2$ in Chapter 5.

ADHM Algebra

Part of the utility of the ADHM construction is the ability to rewrite expressions in a way such that all derivatives can be explicitly evaluated on Δ . An example of this is given in equation (4.3.14). This is a pattern which is repeated throughout many of our calculations. We will present a few identities which will be used without comment when we perform these manipulations in the rest of this thesis.

Due to the conditions on U ,

$$\Delta^\dagger U = 0, \quad U^\dagger U = 1, \quad (4.3.18)$$

we can move a derivative between these terms whenever they appear adjacently,

$$U^\dagger \partial_i U = -(\partial_i U^\dagger)U, \quad \text{and} \quad \partial_i U^\dagger \Delta = -U^\dagger \partial_i \Delta. \quad (4.3.19)$$

Since Δ is linear in x the derivatives are then trivial,

$$\partial_i \Delta = -e_i b, \quad \text{and} \quad \partial_i \Delta^\dagger = -b^\dagger \bar{e}_i. \quad (4.3.20)$$

The expression

$$P = UU^\dagger \quad (4.3.21)$$

is a projector onto the subspace of \mathbb{H}^{k+1} spanned by U . To see this we note that together the columns of Δ and U span \mathbb{H}^{k+1} and

$$PU = U, \quad \text{and} \quad P\Delta = 0. \quad (4.3.22)$$

The following expression for P has the same action on U and Δ and is therefore identical,

$$P = \mathbb{1}_{k+1} - \Delta f \Delta^\dagger. \quad (4.3.23)$$

The derivative of U with respect to any of the parameters in the ADHM data, z^r , is

$$\partial_r U = -\Delta f \partial_r \Delta^\dagger U + P \partial_r U. \quad (4.3.24)$$

We can see this by differentiating the identity $U = PU$.

4.4 The moduli space of instantons

We saw at the end of the last section that the ADHM construction provides a convenient and comprehensive way of parameterising the moduli space of all instantons of a given charge. In this section we will see that the moduli space has a natural metric that is fundamentally related to the low-energy dynamics of instantons.

Let us be more precise with what we mean by the moduli space:

The moduli space of charge k instantons is the space of all solutions to the self-dual field equation, of topological charge k , quotiented by local gauge transformations, but including solutions which differ by a global gauge transformation.

The moduli space can therefore be thought of as the space of all physically distinct

instantons. Global gauge transformations are conventionally included for reasons that will become clear when we consider dyonic instantons. The moduli space for each topological charge is connected and generally has a complicated topology and geometry.

The moduli space has received much study as a geometric space, and efforts to understand the instanton moduli space have led to important developments within mathematics [79]. Our interest in the moduli space is primarily in its relevance to the dynamics of low energy instantons, so we will approach it from this angle.

To investigate the low energy dynamics of instantons we need to ask what happens when we give the static instantons a small velocity. Of course these configurations will no longer strictly be instantons, but for small velocities they will remain close to the minimum energy solutions corresponding to instantons in the moduli space. Solving the full field theory equations for their motion would be extremely complicated, but for small velocities the problem can be approximated by motion on the moduli space [80]. Since the initial field configuration starts close to a minimum energy solution, the evolution of the fields must always stay close to a minimum energy solution by energy conservation and therefore close to solutions which lie in the moduli space. In fact this motion can be approximated by geodesic motion which remains on the moduli space. If the coordinates on the moduli space are labelled as z^r then we allow a time dependence in $A_\mu(\mathbf{z}(t); \mathbf{x})$ only through $\mathbf{z}(t)$. This is an approximation that is well understood for monopoles and a useful review is provided in reference [60]. We follow a very similar argument for instantons.

Once our fields have a time dependence through the \mathbf{z} parameter, they will not automatically satisfy the Yang-Mills equations of motion as the static fields did. Gauss's law becomes

$$D_i F_{i0} = D_i(D_i A_0 - \dot{z}^r \partial_r A_i) = 0. \quad (4.4.1)$$

This can be solved by modifying A_0 by an amount proportional to the velocity,

$$A_0 = \dot{z}^r \epsilon_r, \quad (4.4.2)$$

where ϵ_r is chosen so that $D_i(D_i \epsilon_r - \partial_r A_i) = 0$, and Gauss's law is satisfied.

The electric components of the field strength can now be written as

$$F_{i0} = -\dot{z}^r \delta_r A_i, \quad (4.4.3)$$

where

$$\delta_r A_i = \partial_r A_i - D_i \epsilon_r. \quad (4.4.4)$$

We refer to $\delta_r A_i$ as a zero-mode since it is the gauge-invariant variation of A_i in a direction that does not change the energy of the fields.

Substituting our time dependent ansatz into the Yang-Mills action gives an effective

action for the evolution of $z^r(t)$ through the moduli space,

$$S = \frac{1}{2} \int d^5x \operatorname{Tr} (F_{i0} F_{i0}) = \frac{1}{2} \int dt g_{rs} \dot{z}^r \dot{z}^s, \quad (4.4.5)$$

where

$$g_{rs} = \int d^4x \operatorname{Tr} (\delta_r A_i \delta_s A_i). \quad (4.4.6)$$

The metric, g_{rs} , defines a metric on the moduli space and the evolution of our ansatz is given by geodesic motion on the moduli space with this metric.

The low energy dynamics of instantons can therefore be approximated by a series of snapshots of static instanton solutions, where the evolution through these snapshots is given by geodesic motion on the moduli space.

The metric which has appeared in understanding the low energy dynamics of instantons can also be derived in a way that is intrinsic to the moduli space itself. We will begin by considering the unquotiented moduli space which includes local gauge transformations. Each point on this space corresponds to some instanton solution, $A_i(\tilde{\mathbf{z}}, x)$, where the $\tilde{\mathbf{z}}$ coordinates now also index the infinite dimensional space of local gauge transformations. To define the tangent vectors to this space, let us briefly return to first principles. Let $A_i(\tilde{\mathbf{z}}(\tau), x)$ be some curve through the moduli space parameterised by τ . This should pass through the point in the moduli space that we are interested in when $\tau = 0$. Then a tangent vector is defined by

$$\tilde{\delta} A_i = \partial_\tau A_i(\tilde{\mathbf{z}}(\tau), x) \Big|_{\tau=0}. \quad (4.4.7)$$

This is the directional derivative in the direction of the curve. Intuitively, $\tilde{\delta} A_i$ can be thought of as a perturbation to A_i which remains in the moduli space to first order. After substituting this curve into the self-dual field equation and differentiating with respect to τ we find the linearised self-dual field equation that $\tilde{\delta} A_i$ must satisfy:

$$D_i(\tilde{\delta} A_j) - D_j(\tilde{\delta} A_i) = \varepsilon_{ijkl} D_k(\tilde{\delta} A_l). \quad (4.4.8)$$

Note that gauge transformations automatically satisfy this linear self-dual field equation.

There is a natural inner product on the unquotiented moduli space,

$$\tilde{g}(\tilde{\delta} A_i, \tilde{\delta}' A_i) = \int d^4x \operatorname{Tr} (\tilde{\delta} A_i \tilde{\delta}' A_i). \quad (4.4.9)$$

This metric will induce a metric on the moduli space when we quotient by gauge transformations. However, we have to take care to ensure that the metric on the moduli space is well-defined, regardless of our choice of gauge. That is, the metric must be

invariant under gauge transformations and so must act identically on tangent vectors which differ only by a gauge transformation. We can therefore define the metric on the moduli space as the above metric on the unquotiented space but with the tangent vectors first projected orthogonal to gauge transformations. These projected tangent vectors are our canonical choice of representatives for tangent vectors in the quotiented moduli space.

For a tangent vector, $\tilde{\delta}A_i$, to be orthogonal to gauge transformations, it must satisfy

$$g\left(\tilde{\delta}A_i, D_i\Lambda\right) = - \int d^4x \operatorname{Tr}\left(D_i(\tilde{\delta}A_i)\Lambda\right) = 0, \quad (4.4.10)$$

for all Λ . Equivalently,

$$D_i(\tilde{\delta}A_i) = 0. \quad (4.4.11)$$

The variations which satisfy the linear self-dual field equation and this gauge fixing condition are known as zero-modes and form the tangent space at each point in the moduli space.

With the gauge transformations quotiented out, recall that the parameters in the ADHM data provide a coordinate system on the moduli space. If we label the $8k$ parameters of the ADHM construction as z^r , $r = 1, \dots, 8k$ then each choice corresponds to an instanton solution, $A_i(\mathbf{z}; \mathbf{x})$. The obvious tangent vectors in this coordinate system are $\partial_r A_i$, except that these may also include variations which are gauge transformations. To obtain a zero-mode, we must project out this gauge transformation. The canonical zero-modes on the moduli space are therefore

$$\delta_r A_i = \partial_r A_i - D_i \epsilon_r, \quad (4.4.12)$$

where ϵ_r is chosen so that $D_i(\delta_r A_i) = 0$. The metric on the moduli space is defined as

$$g_{rs} = \int d^4x \operatorname{Tr}(\delta_r A_i \delta_s A_i). \quad (4.4.13)$$

These zero-modes, $\delta_r A_i$, are exactly the same as those we came across in our ansatz for the low energy dynamics of instantons, and the metric is identical to that in our effective sigma-model action for their evolution. We have seen here however that the metric on the moduli space is intrinsic and does not require the instantons to be embedded in a higher dimensional theory for it to be apparent.

4.4.1 The moduli space metric

To make further progress in understanding the low energy dynamics of instantons we will need an explicit form of the metric in terms of the ADHM parameters, or coordinates on the moduli space. In principle we could find the metric by finding an

explicit expression for $A_i(\mathbf{z}; x)$, solving the gauge fixing condition for ϵ_r and taking the trace of each pair of zero-modes. In practice this approach is intractable. Fortunately we can use the ADHM construction to once again reduce this to an algebraic calculation which can be readily done for charge two instantons with an $SU(2)$ gauge group.

What follows is a method developed by Osborn [94] which was originally used for calculating the metric determinant and has been applied by Peeters and Zamaklar [95] to calculate the metric directly when the instantons are well separated.

An algebraic constraint on zero-modes

Recall that the gauge field, A_i , is constructed from the ADHM data, Δ as

$$A_i = iU^\dagger \partial_i U, \quad \text{where} \quad \Delta^\dagger U = 0, \quad U^\dagger U = 1. \quad (4.4.14)$$

The derivative of A_i in one of the coordinate directions on the moduli space can be calculated in terms of the ADHM data, making use of the ADHM algebra,

$$\partial_r A_i = -iU^\dagger \partial_r \Delta f \bar{e}_i b^\dagger U + iU^\dagger b e_i f \partial_r \Delta^\dagger U + D_i(iU^\dagger \partial_r U). \quad (4.4.15)$$

The last term is an explicit gauge transformation but the first two terms may also contain components which are gauge transformations. Our aim is to perform appropriate transformations on Δ so that all of the gauge transformation components are shifted into the final term and the first two terms can then be taken together as the zero-mode. Let us again consider the tangent vector from first principles: $\delta_r A_i$ is the derivative of a curve through the z^r coordinate on the moduli space, $A_i(z^r(\tau); x)$, at $\tau = 0$. At each point on this curve the field configuration, A_i , has some underlying ADHM data, Δ . However, this ADHM data is not unique since the gauge field is invariant under a transformation of the ADHM data of the following form:

$$\Delta \mapsto Q\Delta R, \quad U \mapsto QU. \quad (4.4.16)$$

We can therefore choose a different underlying Δ at each point on our curve. Let us parameterise this transformation along the curve in the following way:

$$\Delta(z^r(\tau)) \mapsto \exp(\tau \delta_r Q) \Delta \exp(\tau \delta_r R). \quad (4.4.17)$$

This transformation does not change $\partial_r A_i$ but instead allows us to write it as

$$\partial_r A_i = -iU^\dagger C_r f \bar{e}_i b^\dagger U + iU^\dagger b e_i f C_r^\dagger U + D_i(iU^\dagger \partial_r U + iU^\dagger \delta_r QU), \quad (4.4.18)$$

where

$$C_r = \partial_r \Delta + \delta_r Q \Delta + \Delta \delta_r R. \quad (4.4.19)$$

We can use this freedom to choose an appropriate $\delta_r Q$ and $\delta_r R$ such that the only components of $\partial_r A_i$ which are gauge transformations appear explicitly in the final term. The first two terms will then together be a zero-mode. The appropriate $\delta_r Q$ and $\delta_r R$ can be found by imposing the zero-mode conditions on

$$\delta_r A_i = -iU^\dagger C_r f \bar{e}_i b^\dagger U + iU^\dagger b e_i f C_r^\dagger U. \quad (4.4.20)$$

That is, asking that this $\delta_r A_i$ satisfy the linearised self-dual field equation and that it is orthogonal to gauge transformations. The conditions that this imposes on C_r are provided in the following claim:

Claim 4.4.1. *The expression*

$$\delta_r A_i = -iU^\dagger C_r f \bar{e}_i b^\dagger U + iU^\dagger b e_i f C_r^\dagger U, \quad (4.4.21)$$

is a zero-mode if C_r is independent of x and

$$\Delta^\dagger C_r = (\Delta^\dagger C_r)^\top. \quad (4.4.22)$$

Equivalently, if

$$a^\dagger C_r = (a^\dagger C_r)^\top, \quad \text{and} \quad b^\dagger C_r = (b^\dagger C_r)^\top. \quad (4.4.23)$$

Proof. Consider the expression

$$a_i \equiv U^\dagger b f e_i, \quad (4.4.24)$$

which makes up part of $\delta_r A_i$. If we treat this as a vector in the fundamental representation we can work out its covariant derivative,

$$\begin{aligned} D_i a_j &\equiv \partial_i a_j - i A_i a_j \\ &= U^\dagger e_i b f \Delta^\dagger b f e_j + U^\dagger b f (\bar{e}_i b^\dagger \Delta + \Delta^\dagger b e_i) f e_j. \end{aligned} \quad (4.4.25)$$

If we write $\Delta^\dagger b = c_k \bar{e}_k$ with the quaternion components made explicit, where c_k are some real valued matrices, then we can write this covariant derivative as

$$\begin{aligned} D_i a_j &= U^\dagger b f c_k f (e_i \bar{e}_k e_j + \bar{e}_i e_k e_j + \bar{e}_k e_i e_j) \\ &= -U^\dagger b f c_k f (e_i \bar{e}_j e_k - 2\delta_{jk} e_i - 2\delta_{ik} e_j). \end{aligned} \quad (4.4.26)$$

In the final line we have used the quaternion identity,

$$\bar{e}_i e_j = -\bar{e}_j e_i + 2\delta_{ij}. \quad (4.4.27)$$

In this form it is straightforward to see that a_i satisfies the linear self-dual field equation and background gauge condition,

$$D_{[i}a_{j]} = \frac{1}{2}\varepsilon_{ijkl}D_k a_l, \quad \text{and} \quad D_i a_i = 0. \quad (4.4.28)$$

The covariant derivative of $\delta_r A_i$ can now be written as

$$\begin{aligned} D_i(\delta_r A_j) &= -i(D_i U^\dagger)C_r a_j^\dagger + ia_j C_r^\dagger(D_i U) - iU^\dagger C_r(D_i a_j^\dagger) + i(D_i a_j)C_r^\dagger U \\ &= -iU^\dagger b f \left(e_i \Delta^\dagger C_r \bar{e}_j - e_j C_r^\dagger \Delta \bar{e}_i \right) f b^\dagger U - iU^\dagger C_r(D_i a_j^\dagger) + i(D_i a_j)C_r^\dagger U. \end{aligned} \quad (4.4.29)$$

Here U^\dagger is also treated as a vector in the fundamental representation and its covariant derivative is

$$D_i U^\dagger \equiv \partial_i U^\dagger - iA_i U^\dagger = U^\dagger e_i b f \Delta^\dagger. \quad (4.4.30)$$

We have already shown that the last two terms in $D_i(\delta_r A_j)$ satisfy the conditions of a zero-mode so we only need to consider the first. Let us define

$$K_{ij} \equiv e_i \Delta^\dagger C_r \bar{e}_j - e_j C_r^\dagger \Delta \bar{e}_i. \quad (4.4.31)$$

Then $\delta_r A_i$ will be a zero-mode if

$$K_{[ij]} = \frac{1}{2}\varepsilon_{ijkl}K_{kl}, \quad \text{and} \quad K_{ii} = 0. \quad (4.4.32)$$

This is true if and only if

$$\Delta^\dagger C_r = (\Delta^\dagger C_r)^\top. \quad (4.4.33)$$

Since $\Delta = a - bx$ is linear in x , and C_r has no dependence on x , we can split this into two conditions,

$$a^\dagger C_r = (a^\dagger C_r)^\top, \quad \text{and} \quad b^\dagger C_r = (b^\dagger C_r)^\top. \quad (4.4.34)$$

□

It now remains to establish the conditions on $\delta_r Q$ and $\delta_r R$ so that the conditions on C_r are satisfied and $\delta_r A_i$ is a zero-mode. In our canonical choice for the ADHM data, b is given by

$$b = \begin{pmatrix} 0 \\ \mathbb{1}_k \end{pmatrix}, \quad (4.4.35)$$

and the transformation parameter Q takes the form

$$Q = \begin{pmatrix} q & 0 \\ 0 & R^{-1} \end{pmatrix}. \quad (4.4.36)$$

We do not need a variation in q so we can set $\delta_r q = 0$. The variation of Q can now be

expressed entirely in terms of the variation of R ,

$$\delta_r Q = -b \delta_r R b^\dagger. \quad (4.4.37)$$

The linear coefficient of x in C_r is automatically zero,

$$\partial_r b + \delta_r Q b + b \delta_r R = 0, \quad (4.4.38)$$

since $\partial_r b = 0$. Therefore C_r is indeed independent of x ,

$$C_r = \partial_r a + \delta_r Q a + a \delta_r R. \quad (4.4.39)$$

It is straightforward to see that C_r satisfies the first condition to be a zero-mode, $a^\dagger C_r = (a^\dagger C_r)^\top$, since R is an orthogonal matrix and $\delta_r R^\top = -\delta_r R$. For the second condition, $b^\dagger C_r = (b^\dagger C_r)^\top$, we require

$$a^\dagger \partial_r a - (a^\dagger \partial_r a)^\top - a^\dagger b \delta_r R b^\dagger a - b^\dagger a \delta_r R a^\dagger b + \mu^{-1} \delta_r R + \delta_r R \mu^{-1} = 0, \quad (4.4.40)$$

where

$$a^\dagger a = \mu^{-1} \quad (4.4.41)$$

is real and invertible. To find the zero-mode in the r direction we need to solve this constraint for $\delta_r R$ in terms of parameters appearing in a . This is now a purely algebraic constraint on zero-modes.

The inner product of zero-modes

Now that we have an expression for the zero-modes we may substitute them into the inner product and find the metric. Once again this appears to be a difficult problem involving evaluating an integral over the spatial directions. However, there is an identity of Corrigan [96] that allows us to express the trace of the zero-modes as a total derivative and avoid having to evaluate the integral.

Claim 4.4.2. *If $\delta_r A_i$ are zero-modes in the form*

$$\delta_r A_i = -iU^\dagger C_r \bar{e}_i f b^\dagger U + iU^\dagger b f e_i C_r^\dagger U, \quad (4.4.42)$$

then

$$\text{Tr}(\delta_r A_i \delta_s A_i) = -\frac{1}{2} \partial^2 \text{Tr} \left(C_r^\dagger (1 + P) C_s f \right). \quad (4.4.43)$$

A brute force proof of this claim is given in the appendix of [97]. Below we present an independently derived proof by a similar brute force method.

Proof. We can show this identity directly by expanding both sides and checking that the terms match. We begin with the right hand side,

$$\begin{aligned} & -\frac{1}{2}\partial^2 \operatorname{Tr} \left(C_r^\dagger (1+P) C_s f \right) \\ & = -\frac{1}{2} \operatorname{Tr} \left(C_r^\dagger \partial^2 P C_s f + 2C_r^\dagger \partial_i P C_s \partial_i f + C_r^\dagger (1+P) C_s \partial^2 f \right). \end{aligned} \quad (4.4.44)$$

Expanding out the derivatives we find

$$\partial_i f = -f(\bar{e}_i b^\dagger \Delta + \Delta^\dagger b e_i) f, \quad (4.4.45)$$

$$\partial^2 f = -2f \bar{e}_i b^\dagger P b e_i f, \quad (4.4.46)$$

$$\partial_i P = -P e_i b f \Delta^\dagger - \Delta f b^\dagger \bar{e}_i P, \quad (4.4.47)$$

$$\partial^2 P = -4f b f^\dagger P - 4P b f b^\dagger + 2\Delta f \bar{e}_i b^\dagger P b e_i f \Delta^\dagger. \quad (4.4.48)$$

The initial expressions are clearly symmetric in r and s , and when we expand the derivatives many terms appear alongside their conjugate but with r and s swapped over. We will assume that all appearances of r and s are implicitly symmetric so that these terms can be written as one. For example,

$$\operatorname{Tr} \left(C_r^\dagger b f b^\dagger P C_s f + C_r^\dagger P b f b^\dagger C_s f \right) = 2 \operatorname{Tr} \left(C_r^\dagger b f b^\dagger P C_s f \right). \quad (4.4.49)$$

With this implicit symmetry between r and s , the right hand side becomes,

$$\begin{aligned} & -\frac{1}{2}\partial^2 \operatorname{Tr} \left(C_r^\dagger (1+P) C_s f \right) \\ & = \operatorname{Tr} \left(4C_r^\dagger b f b^\dagger P C_s f \right. \\ & \quad - C_r^\dagger \Delta f \bar{e}_i b^\dagger P b e_i f \Delta^\dagger C_s f + C_r^\dagger (1+P) C_s f \bar{e}_i b^\dagger P b e_i f \\ & \quad \left. - 2C_r^\dagger P e_i b f \Delta^\dagger C_s f \bar{e}_i b^\dagger \Delta f - 2C_r^\dagger \Delta f b^\dagger \bar{e}_i P C_s f \bar{e}_i b^\dagger \Delta f \right). \end{aligned} \quad (4.4.50)$$

We will eliminate all explicit references to e_i by making use of the following quaternion identities,

$$e_i q \bar{e}_i = 4 \operatorname{Re}(q) = 2 \operatorname{Tr}(q) e_4, \quad (4.4.51)$$

$$e_i q e_i = \bar{e}_i q \bar{e}_i = -2\bar{q}. \quad (4.4.52)$$

We also make use of the invariance of $b^\dagger C_r$, $b^\dagger \Delta$ and $\Delta^\dagger C_r$ under transposition, so

that we can write

$$e_i \Delta^\dagger C_s \bar{e}_i = 2(\Delta^\dagger C_s + C_s^\dagger \Delta), \quad (4.4.53)$$

$$\bar{e}_i b^\dagger P C_s \bar{e}_i = -2(C_s^\dagger b - \Delta^\dagger b f C_s^\dagger \Delta), \quad (4.4.54)$$

$$\bar{e}_i b^\dagger P b e_i = 2(b^\dagger P b + b^\dagger b - \Delta^\dagger b f b^\dagger \Delta). \quad (4.4.55)$$

These can be used to express the right hand side of the identity as

$$\begin{aligned} & -\frac{1}{2} \partial^2 \text{Tr} \left(C_r^\dagger (1 + P) C_s f \right) \\ & = 4 \text{Tr} \left(C_r^\dagger b f b^\dagger P C_s f + C_r^\dagger P C_s f b^\dagger P b f + C_r^\dagger P C_s f b^\dagger b f \right. \\ & \quad \left. - C_r^\dagger P C_s f \Delta^\dagger b f b^\dagger \Delta f - C_r^\dagger P b f \Delta^\dagger C_s f b^\dagger \Delta f \right). \end{aligned} \quad (4.4.56)$$

The left hand side can be expanded in a similar way, again with an implicit symmetry between r and s , and using $U U^\dagger = P$, to give

$$\begin{aligned} & \text{Tr} (\delta_r A_i \delta_s A_i) \\ & = -2 \text{Tr} \left(C_r \bar{e}_i f b^\dagger P C_s \bar{e}_i f b^\dagger P - b f e_i C_r^\dagger P C_s \bar{e}_i f b^\dagger P \right) \\ & = 4 \text{Tr} \left((C_r^\dagger b - \Delta^\dagger f C_r^\dagger \Delta) f b^\dagger P C_s f + C_r^\dagger P C_s f (b^\dagger P b + b^\dagger b - \Delta^\dagger b f b^\dagger \Delta) f \right). \end{aligned} \quad (4.4.57)$$

These expressions can now clearly be seen to be equal. □

The metric can now be expressed as

$$\begin{aligned} g_{rs} & = \int d^4 x \text{Tr} (\delta_r A_i \delta_s A_i) \\ & = 2\pi^2 \text{Tr} \left(C_r^\dagger P_\infty C_s + C_r^\dagger C_s \right), \end{aligned} \quad (4.4.58)$$

where we have used Stokes' theorem in the final line to integrate over the boundary at infinity, and the projector becomes

$$P_\infty \equiv \lim_{|x| \rightarrow \infty} P = \lim_{|x| \rightarrow \infty} \left(\mathbb{1}_{k+1} - \Delta f \Delta^\dagger \right). \quad (4.4.59)$$

If we expand C_r in terms of $\partial_r a$ and $\delta_r R$ then we arrive at our final algebraic expression for the metric:

$$g_{rs} = 2\pi^2 \text{Tr} \left(\partial_r a^\dagger (1 + P_\infty) \partial_s a - \left(a^\dagger \partial_r a - (a^\dagger \partial_r a)^\top \right) \delta_s R \right). \quad (4.4.60)$$

The quantity $\partial_r a$ is given directly in terms of the ADHM data, and $\delta_r R$ is determined by the purely algebraic constraint in equation (4.4.40), again in terms of the ADHM

data. We will use this form of the metric in Chapter 5 to calculate the metric on the moduli space of charge two instantons with an $SU(2)$ gauge group.

4.5 Dyonic instantons

Dyonic instantons are instanton solutions with an additional excited scalar field [64]. These appear naturally in the low energy world-volume theory of parallel D4-branes which is described by five dimensional maximally supersymmetric Yang-Mills. This theory contains five scalar fields corresponding to the five transverse directions of the D4-branes, but we will only consider a single excited scalar field, Φ . The bosonic part of the action is then

$$S = - \int d^5x \operatorname{Tr} \left(\frac{1}{4} F_{\mu\nu} F^{\mu\nu} + \frac{1}{2} D_\mu \Phi D^\mu \Phi \right). \quad (4.5.1)$$

The energy of this system is

$$E = \int d^4x \operatorname{Tr} \left(\frac{1}{2} F_{i0} F_{i0} + \frac{1}{4} F_{ij} F_{ij} + \frac{1}{2} D_0 \Phi D_0 \Phi + \frac{1}{2} D_i \Phi D_i \Phi \right). \quad (4.5.2)$$

Once again the Bogomol'nyi bound on the energy can be found by completing the square,

$$\begin{aligned} E &= \int d^4x \operatorname{Tr} \left(\frac{1}{8} (F_{ij} \pm \frac{1}{2} \varepsilon_{ijkl} F_{kl})^2 + \frac{1}{2} (F_{i0} \pm D_i \Phi)^2 + \frac{1}{2} (D_0 \Phi)^2 \right. \\ &\quad \left. \mp \frac{1}{8} \varepsilon_{ijkl} F_{ij} F_{kl} \mp F_{i0} D_i \Phi \right) \\ &\geq 2\pi^2 |k| + |Q_E|. \end{aligned} \quad (4.5.3)$$

The energy is bounded below by the topological charge, k , as before,

$$k = \frac{1}{8\pi^2} \int d^4x \operatorname{Tr} \left(\frac{1}{2} \varepsilon_{ijkl} F_{ij} F_{kl} \right), \quad (4.5.4)$$

but there is now another conserved charge, Q_E , which is the electric charge,

$$Q_E = \int d^4x \operatorname{Tr} (F_{i0} D_i \Phi) = \int d^4x \partial_i \operatorname{Tr} (F_{i0} \Phi). \quad (4.5.5)$$

The energy bound is saturated by static solutions which satisfy the following BPS equations:

$$F_{ij} = \pm \frac{1}{2} \varepsilon_{ijkl} F_{kl}, \quad (4.5.6)$$

$$F_{i0} = \pm D_i \Phi. \quad (4.5.7)$$

We will again restrict our attention to the solutions with positive signs. The self-dual field equation for the four spatial components of A_i is unmodified so the instanton is undistorted in the spatial directions by the addition of a scalar field. The second BPS equation can be satisfied by taking

$$A_0 = \Phi. \tag{4.5.8}$$

This does not place any additional constraints on Φ , but it must still satisfy its equation of motion,

$$D^2\Phi = 0. \tag{4.5.9}$$

The D4-brane system is BPS so Φ may have an arbitrary vacuum expectation value (VEV) corresponding to the branes being separated in one of the transverse directions,

$$\Phi|_{|x|=\infty} = iq, \tag{4.5.10}$$

where q is a purely imaginary quaternion in the 2×2 complex matrix representation we used previously in the ADHM construction. The value of Φ must be constant at infinity so that the energy is finite.

For each possible VEV, the equation of motion for Φ has a unique solution in the background of each instanton. In general we will also work with a specific VEV so that instantons and dyonic instantons are in one-to-one correspondence with each other, with the only difference being the presence of the scalar field or not. This means that the moduli space of instantons is identical to the moduli space of dyonic instantons, at least topologically. In a moment we will see that the scalar field does not distort the metric on the moduli space but it does introduce a potential term to the low energy dynamics.

We previously chose $A_0 = \Phi$ in our solution to the BPS equations, but we may perform a gauge transformation by $\Omega = \exp(t\Phi)$ which will set A_0 to zero. The spatial components are then rotating through the gauge group in the remaining unbroken $U(1)$ symmetry picked out by the direction of the scalar VEV, q . The speed of rotation is determined by the magnitude of q . This situation is analogous to 1/4-BPS monopole dyons where there is an additional scalar field and the electric charge can be seen as a rotation through the gauge group [68].

4.5.1 The ADHM construction of the scalar field

We want to find the solution for Φ in the background of a general instanton, and once again the ADHM construction renders solving a differential equation unnecessary and lets us use the ADHM algebra to reduce the problem to an algebraic one. The following ansatz for Φ and the techniques shown below for solving the equations of motion were

first introduced in reference [97]. The ansatz for Φ is:

$$\Phi = iU^\dagger \mathcal{A}U, \quad \mathcal{A} = \begin{pmatrix} q & 0 \\ 0 & P \end{pmatrix}. \quad (4.5.11)$$

Here U is the null vector from the ADHM construction, q is a pure imaginary quaternion and P is a $k \times k$ real anti-symmetric matrix. The VEV of Φ is given by iq .

The matrix P is determined by solving the equation of motion $D^2\Phi = 0$. Using the ADHM algebra presented previously, a straightforward but lengthy calculation gives

$$D^2\Phi = -4iU^\dagger \{bf b^\dagger, \mathcal{A}\}U + 4iU^\dagger bf \operatorname{Tr}_2(\Delta^\dagger \mathcal{A} \Delta) f b^\dagger U. \quad (4.5.12)$$

The trace, Tr_2 , in the second term is only over the quaternionic blocks and therefore picks out twice the real part of its argument. Using the block diagonal form of \mathcal{A} , the first term is $-4iU^\dagger \{f, P\}U$. The lower $k \times k$ block of the ADHM data is $M' = M - \mathbb{1}_k x$ and so we can rewrite the trace in the second term as

$$\begin{aligned} \operatorname{Tr}_2(\Delta^\dagger \mathcal{A} \Delta) &= \operatorname{Tr}_2(L^\dagger q L) + \operatorname{Tr}_2(M'^\dagger P M') \\ &= \operatorname{Tr}_2(L^\dagger q L) + \frac{1}{2} \operatorname{Tr}_2([M'^\dagger, P]M' - M'^\dagger[M', P] + \{P, M'^\dagger M'\}) \\ &= \operatorname{Tr}_2(L^\dagger q L) + \frac{1}{2} \operatorname{Tr}_2([M'^\dagger, P]M' - M'^\dagger[M', P] + \{P, f^{-1}\} - \{P, L^\dagger L\}), \end{aligned} \quad (4.5.13)$$

where we have used $\Delta^\dagger \Delta = L^\dagger L + M'^\dagger M' = f^{-1}$. In the commutator terms all x dependence is proportional to $\mathbb{1}_k$ and vanishes. Thus

$$\begin{aligned} \frac{1}{2} \operatorname{Tr}_2([M'^\dagger, P]M' - M'^\dagger[M', P]) &= \frac{1}{2} \operatorname{Tr}(\bar{e}_i e_j)([M_i, P]M_j - M_i[M_j, P]) \\ &= -[M_i, [M_i, P]]. \end{aligned} \quad (4.5.14)$$

Combining all of this we have

$$\begin{aligned} D^2\Phi &= -4i \left(U^\dagger \{f, P - \frac{1}{2} \operatorname{Tr}_2(P)\} U \right. \\ &\quad \left. + U^\dagger b f \left(\operatorname{Tr}_2(L^\dagger q L) - [M_i, [M_i, P]] - \{P, L_i^\dagger L_i\} \right) f b^\dagger U \right). \end{aligned} \quad (4.5.15)$$

Since P is real, the quantity $(P - \frac{1}{2} \operatorname{Tr}(P))$ is zero. So P must satisfy

$$\operatorname{Tr}_2(L^\dagger q L) - [M_i, [M_i, P]] - \{P, L_i^\dagger L_i\} = 0. \quad (4.5.16)$$

We can see from the symmetry properties of the other quantities involved that P must be antisymmetric as expected. Note that the i and j indices in this expression are for the quaternion components of the matrices, not the matrix entries.

Finding the scalar field Φ is now simply a matter of solving these linear equations

for the components of P in terms of the ADHM data matrices, L and M , in the appropriate instanton background.

4.5.2 The moduli space potential

We have seen that for instantons the effective action for their low energy dynamics is a sigma-model action with a metric given by the natural metric on the moduli space. For dyonic instantons the additional scalar field does not alter this metric, but the effective action now contains a potential on the moduli space. The potential arises from the electric charge which now varies across the moduli space, unlike the topological charge. For lack of a better term, we will continue to use the expression ‘zero-mode’ to describe directions in the moduli space even though they now no longer strictly correspond to flat energy directions. We will also continue to use the term ‘geodesic’ to describe motion on this space in the presence of a potential.

Our approach to the low energy dynamics is identical to before. The only time dependence in A_i and Φ is through the moduli space coordinates: $A_i(\mathbf{z}(t); \mathbf{x})$ and $\Phi(\mathbf{z}(t); \mathbf{x})$. Once again we ask that our ansatz satisfy Gauss’s law, which is now

$$D_i F_{i0} + [D_0 \Phi, \Phi] = 0. \quad (4.5.17)$$

This can no longer be satisfied exactly, but we can solve Gauss’s law to first order if we again modify A_0 away from the stationary solution by an amount proportional to the velocity:

$$A_0 = \Phi + \dot{z}^r \epsilon_r. \quad (4.5.18)$$

The electric component of the field strength, F_{i0} , is then

$$F_{i0} = -(\dot{z}^r \delta_r A_i - D_i \Phi), \quad (4.5.19)$$

where $\delta_r A_i$ is the same zero-mode as before. The first term in Gauss’s law, $D_i F_{i0}$, is still zero since the static equation of motion for the scalar field, $D_i D_i \Phi = 0$, is unchanged by the additional time dependence. The second term in Gauss’s law, $[D_0 \Phi, \Phi]$, is non-zero but is of order $\dot{z}^r |q|^2$ where $|q|$ is the magnitude of the VEV of Φ . We will see more explicitly below that the moduli space approximation is valid when \dot{z} and q are small, so Gauss’s law is satisfied in this regime.

Before finding the effective action on the dyonic instanton moduli space, we note that $D_i \Phi$ satisfies the same conditions as $\delta_r A_i$ for being a zero mode. It is a solution to the linear self-dual equation and satisfies the gauge fixing condition, $D_i D_i \Phi = 0$. Since the zero-modes $\delta_r A_i$ ($r = 1, \dots, 8k$) form a basis for zero-modes on the moduli space, we can express $D_i \Phi$ as

$$D_i \Phi = |q| K^r \delta_r A_i, \quad (4.5.20)$$

for some vector K^r , where we have factored out the magnitude of the scalar VEV, $|q|$. If we consider $D_i\Phi$ at infinity then it is a global gauge transformation by iq . For $SU(2)$ there will be three zero-modes corresponding to a global gauge transformation and since such a gauge rotation is a symmetry of the full Yang-Mills theory, these transformations descend to Killing vectors of the moduli space metric. The vector K^r is therefore a Killing vector of the metric, corresponding to the unbroken global gauge transformation in the $U(1)$ direction specified by q .

As with 1/4-BPS monopole dyons, we can perform a coordinate transformation of the moduli space [83, 82] so that the effective action may be written neatly as the sum of a metric and potential term. Let us define new coordinates by

$$z^r \rightarrow z^r - |q|K^r t. \quad (4.5.21)$$

Recall that dyonic instantons can be put in a gauge where they are rotating in the unbroken $U(1)$ global gauge group. This coordinate transformation corresponds to moving to a coordinate system in which the dyonic instantons are stationary, $\dot{z} = 0$. This is a compelling reason why it is correct to include global gauge transformations in our directions on the moduli space and therefore in our coordinate system. In this rotating coordinate system the electric components of the field strength are

$$F_{i0} = -(\dot{z}^r - |q|K^r)\delta_r A_i \rightarrow -\dot{z}^r \delta_r A_i. \quad (4.5.22)$$

The effective action becomes,

$$\begin{aligned} S &= \frac{1}{2} \int d^5x \operatorname{Tr} (F_{i0}F_{i0} - D_i\Phi D_i\Phi + D_0\Phi D_0\Phi) \\ &= \frac{1}{2} \int dt g_{rs} \dot{z}^r \dot{z}^s - |q|^2 g_{rs} K^r K^s. \end{aligned} \quad (4.5.23)$$

In the final line we have neglected terms of order $\dot{z}^2|q|^2$ coming from the $(D_0\Phi)^2$ term. This effective action is therefore a valid approximation to the low energy dynamics of dyonic instantons in the limit

$$\dot{z}^2 \ll 1, \quad \text{and} \quad |q|^2 \ll 1, \quad (4.5.24)$$

in comparison to the rest mass of the dyonic instantons. Physically, this is the requirement that the potential on the moduli space is shallow compared to the potential around the moduli space and that the kinetic energy is small. This prevents the motion from being able to climb the sides of the potential surrounding the moduli space and move away from the regime in which this approximation is valid.

Note that the potential on the moduli space is expressed as the square of a Killing

vector of the moduli space metric,

$$V = \frac{1}{2} \int d^5x \operatorname{Tr} (D_i \Phi D_i \Phi) = \frac{1}{2} \int dt |q|^2 g_{rs} K^r K^s. \quad (4.5.25)$$

If we were to consider the full supersymmetric Yang-Mills theory then we would also have fermionic zero modes and a supersymmetric effective action on the moduli space. This form of the potential would then be required by supersymmetry.

For stationary dyonic instantons which satisfy $D_i \Phi = F_{i0}$, the potential is equal to the electric charge, Q_E . However, for slow moving dyonic instantons the electric charge will have additional contributions from the kinetic terms in F_{i0} . As with the equations of motion, the electric charge is conserved to order $\dot{z}|q|^2$ in the moduli space approximation.

Chapter 5

The moduli space

So far we have given an overview of the moduli space of instantons with general topological charge and an $SU(2)$ gauge group. In this chapter we will focus our attention on instantons of charge two and lay the groundwork that will allow us to explore their low energy dynamics in Chapter 6. The contents of this chapter are largely calculational; we will use an explicit parameterisation of the ADHM data to calculate expressions for the metric and potential on the moduli space of charge two instantons.

In Section 5.1 we will begin by understanding the parameterisation of the ADHM data of charge two instantons. The moduli space is 16 dimensional so the ADHM data must have 16 free parameters. We will see that these parameters can be split into four quaternionic parameters, with two parameters describing each instanton's position and two parameters describing the size and internal gauge orientation of each instanton. In Section 5.2 we will use the method outlined previously in Chapter 4 to calculate the metric in terms of these ADHM parameters. In Section 5.3 we will perform a similar calculation for the potential on the moduli space of dyonic instantons. The moduli space has conical singularities corresponding to instantons of zero size and in Section 5.4 we will see how these arise through a quotient of the moduli space by the underlying symmetries of the ADHM data. Finally in Section 5.5 we will exhibit some geodesic submanifolds of the moduli space which will prove useful in limiting the number of parameters we need to consider in the numerical evolution of the equations of motion on the moduli space.

5.1 The ADHM data of charge two instantons

We will begin by finding an explicit parameterisation of the ADHM data for a charge two instanton. We know that the lower block matrix, M , in the ADHM data must be symmetric but we will make no other assumptions, so the following parameterisation

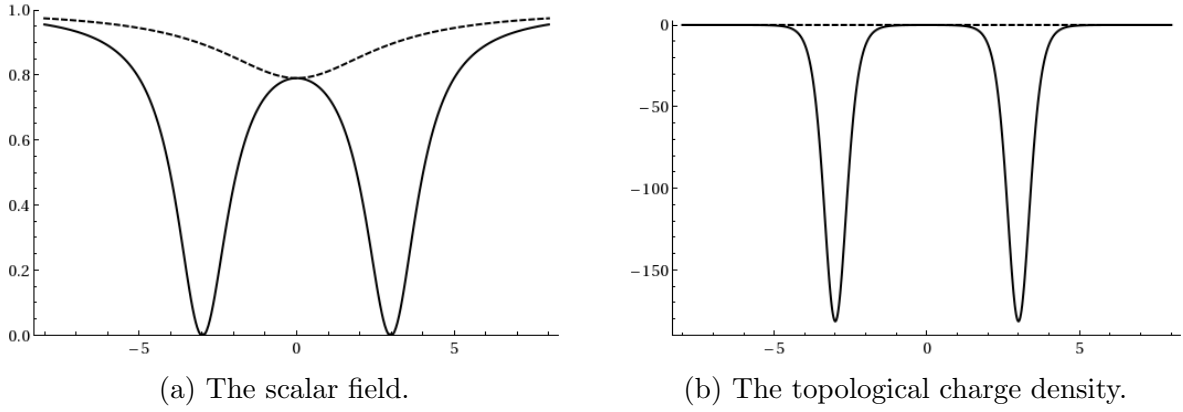


Figure 5.1: Two separated instantons. The solid lines show the fields along the x_4 (real) axis and the dashed lines show the fields along the x_2 -axis. This configuration corresponds to the ADHM parameters $v_1 = e_4$, $v_2 = e_1$ and $\tau = 3e_4$.

is the most general [94]:

$$\Delta(x) = \begin{pmatrix} v_1 & v_2 \\ \tilde{\rho} + \tau & \sigma \\ \sigma & \tilde{\rho} - \tau \end{pmatrix} - x \begin{pmatrix} 0 & 0 \\ 1 & 0 \\ 0 & 1 \end{pmatrix}. \quad (5.1.1)$$

This form is convenient since all of the parameters have a direct physical interpretation in the resulting instanton solution. The quaternionic components of the two diagonal entries in the lower block, $\tilde{\rho} + \tau$ and $\tilde{\rho} - \tau$, can be interpreted as four-vectors and describe the positions of the two instantons in the four spatial dimensions. The parameter $\tilde{\rho}$ is the centre of mass and factors out into an uninteresting flat direction in the metric. We will set $\tilde{\rho}$ to zero for the rest of this thesis. When the magnitude of τ is much larger than the magnitudes of v_1 and v_2 , the instantons are well separated and form two distinct lumps. Each lump can be approximated by a charge one instanton which is rotationally symmetric. An example cross section of the topological charge and scalar field is shown in Figure 5.1 for large τ . As τ decreases the individual lumps move closer together and begin to deform into each other. When the magnitude of τ is equal to the magnitude of σ , the instantons are coincident and form a single lump at the origin with axial symmetry. A cross section of the topological charge and scalar field for this axially symmetric charge two instanton is shown in Figure 5.2. We will discuss the role of σ and the behaviour of coincident instantons more in Chapter 6.

The magnitudes of v_1 and v_2 describe the size of each instanton lump while the unit quaternions, \hat{v}_1 and \hat{v}_2 , describe their alignment in the gauge group. To understand what we mean by the gauge alignment, note that for well separated instantons the gauge field generated by the above ADHM data is approximately that of two superimposed 't

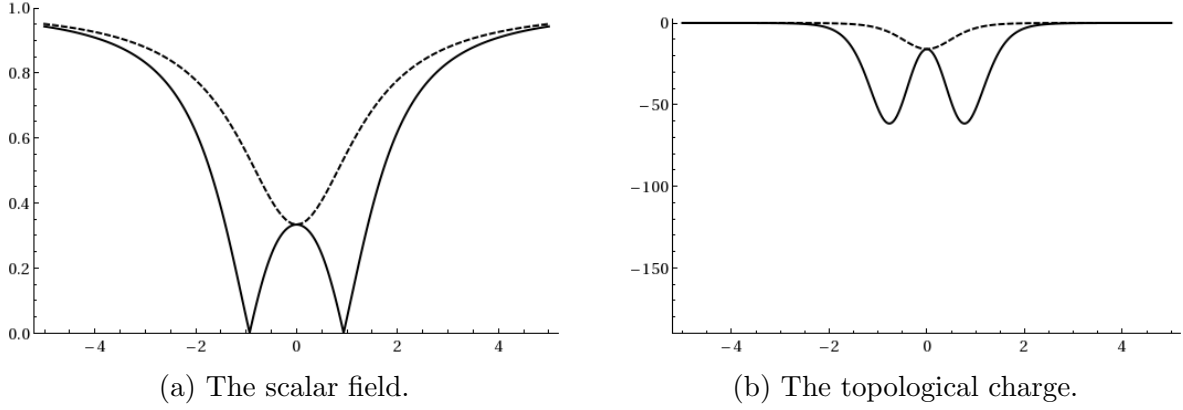


Figure 5.2: Two coincident instantons. The solid lines show the fields along the x_4 (real) axis and the dashed lines show the fields along the x_2 -axis. Note that the fields are rotationally symmetric in the (x_4, x_1) plane when coincident. This configuration corresponds to the ADHM parameters $v_1 = e_4$, $v_2 = e_1$ and $\tau = \frac{1}{\sqrt{2}}e_4$.

Hooft instantons but with a possible global gauge transformation applied to each one,

$$A_i \approx \frac{|v_1|^2(x - \tau)_j \eta_{ij}^a}{|x - \tau|^2(|x - \tau|^2 + |v_1|^2)} \hat{v}_1 \sigma^a \hat{v}_1^\dagger + \frac{|v_2|^2(x + \tau)_j \eta_{ij}^a}{|x + \tau|^2(|x + \tau|^2 + |v_2|^2)} \hat{v}_2 \sigma^a \hat{v}_2^\dagger. \quad (5.1.2)$$

Recall that $SU(2)$ is isomorphic to the unit quaternions so the action of \hat{v}_1 and \hat{v}_2 is a gauge transformation on each separate lump. We could use the global gauge symmetry to set one of \hat{v}_1 or \hat{v}_2 to the identity but we will keep them explicit since the global gauge rotation is a relevant parameter in the moduli space and plays an important role in the dynamics. The relative gauge alignment, $\hat{v}_1^\dagger v_2$, is physically significant even in the static case. When the instantons are close together the gauge field is more complicated and there is no clear notion of separate lumps or of the relative gauge alignment between them.

The parameter σ is fixed by the ADHM constraint to be [94, 95]

$$\sigma = \frac{\tau}{4|\tau|^2} \Lambda + \alpha \tau, \quad \text{where } \Lambda = (\bar{v}_2 v_1 - \bar{v}_1 v_2), \quad (5.1.3)$$

for any real value of α . The symmetry of the ADHM data in equation (4.3.16) always allows us to set α to zero. In doing so we break the continuous $O(2)$ symmetry in equation (4.3.16) to a discrete subgroup.

The scalar field

Now that we have explicit ADHM data for a charge two instanton, we can solve the ansatz for the scalar field from Chapter 4 and write it explicitly in terms of the ADHM parameters, τ , v_1 and v_2 .

Recall that the ansatz for the scalar field contains a $k \times k$ anti-symmetric matrix,

P , which must satisfy

$$\mathrm{Tr}_2(L^\dagger qL) - [M_i, [M_i, P]] - \{P, L_i^\top L_i\} = 0. \quad (5.1.4)$$

The blocks of the charge two ADHM data are

$$L = \begin{pmatrix} v_1 & v_2 \end{pmatrix}, \quad \text{and} \quad M = \begin{pmatrix} \tau & \sigma \\ \sigma & -\tau \end{pmatrix}. \quad (5.1.5)$$

The first term in our constraint on P is therefore

$$\mathrm{Tr}_2(L^\dagger qL) = \begin{pmatrix} 0 & \frac{1}{2} \mathrm{Tr}(\bar{v}_1 q v_2 - \bar{v}_2 q v_1) \\ \frac{1}{2} \mathrm{Tr}(\bar{v}_2 q v_1 - \bar{v}_1 q v_2) & 0 \end{pmatrix}. \quad (5.1.6)$$

Note that the trace of the quaternions in the 2×2 complex representation picks out twice the real component. If we write P as

$$P = \begin{pmatrix} 0 & p \\ -p & 0 \end{pmatrix}, \quad (5.1.7)$$

then the second and third terms in the constraint are

$$[M_i, [M_i, P]] = 4p \begin{pmatrix} 0 & |\tau|^2 + |\sigma|^2 \\ -(|\tau|^2 + |\sigma|^2) & 0 \end{pmatrix}, \quad (5.1.8)$$

and

$$\{P, L_i^\top L_i\} = p \begin{pmatrix} 0 & |v_1|^2 + |v_2|^2 \\ -(|v_1|^2 + |v_2|^2) & 0 \end{pmatrix}. \quad (5.1.9)$$

The off diagonal entry in P is therefore given by

$$p = \frac{1}{2N_A} \mathrm{Tr}(\bar{v}_1 q v_2 - \bar{v}_2 q v_1), \quad (5.1.10)$$

where

$$N_A = |v_1|^2 + |v_2|^2 + 4(|\tau|^2 + |\sigma|^2). \quad (5.1.11)$$

The scalar field is then given by the expression in Section 4.5.1,

$$\Phi = iU^\dagger \mathcal{A} U, \quad \mathcal{A} = \begin{pmatrix} q & 0 \\ 0 & P \end{pmatrix}. \quad (5.1.12)$$

We will not present the expanded expression for Φ since it does not provide any additional insight. However, this implicit form allows us to easily evaluate Φ in different instanton backgrounds. We will also use this solution for P to calculate the potential

in Section 5.3.

The form of the scalar field for charge two and higher dyonic instantons has been previously studied in detail in the context of D4-branes [70, 71], where the zeroes of the scalar field correspond to where the D4-branes intersect. For coincident instantons, the zeroes of the scalar field lie in a circle, and as the instantons separate the circle of zeroes pinches off into two separate loops which shrink down to a point as the instantons separate to infinity. This has an interpretation as supertubes between the D4-branes which collapse as the instantons become well separated.

5.2 The moduli space metric

We saw in Chapter 4 that the metric on the moduli space can be calculated by performing an appropriate transformation of the ADHM data around the point of interest. The transformation is chosen so that the components of the tangent vectors which are orthogonal to gauge transformations are explicit and can be ignored to give us the zero-modes. The zero-modes are expressed in terms of the ADHM data and their inner product can be calculated algebraically. Now that we have an explicit parameterisation for the charge two ADHM data, we can work out these appropriate transformations and the inner product of the zero-modes which gives us the metric on the moduli space.

Recall from Chapter 4 that the metric is given by

$$ds^2 = 2\pi^2 \operatorname{Tr} \left(da^\dagger (1 + P_\infty) da - \left(a^\dagger da - (a^\dagger da)^\top \right) dR \right), \quad (5.2.1)$$

where the transformation of the ADHM data, dR , satisfies the constraint,

$$a^\dagger da - (a^\dagger da)^\top - a^\dagger b dR b^\dagger a - b^\dagger a dR a^\dagger b + \mu^{-1} dR + dR \mu^{-1} = 0. \quad (5.2.2)$$

With the ADHM data for charge two instantons in equation (5.1.1), the projector at infinity is

$$P_\infty = \lim_{|x| \rightarrow \infty} P = \mathbb{1}_3 - b^\dagger b = \begin{pmatrix} 1 & 0 & 0 \\ 0 & 0 & 0 \\ 0 & 0 & 0 \end{pmatrix}. \quad (5.2.3)$$

The first part of the metric expression in equation (5.2.1) is therefore

$$\begin{aligned} ds_1^2 &= 2\pi^2 \operatorname{Tr} \left(da^\dagger (1 + P_\infty) da \right) \\ &= 4\pi^2 \operatorname{Tr} \left(d\bar{\rho} d\tilde{\rho} + d\bar{v}_1 dv_1 + d\bar{v}_2 dv_2 + d\bar{\tau} d\tau + d\bar{\sigma} d\sigma \right). \end{aligned} \quad (5.2.4)$$

We have included $\tilde{\rho}$ to demonstrate that these directions are flat but these can be neglected from now on. The first four terms are all fundamental parameters, but the

last term involving σ needs to be expanded according to equation (5.1.3),

$$\begin{aligned}
 & 4\pi^2 \operatorname{Tr} (d\bar{\sigma} d\sigma) \\
 &= 2\pi^2 \operatorname{Tr} \left(\frac{1}{8|\tau|^2} d\bar{\Lambda} d\Lambda + \frac{1}{4|\tau|^4} \bar{\Lambda} d\bar{\tau} \tau d\Lambda - \frac{1}{4|\tau|^4} d\bar{\Lambda} \Lambda d|\tau|^2 \right. \\
 & \quad \left. + \frac{1}{8|\tau|^4} |\Lambda|^2 d\bar{\tau} d\tau - \frac{1}{4|\tau|^6} |\Lambda|^2 d\bar{\tau} \tau d|\tau|^2 + \frac{1}{8|\tau|^6} |\Lambda|^2 d|\tau|^2 d|\tau|^2 \right). \tag{5.2.5}
 \end{aligned}$$

We note that

$$\operatorname{Tr} (d|\tau|^2) = \operatorname{Tr} (d\bar{\tau} \tau + \bar{\tau} d\tau) = 2 \operatorname{Tr} (d\bar{\tau} \tau), \tag{5.2.6}$$

so that the terms at order $|\tau|^{-6}$ cancel. The terms at order $|\tau|^{-2}$ have been calculated previously [95] and are

$$\begin{aligned}
 & \frac{1}{8|\tau|^2} \operatorname{Tr} (d\bar{\Lambda} d\Lambda) \\
 &= \frac{1}{|\tau|^2} \left(|v_1|^2 (dv_2 \cdot dv_2) + |v_2|^2 (dv_1 \cdot dv_1) + 2(v_1 \cdot dv_1)(v_2 \cdot dv_2) \right. \\
 & \quad - (dv_2 \cdot v_1)(dv_2 \cdot v_1) - (dv_1 \cdot v_2)(dv_1 \cdot v_2) - 2(v_1 \cdot v_2)(dv_1 \cdot dv_2) \\
 & \quad \left. + 2\varepsilon_{ijkl} v_1^i v_2^j dv_1^k dv_2^l \right), \tag{5.2.7}
 \end{aligned}$$

where

$$p \cdot q = p_a q^a \tag{5.2.8}$$

is the scalar product of quaternions treated as four-vectors. The terms at order $|\tau|^{-4}$ are

$$\frac{1}{8|\tau|^4} \operatorname{Tr} (|\Lambda|^2 d\bar{\tau} d\tau) = \frac{1}{|\tau|^4} (|v_1|^2 |v_2|^2 - (v_1 \cdot v_2)^2) (d\tau \cdot d\tau), \tag{5.2.9}$$

and

$$\begin{aligned}
 & \frac{1}{4|\tau|^4} \operatorname{Tr} (\bar{\Lambda} d\bar{\tau} \tau d\Lambda - d\bar{\Lambda} \Lambda d(\bar{\tau} \tau)) \\
 &= -\frac{1}{4|\tau|^4} \operatorname{Tr} (d\Lambda \bar{\Lambda} \bar{\tau} d\tau) \\
 &= -\frac{1}{4|\tau|^4} \left(\operatorname{Tr} (\operatorname{Re}(d\Lambda \bar{\Lambda}) \operatorname{Re}(\bar{\tau} d\tau)) - \operatorname{Tr} (\operatorname{Im}(\Lambda d\bar{\Lambda}) \operatorname{Im}(\bar{\tau} d\tau)) \right) \\
 &= -\frac{2}{|\tau|^4} (\tau \cdot d\tau) \left(|v_1|^2 (v_2 \cdot dv_2) + |v_2|^2 (v_1 \cdot dv_1) \right. \\
 & \quad \left. - (v_1 \cdot v_2)(v_1 \cdot dv_2) - (v_1 \cdot v_2)(v_2 \cdot dv_1) \right) \\
 & \quad + \frac{1}{2|\tau|^4} \left(\varepsilon_{ijkl} \Lambda^i d\Lambda^j \tau^k d\tau^l + (\Lambda \cdot d\tau)(\tau \cdot d\Lambda) - (\Lambda \cdot \tau)(d\Lambda \cdot d\tau) \right). \tag{5.2.10}
 \end{aligned}$$

In this last line we have used the identity,

$$\begin{aligned} \text{Tr}(\text{Im}(p\bar{q})\text{Im}(r\bar{s})) &= \text{Tr}(\bar{\eta}_{ij}^a \bar{\eta}_{kl}^b e_a e_b) p^i q^j r^k s^l \\ &= 2(\varepsilon_{ijkl} - \delta_{ik}\delta_{jl} + \delta_{il}\delta_{jk}) p^i q^j r^k s^l. \end{aligned} \quad (5.2.11)$$

For the second part of the metric, recall that R is an $O(2)$ transformation with one parameter, θ . Since we require a continuous transformation it must be a rotation and its variation is therefore

$$dR = -d\theta \begin{pmatrix} 0 & 1 \\ -1 & 0 \end{pmatrix}. \quad (5.2.12)$$

Let us define a shorthand quantity, dk , by

$$a^\dagger da - (a^\dagger da)^\top = dk \begin{pmatrix} 0 & 1 \\ -1 & 0 \end{pmatrix}, \quad (5.2.13)$$

where the matrix form is determined by the left hand side being an anti-symmetric matrix with real quaternion components. The constraint placed on dR by equation (5.2.2) becomes

$$d\theta = \frac{dk}{N_A}, \quad (5.2.14)$$

where

$$N_A = |v_1|^2 + |v_2|^2 + 4(|\tau|^2 + |\sigma|^2). \quad (5.2.15)$$

The second part of the metric is therefore

$$\begin{aligned} ds_2^2 &= -2\pi^2 \text{Tr} \left((a^\dagger da - (a^\dagger da)^\top) dR \right) \\ &= -8\pi^2 \frac{dk^2}{N_A}. \end{aligned} \quad (5.2.16)$$

We can calculate dk explicitly from equation (5.2.13) and we find

$$dk = \frac{1}{2} \text{Tr} (\bar{v}_1 dv_2 - \bar{v}_2 dv_1 + 2(\bar{\tau} d\sigma - \bar{\sigma} d\tau)). \quad (5.2.17)$$

The argument in the trace is necessarily real but this can also be seen directly by making use of the ADHM constraints or the explicit form of σ . We can expanded dk as

$$\begin{aligned} dk &= (v_1 \cdot dv_2) - (v_2 \cdot dv_1) \\ &\quad - \frac{2}{|\tau|^2} \left(\varepsilon_{ijkl} v_2^i v_1^j \tau^k d\tau^l + (v_2 \cdot \tau)(v_1 \cdot d\tau) - (v_1 \cdot \tau)(v_2 \cdot d\tau) \right). \end{aligned} \quad (5.2.18)$$

Putting all of this together, the metric on the moduli space of charge two instantons

with an $SU(2)$ gauge group is

$$\begin{aligned}
 \frac{ds^2}{8\pi^2} = & dv_1^2 + dv_2^2 + d\tau^2 \\
 & + \frac{1}{4|\tau|^2} \left(|v_1|^2 dv_2^2 + |v_2|^2 dv_1^2 + 2(v_1 \cdot dv_1)(v_2 \cdot dv_2) - (v_1 \cdot dv_2)^2 \right. \\
 & \quad \left. - (v_2 \cdot dv_1)^2 - 2(v_1 \cdot v_2)(dv_1 \cdot dv_2) + 2\varepsilon_{ijkl} v_1^i v_2^j dv_1^k dv_2^l \right) \\
 & + \frac{1}{4|\tau|^4} (|v_1|^2 |v_2|^2 - (v_1 \cdot v_2)^2) d\tau^2 \\
 & - \frac{1}{2|\tau|^4} \left(|v_1|^2 (v_2 \cdot dv_2) + |v_2|^2 (v_1 \cdot dv_1) \right. \\
 & \quad \left. - (v_1 \cdot v_2)(v_1 \cdot dv_2) - (v_1 \cdot v_2)(v_2 \cdot dv_1) \right) \tau \cdot d\tau \\
 & + \frac{1}{8|\tau|^4} \left(\varepsilon_{ijkl} \Lambda^i d\Lambda^j \tau^k d\tau^l + (\Lambda \cdot d\tau)(\tau \cdot d\Lambda) - (\Lambda \cdot \tau)(d\Lambda \cdot d\tau) \right) \tau \cdot d\tau \\
 & - \frac{1}{N_A} \left(v_1 \cdot dv_2 - v_2 \cdot dv_1 \right. \\
 & \quad \left. - \frac{2}{|\tau|^2} (\varepsilon_{ijkl} v_2^i v_1^j \tau^k d\tau^l + (v_2 \cdot \tau)(v_1 \cdot d\tau) - (v_1 \cdot \tau)(v_2 \cdot d\tau)) \right)^2.
 \end{aligned} \tag{5.2.19}$$

The terms on the first line of the metric correspond to the individual movement of each instanton lump in flat space. The remaining terms describe the interaction of the two instanton lumps. Note that these interaction terms fall off quadratically as the separation is increased. This metric has been previously calculated up to order $|\tau|^{-2}$ in reference [95] although we point out that our calculation differs by a factor of two in the final line.

5.3 The moduli space potential

The potential on the moduli space can be calculated directly from the ansatz for Φ in equation (5.1.12) [97]. Recall that the potential on the moduli space arises from the following term in the Yang-Mills action:

$$V = \int d^4x \operatorname{Tr} (D_i \Phi D_i \Phi). \tag{5.3.1}$$

If we integrate by parts and use the equation of motion for Φ , the potential becomes

$$V = \lim_{R \rightarrow \infty} \int_{|x|=R} dS^3 \hat{x}_i \operatorname{Tr} (\Phi D_i \Phi). \tag{5.3.2}$$

In terms of the ADHM data, the covariant derivative of Φ is

$$D_i \Phi = iU^\dagger e_i b f \Delta^\dagger \mathcal{A} U + iU^\dagger \mathcal{A} \Delta f \bar{e}_i b^\dagger U. \quad (5.3.3)$$

For two instantons with ADHM data as in equation (5.1.1), the components of U must satisfy,

$$\bar{v}_1 U_1 + (\bar{\tau} - \bar{x}) U_2 + \bar{\sigma} U_3 = 0, \quad (5.3.4)$$

$$\bar{v}_2 U_1 + \bar{\sigma} U_2 - (\bar{\tau} + \bar{x}) U_3 = 0, \quad (5.3.5)$$

which can be solved in the limit $|x| \rightarrow \infty$ by

$$U_1 \rightarrow 1, \quad (5.3.6)$$

$$U_2 \rightarrow \frac{x}{|x|^2} \bar{v}_1, \quad (5.3.7)$$

$$U_3 \rightarrow \frac{x}{|x|^2} \bar{v}_2. \quad (5.3.8)$$

Expanding the leading order terms in the potential gives

$$\hat{x}_i D_i \Phi = 2 \frac{i}{|x|^3} (v_2 p \bar{v}_1 - v_1 p \bar{v}_2 + q(|v_1|^2 + |v_2|^2)) + \mathcal{O}(|x|^{-4}). \quad (5.3.9)$$

Recall that p is

$$p = \frac{1}{2N_A} \text{Tr} (\bar{v}_1 q v_2 - \bar{v}_2 q v_1), \quad (5.3.10)$$

so that the potential is given by

$$\begin{aligned} V &= -2 \lim_{R \rightarrow \infty} \int_{|x|=R} dS^3 \frac{1}{|x|^3} \text{Tr} (q(v_2 p \bar{v}_1 - v_1 p \bar{v}_2) + q^2(|v_1|^2 + |v_2|^2)) + \mathcal{O}(|x|^{-4}) \\ &= 8\pi^2 |q|^2 \left(|v_1|^2 + |v_2|^2 - \frac{1}{N_A} |\bar{v}_2 \hat{q} v_1 - \bar{v}_1 \hat{q} v_2|^2 \right). \end{aligned} \quad (5.3.11)$$

The first two terms in the potential are the potentials arising from each individual dyonic instanton, while the final term describes their interaction and again falls off quadratically in the separation.

5.4 Singularities in the metric

We have used the ADHM construction to find the metric on the moduli space but we can also use this method to understand the topology of the moduli space. It is well known that the moduli space has singularities corresponding to instantons of zero size and these can be understood as the conical singularities where the moduli space

is quotiented by discrete symmetries of the ADHM data. Recall that by fixing the parameter $\alpha = 0$ in equation (5.1.3) we have broken the continuous $O(2)$ symmetry of the ADHM data in equation (4.3.16). However, there still remains a discrete subgroup of symmetries. The moduli space is quotiented by these symmetries since they identify equivalent parameterisations of the ADHM data which correspond to the same gauge field. The moduli space therefore has an orbifold structure with conical singularities at the fixed points of these symmetries.

Consider a transformation of the ADHM data where R in equation (4.3.16) is a rotation matrix. This gives the equivalent parameterisation:

$$\begin{aligned}\tilde{v}_1 &= v_1 c - v_2 s, & \tilde{v}_2 &= v_1 s + v_2 c, \\ \tilde{\tau} &= (c^2 - s^2)\tau - 2cs\sigma, \\ \tilde{\sigma} &= (c^2 - s^2)\sigma + 2cs\tau,\end{aligned}\tag{5.4.1}$$

where $c = \cos(\theta)$ and $s = \sin(\theta)$. If R is a reflection matrix instead then,

$$\begin{aligned}\tilde{v}_1 &= v_1 c + v_2 s, & \tilde{v}_2 &= v_1 s - v_2 c, \\ \tilde{\tau} &= (c^2 - s^2)\tau + 2cs\sigma, \\ \tilde{\sigma} &= -(c^2 - s^2)\sigma + 2cs\tau.\end{aligned}\tag{5.4.2}$$

For these to leave $\alpha = 0$ invariant we must have either

$$c^2 - s^2 = 0, \quad \text{or} \quad cs = 0,\tag{5.4.3}$$

so that the remaining discrete symmetries are given by rotations or reflections with angle $\theta = (n\pi)/4$ for $n = 0, \dots, 7$. These unbroken symmetries form the dihedral group of order 16.

Let us consider the action of these remaining symmetries and give them a physical interpretation:

1. $c = \pm 1, s = 0$. Under these symmetries, v_1 and v_2 are unchanged or negated. These symmetries correspond to the fact that v_1 and $-v_1$ give the same gauge transformation of A_i , as in equation (5.1.2). Consider a reflection with $c = -1$ where v_1 goes to $-v_1$. Under this symmetry the moduli space is quotiented by \mathbb{Z}_2 with a fixed point at $v_1 = 0$. The moduli space therefore has the topology of a cone around the point $v_1 = 0$, which is a conical singularity. The same arguments apply to the point $v_2 = 0$ when $c = 1$. These singularities correspond to an instanton shrinking to zero size.
2. $c = 0, s = \pm 1$. Under these symmetries, v_1 and v_2 swap roles with a possible change in sign. The parameter describing the instanton separation, τ , is negated.

This corresponds to a relabelling of the instantons so that the instanton described by v_1 is now described by v_2 and vice-versa. The fixed points of these symmetries are when v_1 and v_2 are equal up to a sign, and $\tau = 0$. The singularities at these fixed points are the same singularities described above but in a different parameterisation of the moduli space. To see this, consider the following two equivalent parameterisations,

$$\tau = \varepsilon, \quad \sigma = i, \quad v_1 = 1 + i\varepsilon \quad \text{and} \quad v_2 = 1 - i\varepsilon, \quad (5.4.4)$$

and

$$\tilde{\tau} = i, \quad \tilde{\sigma} = \varepsilon, \quad \tilde{v}_1 = \sqrt{2} \quad \text{and} \quad \tilde{v}_2 = \sqrt{2}i\varepsilon. \quad (5.4.5)$$

These are identified under a reflection with $\theta = \frac{\pi}{4}$. As $\varepsilon \rightarrow 0$, the first of these parameterisations approaches the singularity here. However this is equivalent to the second parameterisation which approaches the zero size instanton singularity mentioned above.

3. $c = \pm \frac{1}{\sqrt{2}}$, $s = \pm \frac{1}{\sqrt{2}}$. These combine v_1 and v_2 in a linear combination, and swap the roles of τ and σ . There are no fixed points except $v_1 = v_2 = \tau = \sigma = 0$. The physical interpretation of this symmetry is less obvious but we will discuss it further in Chapter 6 and see that it is responsible for right angled scattering.

From the string theory viewpoint, the zero size singularities arise from the transition between the Higgs and Coulomb branches of the D4-D0 brane system. It is natural that the world-volume description should break down at this point.

5.5 Geodesic submanifolds

The moduli space has 12 parameters excluding the centre of mass, and integrating the equations of motion on this full space is numerically expensive. We can reduce the range of parameters that we need to consider at one time by finding geodesic submanifolds of the moduli space (we use the term geodesic loosely here to also include motion on the moduli space in the presence of a potential.) If our initial conditions lie within a geodesic submanifold then the evolution will remain within the submanifold for all time. A simple way of finding geodesic submanifolds is as the fixed points of symmetries of the metric and potential.

To be able to see the symmetries more explicitly, let us write the metric in the unexpanded form,

$$ds^2 = 8\pi^2 \left(dv_1 \cdot dv_1 + dv_2 \cdot dv_2 + d\tau \cdot d\tau + d\sigma \cdot d\sigma - \frac{dk^2}{N_A} \right), \quad (5.5.1)$$

where

$$N_A = |v_1|^2 + |v_2|^2 + 4(|\tau|^2 + |\sigma|^2), \quad (5.5.2)$$

and

$$dk = \bar{v}_1 dv_2 - \bar{v}_2 dv_1 + 2(\bar{\tau} d\sigma - \bar{\sigma} d\tau). \quad (5.5.3)$$

The potential is

$$V = 8\pi^2 |q|^2 \left(|v_1|^2 + |v_2|^2 - \frac{1}{N_A} |\bar{v}_2 \hat{q} v_1 - \bar{v}_1 \hat{q} v_2|^2 \right). \quad (5.5.4)$$

The first symmetry that we will consider is conjugation by a unit quaternion, p ,

$$v_1 \rightarrow pv_1\bar{p}, \quad v_2 \rightarrow pv_2\bar{p}, \quad \tau \rightarrow p\tau\bar{p}, \quad \text{under which} \quad \sigma \rightarrow p\sigma\bar{p}. \quad (5.5.5)$$

This is a symmetry of the metric for any p but is only a symmetry of the potential when $p \in \text{span}\{1, q\}$. This symmetry has fixed points when the imaginary parts of v_1 , v_2 and τ are proportional to p . Without loss of generality we can take p and q to be in the direction e_1 so that the geodesic submanifold consists of the points where v_1 , v_2 and τ are complex valued, with their e_2 and e_3 components set to zero. This describes the instantons moving in a two dimensional plane of the full four dimensional space, and each instanton has a gauge orientation in the remaining unbroken $U(1)$ given by the complex phases of v_1 and v_2 . Note that this half-dimensional subspace is the subspace in the Hanany-Tong correspondence between the moduli space of non-commutative instantons and vortices [98]. Since we do not have a non-commutative deformation of the instantons, this subspace corresponds to the strong coupling limit of the vortex theory.

The metric simplifies on this subspace since many of the terms vanish when restricted to only complex values. It is convenient to parameterise this complex submanifold by polar coordinates [95],

$$v_1 = \rho_1(\cos \theta_1 + i \sin \theta_1), \quad (5.5.6)$$

$$v_2 = \rho_2(\cos \theta_2 + i \sin \theta_2), \quad (5.5.7)$$

$$\tau = \omega(\cos \chi + i \sin \chi). \quad (5.5.8)$$

The angles can be combined into a relative and overall gauge rotation,

$$\phi = \theta_1 - \theta_2, \quad (5.5.9)$$

$$\theta = \theta_1 + \theta_2. \quad (5.5.10)$$

The metric and potential on this complex submanifold are then

$$\begin{aligned}
 \frac{ds^2}{8\pi^2} &= d\rho_1^2 + d\rho_2^2 + \frac{1}{4}(\rho_1^2 + \rho_2^2)(d\theta^2 + d\phi^2) + \frac{1}{2}(\rho_1^2 - \rho_2^2) d\theta d\phi \\
 &+ \frac{1}{4\omega^2} (d(R \sin \phi))^2 + \left(1 + \frac{1}{4\omega^4} R^2 \sin^2 \phi\right) (d\omega^2 + \omega^2 d\chi^2) \\
 &- \frac{1}{2\omega^4} (R \sin^2 \phi (\rho_1 d\rho_2 + \rho_2 d\rho_1) + R^2 \cos \phi \sin \phi d\phi) \omega d\omega \\
 &- \frac{1}{N_A} (\cos \phi (\rho_1 d\rho_2 - \rho_2 d\rho_1) + R \sin \phi (d\theta - 2 d\chi))^2,
 \end{aligned} \tag{5.5.11}$$

and

$$\frac{V}{8\pi^2} = |q|^2 \left(\rho_1^2 + \rho_2^2 - \frac{4}{N_A} R^2 \sin^2 \phi \right), \tag{5.5.12}$$

where

$$N_A = \rho_1^2 + \rho_2^2 + 4\omega^2 + \frac{R^2}{\omega^2} \sin^2 \phi, \quad \text{and} \quad R \equiv \rho_1 \rho_2. \tag{5.5.13}$$

Note that the metric has no functional dependence on θ or χ . These correspond respectively to the overall gauge rotation and spatial rotation of the instantons. This is to be expected as these are symmetries of the full field theory and so descend to Killing vectors on the moduli space. In this parameterisation it is clear that V is the square of the Killing vector corresponding to rotations by θ , as described in Chapter 4.

We can restrict to a further submanifold of this complex submanifold by relating the two instantons' sizes and gauge angles. Consider the symmetry,

$$v_1 \rightarrow iv_2, \quad v_2 \rightarrow -iv_1. \tag{5.5.14}$$

The fixed points of this are when $v_1 = iv_2$, or in our polar coordinate parameterisation,

$$\rho_1 = \rho_2, \quad \theta_1 = \theta_2 - \frac{\pi}{2}. \tag{5.5.15}$$

On this submanifold we will drop the subscripts on ρ and θ since they are unnecessary. The metric and potential are

$$\begin{aligned}
 \frac{ds^2}{8\pi^2} &= 2 d\rho^2 + 2\rho^2 d\theta^2 + \frac{\rho^2}{\omega^2} d\rho^2 + \left(1 + \frac{\rho^4}{\omega^4}\right) (d\omega^2 + \omega^2 d\chi^2) \\
 &- \frac{\rho^3}{\omega^3} d\rho d\omega - \frac{4}{N_A} \rho^4 (d\theta - d\chi)^2,
 \end{aligned} \tag{5.5.16}$$

and

$$\frac{V}{8\pi^2} = q^2 \left(2\rho^2 - \frac{4}{N_A} \rho^4 \right), \tag{5.5.17}$$

where

$$N_A = 2\rho^2 + 4\omega^2 + \frac{\rho^4}{\omega^2}. \quad (5.5.18)$$

This submanifold describes two instantons with their gauge orientations locked to be orthogonal.

We can also consider a related symmetry where

$$v_1 \rightarrow v_2, \quad v_2 \rightarrow v_1. \quad (5.5.19)$$

The fixed points of this are when $v_1 = v_2$, and the metric and potential on this submanifold reduce to those of two non-interacting charge one dyonic instantons.

There is another interesting symmetry which will be relevant to our discussion of localised charge two dyonic instantons. We can swap τ and σ with a quaternionic phase,

$$\tau \rightarrow p\sigma, \quad \sigma \rightarrow -p\tau, \quad (5.5.20)$$

where p is a purely imaginary unit quaternion. This has a fixed point when $\tau = p\sigma$ so that $|\tau| = |\sigma|$. We will see in Chapter 6 that this corresponds to the instantons being coincident and axially symmetric. The magnitude of τ must be fixed by

$$|\tau|^2 = \frac{1}{4} |\bar{v}_2 v_1 - \bar{v}_1 v_2|, \quad (5.5.21)$$

which will remove a parameter from the metric on this submanifold. This submanifold is also invariant under the symmetries of ADHM data and is a natural boundary on the fundamental domain of the moduli space.

Chapter 6

Low energy dynamics

In the previous chapter we constructed the metric and potential for the moduli space of two dyonic instantons with an $SU(2)$ gauge group. Armed with these expressions we can now explore the low energy dynamics of two (dyonic) instantons by using the moduli space approximation introduced in Chapter 4. The approximate low energy dynamics of instantons is given by geodesic motion on the moduli space, while the low energy dynamics of dyonic instantons is similar but takes place in the presence of a potential on the moduli space.

The metric and potential are too complicated to solve the equations of motion analytically. We can infer some of the properties of the low energy dynamics from the algebraic properties of the metric, but most of our analysis of the dynamics is through a numerical study. The geodesic submanifolds exhibited in the previous chapter allow us to explore regions of the moduli space with few enough parameters that a numerical study is feasible.

In Section 6.1 we will examine the scattering behaviour of two instantons. We will see that in a head-on collision, instantons will scatter at right angles, like other soliton systems. This can be understood from the symmetries of the underlying ADHM data. We will also see this behaviour explicitly in numerical evolutions of the motion on the moduli space. In Section 6.2 we will review the dynamics of a single dyonic instanton. This will help to put the results for two interacting dyonic instantons in context. In Section 6.3 we will explore the scattering of two dyonic instantons. The addition of a potential has a significant effect on their behaviour, and the scattering angle is modified significantly away from 90° . In Section 6.4 we will look at the geodesic completeness of the moduli space, and we will see that angular momentum may be transferred between the dyonic instantons and one may hit the zero size singularity in finite time. Finally in Section 6.5 we will comment on the stability of localised charge two dyonic instantons.

6.1 Instanton scattering

6.1.1 Right angled scattering

Right angled scattering is a common feature in soliton systems and in this section we will see that instantons are no exception. Right angled scattering of monopoles can be understood from the conical structure of the monopole moduli space which arises when taking the quotient by the symmetry which swaps the identity of the two incoming monopoles. The instanton moduli space has a more complicated structure, but we can still understand right angled scattering by considering the moduli space quotiented by the underlying symmetries of the ADHM data.

Let us begin by understanding the role of the separation parameter τ in describing the different configuration of charge two instantons. When τ is large it describes two well separated charge one instantons at τ and $-\tau$, as can be seen in Figure 6.1a. However, this interpretation as two distinguishable lumps begins to break down when τ is of a similar magnitude to σ . As a first observation, we note that the charge two instanton is axially symmetric when $|\tau| = |\sigma|$, as in Figure 6.1d, and there is no clear notion of two charge one instantons any more. When the magnitude of τ is less than the magnitude of σ , the charge one instantons separate again at right angles, as seen in Figures 6.1e and 6.1f. So clearly σ also plays an important role in describing the position of the instantons.

This relation between τ and σ can be understood from the symmetries of the ADHM data which swap the roles of τ and σ . For example, consider a transformation of the ADHM data as in equation (5.4.2) by a reflection with angle $\theta = \frac{\pi}{4}$,

$$\tilde{\Delta} = \begin{pmatrix} \frac{1}{\sqrt{2}}(v_1 + v_2) & \frac{1}{\sqrt{2}}(v_1 - v_2) \\ \sigma & \tau \\ \tau & -\sigma \end{pmatrix}. \quad (6.1.1)$$

This symmetry leaves the fields unchanged, and these parameters must have an equivalent physical interpretation as those in the original ADHM parameterisation. It follows that σ must have an equal claim to describe the instantons' separation.

Recall that σ is given by

$$\sigma = \frac{\tau}{4|\tau|^2}\Lambda, \quad \text{where } \Lambda = \bar{v}_2 v_1 - \bar{v}_1 v_2, \quad (6.1.2)$$

and so has a magnitude inversely proportional to the magnitude of τ . When τ is large, σ is small and τ provides a good description of the instantons' separation. However, as τ grows smaller and is of a similar magnitude to σ this description breaks down and the instantons become indistinguishable. As τ goes to zero, σ grows large and instead

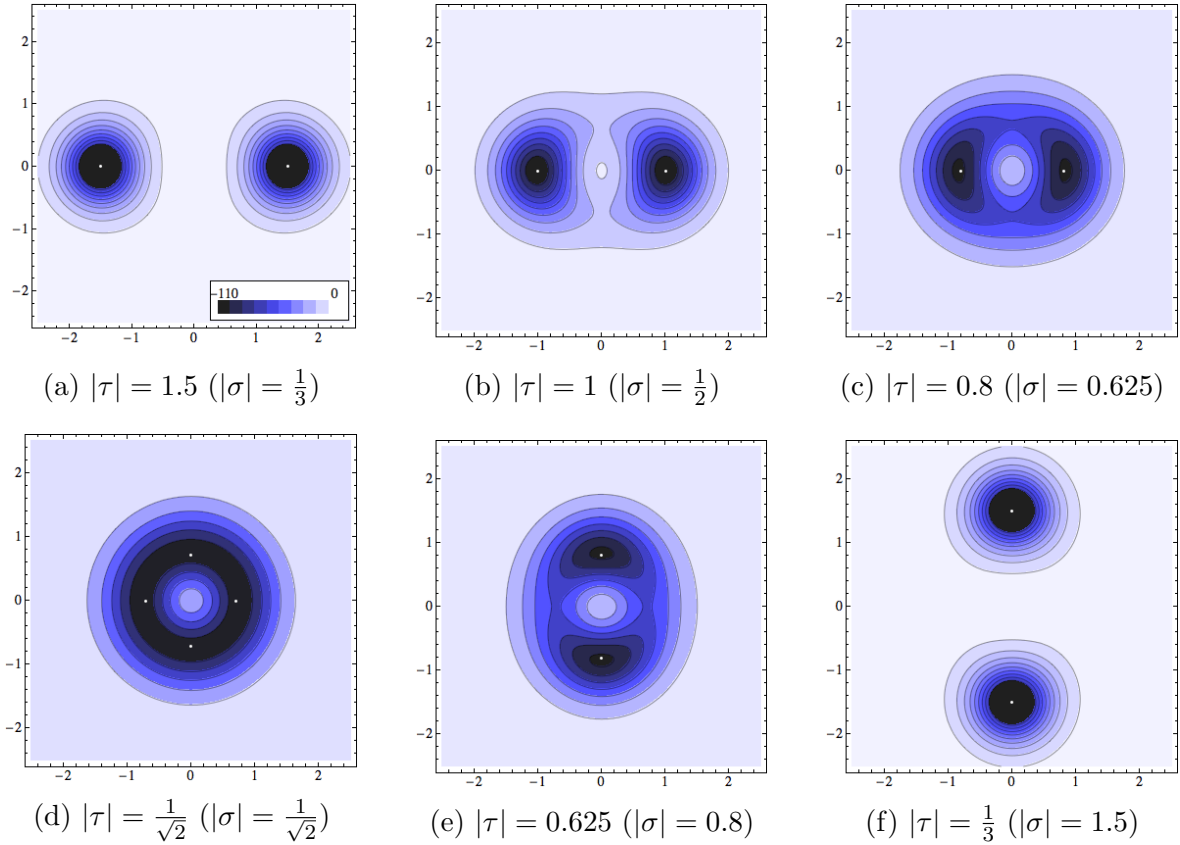


Figure 6.1: The topological charge density of a charge two instanton at various values of τ . Each figure shows the values of the charge density on the complex plane, at zero in the e_2 and e_3 quaternion directions. Each contour shows a fixed value of the charge density with the lighter areas corresponding to less charge. The instantons have size $\rho = 1$ and have an orthogonal gauge orientation ($\phi = \frac{\pi}{2}$). The value of τ is real. The white dots mark the positions of τ and $-\tau$ when $|\tau| \geq |\sigma|$ and the positions of σ and $-\sigma$ when $|\tau| \leq |\sigma|$.

takes on the role of the separation.

Right angled scattering occurs because σ always lies orthogonal to τ . If we treat σ and τ as four-vectors then their inner product is zero,

$$\sigma \cdot \tau = 0. \quad (6.1.3)$$

This is due to fact that Λ in equation (6.1.2) is a pure imaginary quaternion. When σ takes over the role of the separation, the instantons will be separated at right angles to the previous direction τ . This behaviour is what we see in Figure 6.1.

The direction in which the instantons separate will be determined by the direction of σ . The outgoing rotation compared to their incoming direction, τ , is determined by the purely imaginary quantity $\bar{v}_2 v_1 - \bar{v}_1 v_2$, which depends on the internal gauge orientations of the two individual instantons. There are three distinct cases although a general scattering may be some combination of these:

1. τ, v_1 and v_2 in the same plane. When the gauge orientations of the instantons are in the same plane as their separation, the instantons will scatter orthogonally to τ in this plane. This is the only situation possible in the complex geodesic submanifold in equation (5.5.11).
2. τ and v_1 in the same plane with v_2 orthogonal. When v_2 is orthogonal to this plane, the instantons will scatter in the direction of v_2 . Similarly for v_1 and v_2 reversed.
3. τ, v_1 and v_2 all mutually orthogonal. When the gauge orientations are orthogonal to each other and to the instantons' separation, they will scatter in the remaining direction orthogonal to τ, v_1 and v_2 .

When v_1 and v_2 are parallel the instantons do not interact. In this case σ is zero and τ always describes their separation. The instantons do not scatter and will instead pass through each other.

As an alternative interpretation, we note that the ADHM data naturally splits into two parts: L , describing the instanton sizes and gauge alignments, and M , describing the instantons' positions. When an $N \times N$ matrix describes the positions of N D-branes, it is the eigenvalues that actually correspond to the physical positions of the D-branes. In a similar manner, the eigenvalues of M give a suitable description of the instantons' positions. For complex τ and σ , the eigenvalues are

$$\pm \sqrt{\tau^2 + \sigma^2}. \quad (6.1.4)$$

These eigenvalues are approximately equal to $\pm\tau$ when τ is large and to $\pm\sigma$ when τ is small. The eigenvalues will be zero when the instantons are coincident and $|\tau| = |\sigma|$.

The eigenvalues are rotated by 90° in the complex plane when they pass through zero due to a change of sign inside the square root.

Let us briefly compare this behaviour to right angled scattering in monopoles. For two monopoles in $SU(2)$, the moduli space is the Atiyah-Hitchin manifold [99] which has a two dimensional geodesic submanifold corresponding to motion in a plane. This submanifold has the topology of a cone since the system is identical under a rotation by 180° around the origin which swaps the identity of the two monopoles. Head-on scattering is described by a geodesic which passes over the vertex of the cone and therefore emerges at 90° in the spatial coordinates, relative to where it came in. The subspace is smooth at this vertex although the angle jumps by 90° , as expected from passing through the origin in polar coordinates.

For two instantons, the moduli space also has a geodesic submanifold corresponding to motion in a plane. The metric of this is given in equation (5.5.11). This space is still six dimensional and it is not possible to give as simple a description of right-angled scattering as for monopoles. Each instanton has a unique identity and the symmetry under a rotation by 180° no longer exists. Instead, we can understand the 90° scattering through the symmetry of the ADHM data as described above and given in equation (6.1.1).

6.1.2 Geodesic motion

So far we have only considered the variation of parameters within the moduli space, but these parameters do not describe geodesics. However, we also expect to see right angled scattering in the geodesic motion of two instantons whenever the magnitude of τ passes through $|\tau| = |\sigma|$. This is inevitable if $|\tau|$ is decreasing.

The numerical results in the following sections were calculated using Mathematica. The equations of motion were calculated as an analytic expression from the metric and potential in the previous chapter, with the effective action in equation (4.5.23). In the case of the half dimensional geodesic submanifold described around (5.5.11), the equations of motions were numerically integrated using Mathematica's `NDSolve`. For the equations of motion on the full moduli space, a Runge-Kutta method was used to integrate the equations, and the results were checked against the integrations performed on the lower dimensional submanifolds.

We cannot numerically integrate the equations of motion for a head-on collision between two instantons because the symmetry between τ and σ manifests as a discontinuous jump of parameters in the geodesic evolution. This jump is between equivalent parameterisations and so is smooth on the moduli space, but prevents us from finding a numerical solution. However, we can still explore head-on collisions by examining the behaviour as the impact parameter goes to zero.

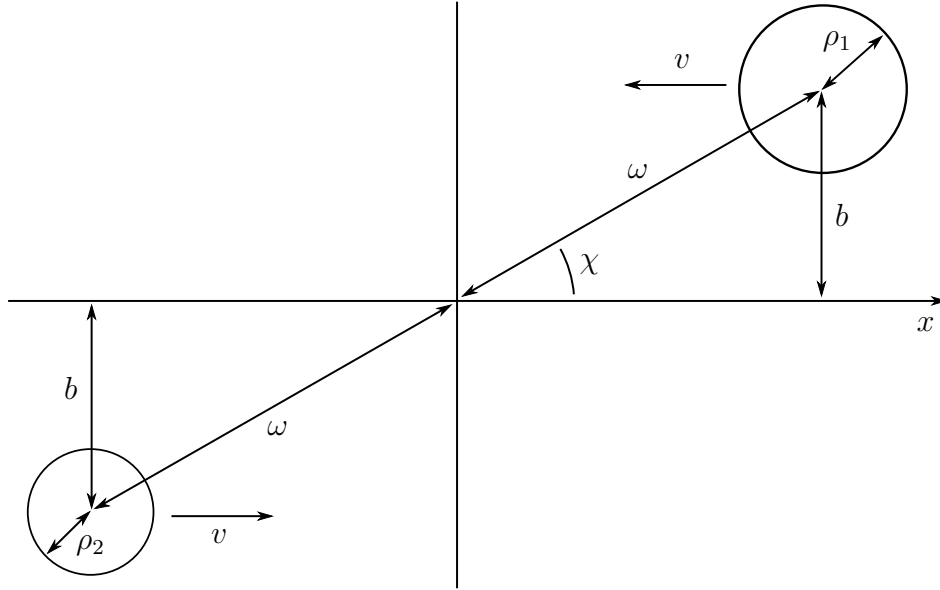


Figure 6.2: The physical interpretation of the parameters in the initial conditions of our scattering processes.

In the rest of this chapter we will only consider motion on the half-dimensional geodesic submanifold described around equation (5.5.11). Recall that we can parameterise the instantons on this submanifold with complex parameters as

$$v_1 = \rho_1 (\cos \theta_1 + i \sin \theta_1), \quad (6.1.5)$$

$$v_2 = \rho_2 (\cos \theta_2 + i \sin \theta_2), \quad (6.1.6)$$

$$\tau = \rho_1 (\cos \chi + i \sin \chi). \quad (6.1.7)$$

The physical interpretation of these parameters is shown in Figure 6.2. The only parameters which are not shown are the gauge orientations, θ_1 and θ_2 . The overall gauge orientation, $\theta = \theta_1 + \theta_2$ does not have a physical effect on the static instantons, but its rate of change is important in the dynamics. The dynamics are therefore invariant under the initial value of θ , and we will not specify it when we list initial conditions. The relative angle, $\phi = \theta_1 - \theta_2$, is significant however. It is convenient to work with a slightly different parameterisation of our initial positions; we introduce the impact parameter, b , and the separation along the x -axis, x , as shown in Figure 6.2. To consider the scattering of two instantons we start with well separated static instantons and send them towards each other with an initial velocity parallel to the x -axis, $\dot{x} = -v$. Ideally we are interested in the behaviour as the instantons come from infinity but we will settle on $x = 50$ as a practical initial separation in our numerical study. Unless otherwise stated we will take the incoming velocity to be $v = 0.03$ and the initial instanton sizes to be $\rho_1 = \rho_2 = 1$.

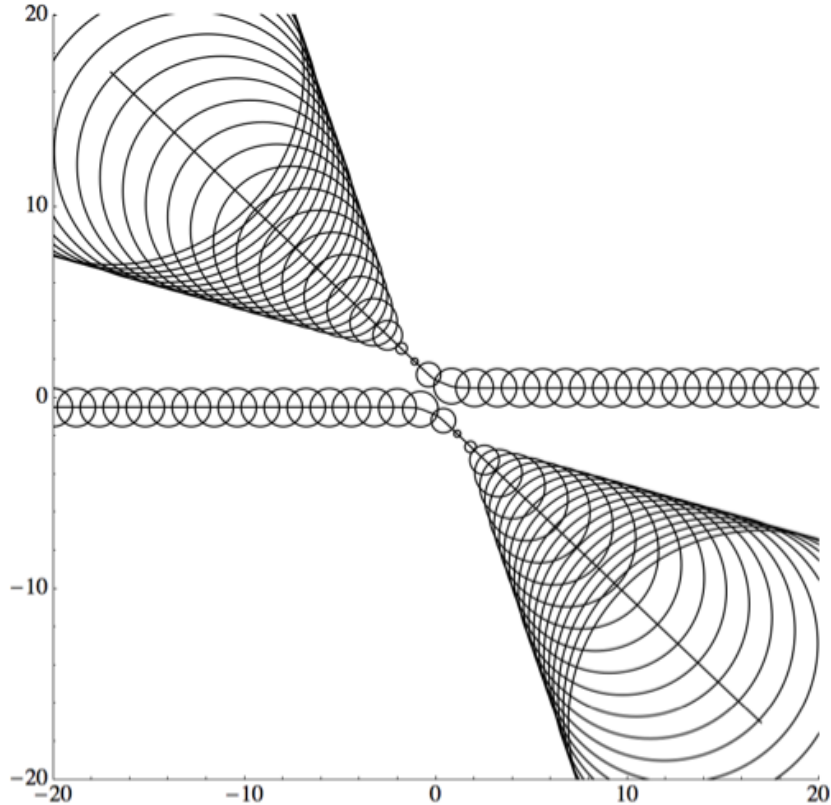


Figure 6.3: The collision of two instantons with an impact parameter of $b = 0.5$. The relative gauge angle begins and remains fixed at $\phi = \frac{\pi}{2}$.

For simplicity we will begin by exploring the lower dimensional geodesic submanifold where the instantons are of identical size and have a fixed orthogonal gauge orientation, $\phi = \frac{\pi}{2}$. Figure 6.3 shows the scattering of two instantons on this submanifold with an impact parameter of $b = 0.5$. The solid lines in Figure 6.3 show the evolution of $\pm\tau$ and trace the instantons' positions. The circles show snapshots of the instantons at discrete moments in the evolution. The circles' centres correspond to the instantons' positions and the radii are given by the values of ρ_1 and ρ_2 at each point, showing the instantons' sizes. These figures give a good high level impression of how the instantons evolve, although care has to be taken with their interpretation when the instantons are very close.

We can see that after the interaction shown in Figure 6.3, the instanton sizes are perturbed and they begin to shrink. To the limits of our numerical accuracy the instantons appear to pass through the zero size singularity and emerge with an increasing size, spreading out indefinitely. It may seem concerning that the instantons pass through the singularity on the moduli space, but this is not a generic behaviour. If we move away from this submanifold and give the instantons an initial difference in size or relative gauge angle then they will no longer hit the singularity. The value of v_1 and v_2 will no longer pass through the origin and the instantons' minimum sizes will be greater than zero. We will see evidence of this later.

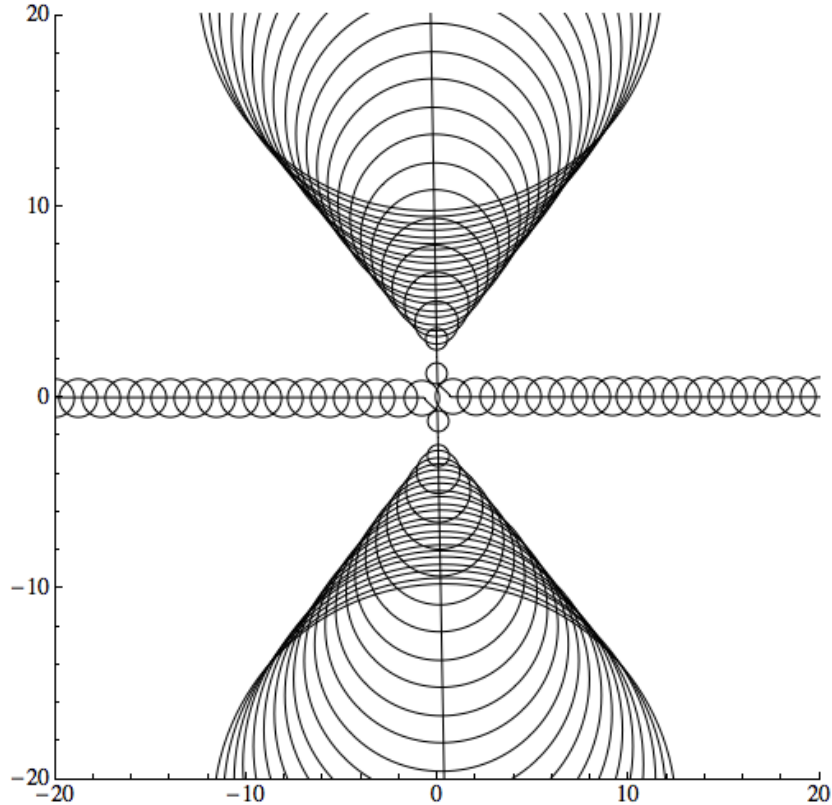


Figure 6.4: The collision of two instantons with an impact parameter of $b = 0.01$. The relative gauge angle begins and remains fixed at $\phi = \frac{\pi}{2}$.

As the impact parameter decreases towards zero the scattering angle increases towards 90° . Figure 6.4 shows the scattering of two instantons with a small impact parameter of $b = 0.01$ where the scattering is at almost exactly 90° . As mentioned previously, we cannot numerically integrate a direct head-on collision due to the discontinuous jump between equivalent parameterisations when the instantons become coincident. This jump is shown more clearly in Figure 6.5 where the evolution of $|\tau|$ and $|\sigma|$ is shown for impact parameters of $b = 0.1$ and $b = 0.01$. The interpolation between the two becomes increasingly quick as the impact parameter is reduced. The angle χ also jumps by $\frac{\pi}{2}$. This jump can also be seen near the origin in Figure 6.4.

Figure 6.6 shows how the scattering angle varies with impact parameter. The scattering angle clearly tends towards 90° as the impact parameter goes to zero. The scattering angle decreases to zero asymptotically as the impact parameter increases, as expected.

So far we have only considered the subset of the possible initial conditions where the gauge alignment of the two instantons is orthogonal. We will now lift that restriction to explore the effect of this angle. We will still remain in the complex submanifold of equation (5.5.11) where the instantons only move in a plane.

After scattering head on, the instantons are more suitably described in terms of the alternative parameterisation given in (6.1.1). From this, we can expect the instantons

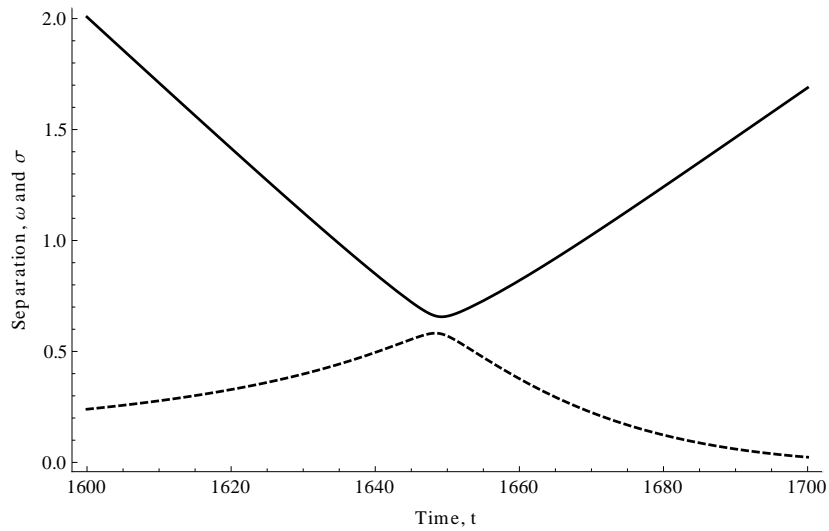
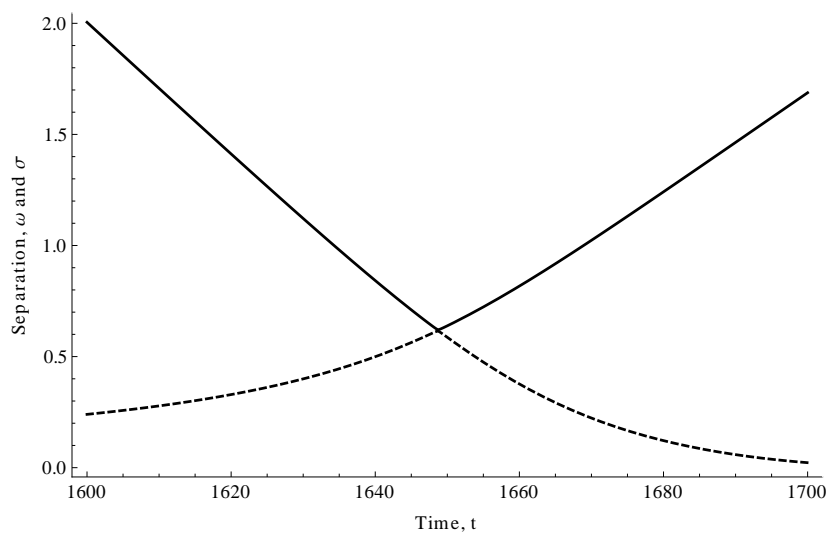
(a) Impact parameter $b = 0.1$ (b) Impact parameter $b = 0.01$

Figure 6.5: The evolution of $|\tau|$ (solid) and $|\sigma|$ (dashed) during two collisions of instantons with different impact parameters.

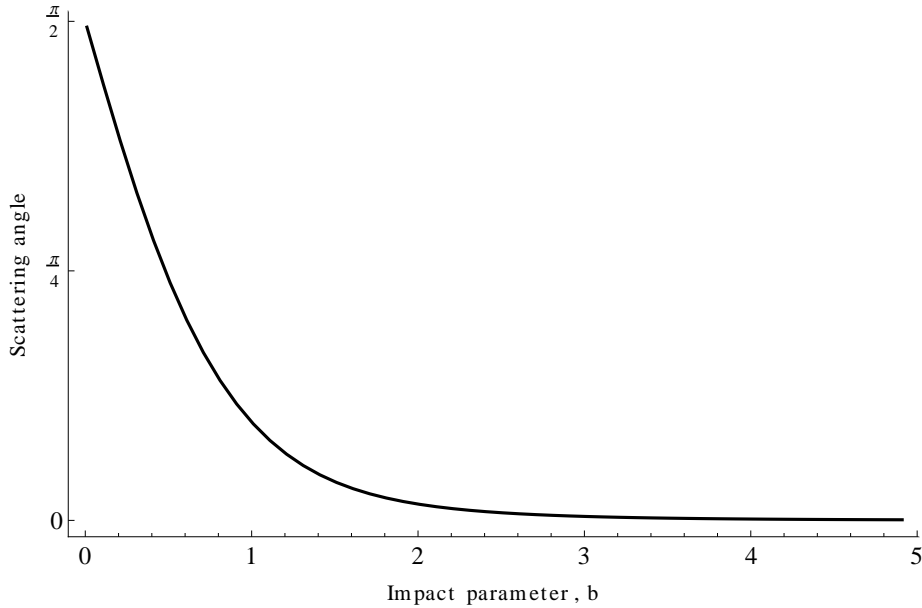


Figure 6.6: The variation of the scattering angle of a collision of two instantons with different impact parameters, b .

to emerge from the head-on scattering with sizes

$$\tilde{\rho}_1 = \frac{1}{\sqrt{2}}|v_1 + v_2|, \quad \text{and} \quad \tilde{\rho}_2 = \frac{1}{\sqrt{2}}|v_1 - v_2|, \quad (6.1.8)$$

compared to the incoming sizes $\rho_1 = |v_1|$ and $\rho_2 = |v_2|$. The relative angle between v_1 and v_2 obviously plays a key role in this. The outgoing sizes are only equal when the incoming v_1 and v_2 are orthogonal, or $\phi = \frac{\pi}{2}$, but in general they will emerge with different sizes. This is an accurate description immediately before and after the right-angled scattering, but the relation between the asymptotic sizes of the incoming and outgoing instantons is not as clear due to the additional dynamical effects on the size. Figure 6.7 shows the result of a collision with an initial relative gauge angle of $\phi = \frac{\pi}{4}$. We see that the instantons now emerge with a different behaviour in their sizes. The scattering angle is also shallower than when the gauge orientation was orthogonal.

Recall that there is another geodesic submanifold corresponding to instantons with equal size and parallel gauge orientation, $\phi = 0$. In this case the instantons do not interact at all and the metric is flat. The scattering angle is therefore trivially zero. The relative gauge orientation between the two instantons therefore gives some measure of the strength of the interaction between the instantons. Figure 6.8 shows how the scattering angle depends on the initial difference in gauge orientation between the two incoming instantons. The strongest interaction occurs when the gauge orientation is orthogonal and decreases as the gauge orientation becomes parallel, at which point the instantons are completely non-interacting.

Right-angled scattering is a generic feature of two instantons which collide head

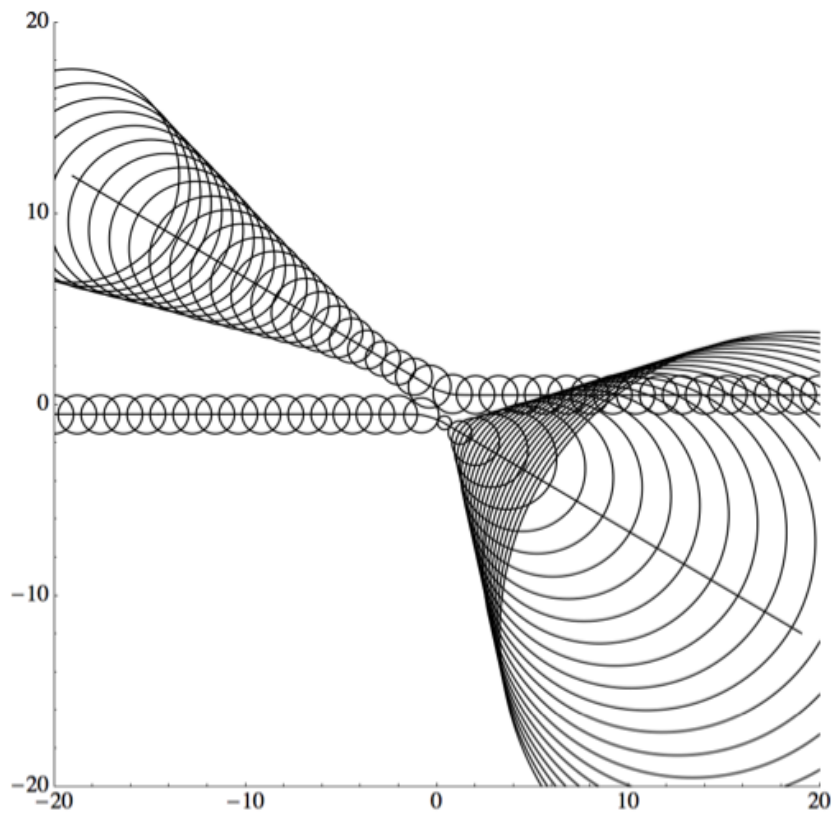


Figure 6.7: The collision of two dyonic instantons with an impact parameter of $b = 0.5$ and an initial relative gauge angle of $\phi = \frac{\pi}{4}$.

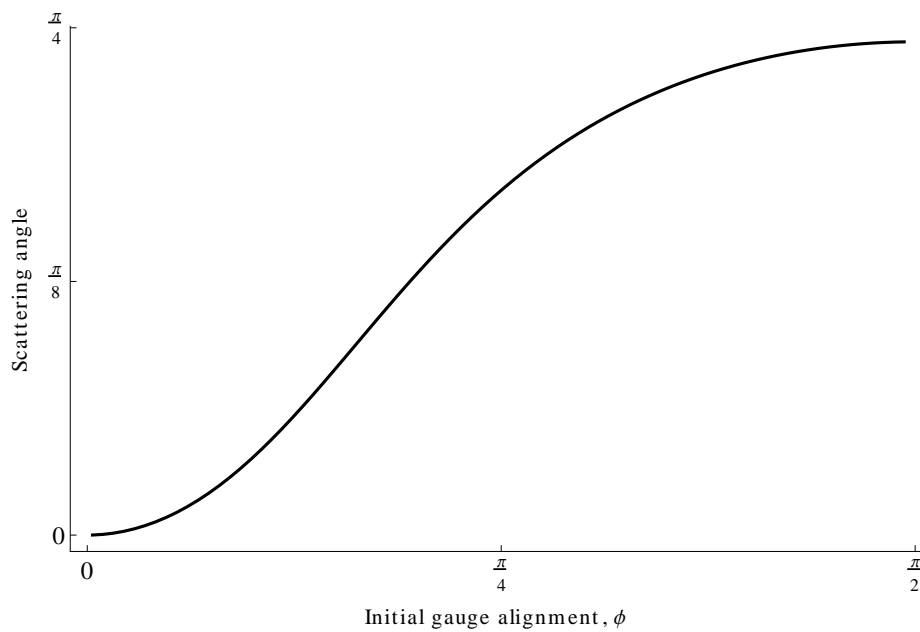


Figure 6.8: The variation of the scattering angle of a collision of two instantons with different initial gauge alignments, ϕ , and impact parameter $b = -0.5$.

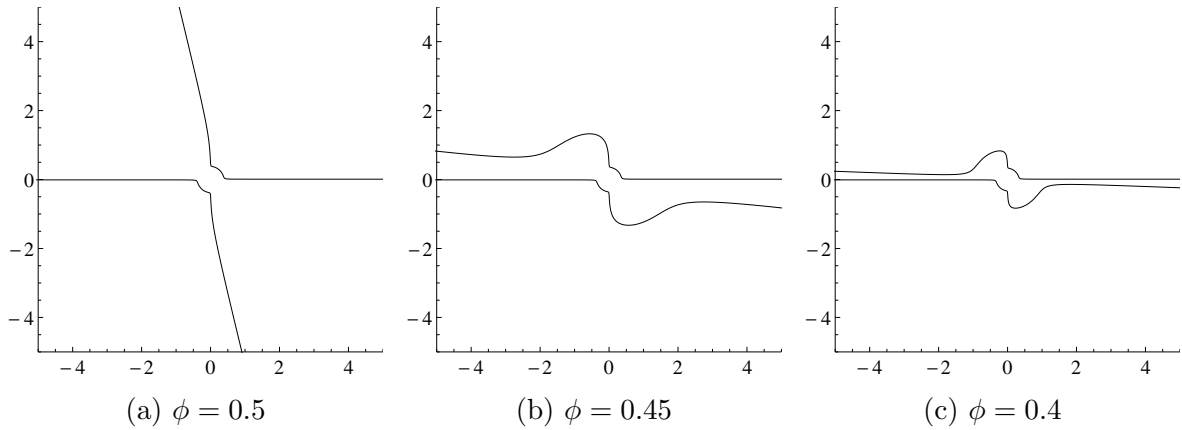


Figure 6.9: The evolutions of the centres of the instantons in a nearly head on collision ($b = 0.01$) for various initial values of the relative gauge angle, ϕ .

on, yet we have seen that when the relative gauge angle is zero the instantons do not interact at all. To reconcile the limit of zero gauge angle with right-angled scattering, we note that for small ϕ one of the instantons emerges with a much larger size than the other. When ϕ is sufficiently small, the large instanton grows in size faster than the instantons separate and so causes them to interact again. This can be seen in Figure 6.9a where the initial gauge alignment is $\phi = 0.5$. The instantons scatter at right angles but then continue to interact and rotate slightly to give them an asymptotic scattering angle of less than 90° . As the initial gauge angle, ϕ , goes to zero this effect becomes more pronounced and the asymptotic scattering angle goes to zero, despite the instantons initially scattering at 90° when they become coincident. Figures 6.9b and 6.9c show this effect for $\phi = 0.45$ and $\phi = 0.4$. The limit of this behaviour is that when $\phi = 0$ the right angled scattering is not apparent and the instantons simply pass through each other after becoming coincident, as expected by examining the appropriate geodesic submanifold.

In the full moduli space, the instantons each have an $SU(2)$ gauge angle and are free to move in four dimensions. As described previously the scattering direction no longer remains in a plane but depends on the direction of the separation of the instantons and the relative gauge orientation of the instantons in $SU(2)$. Moving beyond the complex subspace into the full moduli space becomes computationally expensive but we have been able to explore a few examples. The complex subspace appears to be stable to small perturbations in the full moduli space so that the discussion above can be safely interpreted in the full moduli space. It would be interesting to explore the scattering behaviour of instantons with their gauge alignment in the full $SU(2)$ gauge group and not just constrained to the unbroken $U(1)$. A systematic study of such behaviour is unfortunately beyond our reach at this time.

6.2 Dynamics of a single dyonic instanton

Before discussing the scattering of two dyonic instantons we will review how the potential stabilises a single dyonic instanton. The effective action for a single dyonic instanton rotating in only one direction in the gauge group is

$$S = 8\pi^2 \int dt \dot{\rho}^2 + \rho^2 \dot{\theta}^2 - |q|^2 \rho^2, \quad (6.2.1)$$

where ρ is the size of the dyonic instanton and θ is its U(1) gauge angle. This can be calculated directly from the inner product of zero-modes of the 't Hooft ansatz [95] or from the ADHM data as in Chapter 5. The equation of motion for the gauge angle is a conservation law for gauge angular momentum,

$$\rho^2 \dot{\theta} = l, \quad (6.2.2)$$

where l is some constant. The equation of motion for ρ is

$$\ddot{\rho} - \rho \dot{\theta}^2 + |q|^2 \rho = 0. \quad (6.2.3)$$

We can replace $\dot{\theta}$ by the angular momentum so that

$$\ddot{\rho} - \frac{l^2}{\rho^3} + |q|^2 \rho = 0. \quad (6.2.4)$$

In the absence of a potential ($|q| = 0$), pure instantons suffer from a slow-roll instability where a small perturbation to the static instanton will result in the instanton spreading out at a constant velocity. Eventually the instanton will be spread over the entire space or hit the zero size singularity. We can easily see this behaviour on the moduli space since the metric in the effective action is flat and the equation of motion for ρ becomes $\ddot{\rho} = 0$ in the absence of any angular velocity.

The effective action for a dyonic instanton includes a potential term which stabilises the lumps at a fixed size. We can see from the equation of motions that when $\dot{\theta} = |q|$ the instanton size and rotational velocity remain constant. This describes a static dyonic instanton which satisfies the BPS equations exactly. The apparent motion on the moduli space is due to the coordinate transformation that we made in equation (4.5.21).

If we think of this motion as a point moving around a spherically symmetric potential, like a marble in a bowl, then it is clear that this system is now stable to perturbations in the instanton's size. A small initial velocity for ρ sets up an oscillation around the initial value of ρ , but it will not increase indefinitely. The upper and lower bounds of the oscillation are proportional to the initial perturbation.

Generally, the dyonic instanton will oscillate in size with an amplitude, A , [95]

$$\rho = \sqrt{A \sin(2|q|(t + t_0))} + \sqrt{\frac{l^2}{|q|^2} + A^2}. \quad (6.2.5)$$

The smaller the initial angular velocity, the less angular momentum the instanton has and the closer it comes to zero size. The larger the initial change in size, the larger the amplitude of the oscillation and again the closer it will come to zero size. The instanton can oscillate out to arbitrary size for a sufficiently large initial $\dot{\rho}$ but will always turn around before reaching $\rho = 0$ for non-zero angular momentum.

6.3 Dyonic instanton scattering

The presence of a potential in the effective action for dyonic instantons has a significant effect on their scattering behaviour. In this section we will explore how dyonic instantons behave during head-on collisions and with a non-zero impact parameter. The right angled scattering behaviour of instantons is replaced with a more complex dependence on the potential.

Figure 6.10 shows a head-on collision between two dyonic instantons. The dyonic instantons begin their evolution by moving towards each other along the real axis but they are deflected as they approach each other. The dyonic instantons scatter at an unusual angle of just over 122° and the radial size of the instantons picks up a small stable oscillation. Unless otherwise stated, we will always take $|q| = 0.1$. As with instantons, we will take our canonical initial conditions to be $\rho_1 = \rho_2 = 1$, $v = 0.03$, $x = 50$ and $\phi = \frac{\pi}{2}$.

Figure 6.11 shows the relation between the scattering angle and the magnitude of the potential. As expected, the scattering angle approaches 90° as $|q|$ goes to zero and the system gets closer to describing pure instantons.

When the impact parameter, b , is non-zero the dyonic instantons also display a range of interesting behaviour. From the view point of one of the incoming dyonic instanton lumps they scatter to their left in a head-on collision. If the direction of rotation of the dyonic instantons was reversed, $\dot{\theta} \mapsto -\dot{\theta}$, then the behaviour would be a mirror image. If we move their impact parameter in the left direction so that b is negative then the dyonic instantons continue to repel each other but their scattering angle becomes shallower. Figure 6.12 shows the scattering of two dyonic instantons with impact parameter $b = -2$ and we see that the scattering angle is much shallower than in the head-on collision. Figure 6.13 shows how the scattering angle depends upon the impact parameter in the negative direction. As the impact parameter is increased in the negative direction the strength of the dyonic instantons' interaction decreases

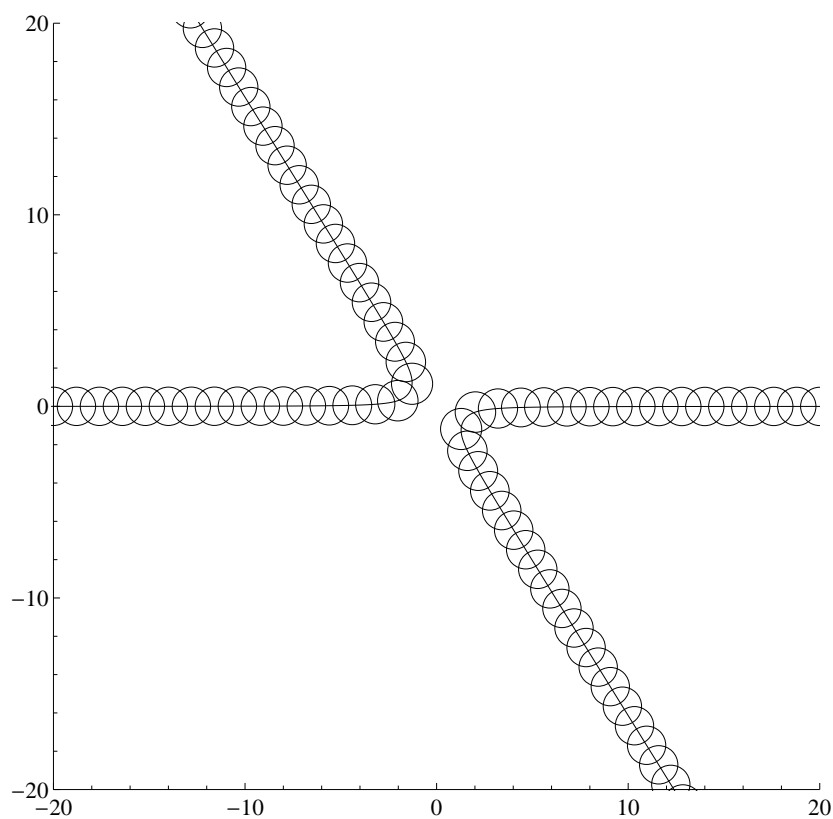


Figure 6.10: A head-on collision of two dyonic instantons with the magnitude of the potential at $|q| = 0.1$.

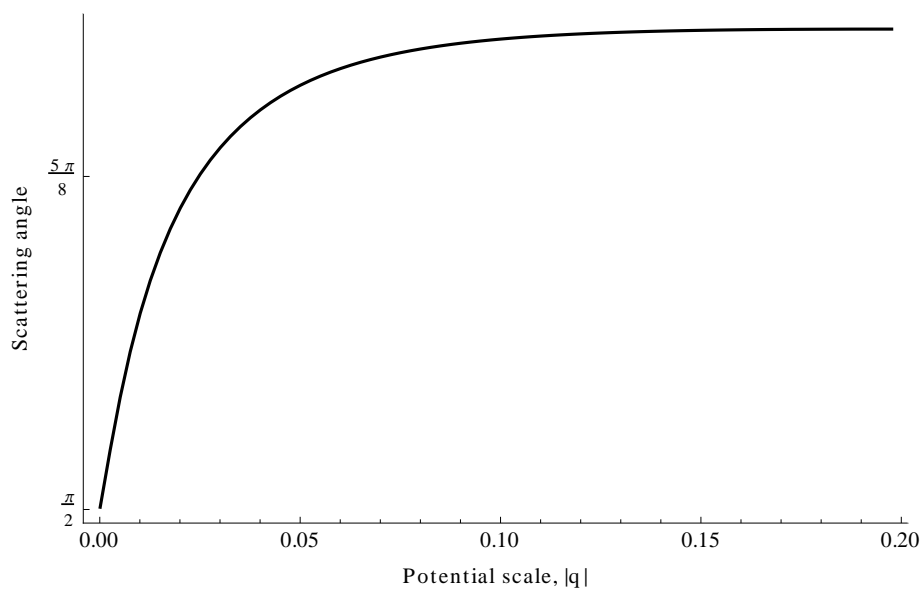


Figure 6.11: The scattering angle of a head-on collision of two dyonic instantons with varying values of the potential scale, $|q|$.

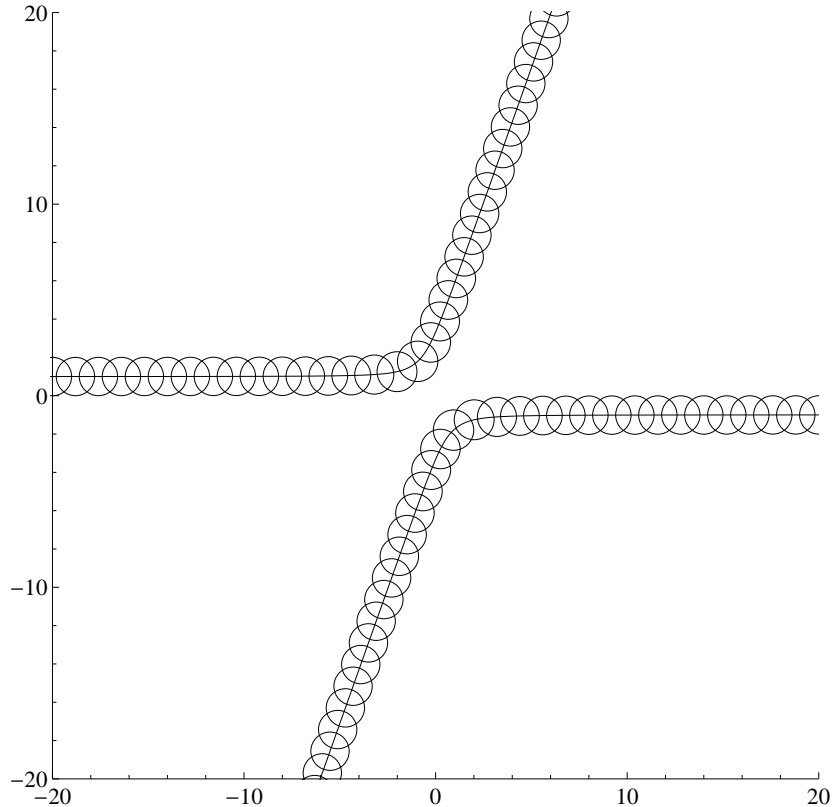


Figure 6.12: The collision of two dyonic instantons with an impact parameter of $b = -1$.

and the scattering angle goes to zero. Comparing this to pure instantons in Figure 6.6 we see that the interaction remains stronger at larger impact parameter in the presence of a potential.

When the impact parameter is positive the behaviour is more interesting. The dyonic instantons are now attracted to each other and it is possible for the instantons to loop around each other before scattering. Figure 6.14 shows one example of this in detail with an impact parameter of $b = 2.9$. Figure 6.15 shows how the outgoing angle varies with the impact parameter for different values of $|q|$. The jumps in the plots correspond to the instantons losing their identity in the scattering process. This happens whenever the instantons come close to the origin at the same time and form a single symmetrical lump. It becomes meaningless to talk about which outgoing instanton corresponds to which incoming instanton and the jumps by 180° are from swapping which parameters are used to label each instanton rather than a physical discontinuity. The tall spikes correspond to scatterings in which the instantons orbit for more than one revolution and so can have an outgoing angle of greater than 360° .

Figure 6.16 shows how the scattering angle depends on the initial difference in gauge angle between the two dyonic instantons. As with instantons, the scattering angle interpolates between zero when the gauge orientations are parallel and the value seen previously when the gauge orientations are orthogonal. The strength of the interaction between the dyonic instantons again depends on their relative gauge orientation

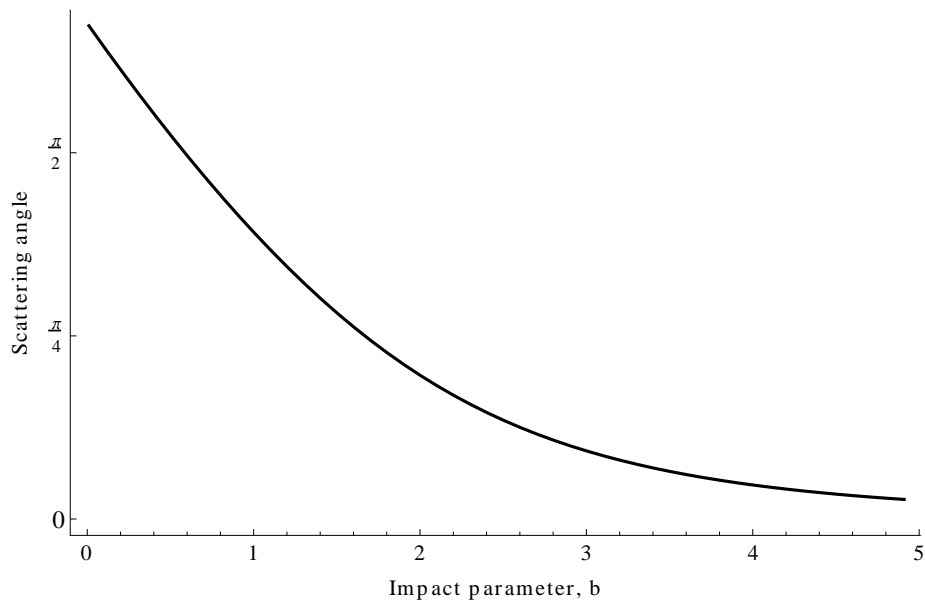


Figure 6.13: The variation of the scattering angle with impact parameter for a collision between two dyonic instantons. The impact parameter, b , is in the negative direction.

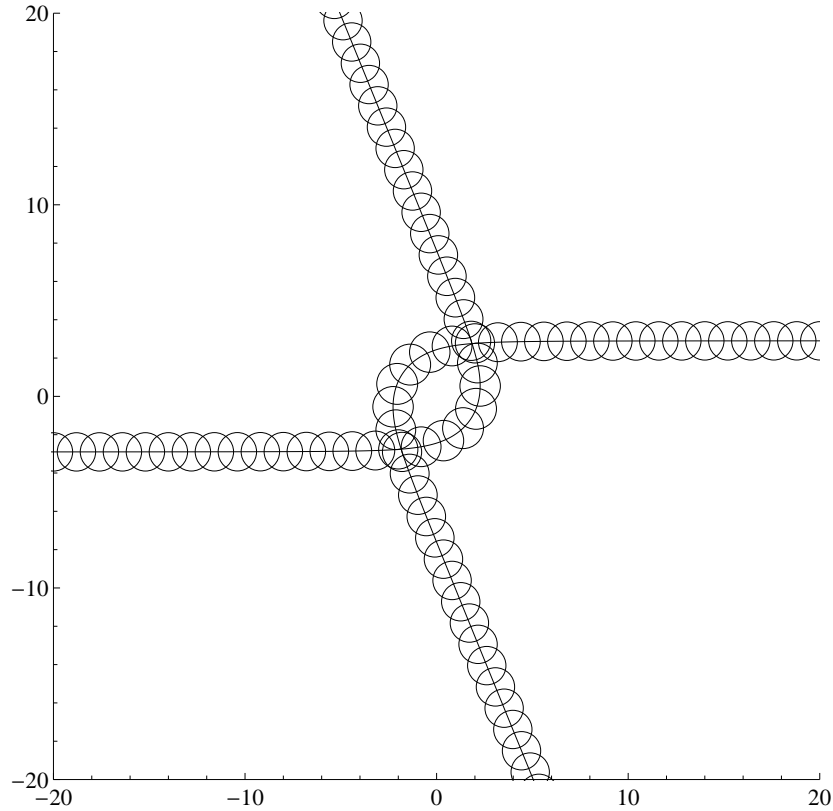


Figure 6.14: A collision of two instantons with an impact parameter of $b = 2.9$.

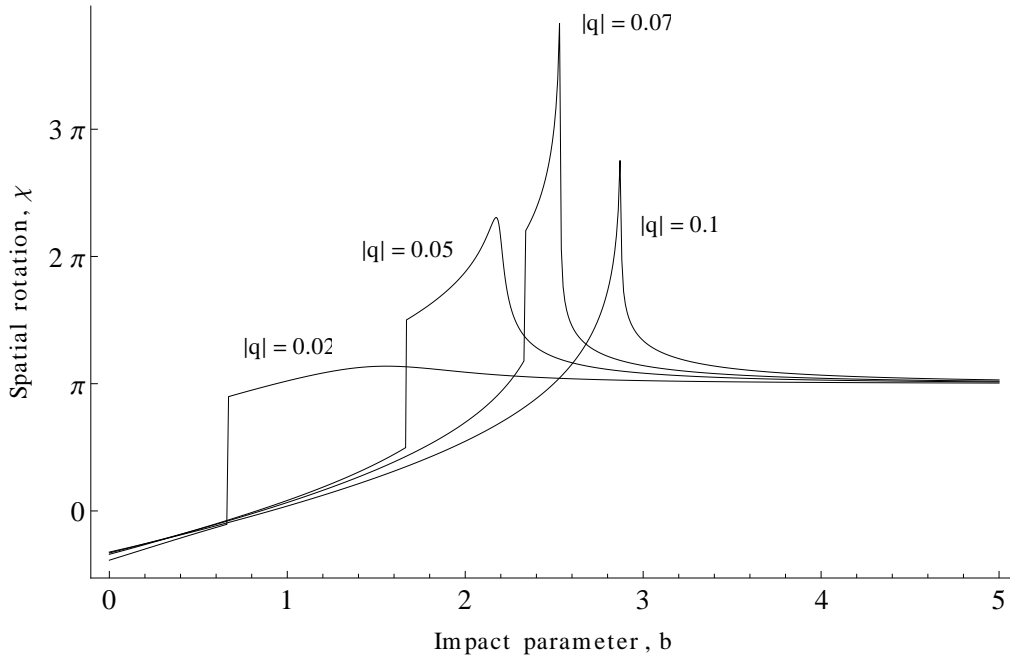


Figure 6.15: The variation of the outgoing angle, χ , with impact parameter for a collision between two dyonic instantons, shown for different values of the potential scale, $|q|$. The impact parameter, b , is in the positive direction.

with the strongest interaction occurring when they are orthogonal. At the other extreme, when the gauge alignment is parallel, the dyonic instantons are completely non-interacting.

The properties of dyonic instantons that we have considered so far are reminiscent of the Q-lumps considered by Leese [100]: both systems have a topological charge and a non-topological Noether charge; the presence of the non-topological charge induces a potential in the effective action for slow moving solitons; and the potential stabilises the solitons against spreading out indefinitely under a small perturbation. Both systems also see similar scattering behaviour with head-on collisions causing a deflection of more than 90° , without the lumps becoming coincident. As far as we are aware dyonic instantons and Q-lumps are the only solitons which have been seen to scatter in this way. Both system also have trajectories where the lumps orbit each other briefly when the impact parameter is in an appropriate range. Leese makes the point that it is difficult to avoid some external perturbation which would introduce a potential and so Q-lumps may be more physically relevant than the underlying pure σ -model soliton. This point seems to be particularly relevant for instantons on D4-branes where the potential is induced by a separation of the branes.

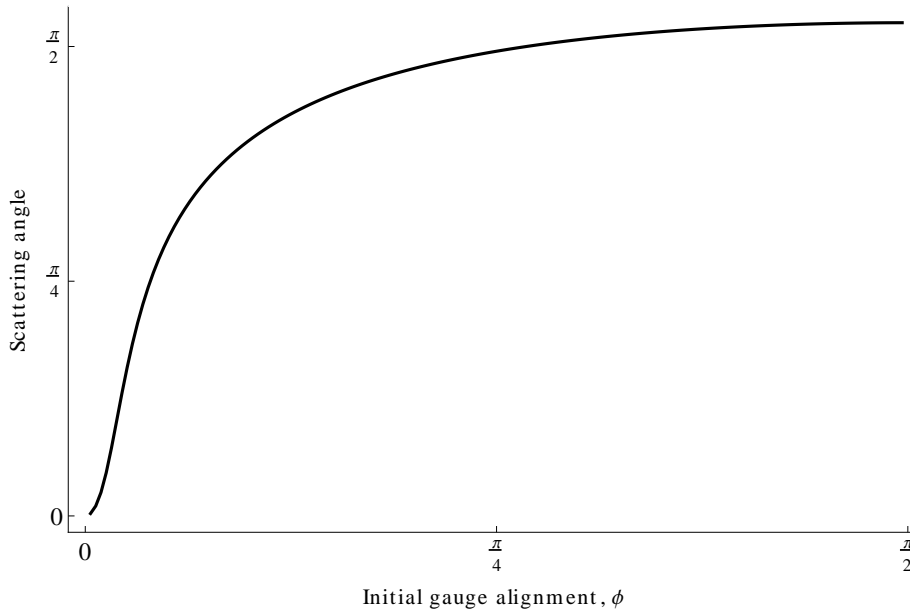


Figure 6.16: The variation of the scattering angle with the initial gauge alignment, ϕ for two dyonic instantons with an impact parameter of $b = -0.5$.

6.4 Geodesic completeness of the moduli space

It is straightforward to see that the instanton moduli space is not geodesically complete, but the equivalent question for motion in the presence of a potential is not so straightforward. For pure instantons, a small negative perturbation in the size parameter will cause the instanton to shrink steadily until it hits the zero size singularity. For dyonic instantons however, there is a non-zero conserved angular momentum on the moduli space from the rotation in the unbroken $U(1)$ gauge group. This prevents the dyonic instanton from shrinking to zero size under small perturbations.

For a single dyonic instanton, the angular momentum is given by

$$l = \rho^2 \dot{\theta}, \quad (6.4.1)$$

but for two dyonic instantons the angular momentum is more complicated and the picture is not as clear. On the two instanton moduli space the conserved gauge angular momentum arises from the Killing direction θ in the metric and is given by

$$l = g_{\theta p} \dot{z}^p, \quad (6.4.2)$$

where θ is the embedding angle in the unbroken $U(1)$ as in equation (5.5.11). Considering just the complex geodesic submanifold, the angular momentum for two dyonic

instantons is

$$l = \rho_1^2 \dot{\theta}_1 + \rho_2^2 \dot{\theta}_2 - \frac{2}{N_A} \rho_1 \rho_2 \cos \phi \sin \phi (\rho_1 \dot{\rho}_2 - \rho_2 \dot{\rho}_1) - \frac{2}{N_A} \rho_1^2 \rho_2^2 \sin^2 \phi (\dot{\theta} - 2\dot{\chi}). \quad (6.4.3)$$

The first two terms describe the angular momentum of each dyonic instanton when they are well separated. However, there is only an overall conserved quantity and the individual instantons are free to transfer angular momentum when close together. It is no longer clear *a priori* whether one of the dyonic instantons can shrink to zero size by exchanging angular momentum with the other.

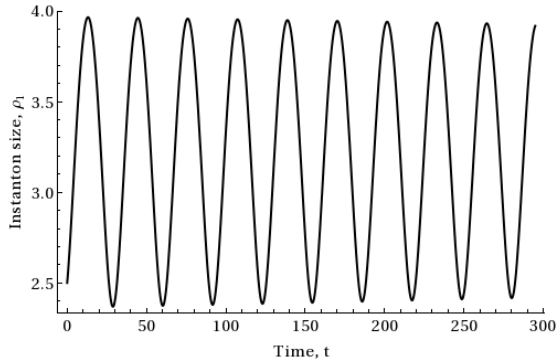
By numerically exploring motion on the moduli space we have been readily able to find trajectories where the instantons do indeed exchange angular momentum in such a way that one dyonic instanton shrinks to zero size. This is most easily observed when the dyonic instantons are far enough apart to be clearly distinct yet still within range of interaction. An illustrative example is shown in Figure 6.17 where both dyonic instantons start with a non-zero angular momentum but one draws angular momentum from the other until it passes through zero size. Both dyonic instantons continue to oscillate at a steady rate and so long as the dyonic instanton reaches the lowest point of its oscillation at the same time as passing through zero angular momentum it will hit the zero size singularity. This requires fine tuning of one of the parameters which we were able to achieve to the limits of our numerical accuracy. This fine tuning suggests there is a subset of initial conditions of codimension one which will evolve to hit a zero size singularity.

If we consider the full moduli space rather than just motion on the complex geodesic submanifold then we observe that the same generic behaviour is possible. The initial parameters now need a further two parameters to be fine tuned so that the additional two components of v_1 or v_2 also pass through their minimum value as the angular momentum passes through zero.

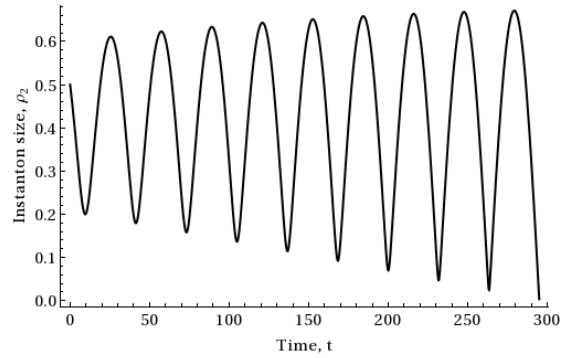
6.5 Localised charge two instantons

In this section we will consider the charge two object formed by two coincident dyonic instantons. For pure instantons, this configuration cannot be considered as an individual object as a small perturbation to the instanton positions will cause the two constituent instantons to drift apart until they are well separated again. Dyonic instantons however, are stabilised at a fixed separation by the potential. Figure 6.18 shows the result of giving two separated dyonic instantons a small initial velocity away from each other. The dyonic instantons now orbit each other in a spiralling pattern.

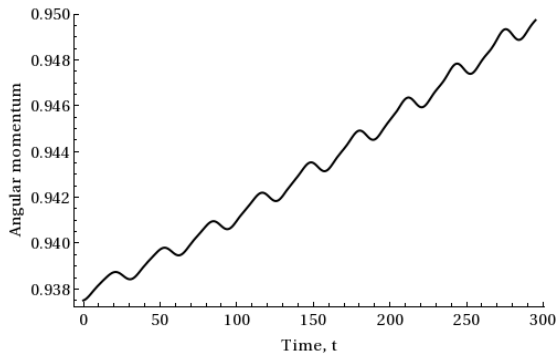
The dyonic instantons will only form a stable orbit for a small enough perturbation and will otherwise continue to move away from each other at a steady speed. When



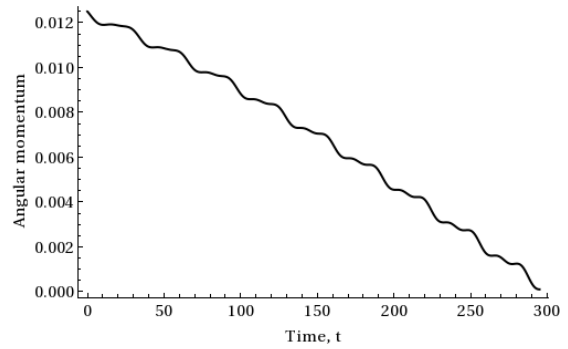
(a) The size of the first instanton, ρ_1 . This is drawing angular momentum away from the second.



(b) The size of the second instanton, ρ_2 . This passes through zero size.



(c) The angular momentum of the first instanton.



(d) The angular momentum of the second instanton. This reaches zero as the size, ρ_2 , reaches the lowest point of its oscillation.

Figure 6.17: The evolution to a zero size singularity of two initially non-singular dyonic instantons. The initial values were $\rho_1 = 2.5$, $\rho_2 = 0.5$, $\omega = 15$, $\phi = -\frac{\pi}{10}$. The initial velocities were $\dot{\rho}_1 = 0.1$, $\dot{\theta} = 0.2$, $\dot{\phi} = 0.1$ and $\dot{\rho}_2 = -0.03$. All other initial velocities were zero.

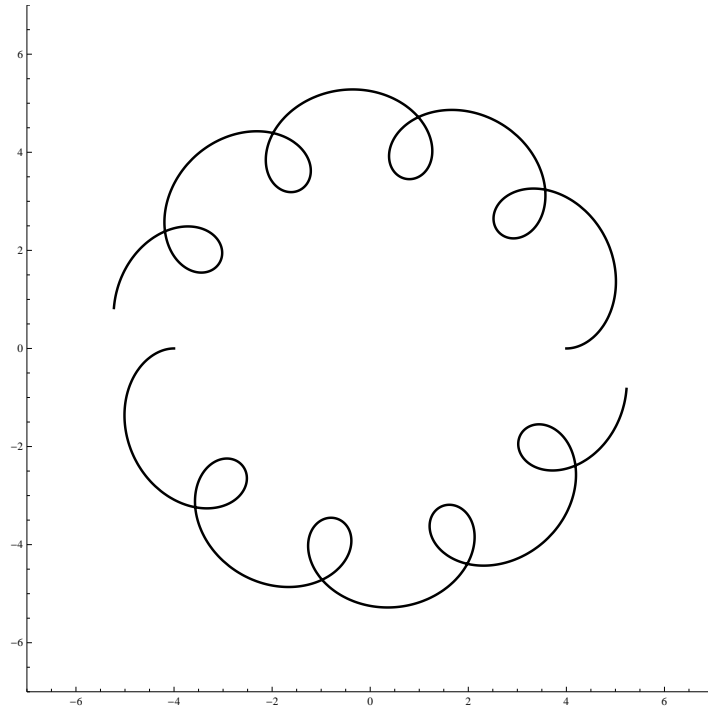


Figure 6.18: Two dyonic instantons in a stable orbit after a small outwards perturbation in their positions. The instantons started at a separation of $x = 4$ with size $\rho = 1$. They were given an initial outwards velocity of $v = 0.0005$.

only moving slightly faster than this ‘escape velocity’ the dyonic instantons display some orbiting behaviour but do not settle into a stable orbit. Figure 6.19 shows how the separation affects the threshold velocity at which the dyonic instantons will no longer form a stable orbit. The threshold velocity decreases as the strength of the interaction between the lumps decreases. The maximum threshold velocity is located close to where the instantons are coincident and axially symmetric, but with a slight shift towards a finite separation.

As a result of this stability, the axially symmetric charge two dyonic instanton is a stable object. It will not separate into two distinct charge one dyonic instantons under a perturbation.

The axially symmetric charge two dyonic instanton also admits the only closed geodesic that we have found. In this closed geodesic the dyonic instantons remain axially symmetric with $|\tau| = |\sigma|$,

$$\omega = \frac{\rho}{\sqrt{2}}, \quad \dot{\omega} = \ddot{\omega} = 0, \quad (6.5.1)$$

and have no oscillations in their size,

$$\dot{\rho} = \ddot{\rho} = 0. \quad (6.5.2)$$

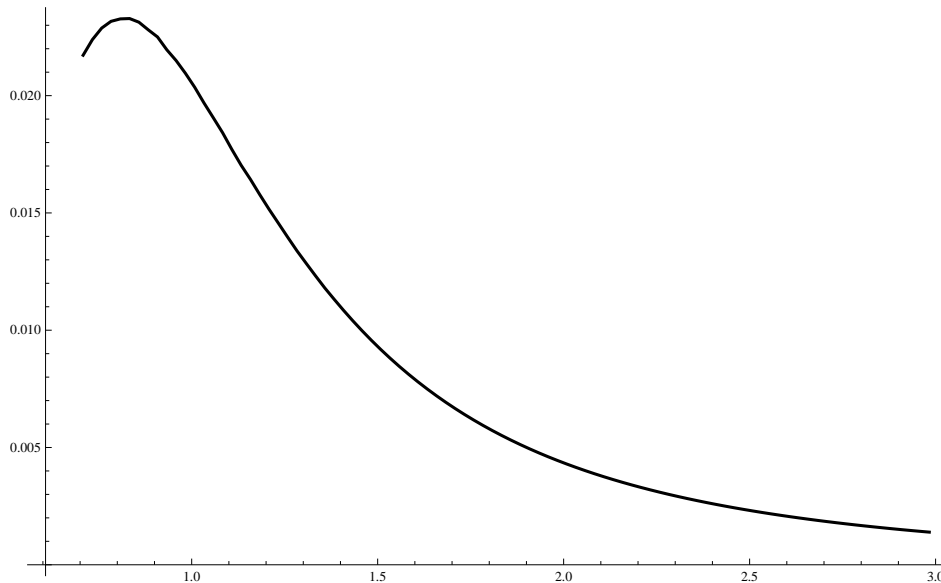


Figure 6.19: The maximum outwards velocity of two dyonic instantons that will lead to a stable orbit with different separations. The instantons have size $\rho = 1$.

The equations of motion are then satisfied by

$$\dot{\chi} = -4|q|, \quad \dot{\theta} = |q|. \quad (6.5.3)$$

This corresponds to a spatially rotating charge two dyonic instanton where the rotational velocity, $\dot{\chi}$, is fixed by the scale of the potential.

It would be interesting to investigate whether such a closed geodesic is stable in the full field theory or whether there are higher order radiative corrections that would cause it to decay. We leave this for future consideration.

6.6 Discussion and conclusions

In this chapter and the previous chapter we have calculated the full metric and potential on the moduli space of two dyonic instantons in terms of the parameters in the ADHM construction. With this construction in mind we have been able to understand some of the structure of the moduli space arising from the quotient of the moduli space by symmetries of the ADHM data. We have also explored the dynamics of two slow moving instantons and dyonic instantons using the moduli space approximation. We have seen that instantons readily undergo right angled scattering like many other soliton systems. This too can be understood from symmetries of the underlying ADHM data. The presence of a potential has a significant effect on the motion of dyonic instantons and we have seen that they behave in a way which is qualitatively similar to Q-lumps [100].

Several questions remain open for future research. We have only explored the

dynamics when the instantons lie in a plane with their relative gauge alignment in the unbroken $U(1)$ symmetry. When the gauge alignment in the full $SU(2)$ symmetry is orthogonal to the unbroken $U(1)$, the final term in the potential vanishes. It would be interesting to explore the effects of this term on the dynamics of collisions between two dyonic instantons. Unfortunately the complexity of the full moduli space makes a systematic exploration of this regime numerically difficult.

In our discussion of the dynamics we have assumed that the moduli space approximation is a suitable approximation in the regimes we have considered and we have discounted any radiative modes as negligible. Certainly this is the case in similar systems [100] and we expect it to hold here as well, but ideally we could check the validity of the approximation with a comparison to the full field theory. Unfortunately a full simulation of the four dimensional field theory is beyond the reach of available computing power at this time. It may be possible to revisit this question in the future.

It would be interesting to explore the dynamics of the full supersymmetric theory and the quantised theory. It would be particularly relevant to the M-theory interpretation of instantons to understand how the singularities affect the quantised theory and to explore the existence of bound states of instantons. Previous studies in this direction (for example [101]) have considered the bound states of periodic instantons and the behaviour in the decompactification limit. With the full metric and potential for two instantons now available it may be possible to consider this decompactified limit for two instantons directly.

Another approach to understanding the singularities would be to look at non-commutative instantons which have a minimum bound on their size [75]. It would be interesting to understand how the non-commutativity affects the moduli space and dynamics of two slow moving (dyonic) instantons.

Finally, this work could be extended to calculate the moduli space metric and potential of dyonic instantons in $SU(3)$ or $SU(N)$. The higher gauge group allows the possibility of bound states that correspond to supertubes passing through intermediate D4-branes and may provide a more direct description of the index counting in reference [78]. Work on this is in progress.

Chapter 7

Regular polytope symmetry

In this final chapter we are interested in finding ADHM data for higher charge instantons with an $SU(2)$ gauge group. A general solution to the ADHM constraints is known for instantons with charge three or less, but the non-linearity of the constraints makes a general solution for higher charges difficult to find. In this chapter we will search for specific solutions to the ADHM constraints by looking for instantons with a large amount of symmetry. For an instanton to be symmetric it must be invariant under the action of some symmetry group, and the underlying ADHM data must also be invariant under the appropriate transformations. This restricts the space of possible ADHM data, and we are left with far fewer parameters in the ADHM constraints, which we can now solve explicitly.

Our motivation for studying symmetric instantons comes from their relation to other systems. Instantons that are symmetric under a subgroup of $SO(3)$, such as the cubic and icosahedral symmetry groups, can be used to generate solutions in the Skyrme model that are approximately Skyrmions and deviate from the Skyrme energy by only a few percent [102, 103]. In Section 7.1 we will review this relationship and present the known instanton solutions with tetrahedral, cubic, and icosahedral symmetries. There is also a connection between instantons and hyperbolic monopoles, where a hyperbolic monopole solution can be constructed from ADHM data which has a circle symmetry [104]. The known symmetric instantons all have this circle symmetry and so immediately give rise to new hyperbolic monopole solutions [105]. We also review this in Section 7.1.

Motivated by the utility of instantons with symmetries which are a subgroup of $SO(3)$, the rest of this chapter is concerned with finding instantons that have a symmetry which is a subgroup of the larger $SO(4)$. These may provide further links to Skyrmions and monopoles, although we will not explore that question in this thesis. The symmetric instantons mentioned so far have the symmetries of the Platonic solids in three dimensions. The analogues of the Platonic solids in four dimensions are the regular polytopes, which are composed of identical three-dimensional cells which are

Platonic solids. The symmetry groups of the regular polytopes are subgroups of $SO(4)$ and are natural candidates for symmetric instantons. There are six regular polytopes in four dimensions and in Section 7.2 we will describe these polytopes in more detail and understand the action of their symmetry groups. In Section 7.3 we will look at how the action of a general symmetry group on the instanton is lifted to act on the underlying ADHM data. In Section 7.4 we will see how the representations of the 5-cell symmetry group can be used to find ADHM data with the symmetries of the 5-cell. The double cover of the 5-cell symmetry group is a subgroup of $SU(2)$, which is the double cover of $SO(3)$. This allows us to use the existing machinery for Platonic symmetries, but in Section 7.5 we will understand how the ADHM data transforms when the symmetry group is a subgroup of $SU(2) \times SU(2)$, which is the double cover of $SO(4)$. This places restrictions on the possible form of the ADHM data, and in Section 7.7 we use these restrictions to search for solutions which have the symmetries of the 16-cell. In Section 7.8 we perform a similar search to find solutions with the symmetries of the 24-cell, where the representations of the symmetry are more complex and so the search is made more difficult. In both cases we recover solutions which have the appropriate symmetries, but these turn out to be equivalent to solutions which can be constructed from the JNR ansatz.

7.1 Symmetric instantons and other soliton systems

In this section we will review two systems in which symmetric instantons can be used to construct new solutions: Skyrmions and hyperbolic monopoles.

7.1.1 Skyrmions

The Skyrme model is a 3+1 dimensional non-linear field theory of low-energy hadronic physics in which protons and neutrons appear as topological solitons [106]. These topological solitons are known as Skyrmions and their topological charge is known as the baryon number, B . When $B = 1$ the Skyrmion solution is spherically symmetric and is an approximate model of a proton or neutron, and there are bound states of multiple Skyrmions which can be viewed as nuclei of low atomic mass number.

The Skyrme field is an $SU(2)$ valued scalar, $U(\mathbf{x})$. The Skyrme field can be parameterised as

$$U(\mathbf{x}, t) = \sigma + i\pi \cdot \tau, \quad (7.1.1)$$

where τ_1, τ_2 and τ_3 are the Pauli matrices. The parameters are constrained by

$$\sigma^2 + \pi_1^2 + \pi_2^2 + \pi_3^2 = 1. \quad (7.1.2)$$

The Lagrangian is written in terms of the $\mathfrak{su}(2)$ -valued current, $L_\mu = U^{-1}\partial_\mu U$, and is

$$\mathcal{L} = -\frac{1}{2} \text{Tr} (L_\mu L^\mu) + \frac{1}{16} \text{Tr} ([L_\mu, L_\nu][L^\mu, L^\nu]). \quad (7.1.3)$$

Note that U and L in the Skyrme model have no relation to the quantities in the ADHM construction with the same labels. Hopefully their meaning will be clear from the context. For finite energy, the Skyrme field must go to a constant value at infinity and can always be rotated to be 1,

$$U(\mathbf{x}, t)|_{|\mathbf{x}| \rightarrow \infty} = 1. \quad (7.1.4)$$

At any given time the Skyrme field can therefore be taken as a field over S^3 by compactifying \mathbb{R}^3 with a point at infinity. As with instantons, such a map has a topological degree, and in the Skyrme model this topological degree is known as the baryon number. Unlike instantons, the BPS equations for Skyrmions do not have any solutions, and there is no simple method of finding the fields that are the minimum energy solutions in each topological sector.

The simplest class of Skyrme fields are the spherically symmetric hedgehog fields,

$$U(\mathbf{x}) = \exp (if(r) \mathbf{x} \cdot \boldsymbol{\tau}). \quad (7.1.5)$$

To satisfy the boundary conditions, we must have $f(r) \rightarrow 0$ as $r \rightarrow \infty$, and for this solution to be smooth at the origin, we must have $f(0) = n\pi$ for some integer n . The integer n is the baryon number of this field, $B = n$. There is a unique f for each baryon number which minimises the energy of fields of this form. The solution for f can only be found numerically, and the minimum energy field for $B = 1$ is known as the Skyrminion. There is strong evidence that the Skyrminion is the lowest energy solution with $B = 1$. The energy of a hedgehog field with $B > 1$ is considerably larger than the energy of B Skyrminions, and these solutions are not stable. For $B = 2$, the minimum energy Skyrminions are toroidal [107, 108, 109].

A Skyrme field can be generated from an $SU(2)$ instanton field via the following formula [102, 103]:

$$U(\mathbf{x}) = \mathcal{P} \exp \left(-i \int_{-\infty}^{\infty} dt A_4(\mathbf{x}, t) \right), \quad (7.1.6)$$

where A_4 is the fourth spatial component of the Yang-Mills gauge field in the instanton solution and \mathcal{P} denotes path ordering.

The minimum energy Skyrminion solutions of charge one and two have spherical and axial symmetry respectively and can both be approximately generated from instantons with the corresponding symmetries. The instanton generated solutions are not exactly

the Skyrmion solutions, but they are very close, and their energy is only 1% greater than the true Skyrmion solutions.

The charge three and four minimum energy Skyrmons have tetrahedral and cubic symmetry respectively. There also exist instanton solutions with these symmetries which generate Skyrme fields which are a very good approximation to the minimum energy Skyrmons [110]. The charge three tetrahedral instanton is found by placing the four poles in the JNR ansatz at the vertices of a tetrahedron with equal weight, but the charge four cubic instanton is a novel solution to the ADHM constraints. The cubic instanton is part of a one parameter family of instantons which has overall tetrahedral symmetry. At one end of the parameter space, the instantons are well separated at the vertices of a tetrahedron. As the parameter varies the instantons come closer together until they have cubic symmetry. They then separate again on the vertices of the dual tetrahedron. After mapping to the Skyrme fields this family of instantons describes the scattering of four Skyrmons in the same way.

The novel charge four instanton with cubic symmetry is given by the ADHM data [110],

$$a = \frac{1}{2\sqrt{2}} \begin{pmatrix} \sqrt{2} & \sqrt{2}i & \sqrt{2}j & \sqrt{2}k \\ 0 & -(j+k) & -(k+i) & -(i+j) \\ -(j+k) & 0 & (j-i) & (i-k) \\ -(k+i) & (j-i) & 0 & (k-j) \\ -(i+j) & (i-k) & (k-j) & 0 \end{pmatrix}. \quad (7.1.7)$$

The topological charge density of this instanton is shown in Figure 7.1. This figure has been plotted using the formula for the topological charge density,

$$\frac{1}{8\pi^2} \varepsilon_{ijkl} \text{Tr} (F_{ij} F_{kl}), \quad (7.1.8)$$

and the expression for F_{ij} in terms of the ADHM data,

$$F_{ij} = -U^\dagger b (\Delta^\dagger \Delta)^{-1} (e_i \bar{e}_j - e_j \bar{e}_i) b^\dagger U, \quad (7.1.9)$$

where $e_i = \{i, j, k, 1\}$.

The minimum energy charge seven Skyrmon forms a shell with the structure of a dodecahedron, which has icosahedral symmetry [111]. The corresponding charge seven instanton with the same structure has been found by searching for charge seven ADHM data which is invariant under the icosahedral symmetry group [112]. This dodecahedral instanton fits into a one parameter family with overall tetrahedral symmetry. This one parameter family describes the scattering of six Skyrmons which are initially positioned along the three axes at plus and minus infinity, and a Skyrmon positioned at the origin. The Skyrmons move in towards the origin where they form a shell with the

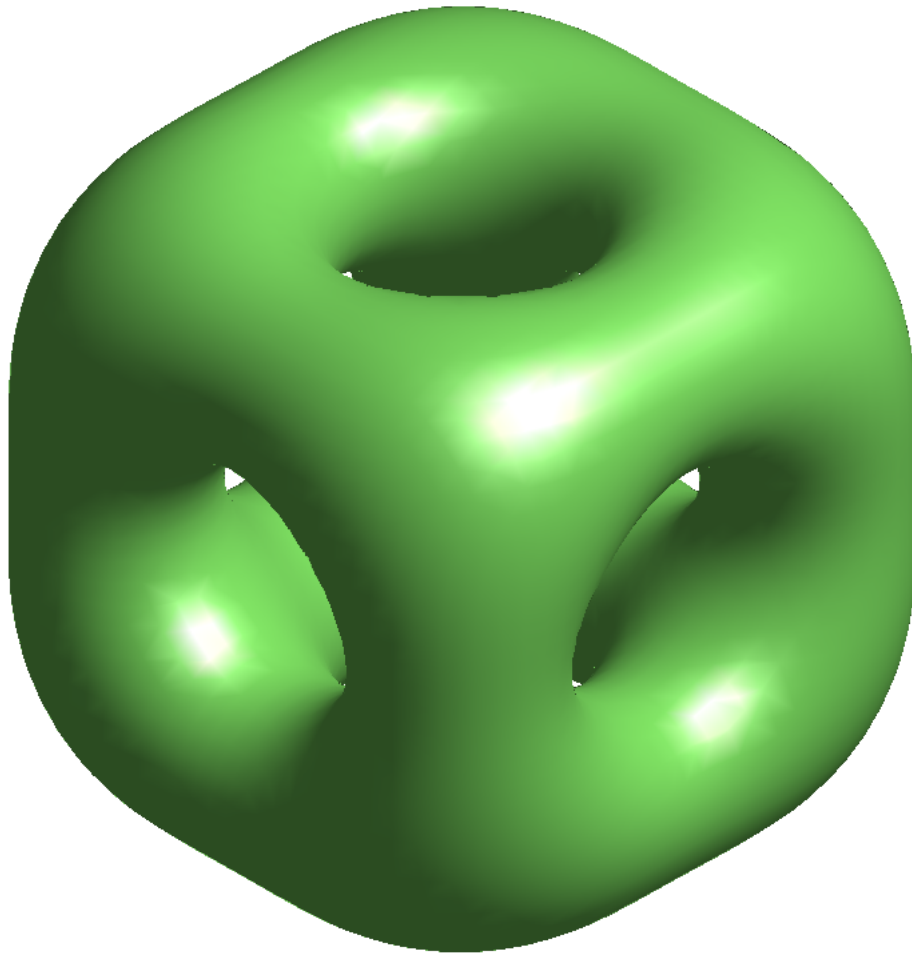


Figure 7.1: A surface of constant topological charge density of the charge four instanton with cubic symmetry.

dodecahedral structure and then a cube. They then form the dual dodecahedron and move out along the same axes again. This process is illustrated in Figure 1 of reference [112].

The ADHM data of the charge seven icosahedral instanton is [112].

$$a = \begin{pmatrix} 1 & i & j & k & 0 & 0 & 0 \\ 0 & 0 & 0 & 0 & i & j & k \\ 0 & 0 & 0 & 0 & 0 & \tau k & \tau^{-1}j \\ 0 & 0 & 0 & 0 & \tau^{-1}k & 0 & \tau i \\ 0 & 0 & 0 & 0 & \tau j & \tau^{-1}i & 0 \\ i & 0 & \tau^{-1}k & \tau j & 0 & 0 & 0 \\ j & \tau k & 0 & \tau^{-1}i & 0 & 0 & 0 \\ k & \tau^{-1}j & \tau i & 0 & 0 & 0 & 0 \end{pmatrix}. \quad (7.1.10)$$

Here $\tau = (\sqrt{5} + 1)/2$. The topological charge density takes the form of a dodecahedron and is shown in Figure 7.2.

There is also a known charge 17 icosahedral instanton which resembles a buckyball [113] which we will not discuss here.

7.1.2 Hyperbolic monopoles

Monopoles are the solutions to the BPS equations in four-dimensional Yang-Mills-Higgs theory and carry a topological magnetic charge. There are many thorough reviews on the subject of monopoles, for example [7, 60]. The moduli space of monopoles is well understood, but explicit solutions to the BPS equations are known only for charge one and charge two monopoles [114, 115, 116] or axially symmetric monopoles of any charge [117]. Like with instantons, monopoles can be constructed by solving an easier constraint. For monopoles this procedure is known as the Nahm transform, and the Nahm data is a set of one parameter matrix-valued functions which satisfy the Nahm equations [118]. In general the corresponding monopole solutions can only be constructed numerically. Monopoles can also exist in a hyperbolic background geometry, and in this case it is possible to find additional explicit solutions.

Monopoles can be recovered from instantons by compactifying one of the four spatial directions so that one of the components of the gauge field becomes a scalar, $A_4 = \Phi$. The BPS equations for monopoles are the dimensionally reduced self-dual field equations,

$$\star F = D\Phi, \quad (7.1.11)$$

where \star is the Hodge dual.

Monopoles in a background with hyperbolic geometry have the same BPS equation,

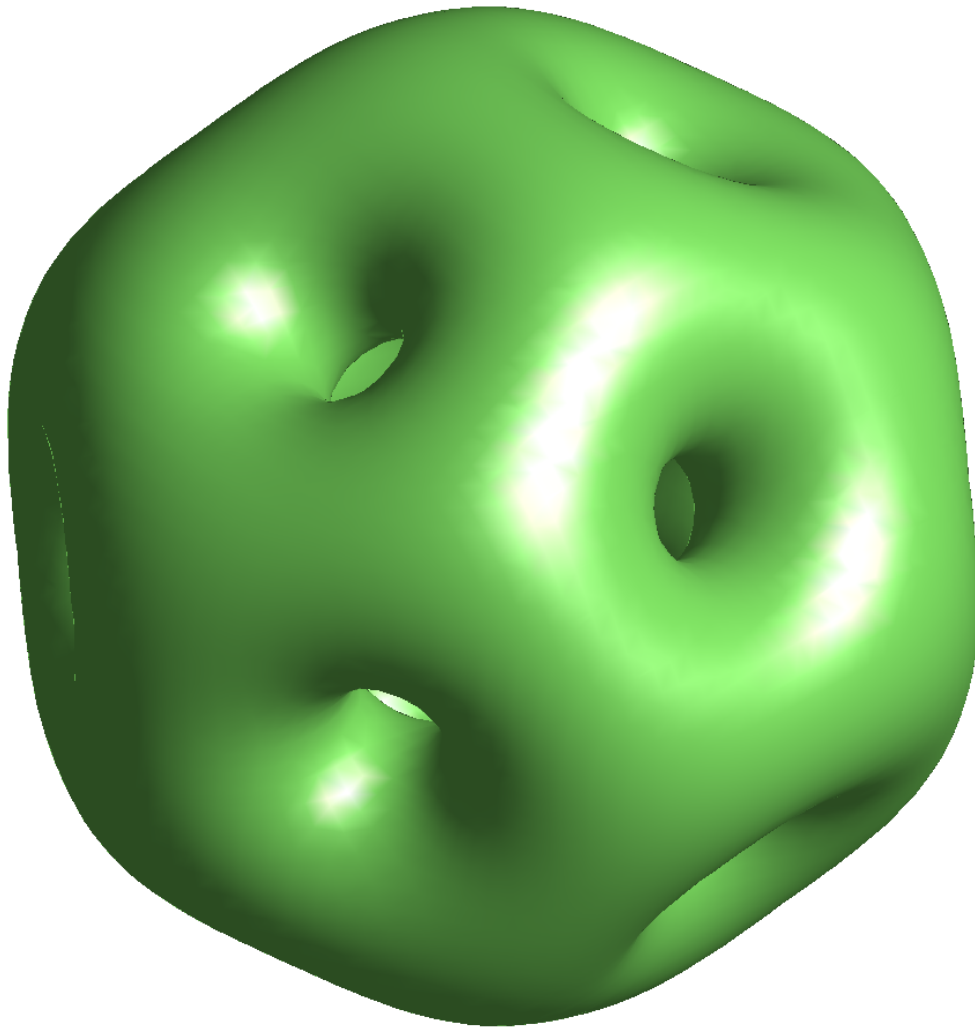


Figure 7.2: A surface of constant topological charge density of the charge 7 instanton with icosahedral symmetry, which resembles a dodecahedron.

although the Hodge dual is now given by

$$(\star F)_k = \sqrt{|\det g|} \varepsilon_{ijk} F^{ij}, \quad (7.1.12)$$

where g is the metric in hyperbolic space.

An instanton reduces to give a monopole in hyperbolic space if the underlying ADHM data has a circle symmetry [104]. Using the JNR ansatz, hyperbolic monopoles with arbitrary Platonic symmetries can be constructed by using the freedom to place the $k + 1$ poles in the JNR ansatz on a two-dimensional subspace that ensures the instanton is invariant under the circle symmetry [105]. In reference [105], examples are constructed with spherical, axial, tetrahedral, octahedral and icosahedral symmetry, at charges 1, 2, 3, 5 and 11 respectively.

The dimension of the hyperbolic monopole moduli space scales as $4k$, but the dimension of the space of JNR solutions only grows like $3k$ and so does not contain all hyperbolic monopole solutions. To obtain all hyperbolic monopoles, one must obtain all ADHM data which is invariant under a circle symmetry. In general, ADHM data is invariant under a circle if the following stronger constraints hold [105]:

- $a^\dagger a = \mathbb{1}_k$,
- M is pure quaternionic,
- $LM = \mu L$ for some pure quaternion μ , and L is non-zero.

Note that the first of these implies that the usual ADHM constraint in equation (4.3.10) is satisfied. A quick check reveals that the charge four cubic instanton and the charge seven dodecahedral instanton shown previously both satisfy these constraints and so reduce to give novel symmetric hyperbolic monopoles which are of a lower charge than the JNR ansatz can produce [105]. In fact, the one parameter families that both of these symmetric instantons fit into give one parameter families describing the scattering of hyperbolic monopoles.

7.2 Regular polytopes

Before we look for instantons with four-dimensional symmetries, we will first understand the regular polytopes that these symmetries arise from. The Platonic solids are regular polyhedra where all of the faces are identical regular polygons. In four dimensions, the analogue of the Platonic solids are the regular polytopes which are constructed from identical cells that are Platonic solids. There are six regular polytopes, which are labelled by the number of three dimensional cells they contain:

- 5-cell, or *pentatope*. This is the four-dimensional generalisation of the tetrahedron. It is dual to itself.
- 8-cell, or *tesseract*. This is the four-dimensional generalisation of the cube.
- 16-cell, or *hyperoctahedron*. This is the four-dimensional generalisation of the octahedron. It is dual to the tesseract.
- 24-cell. The 24-cell is dual to itself. It is unique since it doesn't fit into a family of polytopes which span all dimensions.
- 120-cell. This is the four-dimensional generalisation of the dodecahedron.
- 600-cell. This is the four-dimensional generalisation of the icosahedron. It is dual to the 120-cell.

The regular polytopes that are dual to each other share the same symmetry group, so the only symmetry groups we need to consider are those of the 5-cell, the 16-cell, the 24-cell and the 600-cell. In our treatment of the group action below, the symmetry groups act via the independent left and right multiplication of quaternions. The symmetry group of the 5-cell does not fit into this framework, and the lowest charge instanton with the symmetries of the 5-cell can be found by simpler means [3]. Our general framework is stretched to its limit with the 24-cell symmetry group, so we will only briefly mention the 120-cell and 600-cell in this thesis. In the rest of this section we will review the symmetry groups of the four-dimensional polytopes.

If \mathbb{R}^4 is identified with the quaternions, \mathbb{H} , then the action of any rotation, $\mathfrak{g} \in \text{SO}(4)$, can be expressed as left and right multiplication by unit quaternions,

$$\mathfrak{g} \circ x = g_L x g_R^{-1}, \quad (7.2.1)$$

for some unit quaternions $g_L, g_R \in \text{SU}(2)$. The action of (g_L, g_R) is identical to the action of $(-g_L, -g_R)$, so there are two elements in $\text{SU}(2) \times \text{SU}(2)$ which correspond to the same element in $\text{SO}(4)$. The group $\text{SU}(2) \times \text{SU}(2)$ is therefore the double cover of $\text{SO}(4)$. The symmetry groups of the regular polytopes are all naturally expressed as subgroups of $\text{SU}(2) \times \text{SU}(2)$, and the true symmetry group is the projection into $\text{SO}(4)$.

5-cell or pentatope

The 5-cell is the four-dimensional generalisation of the tetrahedron and the action of its symmetry group is realised in a different way to the 16-cell and 24-cell, so we will consider it first. The vertices of the 5-cell can be taken to be the five quaternions,

$$V_5 = \left\{ 1, \frac{1}{4}(-1 \pm i \pm j \pm k) \right\}, \quad (7.2.2)$$

where an odd number of plus signs is taken for each vertex. These vertices are permuted under the action of the icosahedral group by

$$x \mapsto g^\sharp x g^{-1}, \tag{7.2.3}$$

where g is an element of the binary icosahedral group, which is generated by the unit quaternions,

$$g_1 = i, \quad g_2 = j, \quad \text{and} \quad g_3 = -\frac{1}{2}(i + \tau j - \tau^{-1}k). \tag{7.2.4}$$

In this expression $\tau = \frac{1}{2}(\sqrt{5} + 1)$, and g^\sharp is the dual of g , which is obtained by replacing τ with $-\tau^{-1}$.

The double cover of the symmetry group of the 5-cell is therefore a subgroup of $SU(2)$, and is embedded in $SU(2) \times SU(2)$ via $g \mapsto (g^\sharp, g)$.

16-cell

The 16-cell is the four-dimensional generalisation of the octahedron. It has 8 vertices which lie at ± 1 on each axis and these vertices form the quaternion group,

$$Q_8 = \{\pm 1, \pm i, \pm j, \pm k\}. \tag{7.2.5}$$

The quaternion group is a group under quaternion multiplication and the left and right action of Q_8 therefore permutes the vertices of the 16-cell,

$$x \mapsto g_L x g_R^{-1}, \quad g_L, g_R \in Q_8. \tag{7.2.6}$$

The double cover of the rotational symmetry group of the 16-cell is therefore $Q_8 \times Q_8 \subset SU(2) \times SU(2)$. The quaternion group, Q_8 , is generated by two elements,

$$g_1 = i, \quad \text{and} \quad g_2 = j. \tag{7.2.7}$$

More abstractly, the quaternion group is generated by any two generators that satisfy

$$g_1^\alpha = g_2^\beta = (g_1 g_2)^\gamma = -1, \quad \text{with} \quad \alpha = \beta = \gamma = 2. \tag{7.2.8}$$

The 16-cell is dual to the 8-cell, which shares the same symmetry group.

24-cell

The structure of the symmetries of the 24-cell is very similar. The vertices of the 24-cell form the binary tetrahedral group,

$$\mathbb{T} = \{\pm 1, \pm i, \pm j, \pm k, \frac{1}{2}(\pm 1 \pm i \pm j \pm k)\}. \tag{7.2.9}$$

The double cover of the rotational symmetry group of the 24-cell is $\mathbb{T} \times \mathbb{T}$, with rotations acting via left and right multiplication. The binary tetrahedral group is generated by

$$g_1 = \frac{1}{2}(1 + i + j + k), \quad \text{and} \quad g_2 = \frac{1}{2}(1 + i + j - k), \quad (7.2.10)$$

which in general satisfy,

$$g_1^\alpha = g_2^\beta = (g_1 g_2)^\gamma = -1, \quad \text{with } \alpha = \beta = 3, \gamma = 2. \quad (7.2.11)$$

600-cell

The 120 vertices of the 600-cell form the binary icosahedral group, \mathbb{I} , which is generated by

$$g_1 = \frac{1}{2}(1 + i + j + k), \quad \text{and} \quad g_2 = \frac{1}{2}(\tau + \tau^{-1}i + j). \quad (7.2.12)$$

The double cover of the rotational symmetry group of the 600-cell is therefore $\mathbb{I} \times \mathbb{I}$, with rotations acting via left and right multiplication. In general the generators satisfy,

$$g_1^\alpha = g_2^\beta = (g_1 g_2)^\gamma = -1, \quad \text{with } \alpha = 2, \beta = 3, \gamma = 5. \quad (7.2.13)$$

The 600-cell is dual to the 120-cell which shares the same symmetry group.

Group representations

A representation of a group is a map, ρ , from the group to $\text{GL}(n)$ such that the matrices, $\rho(g)$, preserve the group action. The representation matrices must satisfy the group presentation,

$$\rho(g_1)^\alpha = \rho(g_2)^\beta = (\rho(g_1)\rho(g_2))^\gamma. \quad (7.2.14)$$

A representation, ρ , is *irreducible* if there is no similarity transform which simultaneously puts $\rho(g_1)$ and $\rho(g_2)$ into block diagonal form. For any other representation there exists a transformation which decomposes it into block diagonal form with each block being an irreducible representation. In the ADHM data, the only transformation matrices which we can apply are real and orthogonal. We are therefore only interested in real representations. We note that certain representations may be reducible over \mathbb{C} but are irreducible over \mathbb{R} .

All irreducible representations satisfy

$$\rho(g_1)^\alpha = \rho(g_2)^\beta = (\rho(g_1)\rho(g_2))^\gamma = \varepsilon, \quad \text{where } \varepsilon = \pm 1. \quad (7.2.15)$$

A general irreducible representation may have either sign for ε , and we will call representations where $\varepsilon = +1$ a *positive representation*, and those where $\varepsilon = -1$ a *negative representation*. A positive representation is also a representation of the subgroup of

$\text{SO}(3)$, while a negative representation is only a representation of the double cover. The quaternion representation is a negative representation, while the trivial representation where all group elements map to the identity matrix is a positive representation.

Typically, representations are labelled by a letter which indicates their dimension. One-dimensional representations are labelled by A , while two-dimensional representations are labelled by E , three-dimensional representations by F , and higher dimensions by going through the alphabet in sequence. Negative representations are indicated with a prime, for example, G' . The fundamental quaternion representation is therefore typically labelled E' , since we represent quaternions as 2×2 complex matrices.

7.3 Group actions on the ADHM data

In this section we will understand what it means for an instanton to be symmetric, and how the symmetry group acts on both the instanton and the underlying ADHM data. For an instanton to be symmetric the transformation of the gauge field under the action of the symmetry must be gauge equivalent to the original gauge field. As a consequence of this the topological charge density of the instanton will be invariant under the action of the symmetry group. The symmetry could be any subgroup of $\text{SO}(4)$ such as the symmetry groups of the Platonic solids or of the regular polytopes. Every instanton has some underlying ADHM data from which it can be constructed, and in this section we will see how the action of the symmetry group can be lifted to an action on the ADHM data.

If $\mathcal{G} \subset \text{SO}(4)$ is the symmetry group of an instanton, such as the 16-cell or 24-cell symmetry groups above, then the topological charge density must be invariant under the action of \mathcal{G} . The gauge field may still transform up to a gauge transformation, so if \mathfrak{g} is an element of \mathcal{G} , we must have

$$A_i(\mathfrak{g} \circ x) = \Omega_{\mathfrak{g}}(x)A_i(x)\Omega_{\mathfrak{g}}^{-1}(x) - i\Omega_{\mathfrak{g}}(x)\partial_i(\Omega_{\mathfrak{g}}^{-1}(x)). \quad (7.3.1)$$

To find solutions with this symmetry we need to lift the action of \mathcal{G} on A_i to an action on the underlying ADHM data. Recall that the ADHM data for a charge k instanton with $\text{SU}(2)$ gauge group is given by

$$\Delta(x) = a - bx, \quad (7.3.2)$$

where

$$a = \begin{pmatrix} L \\ M \end{pmatrix}, \quad \text{and} \quad b = \begin{pmatrix} 0 \\ \mathbb{1}_k \end{pmatrix}. \quad (7.3.3)$$

In this expression L is a length k quaternionic row vector and M is a $k \times k$ symmetric

quaternionic matrix. The spatial coordinate, x , is a quaternion in this construction. Recall that the ADHM construction does not choose a particular gauge for the gauge field.

If the gauge field is invariant under the action of \mathcal{G} then the ADHM data, $\Delta(x)$, must also transform in a way that leaves the gauge field invariant up to gauge transformation. The only symmetries of the ADHM data which leave the corresponding gauge equivalence class invariant are

$$\Delta \rightarrow \begin{pmatrix} p & 0 \\ 0 & P \end{pmatrix} \Delta R^{-1}, \quad (7.3.4)$$

where p is a unit quaternion, P is a $k \times k$ quaternionic matrix such that $P^\dagger P = \mathbb{1}_k$, and R is an invertible $k \times k$ quaternionic matrix. For each element of the symmetry group, $\mathfrak{g} \in \mathcal{G}$, the transformed ADHM data is $\Delta(\mathfrak{g} \circ x)$. For a symmetric instanton, this must be equivalent to $\Delta(x)$, so there must exist $p_{\mathfrak{g}}$, $P_{\mathfrak{g}}$ and $R_{\mathfrak{g}}$ such that

$$\Delta(\mathfrak{g} \circ x) = \begin{pmatrix} p_{\mathfrak{g}} & 0 \\ 0 & P_{\mathfrak{g}} \end{pmatrix} \Delta(x) R_{\mathfrak{g}}^{-1}. \quad (7.3.5)$$

Recall that every rotation in \mathbb{R}^4 can be represented by left and right multiplication by unit quaternions,

$$\mathfrak{g} \circ x = g_L x g_R^{-1}. \quad (7.3.6)$$

Since the ADHM data is quaternionic, this is a natural way to represent the action of \mathfrak{g} . By comparing the terms in equation (7.3.4) which are linear in x , we see that $P_{\mathfrak{g}}$ and $R_{\mathfrak{g}}$ must factor into

$$P_{\mathfrak{g}} = Q_{\mathfrak{g}} g_L, \quad \text{and} \quad R_{\mathfrak{g}} = Q_{\mathfrak{g}} g_R, \quad (7.3.7)$$

for some real orthogonal matrix, $Q_{\mathfrak{g}}$. The left quaternion, g_L , may also be factored out of $p_{\mathfrak{g}}$, so that for symmetric ADHM data there must exist a quaternion $q_{\mathfrak{g}}$, and a real orthogonal matrix, $Q_{\mathfrak{g}}$, such that

$$\Delta(g_L x g_R^{-1}) = \begin{pmatrix} q_{\mathfrak{g}} & 0 \\ 0 & Q_{\mathfrak{g}} \end{pmatrix} g_L \Delta(x) g_R^{-1} Q_{\mathfrak{g}}^{-1}. \quad (7.3.8)$$

In terms of the blocks in the ADHM data, L and M , this condition is

$$q_{\mathfrak{g}} g_L L = L g_R Q_{\mathfrak{g}} \quad \text{and} \quad Q_{\mathfrak{g}} g_L M = M g_R Q_{\mathfrak{g}}. \quad (7.3.9)$$

To recap, if we have a symmetric instanton, then its ADHM data must be invariant under the action of each symmetry, $\mathfrak{g} \in \mathcal{G}$. This can be represented by the action of an

element in the double cover of \mathcal{G} , which is a subgroup of $SU(2) \times SU(2)$, and acts by left and right quaternion multiplication. The transformed ADHM data must give the same gauge field, and so there must exist a $q_{\mathfrak{g}}$ and $Q_{\mathfrak{g}}$, as above, that relate it back to the original ADHM data. Later on we will flip this argument, and look for symmetric ADHM data by first finding all possible $q_{\mathfrak{g}}$ and $Q_{\mathfrak{g}}$.

7.4 The 5-cell

The action of the 5-cell symmetry group is different from the 16-cell and 24-cell symmetry group because the left and right actions do not act independently. Put another way, the double cover of the symmetry group is isomorphic to a subgroup of $SU(2)$ and is embedded diagonally in $SU(2) \times SU(2)$. This allows the existing machinery that was used to find the charge seven [112] and charge 17 instanton [113] with icosahedral symmetry to be applied to the 5-cell as well. The symmetric instantons considered previously are symmetric under rotations in $SO(3)$, and the double cover of $SO(3)$ is $SU(2)$, with rotations acting as

$$x \mapsto g x g^{-1}. \quad (7.4.1)$$

For the 5-cell this action is twisted and the left quaternion is replaced by its dual, g^{\sharp} , but the representation theory remains largely the same since the left and right actions are not independent.

The following ADHM data is invariant under the action of the 5-cell symmetry group [3],

$$a = \lambda \begin{pmatrix} -2 & -2i & -2j & -2k \\ -3 & i & j & k \\ i & 1 & -\sqrt{5}k & -\sqrt{5}j \\ j & -\sqrt{5}k & 1 & -\sqrt{5}i \\ k & -\sqrt{5}j & -\sqrt{5}i & 1 \end{pmatrix}, \quad (7.4.2)$$

where λ is a real number that determines the scale of the instanton. This ADHM data is invariant under the action of the 5-cell symmetry group,

$$\begin{pmatrix} L \\ M \end{pmatrix} = \begin{pmatrix} 1 & 0 \\ 0 & G(g_i) \end{pmatrix} g_i^{\sharp} \begin{pmatrix} L \\ M \end{pmatrix} g_i^{-1} G(g_i)^{-1}, \quad (7.4.3)$$

where g_i are the generators of the binary icosahedral group in equation (7.2.4), and G

is a four-dimensional irreducible representation of the binary icosahedral group,

$$\begin{aligned}
 G(g_1) &= \begin{pmatrix} 1 & 0 & 0 & 0 \\ 0 & 1 & 0 & 0 \\ 0 & 0 & -1 & 0 \\ 0 & 0 & 0 & -1 \end{pmatrix}, & G(g_2) &= \begin{pmatrix} 1 & 0 & 0 & 0 \\ 0 & -1 & 0 & 0 \\ 0 & 0 & 1 & 0 \\ 0 & 0 & 0 & -1 \end{pmatrix}, \\
 G(g_3) &= \frac{1}{4} \begin{pmatrix} -1 & \sqrt{5} & -\sqrt{5} & -\sqrt{5} \\ \sqrt{5} & 3 & 1 & 1 \\ -\sqrt{5} & 1 & -1 & 3 \\ -\sqrt{5} & 1 & 3 & -1 \end{pmatrix}.
 \end{aligned} \tag{7.4.4}$$

7.5 Independent left and right actions

Suppose that we have ADHM data which is invariant under the symmetries of the 16-cell or the 24-cell. The crucial difference in this case compared to the 5-cell is that the left and right actions can be applied independently. We will first consider the right action of the generators of the symmetry group, so that $g_R = g_1, g_2$. Then there must exist matrices $Q_R(g_i)$ and quaternions $q_R(g_i)$ which satisfy

$$Q_R(g_i) M = M g_i Q_R(g_i) \quad \text{and} \quad q_R(g_i) L = L g_i Q_R(g_i). \tag{7.5.1}$$

In our framework, the matrices in the right action form a representation of the double cover of the symmetry group,

$$Q_R(g_1)^\alpha = Q_R(g_2)^\beta = (Q_R(g_1)Q_R(g_2))^\gamma. \tag{7.5.2}$$

We are free to choose a basis for this representation, and so can decompose it into the direct sum of irreducible representations. If we order the irreducible representations so that the positive representations form the upper blocks of Q_R and the negative representations form the lower blocks of Q_R then

$$Q_R(g_1)^\alpha = Q_R(g_2)^\beta = (Q_R(g_1)Q_R(g_2))^\gamma = \begin{pmatrix} \mathbb{1}_m & 0 \\ 0 & -\mathbb{1}_n \end{pmatrix}, \tag{7.5.3}$$

where $m + n = k$. We can write Q_R as

$$Q_R(g) = \begin{pmatrix} Q_R^+(g) & 0 \\ 0 & Q_R^-(g) \end{pmatrix}, \tag{7.5.4}$$

where Q_R^+ is an m -dimensional positive representation and Q_R^- is an n -dimensional negative representation of the double cover of the symmetry group.

We can view M as a map from some k -dimensional representation space, W , tensored with the quaternion representation, E' , back to the representation space, W ,

$$M : W \otimes E' \rightarrow W. \quad (7.5.5)$$

Since E' is a negative representation, M must map the subspace of a positive representation in W to the subspace of a negative representation in W , and vice-versa. There can be no invariant maps between two positive representations or between two negative representations in W . Equivalently, when Q_R is in the basis above, the only M which can be invariant have the form

$$M = \begin{pmatrix} 0 & B \\ B^\top & 0 \end{pmatrix}, \quad (7.5.6)$$

where B is an $m \times n$ quaternionic matrix.

If we now consider the left action then there must exist matrices $Q_L(g_i)$ and quaternions $q_L(g_i)$ which satisfy

$$Q_L(g_i) g_i M = M Q_L(g_i) \quad \text{and} \quad q_L(g_i) g_i L = L Q_L(g_i). \quad (7.5.7)$$

We have fixed the basis for the right action and we no longer have the freedom to choose an arbitrary basis for the representation Q_L in the left action. However, by considering the action of $(g_i)^\alpha = -1$, and the form of M shown above, we can take Q_L to satisfy

$$Q_L(g_1)^\alpha = Q_L(g_2)^\alpha = (Q_L(g_1)Q_R(g_2))^\beta = \begin{pmatrix} \mathbb{1}_m & 0 \\ 0 & -\mathbb{1}_n \end{pmatrix}. \quad (7.5.8)$$

The representation of the left action can therefore also be put in the same block form as the right action,

$$Q_L(g) = \begin{pmatrix} Q_L^+(g) & 0 \\ 0 & Q_L^-(g) \end{pmatrix}, \quad (7.5.9)$$

where Q_L^+ is a m -dimensional positive representation and Q_L^- is a n -dimensional negative representation. Unlike the right action, these blocks are not necessarily the direct sum of irreducible representations, since we no longer have the freedom to arbitrarily choose our basis.

So far we have considered the left and right actions independently, but the full set of rotations in $\text{SO}(4)$ are generated by acting with both a left and right action together. Whether we act on the left or the right first is irrelevant to the action on x , but is significant when considering the ordering of Q_L and Q_R . If we compare the action of first acting on the left by g_i and then on the right by g_j with the action of first acting on the right by g_j and then on the left by g_i then we see that the matrices in the left

and right representations must commute,

$$Q_R(g_i) Q_L(g_j) = Q_L(g_j) Q_R(g_i). \quad (7.5.10)$$

Anti-commuting is also a possibility, but we can rule this out by considering the left or right action of $(g_1)^{2\alpha} = 1$ under which $(Q_{L,R}(g_1))^{2\alpha} = \mathbb{1}_k$ and so they must commute. By a similar argument, the quaternion representations, q_L and q_R , must also commute.

The above left and right actions on the ADHM data must also leave the upper row vector, L , invariant. We can write L in block form with the same block structure as Q_R and Q_L ,

$$L = (L^+ \ L^-). \quad (7.5.11)$$

To leave L invariant, q_R and Q_R must then satisfy,

$$q_R(g_i)L^+ = L^+ g_i Q_R^+(g_i) \quad \text{and} \quad q_R(g_i)L^- = L^- g_i Q_R^-(g_i). \quad (7.5.12)$$

When considering the action of $g_1^\alpha = g_2^\beta = (g_1 g_2)^\gamma = -1$ this becomes

$$(q_R(g_1))^\alpha L^+ = (q_R(g_2))^\beta L^+ = (q_R(g_1)q_R(g_2))^\gamma L^+ = -L^+, \quad (7.5.13)$$

and

$$(q_R(g_1))^\alpha L^- = (q_R(g_2))^\beta L^- = (q_R(g_1)q_R(g_2))^\gamma L^- = L^-. \quad (7.5.14)$$

Therefore L^+ can only be non-zero if q_R is a negative representation, and L^- can only be non-zero if q_R is a positive representation. Clearly only one of these blocks can be non-zero. A similar consideration of the left action shows that q_L must be a representation of the same sign as q_R to be able to leave the remaining non-zero block in L invariant. The only negative representations of q_R and q_L are proportional to the quaternion representation $q_{R,L}(g_i) = \pm g_i$, but in this case the left and right actions will not commute, so these can be ruled out.

In this section we have understood the structure of the representations which transform the ADHM data back to its original form after the application of the action of a symmetry group via left and right quaternion multiplication. The 2×2 complex representations q_R and q_L must be positive representations which are a subgroup of the 2×2 complex representation of quaternions. The transformation matrices Q_R and Q_L are k -dimensional real representations and share the same block form. The upper blocks, Q_R^+ and Q_L^+ , are positive representations and the lower blocks, Q_R^- and Q_L^- , are negative representations. We have the freedom to choose a canonical basis for either Q_R and Q_L and will choose to put Q_R in the form of the direct sum of irreducible representations.

ADHM data must then be invariant under the left and right action of this symmetry,

$$Q_{R,u}^+(g_i) B_{uv} = B_{uv} g_i Q_{R,v}^-(g_i), \quad Q_{L,u}^+(g_i) g_i B_{uv} = B_{uv} Q_{L,v}^-(g_i), \quad (7.6.4)$$

and

$$q_R(g_i) L_v^- = L_v^- g_i Q_{R,v}^-(g_i), \quad q_L(g_i) g_i L_v^- = L_v^- Q_{L,v}^-(g_i), \quad (7.6.5)$$

where $u = 1, \dots, s$, and $v = 1, \dots, t$. Note that the u and v indices are not summed over in these expressions.

After we have chosen a representation, we can find the invariant blocks, B_{uv} and L_v , for each choice of u and v by solving equations (7.6.4) and (7.6.5). If these blocks exist they generally have one or two free real parameters. These remaining free parameters are then constrained by the ADHM constraints, and whether an instanton exists for the given representation is determined by whether these constraints may be solved.

The remaining task is to find the possible representations for the blocks in Q_L and Q_R , recalling that Q_L must commute with Q_R . This will depend on the explicit form of the irreducible real representations of the double cover of the symmetry group, and we must consider the 16-cell and the 24-cell separately.

7.7 The 16-cell

In this section we will enumerate all possibilities for the representations Q_L , Q_R , q_R and q_L of the double cover of the 16-cell symmetry group. For each possible representation, we can look for ADHM data which is invariant, and then check whether it can satisfy the ADHM constraints. By starting at low charge and working our way up through higher charges, we hope to systematically search for the lowest charge instanton with the symmetries of the 16-cell.

We have seen in Section 7.3 that the symmetry group of the 16-cell is generated by the left and right actions of the quaternion group, Q_8 . The quaternion group is generated by two generators, $g_1 = i$ and $g_2 = j$, which have the presentation

$$g_1^2 = g_2^2 = (g_1 g_2)^2 = -1. \quad (7.7.1)$$

There are only five distinct irreducible real representations of the quaternion group, and all others are related by a similarity transformation. There are four positive

representations which are all one dimensional:

$$A(g_1) = 1, \quad A(g_2) = 1, \quad (7.7.2)$$

$$A_1(g_1) = -1, \quad A_1(g_2) = -1, \quad (7.7.3)$$

$$A_2(g_1) = -1, \quad A_2(g_2) = 1, \quad (7.7.4)$$

$$A_3(g_1) = 1, \quad A_3(g_2) = -1. \quad (7.7.5)$$

The remaining real representation is four dimensional and is a negative representation:

$$G'(g_1) = \begin{pmatrix} 0 & -1 & 0 & 0 \\ 1 & 0 & 0 & 0 \\ 0 & 0 & 0 & -1 \\ 0 & 0 & 1 & 0 \end{pmatrix}, \quad G'(g_2) = \begin{pmatrix} 0 & 0 & -1 & 0 \\ 0 & 0 & 0 & 1 \\ 1 & 0 & 0 & 0 \\ 0 & -1 & 0 & 0 \end{pmatrix}. \quad (7.7.6)$$

In the framework we have introduced in the previous section, the right action on the ADHM data, Q_R , can be written in block form where the upper block is a positive representation and the lower block is a negative representation. We can always choose a basis in which these blocks are the direct sum of irreducible representations, and the upper block of Q_R must be the direct sum of some combination of A , A_1 , A_2 and A_3 , while the lower block is a direct sum of some number of copies of G' .

Using the JNR ansatz, we can immediately construct a charge seven instanton with the symmetries of the 16-cell by placing the eight poles at the vertices of the 16-cell with equal weight. Since we are interested in the lowest charge solutions there is no need to consider charges higher than this. This immediately rules out the possibility of more than one copy of G' in the lower block of Q_R .

In the left action on the ADHM data, Q_L , the upper block must also be the direct sum of some combination of A , A_1 , A_2 and A_3 , and the lower block must be a copy of G' , but both blocks may be in a different basis to Q_R .

We can take the right action to be in the canonical basis for the representations that we have presented above. To find the left action, we must find representations in a basis which commute with the right action. We note that the representations don't have to be the same in the left and right actions, although as noted, they must have the same signs.

The upper block in the right action, Q_R^+ must be the direct sum of the one-dimensional representations, $Q_R^+ = a_0 A \oplus a_1 A_1 \oplus a_2 A_2 \oplus a_3 A_3$, where

$$a_0 A = \underbrace{A \oplus \dots \oplus A}_{a_0 \text{ times}}. \quad (7.7.7)$$

The matrices which will commute with this upper right action are of the form $C_0 \oplus$

$C_1 \oplus C_2 \oplus C_3$, where the C_i are arbitrary square matrices of dimension a_i . We can perform an arbitrary basis transformation on each of these blocks without affecting the right action, and can also write the left action in its irreducible form as the direct sum of A, A_1, A_2 and A_3 , although not necessarily grouped together as in the right action.

The lower block in the right action must be a single copy of G' . The matrices which commute with $G'(g_1)$ and $G'(g_2)$ are of the form:

$$\begin{pmatrix} a & b & c & d \\ -b & a & -d & c \\ -c & d & a & -b \\ -d & -c & b & a \end{pmatrix}. \quad (7.7.8)$$

For a matrix in this form to square to $-\mathbb{1}$, it must satisfy $a = 0$, $b^2 + c^2 + d^2 = 1$. If we parameterise the two generators in the left action as

$$G'_L(g_1) = \begin{pmatrix} 0 & b & c & d \\ -b & 0 & -d & c \\ -c & d & 0 & -b \\ -d & -c & b & 0 \end{pmatrix}, \quad G'_L(g_2) = \begin{pmatrix} 0 & e & f & g \\ -e & 0 & -g & f \\ -f & g & 0 & -e \\ -g & -f & e & 0 \end{pmatrix}, \quad (7.7.9)$$

then the condition for them to satisfy the group operations is

$$\begin{aligned} b^2 + c^2 + d^2 &= e^2 + f^2 + g^2 = 1, \\ be + cf + dg &= 0. \end{aligned} \quad (7.7.10)$$

This is the condition that (b, c, d) and (e, f, g) are orthogonal unit vectors in \mathbb{R}^3 . These can be rotated to $(1, 0, 0)$ and $(0, 1, 0)$ by transformation matrices of the form in equation (7.7.8) which commute with the right action and so leave it invariant. The representation in the lower block of the left action can therefore always be put in a basis where it has the following form:

$$G'_L(g_1) = \begin{pmatrix} 0 & 1 & 0 & 0 \\ -1 & 0 & 0 & 0 \\ 0 & 0 & 0 & -1 \\ 0 & 0 & 1 & 0 \end{pmatrix}, \quad G'_L(g_2) = \begin{pmatrix} 0 & 0 & 1 & 0 \\ 0 & 0 & 0 & 1 \\ -1 & 0 & 0 & 0 \\ 0 & -1 & 0 & 0 \end{pmatrix}, \quad (7.7.11)$$

Note that this is the right representation transformed by the matrix,

$$P = \text{diag}(1, -1, -1, -1). \quad (7.7.12)$$

To recap, for ADHM data up to charge seven, the lower block of the right action

must be a single copy of G' and can be put in the basis in equation (7.7.6), while the lower block of the left action must also be G' , but in the basis in equation (7.7.11). The upper block of the right and left actions can be any combination of the one-dimensional representations in equation (7.7.2), in diagonal form.

Finally, q_R and q_L must each be one of the representations,

$$q_{R,L} = 2A, 2A_1, 2A_2, \text{ or } 2A_3. \quad (7.7.13)$$

These are always two copies of the same one-dimensional representation in order to be embedded in the quaternion representation.

This presents us with a finite number of representations for the action on the ADHM data, and we can test all possible combinations up to charge seven to see if there is ADHM data which is both invariant under the given left and right actions and can satisfy the ADHM constraints.

Given that the lower blocks must be the four-dimensional G' representation, and the upper blocks are one-dimensional representations, the ADHM data must be composed of 1×4 blocks as in Section 7.6. For example, for charge seven ADHM data,

$$a = \begin{pmatrix} 0 & 0 & 0 & L_1^- \\ 0 & 0 & 0 & B_{11} \\ 0 & 0 & 0 & B_{21} \\ 0 & 0 & 0 & B_{31} \\ B_{11}^\top & B_{21}^\top & B_{31}^\top & 0 \end{pmatrix}, \quad (7.7.14)$$

where L_1^- , B_{11} , B_{21} and B_{31} are 1×4 quaternionic matrices.

Depending on the choice of representations for q_R and q_L , some of the possibilities for L_1^- that are invariant under the left and right action of G' in the bases presented above are:

$$L_1^- = l_0(-1, k, j, i) \text{ when } q_R = 2A, q_L = 2A, \quad (7.7.15)$$

$$L_1^- = l_0(k, -j, i, 1) \text{ when } q_R = 2A, q_L = 2A_1, \quad (7.7.16)$$

$$L_1^- = l_0(k, j, -i, 1) \text{ when } q_R = 2A_1, q_L = 2A, \quad (7.7.17)$$

$$L_1^- = l_0(1, i, j, -k) \text{ when } q_R = 2A_1, q_L = 2A_1, \quad (7.7.18)$$

where l_0 is an arbitrary real constant. When q_R and q_L are the representations $2A_2$ or $2A_3$, there exist similar invariant L_1^- rows but with different permutations of $1, i, j, k$ and different choices of sign.

Each block in the ADHM data, B_{uv} , must be a right invariant map between the one-dimensional representation in the corresponding diagonal entry of Q_R^+ and the rep-

representation in the lower block, $Q_R^- = G'$. The block B_{uv} must also be a left invariant map between the corresponding one-dimensional representation in Q_L^+ , and the representation in the lower block $Q_L^- = G'_L$,

$$A_{R_u}(g_i) B_{u1} = B_{u1} g_i G'(g_i), \quad \text{and} \quad A_{L_u}(g_i) g_i B_{u1} = B_{u1} G'_L(g_i). \quad (7.7.19)$$

In this expression, $A_{L_u}, A_{R_u} = A, A_1, A_2$ or A_3 , depending on the representations chosen for Q_R^+ and Q_L^+ . It will not be very illuminating to list all of the invariant blocks for all combinations of the one-dimensional representations, but they all have a similar form to the invariant L^- blocks shown above and have a single free real parameter.

The remaining challenge is to find an appropriate representation such that the free parameters in the blocks in the ADHM data can satisfy the ADHM constraint. There are a maximum of four free parameters in the ADHM data up to charge seven and it is straightforward to see whether there exists a non-trivial solution. For example, if we take the upper representation in the right action to be $Q_R^+ = A \oplus A_2 \oplus A_3$; the upper representation in the left action to be $Q_L^+ = A \oplus A_2 \oplus A_3$; and the quaternion actions to be $q_R = 2A_1$ and $q_L = 2A_1$, then the following ADHM data is invariant under this action:

$$a = \begin{pmatrix} 0 & 0 & 0 & L_1^- \\ 0 & 0 & 0 & B_{11} \\ 0 & 0 & 0 & B_{21} \\ 0 & 0 & 0 & B_{31} \\ B_{11}^\top & B_{21}^\top & B_{31}^\top & 0 \end{pmatrix}, \quad (7.7.20)$$

where

$$L_1^- = l_0(1, i, j, -k), \quad (7.7.21)$$

$$B_{11} = b_1(1, -i, -j, -k), \quad (7.7.22)$$

$$B_{21} = b_2(1, i, -j, k), \quad (7.7.23)$$

$$B_{31} = b_3(1, -i, j, k). \quad (7.7.24)$$

Note that L_1^- is a left and right invariant map between A_1 and G' ; B_{11} is a left and right invariant map between A and G' ; B_{21} is a left and right invariant map between A_2 and G' ; and B_{31} is a left and right invariant map between A_3 and G' . For this ADHM data to solve the ADHM constraint, the remaining free parameters must satisfy

$$l_0^2 = b_1^2 = b_2^2 = b_3^2. \quad (7.7.25)$$

Without loss of generality, we can take $l_0 = b_1 = b_2 = b_3 = \lambda$, with alternative choices

of sign giving equivalent ADHM data. The remaining parameter is just an overall scale:

$$a = \lambda \begin{pmatrix} 0 & 0 & 0 & 1 & i & j & -k \\ 0 & 0 & 0 & 1 & -i & -j & -k \\ 0 & 0 & 0 & 1 & i & -j & k \\ 0 & 0 & 0 & 1 & -i & j & k \\ 1 & 1 & 1 & 0 & 0 & 0 & 0 \\ -i & i & -i & 0 & 0 & 0 & 0 \\ -j & -j & j & 0 & 0 & 0 & 0 \\ -k & k & k & 0 & 0 & 0 & 0 \end{pmatrix}. \quad (7.7.26)$$

This ADHM data now describes an instanton with the symmetries of the 16-cell. If we take the vertices of the 16-cell which lie in the hyperplane $x_4 = 0$ then they form an octahedron. The topological charge density of this 16-cell instanton in this hyperplane is plotted in Figure 7.3.

By trying all possible combinations of one-dimensional representations in Q_R^+ and Q_L^+ , as well as the possible representations for q_R and q_L we are able to construct many different parameterisations of the charge seven ADHM data which are invariant under the symmetries of the 16-cell. In general, the representations which have invariant ADHM data have $Q_R^+ = A_i \oplus A_j \oplus A_k$ for $i, j, k = 0, 1, 2, 3$, $i \neq j \neq k$, and q_R is equal to the remaining one-dimensional representation which is not included in Q_R^+ . Note that we have used the notation $A_0 \equiv A$. The upper block of the left representation is also given by $Q_R^+ = A_i \oplus A_j \oplus A_k$ for $i \neq j \neq k$, although there exists invariant ADHM data for any choice of q_L , unlike q_R . In all cases, the ADHM data has a very similar form to equation (7.7.20), with four free parameters which are constrained to an overall scale after applying the ADHM constraint. These different representations all give ADHM data which describe instantons with identical topological charge density.

The solution we have found is the lowest charge instanton which has the symmetries of the 16-cell within our framework. As we will see in Section 7.10, these solutions are equivalent to the charge seven JNR ansatz with the eight poles placed at the vertices of the 16-cell.

7.8 The 24-cell

As quaternions, the vertices of the 24-cell form the binary tetrahedral group,

$$\mathbb{T} = \{\pm 1, \pm i, \pm j, \pm k, \frac{1}{2}(\pm 1 \pm i \pm j \pm k)\}. \quad (7.8.1)$$

Our treatment of the 24-cell is similar to the 16-cell in the previous section. The main difference is that all but one of the real irreducible representations of the binary tetra-

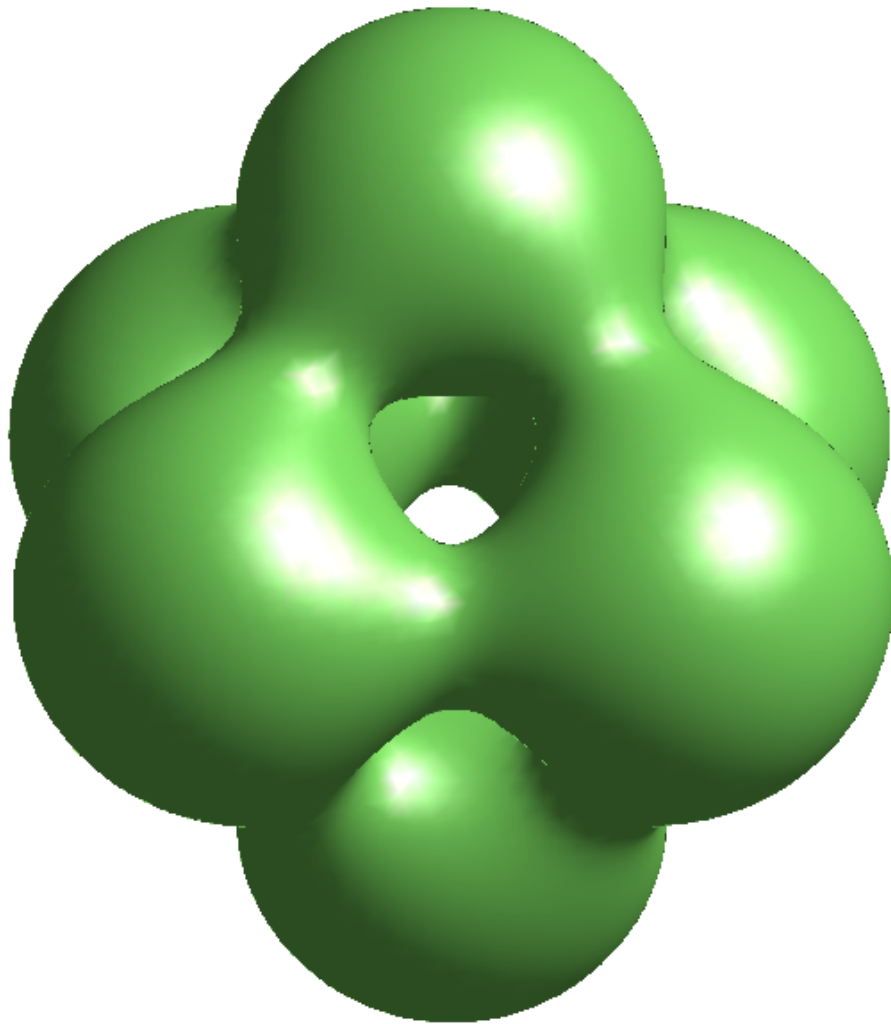


Figure 7.3: A surface of constant topological charge density in the $x_4 = 0$ hyperplane of the charge 7 instanton with the symmetries of the 16-cell. The vertices in this hyperplane form an octahedron.

hedral group have dimension greater than one, and finding appropriate representations is more complicated. We also need to search up to at least charge 23 where the JNR ansatz guarantees an instanton with the symmetries of the 24-cell.

We will first present the real irreducible representations of the binary tetrahedral group in some canonical basis that can be taken as the basis for the representations in the right action. We will then find the form that the representations in the left action must take in order to commute with the representations in the right action. Finally, we will enumerate all the possible combinations of these representations up to charge 23 to find ADHM data with the symmetries of the 24-cell.

7.8.1 Representations of the right action

The positive real irreducible representations of the binary tetrahedral group are

$$A(g_1) = 1, \quad A(g_2) = 1, \quad (7.8.2)$$

$$E(g_1) = \frac{1}{2} \begin{pmatrix} -1 & -\sqrt{3} \\ \sqrt{3} & -1 \end{pmatrix}, \quad E(g_2) = \frac{1}{2} \begin{pmatrix} -1 & \sqrt{3} \\ -\sqrt{3} & -1 \end{pmatrix}, \quad (7.8.3)$$

$$F(g_1) = \begin{pmatrix} 0 & 0 & 1 \\ 1 & 0 & 0 \\ 0 & 1 & 0 \end{pmatrix}, \quad F(g_2) = \begin{pmatrix} 0 & 1 & 0 \\ 0 & 0 & -1 \\ -1 & 0 & 0 \end{pmatrix}. \quad (7.8.4)$$

The negative real representations of the binary tetrahedral group are

$$G'(g_1) = \frac{1}{2} \begin{pmatrix} 1 & -1 & -1 & 1 \\ 1 & 1 & -1 & -1 \\ 1 & 1 & 1 & 1 \\ -1 & 1 & -1 & 1 \end{pmatrix}, \quad G'(g_2) = \frac{1}{2} \begin{pmatrix} 1 & -1 & -1 & -1 \\ 1 & 1 & 1 & -1 \\ 1 & -1 & 1 & 1 \\ 1 & 1 & -1 & 1 \end{pmatrix}, \quad (7.8.5)$$

$$G'_1(g_1) = \frac{1}{4} \begin{pmatrix} -1 + \sqrt{3} & -1 - \sqrt{3} & 1 + \sqrt{3} & -1 + \sqrt{3} \\ 1 + \sqrt{3} & -1 + \sqrt{3} & 1 - \sqrt{3} & 1 + \sqrt{3} \\ -1 + \sqrt{3} & -1 - \sqrt{3} & -1 - \sqrt{3} & 1 - \sqrt{3} \\ 1 + \sqrt{3} & -1 + \sqrt{3} & -1 + \sqrt{3} & -1 - \sqrt{3} \end{pmatrix}, \quad (7.8.6)$$

$$G'_1(g_2) = \frac{1}{4} \begin{pmatrix} -1 + \sqrt{3} & 1 + \sqrt{3} & 1 - \sqrt{3} & -1 - \sqrt{3} \\ -1 - \sqrt{3} & -1 + \sqrt{3} & 1 + \sqrt{3} & 1 - \sqrt{3} \\ -1 - \sqrt{3} & -1 + \sqrt{3} & -1 - \sqrt{3} & -1 + \sqrt{3} \\ 1 - \sqrt{3} & -1 - \sqrt{3} & 1 - \sqrt{3} & -1 - \sqrt{3} \end{pmatrix}.$$

The representation of the right action, Q_R , can be put into a basis where its upper block is the direct sum of a combination of these positive representations and the lower block is the direct sum of a combination of these negative representations. From now

on we will assume that our representations are in the bases above unless otherwise noted.

7.8.2 Representations of the left action

To find appropriate representations of the left action we need to find a basis in which the representations commute with those given for the right action. If ρ_1 and ρ_2 are two different irreducible representations in the right action then there are no matrices, P , which satisfy

$$\rho_1 P = P \rho_2. \quad (7.8.7)$$

The only matrices which commute with the right action are therefore also block diagonal with blocks corresponding to the right irreducible representations. Note that the right representation may include multiple copies of the same irreducible representation, such as $E \oplus E$. The corresponding left block may then be a 4×4 block rather than two separate 2×2 blocks, because the off-diagonal blocks may be non-zero here.

We will systematically go through the blocks in the representation of the right action and find the possible commuting representations of the left action. We will only consider the most granular blocks, so for example, if the right representation contains the 4×4 block $E \oplus E$, we would not consider the representation where the left block is also $E \oplus E$, since these both split into two 2×2 blocks. However, we will consider the representation where the left block is $E \otimes E$ since this is not composed of smaller blocks, and the whole 4×4 block must be considered together.

Note that when we talk about representations in the section below, we are referring to the explicit matrices in Section 7.8.1, not the abstract representation. Likewise, when we use the tensor product and direct sum, we are referring to the concrete Kronecker product and direct sum of the matrices respectively.

Let us start with the trivial cases. If a block in the right action is simply the identity matrix then any positive representation of the appropriate size may be used as the block in the left action. We can take these to be in the canonical basis since we can perform any basis transformation without affecting the form of the right block. Likewise, for any block in the right action that is a positive non-trivial representation, the block in the left action may be taken to be the identity matrix.

Now consider the right representation E . The only matrices which commute with both $E(g_1)$ and $E(g_2)$ are of the form

$$\begin{pmatrix} a & -b \\ b & a \end{pmatrix}. \quad (7.8.8)$$

These must be rotation matrices and the only non-trivial rotation matrices which form

a representation of the binary tetrahedral group are $E(g_1)$ and $E(g_2)$. These two matrices are similar and the transformation between them is $Q = \text{diag}(1, -1)$, which does not commute with the right representation. So there are two possibilities for the left block: the original representation, E , and a twisted representation, E^t , where

$$E^t(g_1) = E(g_2), \quad E^t(g_2) = E(g_1). \quad (7.8.9)$$

When the right representation is $2E \equiv E \oplus E = \mathbb{1}_2 \otimes E$, the commuting matrices are of the form

$$\begin{pmatrix} a & -b & c & -d \\ b & a & d & c \\ e & -f & g & -h \\ f & e & h & g \end{pmatrix}. \quad (7.8.10)$$

Here $E \otimes E$, $E \otimes E^t$ and $E \otimes 2A$ are possible representations for the left block. The twisted product, $E \otimes E^t$, is related to $E \otimes E$ via the transformation matrix $P = \text{diag}(1, -1, 1, -1)$. However, this does not leave the right action invariant and so $E \otimes E^t$ must be considered separately. Applying a twist to the first E in the product can be undone since the transformation will apply only to the identity part of the right representation, $2E = \mathbb{1}_2 \otimes E$, and therefore leave it invariant. There is no need to consider $E \oplus E$ as a left representation, because both representations are then composed of smaller blocks that we have already considered.

It is not clear that these are all possible left representations for the right block $2E$. There may be other 4×4 matrices which are of the form in equation (7.8.10) and form a representation but that are not related to $E \otimes E$ or $E \otimes 2A$ by a transformation which leaves the right action, $2E$, invariant. The condition for matrices of this form to be a representation is non-linear and we have not been able to systemically rule out other possibilities. From now on we will simply list possibilities for the left representations without claiming that these are exhaustive.

When the right representation is $3E$, the left representation must be 6-dimensional and in the form of equation (7.8.10) generalised to a 6×6 matrix. Three such representations are $F \otimes E$, $F \otimes E^t$ and $F \otimes 2A$. We are free to choose the basis for F since a transformation on the first term in the tensor product leaves the right block, $\mathbb{1}_3 \otimes E$, invariant. We will therefore take F to be in the canonical basis above.

When the right representation is $4E$, let us start by considering the left representations in the form $\tilde{G} \otimes E$, where \tilde{G} is some four-dimensional representation. These will commute with the right representation for any choice of \tilde{G} . We are free to choose a basis for \tilde{G} without affecting the right representation, and so can always take it to be composed of irreducible blocks. There is no irreducible four-dimensional positive representation, so in the appropriate basis $\tilde{G} \otimes E$ must be a direct sum of smaller blocks

considered previously. Similarly, there is no need to consider left representations of the form $\tilde{G} \otimes E^t$ or $\tilde{G} \otimes 2A$.

We can also consider left representations in the form $\tilde{E} \otimes (E \oplus E)$, where \tilde{E} is some two-dimensional representation for which we are free to choose the basis. The only choice for \tilde{E} that does not decompose into smaller blocks is $\tilde{E} = E$, so that the left representation is $E \otimes (E \oplus E)$. By a similar argument, other possible left representations are of the form $E \otimes (\tilde{E}_1 \oplus \tilde{E}_2)$, where $\tilde{E}_1, \tilde{E}_2 = E, E^t$, or $2A$. Note that the ordering of the terms in the direct sum does not matter since these can be permuted without affecting the right representation.

There is no need to consider the left blocks in the form $\tilde{E}_1 \oplus \tilde{E}_2 \oplus \tilde{E}_3 \oplus \tilde{E}_4$ since these decompose into blocks considered previously.

When the right representation is $5E$, there are no obvious possible 10-dimensional representations for the left representation which do not decompose into blocks we have already considered.

Following the same pattern when the right representation is $6E$, the following left representations are possible and inequivalent: $F \otimes (\tilde{E}_1 \oplus \tilde{E}_2)$ and $E \otimes (\tilde{E}_1 \oplus \tilde{E}_2 \oplus \tilde{E}_3)$, where $\tilde{E}_1, \tilde{E}_2, \tilde{E}_3 = E, E^t$, or $2A$, and permutations of the direct sum are again equivalent. As before, if the left action is in the form $\tilde{I} \otimes \tilde{E}_1$ for some six-dimensional representation \tilde{I} then it can be written as the sum of blocks considered previously, after the appropriate basis transformation.

This pattern also extends to when the right representation is $7E$, $8E$ or $9E$, and the possibilities for the left action are shown in Table 7.1.

There are additional possibilities for the left representation when the right representation is $8E$. The matrices in G' and G'_1 are all in the form of equation (7.8.10) and so commute with $2E$. We can also consider the twisted representations, G'^t and $G'_1{}^t$. With G' , the following transformation matrix swaps $G'(g_1)$ and $G'(g_2)$:

$$P = \frac{1}{\sqrt{2}} \begin{pmatrix} 1 & 0 & 0 & -1 \\ 0 & 1 & 1 & 0 \\ 0 & 1 & -1 & 0 \\ -1 & 0 & 0 & -1 \end{pmatrix}. \quad (7.8.11)$$

This commutes with $2E$ in the canonical basis, so there is no need to consider G'^t separately. However, the transformation between G'_1 and $G'_1{}^t$ does not commute with $2E$, so these must be considered separately. The representations $G' \otimes G'$, $G' \otimes G'_1$, $G' \otimes G'_1{}^t$, $G'_1 \otimes G'_1$, $G'_1 \otimes G'_1{}^t$ and $G'_1 \otimes G'$ are therefore also possible representations for the left representation when the right representation is $8E$. Note that these representations are positive as they are the tensor product of two negative representations.

There is no need to consider $10E$ or higher, since the lower block must be at least

four dimensional, and the highest charge that we need to consider is charge 23.

The F representation commutes only with the identity. If the right representation is F there is therefore no non-trivial left representation.

When the right representation is $2F$, the only possible left representation is $E \otimes \mathbb{1}_3$.

When the right representation is $3F$, the only possible left representation is $F \otimes \mathbb{1}_3$.

For any higher dimensional right representation, nF , with $n > 3$, the left representation must be in the form $\rho_n \otimes \mathbb{1}_3$, where ρ_n is a n -dimensional representation. However, we are free to choose the basis of ρ_n and so can decompose it into irreducible representations, where each block has been considered previously.

The G'_1 representation commutes with matrices of the form

$$\begin{pmatrix} a & -b & 0 & 0 \\ b & a & 0 & 0 \\ 0 & 0 & a & -b \\ 0 & 0 & b & a \end{pmatrix}. \tag{7.8.12}$$

Neither G' or G'_1 can be put in this form since they are irreducible. For higher multiples of G'_1 in the right representation, the left representation must always occur with blocks of this form. For example, when the right representation is $2G'_1$, the left representation must be in the form

$$\begin{pmatrix} a & -b & 0 & 0 & c & -d & 0 & 0 \\ b & a & 0 & 0 & d & c & 0 & 0 \\ 0 & 0 & a & -b & 0 & 0 & c & -d \\ 0 & 0 & b & a & 0 & 0 & d & c \\ e & -f & 0 & 0 & g & -h & 0 & 0 \\ f & e & 0 & 0 & h & g & 0 & 0 \\ 0 & 0 & e & -f & 0 & 0 & g & -h \\ 0 & 0 & f & e & 0 & 0 & h & g \end{pmatrix} \equiv \begin{pmatrix} a & -b & c & -d \\ b & a & d & c \\ e & -f & g & -h \\ f & e & h & g \end{pmatrix} \tilde{\otimes} \mathbb{1}_2, \tag{7.8.13}$$

where we have defined $\tilde{\otimes}$ as the Kronecker product acting on each 2×2 block. We therefore see that $G' \tilde{\otimes} \mathbb{1}_2$, $G'_1 \tilde{\otimes} \mathbb{1}_2$ and $G_1{}^{t'} \tilde{\otimes} \mathbb{1}_2$ are possible left representations. The left representation $G_1{}^{t'} \tilde{\otimes} \mathbb{1}_2$ is equivalent to $G' \tilde{\otimes} \mathbb{1}_2$ since the transformation matrix between them is $P \tilde{\otimes} \mathbb{1}_2$ where P is given in equation (7.8.11) and commutes with the right action.

There are no additional possibilities when the right representation is $3G'_1$, or $5G'_1$. There is no need to consider $6G'_1$ or higher as we would exceed charge 23.

When the right representation is $4G'_1$, both $G' \otimes \tilde{G}$ and $G'_1 \otimes \tilde{G}$ are suitable left representations, where $\tilde{G} = \mathbb{1}_4$, $E \oplus E$ or $E^t \oplus E^t$.

The following left representations are also possible when the right block is $4G'_1$:

$(E \otimes G') \tilde{\otimes} \mathbb{1}_2$, $(E \otimes G'_1) \tilde{\otimes} \mathbb{1}_2$, $(E \otimes G'_1{}^t) \tilde{\otimes} \mathbb{1}_2$, $(G' \otimes E) \tilde{\otimes} \mathbb{1}_2$, $(G' \otimes E^t) \tilde{\otimes} \mathbb{1}_2$, $(G'_1 \otimes E) \tilde{\otimes} \mathbb{1}_2$, and $(G'_1 \otimes E^t) \tilde{\otimes} \mathbb{1}_2$. The left representations in this form where the first term is twisted are related to these untwisted representations by transformations which do not affect the right action. Once again, the transformation between $(E \otimes G') \tilde{\otimes} \mathbb{1}_2$ and $(E \otimes G'^t) \tilde{\otimes} \mathbb{1}_2$ commutes with the right representation and so these do not need to be considered separately.

The final right representation to consider is G' , which commutes with matrices of the form

$$\begin{pmatrix} a & -b & c & d \\ b & a & d & -c \\ -c & -d & a & -b \\ -d & c & b & a \end{pmatrix}. \quad (7.8.14)$$

The left representation can be $PG'P^\top$ or PG'^tP^\top , where $P = \text{diag}(-1, 1, 1, 1)$. We can see from the discussion above that G'_1 can never commute with G' in any basis.

When the right representation is $2G'$, the left representation may be $E \otimes (PG'P^\top)$ or $E \otimes (PG'^tP^\top)$.

Similarly, when the right representation is $3G'$, the left representation may be $F \otimes PG'P^\top$ or $F \otimes PG'^tP^\top$.

When the right representation is $4G'$, both $G' \otimes \tilde{G}$ and $G'_1 \otimes \tilde{G}$ are suitable left representations, where \tilde{G} is a positive representation in the form of equation (7.8.14), $\tilde{G} = 4A$, $E \oplus E$, or $E^t \oplus E^t$.

Any left representation of the form $\tilde{G} \otimes (PG'P^\top)$ or $\tilde{G} \otimes (PG'^tP^\top)$, can be decomposed into blocks which we have considered previously by transforming \tilde{G} to a basis where it is the direct sum of irreducible representations.

When the right representation is $5G'$, all possibilities are composed of blocks that we have previously considered.

We have now considered all possible blocks in the right representation which can appear up to charge 23. For each block in the right representation in the canonical basis, we have found possibilities for the equivalent block in the left representation, many of which are actually the same representation but in a different basis. However, we cannot transform between these bases without affecting the right block and so we must consider these as inequivalent representations of the left action. A summary of these possible representations is given in Table 7.1. Unfortunately we have no method of systematically finding commuting representations and so we cannot rule out the possibility that there are other inequivalent left representations that we have not been able to find by inspection.

Right representation	Left representation
$\mathbb{1}_k$	$A, E, \text{ or } F$ (for $k = 1, 2, 3$ respectively)
E	$2A, E, \text{ or } E^t$
$2E$	$E \otimes \tilde{E}_1$, where $\tilde{E}_1 = 2A, E, \text{ or } E^t$.
$3E$	$F \otimes \tilde{E}_1$
$4E$	$E \otimes (\tilde{E}_1 \oplus \tilde{E}_2)$
$5E$	—
$6E$	$F \otimes (\tilde{E}_1 \oplus \tilde{E}_2)$ or $E \otimes (\tilde{E}_1 \oplus \tilde{E}_2 \oplus \tilde{E}_3)$
$7E$	—
$8E$	$E \otimes (\tilde{E}_1 \oplus \tilde{E}_2 \oplus \tilde{E}_3 \oplus \tilde{E}_4)$, $G' \otimes \tilde{G}'$ or $G'_1 \otimes \tilde{G}'$, where $\tilde{G}' = G', G'_1$ or $G_1'^t$.
$9E$	$F \otimes (\tilde{E}_1 \oplus \tilde{E}_2 \oplus \tilde{E}_3)$
F	$\mathbb{1}_3$
$2F$	$E \otimes \mathbb{1}_3$
$3F$	$F \otimes \mathbb{1}_3$
$nF, n > 3$	—
G'	$PG'P^\top$, or PG'^tP^\top , where $P = \text{diag}(-1, 1, 1, 1)$.
$2G'$	$E \otimes (PG'P^\top)$, or $E \otimes (PG'^tP^\top)$
$3G'$	$F \otimes (PG'P^\top)$, or $F \otimes (PG'^tP^\top)$
$4G'$	$G' \otimes \tilde{G}$, or $G'_1 \otimes \tilde{G}$, where $\tilde{G} = 4A, E \oplus E, \text{ or } E^t \oplus E^t$.
$5G'$	—
G'_1	—
$2G'_1$	$G' \tilde{\otimes} \mathbb{1}_2, G'_1 \tilde{\otimes} \mathbb{1}_2$ or $G_1'^t \tilde{\otimes} \mathbb{1}_2$
$3G'_1$	—
$4G'_1$	$G' \otimes \tilde{G}$, or $G'_1 \otimes \tilde{G}$, where $\tilde{G} = \mathbb{1}_4, E \oplus E$ or $E^t \oplus E^t$; or $(E \otimes G') \tilde{\otimes} \mathbb{1}_2, (E \otimes G'_1) \tilde{\otimes} \mathbb{1}_2, (E \otimes G_1'^t) \tilde{\otimes} \mathbb{1}_2, (G' \otimes E) \tilde{\otimes} \mathbb{1}_2, (G' \otimes E^t) \tilde{\otimes} \mathbb{1}_2, (G'_1 \otimes E) \tilde{\otimes} \mathbb{1}_2, \text{ or } (G'_1 \otimes E^t) \tilde{\otimes} \mathbb{1}_2$.
$5G'_1$	—

Table 7.1: A summary of the possible blocks that make up the representations of the right and left actions of the binary tetrahedral group when acting on the ADHM data.

7.9 A charge 23 solution

After testing every combination of representations from the previous section for ADHM data up to charge 23, we have found the following charge 23 solution. The right and left representations are

$$Q_R = \text{diag}(E, 3F, G', 2G'_1), \quad (7.9.1)$$

and

$$Q_L = \text{diag}(E, F \otimes \mathbb{1}_3, PG'P^\top, G'_1 \tilde{\otimes} \mathbb{1}_2), \quad (7.9.2)$$

where $P = \text{diag}(-1, 1, 1, 1)$ and $\tilde{\otimes}$ is the Kronecker product on 2×2 blocks as in equation (7.8.13). In the block form described above,

$$Q_{R,1}^+ = E, \quad Q_{R,2}^+ = 3F, \quad Q_{R,1}^- = G', \quad Q_{R,2}^- = 2G'_1, \quad (7.9.3)$$

$$Q_{L,1}^+ = E, \quad Q_{L,2}^+ = F \otimes \mathbb{1}_3, \quad Q_{L,1}^- = PG'P^\top, \quad Q_{L,2}^- = G'_1 \tilde{\otimes} \mathbb{1}_2. \quad (7.9.4)$$

The blocks which are invariant under the action of this representation are

$$B_{12} = b_1 \begin{pmatrix} -i & j & k & 1 & k & -1 & i & j \\ -j & -i & -1 & k & 1 & k & -j & i \end{pmatrix} + b_2 \begin{pmatrix} j & i & 1 & -k & -1 & -k & j & -i \\ -i & j & k & 1 & k & -1 & i & j \end{pmatrix}, \quad (7.9.5)$$

and

$$B_{21} = b_3 \begin{pmatrix} 1 & -i & j & -k \\ -k & -j & -i & -1 \\ j & -k & -1 & i \\ k & -j & -i & 1 \\ 1 & i & -j & -k \\ -i & 1 & -k & j \\ -j & -k & 1 & i \\ i & -1 & -k & j \\ 1 & i & j & k \end{pmatrix}, \quad (7.9.6)$$

where b_1, b_2 and b_3 are arbitrary real coefficients. The invariant matrix, B_{22} , is shown in Figure 7.4 and there is no invariant block, B_{11} between $Q_{(R,L),1}^+$ and $Q_{(R,L),1}^-$.

The only block which has an invariant L_v^- is $Q_{R,1}^-$ and $Q_{L,1}^-$, and it leaves the following row vector invariant,

$$L_1^- = l_1 \begin{pmatrix} 1 & -i & -j & -k \end{pmatrix}, \quad (7.9.7)$$

where l_1 is any real number.

$$\begin{aligned}
& \begin{pmatrix} \frac{1}{2}(-i+\sqrt{3}j) & \frac{1}{2}(-\sqrt{3}i-j) & \frac{1}{2}(-\sqrt{3}-k) & \frac{1}{2}(1-\sqrt{3}k) & \frac{1}{2}(\sqrt{3}-k) & \frac{1}{2}(-1-\sqrt{3}k) & \frac{1}{2}(i+\sqrt{3}j) & \frac{1}{2}(\sqrt{3}i-j) \\ j & -i & 1 & k & 1 & -k & -j & -i \\ \frac{1}{2}(\sqrt{3}-k) & \frac{1}{2}(1+\sqrt{3}k) & \frac{1}{2}(i+\sqrt{3}j) & \frac{1}{2}(-\sqrt{3}i+j) & \frac{1}{2}(i-\sqrt{3}j) & \frac{1}{2}(-\sqrt{3}i-j) & \frac{1}{2}(\sqrt{3}+k) & \frac{1}{2}(1-\sqrt{3}k) \\ j & -i & -1 & -k & -1 & k & -j & -i \\ \frac{1}{2}(i+\sqrt{3}j) & \frac{1}{2}(-\sqrt{3}i+j) & \frac{1}{2}(\sqrt{3}-k) & \frac{1}{2}(1+\sqrt{3}k) & \frac{1}{2}(-\sqrt{3}-k) & \frac{1}{2}(-1+\sqrt{3}k) & \frac{1}{2}(-i+\sqrt{3}j) & \frac{1}{2}(\sqrt{3}i+j) \\ \frac{1}{2}(1-\sqrt{3}k) & \frac{1}{2}(\sqrt{3}+k) & \frac{1}{2}(\sqrt{3}i+j) & \frac{1}{2}(-i+\sqrt{3}j) & \frac{1}{2}(-\sqrt{3}i+j) & \frac{1}{2}(i+\sqrt{3}j) & \frac{1}{2}(-1-\sqrt{3}k) & \frac{1}{2}(-\sqrt{3}+k) \\ \frac{1}{2}(-\sqrt{3}-k) & \frac{1}{2}(-1+\sqrt{3}k) & \frac{1}{2}(i-\sqrt{3}j) & \frac{1}{2}(-\sqrt{3}i-j) & \frac{1}{2}(i+\sqrt{3}j) & \frac{1}{2}(-\sqrt{3}i+j) & \frac{1}{2}(-\sqrt{3}+k) & \frac{1}{2}(-1-\sqrt{3}k) \\ \frac{1}{2}(-1-\sqrt{3}k) & \frac{1}{2}(-\sqrt{3}+k) & \frac{1}{2}(-\sqrt{3}i+j) & \frac{1}{2}(i+\sqrt{3}j) & \frac{1}{2}(\sqrt{3}i+j) & \frac{1}{2}(-i+\sqrt{3}j) & \frac{1}{2}(1-\sqrt{3}k) & \frac{1}{2}(\sqrt{3}+k) \\ -i & j & -k & -1 & -k & 1 & i & j \end{pmatrix} \\
& B_{22} = b_4 \\
& \begin{pmatrix} \frac{1}{2}(\sqrt{3}i+j) & \frac{1}{2}(-i+\sqrt{3}j) & \frac{1}{2}(-1+\sqrt{3}k) & \frac{1}{2}(-\sqrt{3}-k) & \frac{1}{2}(1+\sqrt{3}k) & \frac{1}{2}(\sqrt{3}-k) & \frac{1}{2}(-\sqrt{3}i+j) & \frac{1}{2}(i+\sqrt{3}j) \\ i & j & -k & 1 & k & 1 & i & -j \\ \frac{1}{2}(-1-\sqrt{3}k) & \frac{1}{2}(\sqrt{3}-k) & \frac{1}{2}(\sqrt{3}i-j) & \frac{1}{2}(i+\sqrt{3}j) & \frac{1}{2}(\sqrt{3}i+j) & \frac{1}{2}(i-\sqrt{3}j) & \frac{1}{2}(-1+\sqrt{3}k) & \frac{1}{2}(\sqrt{3}+k) \\ i & j & k & -1 & -k & -1 & i & -j \\ \frac{1}{2}(\sqrt{3}i-j) & \frac{1}{2}(i+\sqrt{3}j) & \frac{1}{2}(-1-\sqrt{3}k) & \frac{1}{2}(\sqrt{3}-k) & \frac{1}{2}(1-\sqrt{3}k) & \frac{1}{2}(-\sqrt{3}-k) & \frac{1}{2}(-\sqrt{3}i-j) & \frac{1}{2}(-i+\sqrt{3}j) \\ \frac{1}{2}(-\sqrt{3}-k) & \frac{1}{2}(1-\sqrt{3}k) & \frac{1}{2}(i-\sqrt{3}j) & \frac{1}{2}(\sqrt{3}i+j) & \frac{1}{2}(-i-\sqrt{3}j) & \frac{1}{2}(-\sqrt{3}i+j) & \frac{1}{2}(\sqrt{3}-k) & \frac{1}{2}(-1-\sqrt{3}k) \\ \frac{1}{2}(1-\sqrt{3}k) & \frac{1}{2}(-\sqrt{3}-k) & \frac{1}{2}(\sqrt{3}i+j) & \frac{1}{2}(i-\sqrt{3}j) & \frac{1}{2}(\sqrt{3}i-j) & \frac{1}{2}(i+\sqrt{3}j) & \frac{1}{2}(1+\sqrt{3}k) & \frac{1}{2}(-\sqrt{3}+k) \\ \frac{1}{2}(\sqrt{3}-k) & \frac{1}{2}(-1-\sqrt{3}k) & \frac{1}{2}(-i-\sqrt{3}j) & \frac{1}{2}(-\sqrt{3}i+j) & \frac{1}{2}(i-\sqrt{3}j) & \frac{1}{2}(\sqrt{3}i+j) & \frac{1}{2}(-\sqrt{3}-k) & \frac{1}{2}(1-\sqrt{3}k) \\ -j & -i & 1 & -k & -1 & -k & -j & i \end{pmatrix} \\
& + b_5
\end{aligned}$$

Figure 7.4: The invariant matrix between the 3F and G'_1 representations. The coefficients b_4 and b_5 are real and arbitrary.

The ADHM data built up from these invariant blocks is then

$$a = \begin{pmatrix} 0 & 0 & L_1^- & 0 \\ 0 & 0 & 0 & B_{12} \\ 0 & 0 & B_{21} & B_{22} \\ 0 & B_{21}^\top & 0 & 0 \\ B_{12}^\top & B_{22'}^\top & 0 & 0 \end{pmatrix}. \quad (7.9.8)$$

The ADHM constraint gives the following constraints on the coefficients:

$$3(b_4^2 + b_5^2) = 3b_3^2 = 2(b_1^2 + b_2^2) = l_1^2. \quad (7.9.9)$$

These can be solved with the parameterisation

$$\begin{aligned} b_1 &= \frac{\lambda}{2\sqrt{2}} \cos \theta_1, & b_2 &= \frac{\lambda}{2\sqrt{2}} \sin \theta_1, & b_3 &= \frac{\lambda}{2\sqrt{3}}, \\ b_4 &= \frac{\lambda}{2\sqrt{3}} \cos \theta_2, & b_5 &= \frac{\lambda}{2\sqrt{3}} \sin \theta_2, & l_1 &= \frac{\lambda}{2}. \end{aligned} \quad (7.9.10)$$

The overall scale is then given by λ ,

$$a^\dagger a = \lambda^2 \mathbb{1}. \quad (7.9.11)$$

Any choice of the parameters θ_1 and θ_2 gives equivalent ADHM data.

Recall that we took the vertices of the 24-cell to be

$$(\pm 1, 0, 0, 0), (0, \pm 1, 0, 0), (0, 0, \pm 1, 0), (0, 0, 0, \pm 1), \frac{1}{2}(\pm 1, \pm 1, \pm 1, \pm 1). \quad (7.9.12)$$

These vertices can be divided into three hyperplanes:

$$x_1 + x_2 = 0 \quad (7.9.13)$$

$$x_1 + x_2 = \pm 1. \quad (7.9.14)$$

In the first of these hyperplanes the vertices form a cuboctahedron (a cube with each corner cut off to give an equilateral triangle face) in the $\frac{1}{\sqrt{2}}(x_1 - x_2)$, x_3 and x_4 axes. The vertices in the second two hyperplanes form octahedrons.

The instanton that is generated from the ADHM data above is rotated compared to the 24-cell with the vertices in equation (7.9.12). The vertices in equation (7.9.12) instead describe the shape of the instanton on the axes $\frac{1}{\sqrt{2}}(x_1 \pm x_2)$ and $\frac{1}{\sqrt{2}}(x_3 \pm x_4)$. Figure 7.5 shows a surface of constant topological charge density in the $x_4 = 0$ hyperplane where the cuboctahedral shape is clear. Figure 7.6 shows a similar surface in the $x_4 = 1$ hyperplane where the octahedral shape is clear.

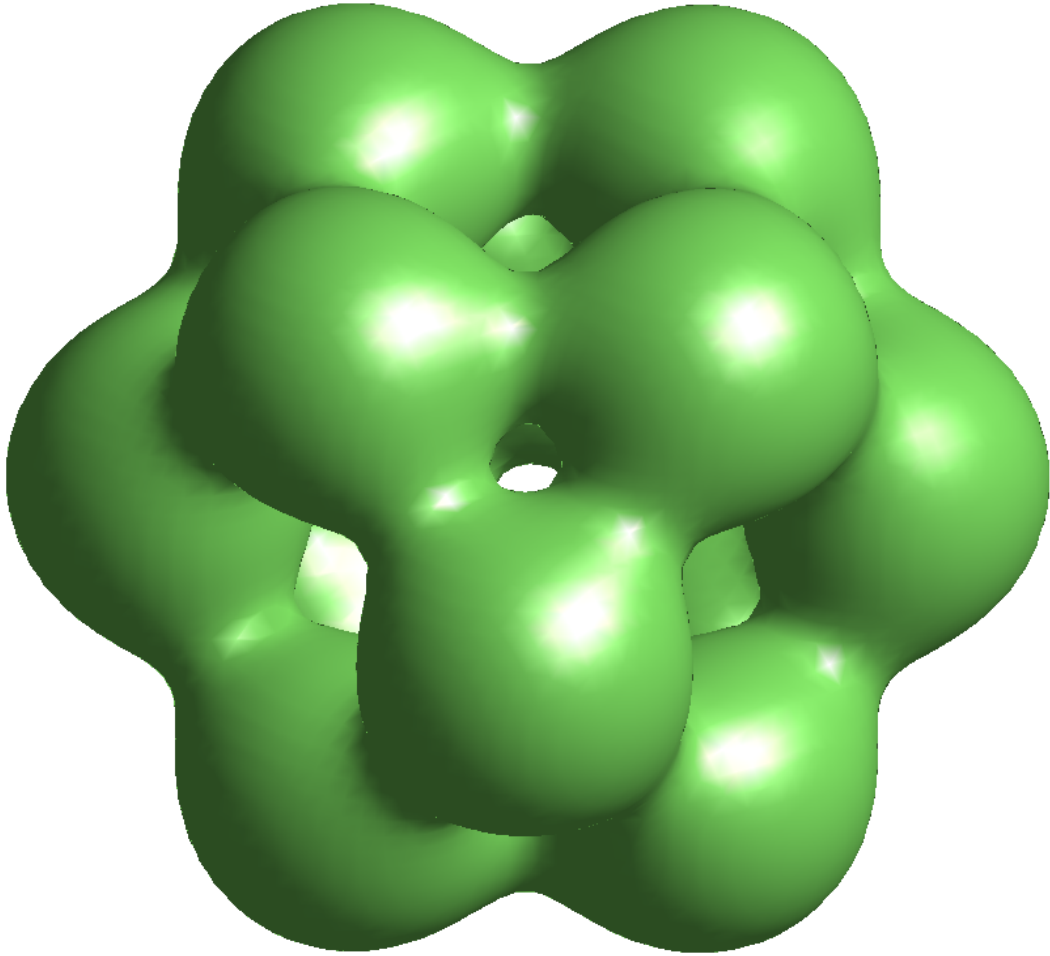


Figure 7.5: A surface of constant topological charge density in the $x_4 = 0$ hyperplane of the charge 23 instanton with the symmetries of the 24-cell. The vertices in this hyperplane form a cuboctahedron.

We did not find any lower charge instantons with the symmetries of the 24-cell.

7.10 Equivalence to JNR ansatz

Recall that the JNR ansatz for a charge k instanton has $k + 1$ free poles. We can therefore use the JNR ansatz to construct a charge seven instanton with the symmetries of the 16-cell by placing the eight poles in the JNR ansatz at the vertices of the 16-cell with equal weight. Similarly, we can use the JNR ansatz to construct a charge 23 instanton with the symmetries of the 24-cell by placing the 24 poles at the vertices in equation (7.2.9).

The lowest charge solutions that we have found for the 16-cell and the 24-cell are also of charge seven and charge 23 respectively, and are in fact equivalent parameterisations of the JNR solution. The ADHM data for the JNR ansatz takes a different form from the canonical form that we have used above. For a charge k JNR instanton with poles

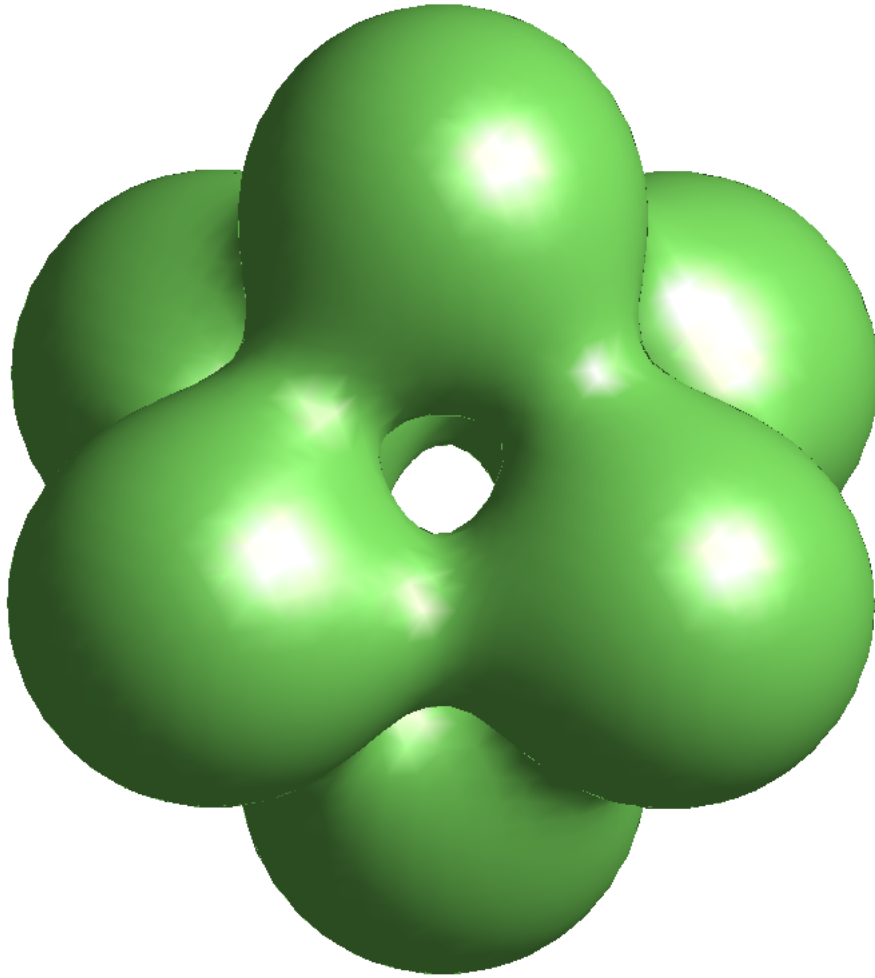


Figure 7.6: A surface of constant topological charge density in the $x_4 = 1$ hyperplane of the charge 23 instanton with the symmetries of the 24-cell. The vertices in this hyperplane form an octahedron.

at y_0, \dots, y_k with equal weights, the ADHM data is [93]

$$\Delta(x) = \begin{pmatrix} y_0 & \cdots & y_0 \\ y_1 & & \\ & \ddots & \\ & & y_k \end{pmatrix} - \begin{pmatrix} 1 & \cdots & 1 \\ 1 & & \\ & \ddots & \\ & & 1 \end{pmatrix} x. \quad (7.10.1)$$

To convert this ADHM data to the canonical form, we need matrices $S \in O(k+1)$ and $C \in GL(k, \mathbb{R})$ such that

$$\begin{pmatrix} 0 & \cdots & 0 \\ 1 & & \\ & \ddots & \\ & & 1 \end{pmatrix} = S \begin{pmatrix} 1 & \cdots & 1 \\ 1 & & \\ & \ddots & \\ & & 1 \end{pmatrix} C. \quad (7.10.2)$$

The following matrices will perform this transformation for general charge, k :

$$C_{ij} = \begin{cases} 0 & \text{if } i > j \\ \frac{j}{\sqrt{j(j+1)}} & \text{if } i = j \\ -\frac{1}{\sqrt{j(j+1)}} & \text{if } i < j \end{cases} \quad \text{where } i, j = 1, \dots, k, \quad (7.10.3)$$

and

$$S = \begin{pmatrix} -\frac{1}{\sqrt{k+1}} & \frac{1}{\sqrt{k+1}} & \cdots & \frac{1}{\sqrt{k+1}} \\ C_{11} & & & \\ -C_{12} & & & \\ \vdots & & (C^T)_{ij} & \\ -C_{1k} & & & \end{pmatrix}. \quad (7.10.4)$$

This is a generalisation of the transformation presented in reference [94] for $k = 1, 2$.

To construct JNR data with the symmetries of the 5-cell, we can take the poles of the charge five JNR instanton to be the 5-cell vertices, with equal weight,

$$\begin{aligned} y_0 &= \frac{1}{4} \left(-1 + \sqrt{5} (i + j + k) \right), & y_1 &= \frac{1}{4} \left(-1 + \sqrt{5} (i - j - k) \right), \\ y_2 &= \frac{1}{4} \left(-1 + \sqrt{5} (-i + j - k) \right), & y_3 &= \frac{1}{4} \left(-1 + \sqrt{5} (-i - j + k) \right), \\ & & y_4 &= 1. \end{aligned} \quad (7.10.5)$$

The solution we presented earlier in equation (7.4.2) is then related to the JNR ansatz

by

$$a = \begin{pmatrix} 1 & 0 \\ 0 & Q \end{pmatrix} S \begin{pmatrix} y_0 & \cdots & y_0 \\ y_1 & & \\ & \ddots & \\ & & y_4 \end{pmatrix} C Q^{-1}, \quad (7.10.6)$$

where S and C are given as above, and [3]

$$Q = \begin{pmatrix} 0 & 0 & 0 & 1 \\ 0 & -\frac{\sqrt{2}}{\sqrt{3}} & -\frac{1}{\sqrt{3}} & 0 \\ -\frac{1}{\sqrt{2}} & \frac{1}{\sqrt{6}} & -\frac{1}{\sqrt{3}} & 0 \\ -\frac{1}{\sqrt{2}} & -\frac{1}{\sqrt{6}} & \frac{1}{\sqrt{3}} & 0 \end{pmatrix}. \quad (7.10.7)$$

The scale factor in the solution in equation (7.4.2) should be taken to be $\lambda = -\frac{1}{4}$ for the solutions to be equivalent. Of course, the JNR ansatz can be arbitrarily scaled as well.

To construct JNR data with the symmetries of the 16-cell, we can take the poles of the charge seven JNR instanton to be the 16-cell vertices,

$$\begin{aligned} y_0 = 1, \quad y_1 = -1, \quad y_2 = i, \quad y_3 = -i, \\ y_4 = j, \quad y_5 = -j, \quad y_6 = k, \quad y_7 = -k. \end{aligned} \quad (7.10.8)$$

The solution we found previously, in equation (7.7.26), is then related to the JNR ansatz as above, but with

$$Q = \begin{pmatrix} 0 & -\frac{1}{\sqrt{3}} & -\frac{1}{\sqrt{6}} & -\frac{1}{\sqrt{10}} & -\frac{1}{\sqrt{15}} & \frac{2}{\sqrt{21}} & \frac{1}{\sqrt{7}} \\ 0 & 0 & 0 & -\frac{\sqrt{2}}{\sqrt{5}} & -\frac{2}{\sqrt{15}} & -\frac{2}{\sqrt{21}} & -\frac{1}{\sqrt{7}} \\ 0 & -\frac{1}{\sqrt{3}} & -\frac{1}{\sqrt{6}} & \frac{1}{\sqrt{10}} & \frac{1}{\sqrt{15}} & -\frac{2}{\sqrt{21}} & -\frac{1}{\sqrt{7}} \\ -1 & 0 & 0 & 0 & 0 & 0 & 0 \\ 0 & \frac{1}{\sqrt{3}} & -\frac{\sqrt{2}}{\sqrt{3}} & 0 & 0 & 0 & 0 \\ 0 & 0 & 0 & \frac{\sqrt{2}}{\sqrt{5}} & -\frac{\sqrt{3}}{\sqrt{5}} & 0 & 0 \\ 0 & 0 & 0 & 0 & 0 & -\frac{\sqrt{3}}{\sqrt{7}} & \frac{2}{\sqrt{7}} \end{pmatrix}. \quad (7.10.9)$$

The scale factor in equation (7.7.26) should be taken to be $\lambda = \frac{1}{2}$.

Due to the large dimension of the charge 23 ADHM data, it is difficult to find an appropriate transformation matrix between the solution in equation (7.9.8) and the JNR ansatz. However, by examining the eigenvalues of the matrices Q_L and Q_R that leave the JNR ansatz invariant under the left and right action of the binary tetrahedral group generators, we are able to confirm that they are the same representations as appear in the solution in equation (7.9.8). Furthermore, all of the blocks can be put

in the same basis as in equation (7.9.8), except for the left $\mathbb{1}_2 \tilde{\otimes} G'$ block. It is possible that the JNR ansatz is actually a slightly different solution, where the left action is in a different basis that we have not considered in the previous section, but the solutions are otherwise very similar.

7.11 Discussion and conclusions

In this chapter we have understood how the ADHM data of a symmetric instanton must transform under the action of the symmetry group. Given the description of the ADHM data in terms of quaternions, the natural way to represent the action of such a symmetry group is via the lift to the double cover, which is a subgroup of $SU(2) \times SU(2)$ and acts via right and left quaternion multiplication. For any symmetry which is a subgroup of $SO(3)$, and also the symmetry group of the 5-cell, the double cover is isomorphic to a subgroup of $SU(2)$, and the left and right actions are not independent. For each action by a member of the double cover, (g^\sharp, g) , where g^\sharp is dependent on g , the ADHM data must transform under a single k -dimensional real representation and a single one-dimensional quaternionic representation. We can always take these to be in the canonical basis where they are the direct sum of irreducible representations. It is then straightforward to enumerate all combinations of irreducible representations and search for ADHM data which is invariant under each possible combination. This procedure allowed us to construct an instanton with the symmetries of the 5-cell, and the lowest charge solution we found with these symmetries was of charge four.

The double cover of the symmetry group of the 16-cell and of the 24-cell are $Q_8 \otimes Q_8$ and $\mathbb{T} \otimes \mathbb{T}$ respectively, and the left and right actions of these groups are independent. This means that there are two independent actions which form representations, Q_R and Q_L . We now only have the freedom to choose a basis in which either Q_R or Q_L is explicitly the direct sum of irreducible representations. However, Q_R and Q_L must commute, since the left and right actions commute, so the possible form of the representations in Q_L is restricted when Q_R is in a given basis. In the case of the 16-cell, this has allowed us to uniquely determine all possibilities for Q_L given a choice of Q_R . For the 24-cell, we have only been able to determine the non-linear constraints on the form of the representations in Q_L , and find the obvious examples by inspection.

With all possible combinations of Q_R and Q_L known for the 16-cell, and a large number known for the 24-cell, we have tested each combination to determine if there is ADHM data which is invariant under the representation and which satisfies the ADHM constraints. For the 16-cell, we have found a selection of solutions at charge seven which are equivalent to the JNR ansatz. For the 24-cell, we have found a solution at charge 23 which is also equivalent to the JNR ansatz.

In the case of the cubic and icosahedral symmetries, there exist symmetric instanton

solutions with lower charge than the JNR ansatz. It is curious that we have not found any such lower charge solutions for the polytope symmetries. This may be due to a fundamental difference in the way that the symmetry acts as a subgroup of $SU(2) \times SU(2)$ rather than as a subgroup of $SU(2)$. It is also possible that lower charge solutions exist, but outside of our framework. In the 24-cell, there may be representations in the left action that we have not found but that may give a lower charge solution. We would need to be able to solve a set of non-linear constraints on the matrix coefficients to find the general form of representations that commute with the right action, and it is not clear how to proceed in this case.

We have also assumed that Q_R and Q_L form representations of the appropriate groups. It is possible that there are symmetric instantons with ADHM data which are invariant under some matrices Q_R and Q_L which are not strictly representations. For example, consider the right action of $g_i^2 = -1$ in the double cover of the 16-cell symmetry group. Then there must exist matrices, $Q_R(g_i)$, such that

$$Q_R(g_i)^2 M = -M Q_R(g_i)^2. \quad (7.11.1)$$

If Q_R is composed of irreducible representations then we saw previously that $Q_R(g_i)^2 = \text{diag}(\mathbb{1}_m, -\mathbb{1}_n)$ in the appropriate basis. However, the following is also a possible solution,

$$Q_R(g_i)^2 = \begin{pmatrix} 0 & \mathbb{1}_{k/2} \\ -\mathbb{1}_{k/2} & 0 \end{pmatrix}, \quad (7.11.2)$$

when k is even, and M is in the form

$$M = \begin{pmatrix} A & B \\ B & A \end{pmatrix}, \quad (7.11.3)$$

with A and B symmetric matrices. The matrices $Q_R(g_i)$ do not form a representation because $g_1^4 = 1$, yet $Q_R(g_1)^4 = -\mathbb{1}_k$, which is not the identity element. However, they still obey the group action when applied to M since the sign is projected out.

Another possibility is that Q_R and Q_L are representations of opposite sign. We took Q_R to be composed of positive representations in the upper block and negative representations in the lower block, so that $Q_R(g_i)^\alpha = \text{diag}(\mathbb{1}_m, -\mathbb{1}_n)$. We also took a similar block structure for Q_L , but it is possible that Q_L instead consists of negative representations in the upper block and positive representations in the lower block so that $Q_L(g_i)^\alpha = \text{diag}(-\mathbb{1}_m, \mathbb{1}_n)$. Again, this difference of sign is irrelevant in the action on the ADHM data.

Finally, it is possible that the matrices Q_R and Q_L only satisfy the group presen-

tation up to a sign,

$$Q_{R,L}(g_1)^\alpha = \pm Q_{R,L}(g_2)^\beta = \pm (Q_{R,L}(g_1)Q_{R,L}(g_2))^\gamma. \quad (7.11.4)$$

With the 24-cell symmetry group, where $\alpha = \beta = 3$, we can always choose the sign of $Q_{R,L}(g_i)$ such that the signs in this expression match. However, for the 16-cell, where $\alpha = \beta = 2$, it would be possible to have symmetric ADHM data which is invariant under some matrices $Q_{R,L}$ where the signs do not match. These matrices would not be a representation.

The core problem is that the transformation of the ADHM data is unaffected by the signs of Q_R and Q_L , so Q_R and Q_L only need to satisfy the group operation up to a sign,

$$Q_{R,L}(g)Q_{R,L}(h) = \pm Q_{R,L}(gh). \quad (7.11.5)$$

Our treatment in terms of representations is only applicable when the signs agree with the group operation. However, we have been unable to find meaningful examples of suitable matrices when the signs do not agree and we do not have the body of representation theory to fall back on.

Chapter 8

Conclusions and outlook

In the first half of this thesis we looked at the BLG and ABJM actions of multiple M2-branes, and we saw how these can be extended to include couplings to the background 3-form in M-theory. A variety of approaches to this problem have been explored in the literature, but our method was to compare the possible terms in the M2-brane action with those that must be recovered in the reduction to D2-branes where the form of the coupling to the background fields is known. A proposal for the extension of the ABJM action to include linear couplings to the background 3-form was given in reference [52], and the main result of the first part of this thesis was the further extension of the ABJM action to include quadratic couplings to the background fields, as given in equation (3.1.67). The extension of the action to quadratic couplings relies on the couplings determined from the linear extension and provides further evidence that the linear extension is correct. We were only able to construct the extension when the gauge symmetry was broken from $U(N) \times U(N)$ to the diagonal $U(N)$ subgroup, and we have commented on the subtleties in constructing a fully gauge-invariant pullback of the background 3-form in the ABJM action.

The discovery of the BLG and ABJM actions was a significant step forward in our understanding of M-theory, but there is much that still remains unknown. We are certainly a long way from having a unified understanding of all aspects of M-theory, but the research in this thesis hopefully takes us a little closer to the full picture by helping to link together the world-volume action of multiple M2-branes with the low-energy massless fields in M-theory. We have only considered the background 3-form in this thesis, but for future work it would be interesting to understand multiple M2-branes in an arbitrary curved background, with non-trivial metric, 3-form and 6-form fields.

The M5-brane still remains more of a mystery, although the recent developments for M2-branes have inspired the search for a theory of multiple M5-branes. There are some non-trivial difficulties to overcome in describing multiple M5-branes, but some promising steps have been taken in this direction [33, 34, 35, 36, 37]. Perhaps the most interesting possibility is the conjecture that the theory of multiple M5-branes on

a circle is dual to five dimensional super-Yang-Mills at all sizes of the radius of the M-theory circle, not just in the compactification limit [72, 73]. If this is true then it is a profound duality with the result that five-dimensional super-Yang-Mills is UV complete.

Five dimensional super-Yang-Mills is therefore in the spotlight at the moment, but instantons in this theory have received much less attention than their lower dimensional cousins, monopoles, skyrmions and vortices, perhaps due to the previous lack of motivation to study a five dimensional theory. In the second half of this thesis we turned our attention to these instantons, first as dynamic solitons in five dimensional Yang-Mills, and then to look for instantons which have some high amount of symmetry in the four spatial dimensions.

The main result of Chapter 5 was the explicit calculation of the moduli space metric for charge two instantons, and the potential for charge two dyonic instantons. The calculation of these through the ADHM construction has also allowed us to understand some of the structure and topology of the moduli space, as well as to identify a number of geodesic submanifolds with various physical interpretations. In Chapter 6 we used these explicit expressions for the metric and potential to explore the evolution of two slow moving (dyonic) instantons via geodesic motion on the moduli space using the moduli space approximation of Manton. We saw that instantons undergo right angled scattering as expected by comparison to similar soliton systems, and we also understood the underlying reason for this due to the quotient structure of moduli space under symmetries of the ADHM data. Our final result in Chapter 6 was that it is possible for dyonic instantons to exchange angular momentum in such a way that one shrinks to zero size. This corresponds to the geodesic evolution hitting a singularity in the moduli space, which is in contrast to a single dyonic instanton where the overall conserved angular momentum prevents it from shrinking. The implications of this behaviour are still unclear for the full field theory. If Yang-Mills is UV complete then these singularities must be avoided somehow, possibly by a breakdown of the moduli space approximation near to the singularities or by quantum effects.

We have seen that instantons are related to Skyrmons, and it may be possible to use our understanding of the two instanton moduli space to further explore charge two Skyrmons. Instantons are also related to vortices, and a half dimensional subspace of the non-commutative instanton moduli space can be identified with the vortex moduli space [98]. We have not considered the non-commutative deformation of the instanton moduli space in this thesis so our results would only apply to the strong coupling limit of the vortex theory, but work on the non-commutative instanton moduli space is in progress. Our understanding of the moduli space of two instantons may also be useful in further understanding the correspondence between the multiple M5-brane theory and five dimensional super-Yang-Mills, particularly if the supersymmetric and

quantum theory can be further developed.

In Chapter 7 we have understood how the action of a symmetry on an instanton lifts to an action by left and right quaternion multiplication on the ADHM data. For an instanton to be symmetric under a symmetry, the ADHM data must also be invariant and we can find a representation of real matrices that transform the ADHM data appropriately. With this representation theory approach we have been able to find solutions with the symmetries of three of the four symmetry groups of the regular polytopes. The 5-cell was straightforward since the right and left action are not independent, and the single representation of the transformation matrices can be put in a canonical basis. The symmetries of the 16-cell and 24-cell act with independent left and right actions, and we only have the freedom to take one of these representations to be in a canonical basis. Nevertheless, we were able to sufficiently restrict the possible form of the other representations and find solutions within our framework that have the symmetries of the 16-cell and 24-cell. The solutions we found turned out to be equivalent to solutions which can be constructed from the JNR ansatz, but we have developed a framework which can be used to understand the action of any subgroups of $SO(3)$ and $SO(4)$ on the ADHM data.

We have seen previously that instantons are related to many other soliton systems: Skymions via their holonomy; vortices via their moduli space; monopoles via dimensional reduction; and hyperbolic monopoles when the instantons have a circle symmetry. It is encouraging that new relationships are still being discovered, and the relationship between instantons with Platonic symmetries and hyperbolic monopoles was only recently realised. Instantons with the symmetries of the regular polytopes may turn out to be similarly related to other systems in the future.

Bibliography

- [1] J. P. Allen and D. J. Smith, “Coupling M2-branes to background fields,” *JHEP* **1108** (2011) 078, [arXiv:1104.5397 \[hep-th\]](#).
- [2] J. P. Allen and D. J. Smith, “The low energy dynamics of charge two dyonic instantons,” *JHEP* **1302** (2013) 113, [arXiv:1210.3208 \[hep-th\]](#).
- [3] J. Allen and P. Sutcliffe, “ADHM Polytopes,” [arXiv:1302.4664 \[hep-th\]](#).
- [4] J. Polchinski, *String theory. Vol. 1: An introduction to the bosonic string*. Cambridge University Press, 1998.
- [5] J. Polchinski, *String theory. Vol. 2: Superstring theory and beyond*. Cambridge University Press, 1998.
- [6] C. Johnson, *D-branes*. Cambridge University Press, 2003.
- [7] N. Manton and P. Sutcliffe, *Topological solitons*. Cambridge University Press, 2004.
- [8] J. Polchinski, “Dirichlet Branes and Ramond-Ramond charges,” *Phys.Rev.Lett.* **75** (1995) 4724–4727, [arXiv:hep-th/9510017 \[hep-th\]](#).
- [9] M. B. Green and J. H. Schwarz, “Supersymmetrical String Theories,” *Phys.Lett.* **B109** (1982) 444–448.
- [10] J. H. Schwarz and P. C. West, “Symmetries and Transformations of Chiral N=2 D=10 Supergravity,” *Phys.Lett.* **B126** (1983) 301.
- [11] P. S. Howe and P. C. West, “The Complete N=2, D=10 Supergravity,” *Nucl.Phys.* **B238** (1984) 181.
- [12] D. J. Smith, “Intersecting brane solutions in string and M theory,” *Class.Quant.Grav.* **20** (2003) R233, [arXiv:hep-th/0210157 \[hep-th\]](#).
- [13] E. Cremmer, B. Julia, and J. Scherk, “Supergravity Theory in Eleven-Dimensions,” *Phys.Lett.* **B76** (1978) 409–412.

- [14] M. Duff and K. Stelle, “Multimembrane solutions of $D = 11$ supergravity,” *Phys.Lett.* **B253** (1991) 113–118.
- [15] Güven, Rahmi, “Black p-brane solutions of $D = 11$ supergravity theory,” *Phys.Lett.* **B276** (1992) 49–55.
- [16] F. Giani and M. Pernici, “ $N=2$ supergravity in ten-dimensions,” *Phys.Rev.* **D30** (1984) 325–333.
- [17] M. Huq and M. Namazie, “Kaluza-Klein supergravity in ten-dimensions,” *Class.Quant.Grav.* **2** (1985) 293.
- [18] I. Campbell and P. C. West, “ $N=2$ $D=10$ Nonchiral Supergravity and Its Spontaneous Compactification,” *Nucl.Phys.* **B243** (1984) 112.
- [19] P. Townsend, “The eleven-dimensional supermembrane revisited,” *Phys.Lett.* **B350** (1995) 184–187, [arXiv:hep-th/9501068 \[hep-th\]](#).
- [20] E. Witten, “String theory dynamics in various dimensions,” *Nucl.Phys.* **B443** (1995) 85–126, [arXiv:hep-th/9503124 \[hep-th\]](#).
- [21] J. H. Schwarz, “The power of M theory,” *Phys.Lett.* **B367** (1996) 97–103, [arXiv:hep-th/9510086 \[hep-th\]](#).
- [22] P. Townsend, “D-branes from M-branes,” *Phys.Lett.* **B373** (1996) 68–75, [arXiv:hep-th/9512062 \[hep-th\]](#).
- [23] C. Schmidhuber, “D-brane actions,” *Nucl.Phys.* **B467** (1996) 146–158, [arXiv:hep-th/9601003 \[hep-th\]](#).
- [24] M. Duff, P. S. Howe, T. Inami, and K. Stelle, “Superstrings in $D=10$ from Supermembranes in $D=11$,” *Phys.Lett.* **B191** (1987) 70.
- [25] N. Lambert, “M-Theory and Maximally Supersymmetric Gauge Theories,” [arXiv:1203.4244 \[hep-th\]](#).
- [26] J. Bagger, N. Lambert, S. Mukhi, and C. Papageorgakis, “Multiple Membranes in M-theory,” [arXiv:1203.3546 \[hep-th\]](#).
- [27] E. Fradkin and A. A. Tseytlin, “Nonlinear Electrodynamics from Quantized Strings,” *Phys.Lett.* **B163** (1985) 123.
- [28] G. Gibbons, “Born-Infeld particles and Dirichlet p-branes,” *Nucl.Phys.* **B514** (1998) 603–639, [arXiv:hep-th/9709027 \[hep-th\]](#).

- [29] R. Leigh, “Dirac-Born-Infeld Action from Dirichlet Sigma Model,” *Mod.Phys.Lett.* **A4** (1989) 2767.
- [30] M. R. Douglas, “Branes within branes,” [arXiv:hep-th/9512077](#) [hep-th].
- [31] E. Witten, “Bound states of strings and p-branes,” *Nucl.Phys.* **B460** (1996) 335–350, [arXiv:hep-th/9510135](#) [hep-th].
- [32] R. C. Myers, “Dielectric-branes,” *JHEP* **12** (1999) 022, [arXiv:hep-th/9910053](#).
- [33] P.-M. Ho, K.-W. Huang, and Y. Matsuo, “A Non-Abelian Self-Dual Gauge Theory in 5+1 Dimensions,” *JHEP* **1107** (2011) 021, [arXiv:1104.4040](#) [hep-th].
- [34] C.-S. Chu and S.-L. Ko, “Non-abelian Action for Multiple Five-Branes with Self-Dual Tensors,” *JHEP* **1205** (2012) 028, [arXiv:1203.4224](#) [hep-th].
- [35] F. Bonetti, T. W. Grimm, and S. Hohenegger, “Non-Abelian Tensor Towers and (2,0) Superconformal Theories,” [arXiv:1209.3017](#) [hep-th].
- [36] H.-C. Kim and K. Lee, “Supersymmetric M5 Brane Theories on $R \times CP^2$,” [arXiv:1210.0853](#) [hep-th].
- [37] N. Lambert, C. Papageorgakis, and M. Schmidt-Sommerfeld, “Deconstructing (2,0) Proposals,” [arXiv:1212.3337](#) [hep-th].
- [38] J. Bagger and N. Lambert, “Gauge Symmetry and Supersymmetry of Multiple M2-Branes,” *Phys. Rev.* **D77** (2008) 065008, [arXiv:0711.0955](#) [hep-th].
- [39] J. Bagger and N. Lambert, “Comments On Multiple M2-branes,” *JHEP* **02** (2008) 105, [arXiv:0712.3738](#) [hep-th].
- [40] A. Gustavsson, “Algebraic structures on parallel M2-branes,” *Nucl. Phys.* **B811** (2009) 66–76, [arXiv:0709.1260](#) [hep-th].
- [41] G. Papadopoulos, “M2-branes, 3-Lie Algebras and Plucker relations,” *JHEP* **0805** (2008) 054, [arXiv:0804.2662](#) [hep-th].
- [42] J. P. Gauntlett and J. B. Gutowski, “Constraining Maximally Supersymmetric Membrane Actions,” *JHEP* **06** (2008) 053, [arXiv:0804.3078](#) [hep-th].
- [43] N. Lambert and D. Tong, “Membranes on an Orbifold,” *Phys.Rev.Lett.* **101** (2008) 041602, [arXiv:0804.1114](#) [hep-th].

- [44] J. Distler, S. Mukhi, C. Papageorgakis, and M. Van Raamsdonk, “M2-branes on M-folds,” *JHEP* **0805** (2008) 038, [arXiv:0804.1256 \[hep-th\]](#).
- [45] O. Aharony, O. Bergman, D. L. Jafferis, and J. Maldacena, “N=6 superconformal Chern-Simons-matter theories, M2-branes and their gravity duals,” *JHEP* **10** (2008) 091, [arXiv:0806.1218 \[hep-th\]](#).
- [46] S. Mukhi and C. Papageorgakis, “M2 to D2,” *JHEP* **05** (2008) 085, [arXiv:0803.3218 \[hep-th\]](#).
- [47] Y. Pang and T. Wang, “From N M2’s to N D2’s,” *Phys. Rev.* **D78** (2008) 125007, [arXiv:0807.1444 \[hep-th\]](#).
- [48] T. Li, Y. Liu, and D. Xie, “Multiple D2-Brane Action from M2-Branes,” *Int.J.Mod.Phys.* **A24** (2009) 3039–3052, [arXiv:0807.1183 \[hep-th\]](#).
- [49] E. Bergshoeff, E. Sezgin, and P. Townsend, “Supermembranes and Eleven-Dimensional Supergravity,” *Phys.Lett.* **B189** (1987) 75–78.
- [50] N. Lambert and P. Richmond, “M2-Branes and Background Fields,” *JHEP* **10** (2009) 084, [arXiv:0908.2896 \[hep-th\]](#).
- [51] M. Li and T. Wang, “M2-branes Coupled to Antisymmetric Fluxes,” *JHEP* **0807** (2008) 093, [arXiv:0805.3427 \[hep-th\]](#).
- [52] Y. Kim, O.-K. Kwon, H. Nakajima, and D. D. Tolla, “Interaction between M2-branes and Bulk Form Fields,” [arXiv:1009.5209 \[hep-th\]](#).
- [53] M. R. Douglas, “D-branes and matrix theory in curved space,” *Nucl.Phys.Proc.Suppl.* **68** (1998) 381–393, [arXiv:hep-th/9707228 \[hep-th\]](#).
- [54] M. R. Douglas, “D-branes in curved space,” *Adv.Theor.Math.Phys.* **1** (1998) 198–209, [arXiv:hep-th/9703056 \[hep-th\]](#).
- [55] J. Adam, J. Gheerardyn, B. Janssen, and Y. Lozano, “The gauge invariance of the non-Abelian Chern-Simons action for D-branes revisited,” *Phys. Lett.* **B589** (2004) 59–69, [arXiv:hep-th/0312264](#).
- [56] A. Belavin, A. M. Polyakov, A. Schwartz, and Y. Tyupkin, “Pseudoparticle Solutions of the Yang-Mills Equations,” *Phys.Lett.* **B59** (1975) 85–87.
- [57] T. Schafer and E. V. Shuryak, “Instantons in QCD,” *Rev.Mod.Phys.* **70** (1998) 323–426, [arXiv:hep-ph/9610451 \[hep-ph\]](#).
- [58] M. Bianchi, S. Kovacs, and G. Rossi, “Instantons and Supersymmetry,” *Lect.Notes Phys.* **737** (2008) 303–470, [arXiv:hep-th/0703142 \[HEP-TH\]](#).

- [59] D. Tong, “TASI lectures on solitons: Instantons, monopoles, vortices and kinks,” [arXiv:hep-th/0509216 \[hep-th\]](#).
- [60] E. J. Weinberg and P. Yi, “Magnetic Monopole Dynamics, Supersymmetry, and Duality,” *Phys.Rept.* **438** (2007) 65–236, [arXiv:hep-th/0609055 \[hep-th\]](#).
- [61] E. Witten, “Sigma models and the ADHM construction of instantons,” *J.Geom.Phys.* **15** (1995) 215–226, [arXiv:hep-th/9410052 \[hep-th\]](#).
- [62] E. Witten, “Small instantons in string theory,” *Nucl.Phys.* **B460** (1996) 541–559, [arXiv:hep-th/9511030 \[hep-th\]](#).
- [63] M. R. Douglas, “Gauge fields and D-branes,” *J.Geom.Phys.* **28** (1998) 255–262, [arXiv:hep-th/9604198 \[hep-th\]](#).
- [64] N. D. Lambert and D. Tong, “Dyonic instantons in five-dimensional gauge theories,” *Phys.Lett.* **B462** (1999) 89–94, [arXiv:hep-th/9907014 \[hep-th\]](#).
- [65] O. Bergman, “Three pronged strings and 1/4 BPS states in N=4 superYang-Mills theory,” *Nucl.Phys.* **B525** (1998) 104–116, [arXiv:hep-th/9712211 \[hep-th\]](#).
- [66] O. Bergman and B. Kol, “String webs and 1/4 BPS monopoles,” *Nucl.Phys.* **B536** (1998) 149–174, [arXiv:hep-th/9804160 \[hep-th\]](#).
- [67] K.-M. Lee and P. Yi, “Dyons in N=4 supersymmetric theories and three pronged strings,” *Phys.Rev.* **D58** (1998) 066005, [arXiv:hep-th/9804174 \[hep-th\]](#).
- [68] B. Julia and A. Zee, “Poles with Both Magnetic and Electric Charges in Nonabelian Gauge Theory,” *Phys.Rev.* **D11** (1975) 2227–2232.
- [69] M. Zamaklar, “Geometry of the nonAbelian DBI dyonic instanton,” *Phys.Lett.* **B493** (2000) 411–420, [arXiv:hep-th/0006090 \[hep-th\]](#).
- [70] S. Kim and K.-M. Lee, “Dyonic instanton as supertube between D-4 branes,” *JHEP* **0309** (2003) 035, [arXiv:hep-th/0307048 \[hep-th\]](#).
- [71] M.-Y. Choi, K. K. Kim, C. Lee, and K.-M. Lee, “Higgs structures of dyonic instantons,” *JHEP* **0804** (2008) 097, [arXiv:0712.0735 \[hep-th\]](#).
- [72] N. Lambert, C. Papageorgakis, and M. Schmidt-Sommerfeld, “M5-Branes, D4-Branes and Quantum 5D super-Yang-Mills,” *JHEP* **01** (2011) 083, [arXiv:1012.2882 \[hep-th\]](#).

- [73] M. R. Douglas, “On D=5 super Yang-Mills theory and (2,0) theory,” *JHEP* **1102** (2011) 011, [arXiv:1012.2880 \[hep-th\]](#).
- [74] O. Aharony, M. Berkooz, and N. Seiberg, “Light cone description of (2,0) superconformal theories in six-dimensions,” *Adv.Theor.Math.Phys.* **2** (1998) 119–153, [arXiv:hep-th/9712117 \[hep-th\]](#).
- [75] N. Nekrasov and A. S. Schwarz, “Instantons on noncommutative R^{*4} and (2,0) superconformal six-dimensional theory,” *Commun.Math.Phys.* **198** (1998) 689–703, [arXiv:hep-th/9802068 \[hep-th\]](#).
- [76] N. Lambert and P. Richmond, “(2,0) Supersymmetry and the Light-Cone Description of M5-branes,” *JHEP* **1202** (2012) 013, [arXiv:1109.6454 \[hep-th\]](#).
- [77] N. Lambert, H. Nastase, and C. Papageorgakis, “5D Yang-Mills instantons from ABJM Monopoles,” *Phys.Rev.* **D85** (2012) 066002, [arXiv:1111.5619 \[hep-th\]](#).
- [78] H.-C. Kim, S. Kim, E. Koh, K. Lee, and S. Lee, “On instantons as Kaluza-Klein modes of M5-branes,” *JHEP* **1112** (2011) 031, [arXiv:1110.2175 \[hep-th\]](#).
- [79] S. Donaldson and P. Kronheimer, *The Geometry of Four-Manifolds*. Oxford Mathematical Monographs. Oxford University Press, USA, 1997.
- [80] N. Manton, “A Remark on the Scattering of BPS Monopoles,” *Phys.Lett.* **B110** (1982) 54–56.
- [81] D. Tong, “A Note on 1/4 BPS states,” *Phys.Lett.* **B460** (1999) 295–301, [arXiv:hep-th/9902005 \[hep-th\]](#).
- [82] D. Bak, C.-k. Lee, K.-M. Lee, and P. Yi, “Low-energy dynamics for 1/4 BPS dyons,” *Phys.Rev.* **D61** (2000) 025001, [arXiv:hep-th/9906119 \[hep-th\]](#).
- [83] D. Bak and K.-M. Lee, “Comments on the moduli dynamics of 1/4 BPS dyons,” *Phys.Lett.* **B468** (1999) 76–80, [arXiv:hep-th/9909035 \[hep-th\]](#).
- [84] E. Bogomolny, “Stability of Classical Solutions,” *Sov.J.Nucl.Phys.* **24** (1976) 449.
- [85] G. 't Hooft, “Computation of the Quantum Effects Due to a Four-Dimensional Pseudoparticle,” *Phys.Rev.* **D14** (1976) 3432–3450.
- [86] R. Jackiw, C. Nohl, and C. Rebbi, “Conformal Properties of Pseudoparticle Configurations,” *Phys.Rev.* **D15** (1977) 1642.

- [87] M. Atiyah, N. J. Hitchin, and I. Singer, “Deformations of instantons,” *Proc.Nat.Acad.Sci.* **74** (1977) 2662–2663.
- [88] A. S. Schwarz, “On Regular Solutions of Euclidean Yang-Mills Equations,” *Phys.Lett.* **B67** (1977) 172–174.
- [89] M. Atiyah, A. nazionale dei Lincei, and S. normale superiore (Italy), *Geometry of Yang-Mills fields*. Lezioni fermiane. Scuola normale superiore, 1979.
- [90] M. Atiyah, N. J. Hitchin, V. Drinfeld, and Y. Manin, “Construction of Instantons,” *Phys.Lett.* **A65** (1978) 185–187.
- [91] R. Ward, “On Selfdual gauge fields,” *Phys.Lett.* **A61** (1977) 81–82.
- [92] N. H. Christ, E. J. Weinberg, and N. K. Stanton, “General Selfdual Yang-Mills Solutions,” *Phys.Rev.* **D18** (1978) 2013.
- [93] E. Corrigan, D. Fairlie, S. Templeton, and P. Goddard, “A Green’s Function for the General Selfdual Gauge Field,” *Nucl.Phys.* **B140** (1978) 31.
- [94] H. Osborn, “Semiclassical Functional Integrals for Selfdual Gauge Fields,” *Annals Phys.* **135** (1981) 373.
- [95] K. Peeters and M. Zamaklar, “Motion on moduli spaces with potentials,” *JHEP* **12** (2001) 032, [arXiv:hep-th/0107164](#).
- [96] E. Corrigan, P. Goddard, H. Osborn, and S. Templeton, “Zeta function regularization and multi-instanton determinants,” *Nucl.Phys.* **B159** (1979) 469.
- [97] N. Dorey, V. V. Khoze, and M. P. Mattis, “Multi-Instanton Calculus in N=2 Supersymmetric Gauge Theory,” *Phys. Rev.* **D54** (1996) 2921–2943, [arXiv:hep-th/9603136](#).
- [98] A. Hanany and D. Tong, “Vortices, instantons and branes,” *JHEP* **0307** (2003) 037, [arXiv:hep-th/0306150](#) [hep-th].
- [99] M. Atiyah and N. J. Hitchin, “Low-Energy Scattering of Nonabelian Monopoles,” *Phys.Lett.* **A107** (1985) 21–25.
- [100] R. Leese, “Q-lumps and their interactions,” *Nucl.Phys.* **B366** (1991) 283–314.
- [101] K.-M. Lee and P. Yi, “Quantum spectrum of instanton solitons in five-dimensional noncommutative U(N) theories,” *Phys.Rev.* **D61** (2000) 125015, [arXiv:hep-th/9911186](#) [hep-th].

- [102] M. Atiyah and N. Manton, “Skyrmions from instantons,” *Phys.Lett.* **B222** (1989) 438–442.
- [103] M. Atiyah and N. Manton, “Geometry and kinematics of two skyrmions,” *Commun.Math.Phys.* **153** (1993) 391–422.
- [104] M. Atiyah, “Magnetic monopoles in hyperbolic spaces,” in *Proceedings of the International Conference on Vector Bundles on Algebraic Varieties, Bombay 1984*, pp. 1–34. Oxford University Press, 1986.
- [105] N. Manton and P. Sutcliffe, “Platonic hyperbolic monopoles,” [arXiv:1207.2636](https://arxiv.org/abs/1207.2636) [hep-th].
- [106] T. Skyrme, “A unified field theory of mesons and baryons,” *Nucl.Phys.* **31** (1962) 556–569.
- [107] V. Kopeliovich and B. Stern, “Exotic Skyrmions,” *JETP Lett.* **45** (1987) 203–207.
- [108] N. Manton, “Is the B=2 Skyrminion axially symmetric?,” *Phys.Lett.* **B192** (1987) 177.
- [109] J. Verbaarschot, “Axial symmetry of bound baryon number two solution of the Skyrme model,” *Phys.Lett.* **B195** (1987) 235.
- [110] R. Leese and N. Manton, “Stable instanton generated Skyrme fields with baryon numbers three and four,” *Nucl.Phys.* **A572** (1994) 575–599.
- [111] R. A. Battye and P. M. Sutcliffe, “Symmetric Skyrmions,” *Phys.Rev.Lett.* **79** (1997) 363–366, [arXiv:hep-th/9702089](https://arxiv.org/abs/hep-th/9702089) [hep-th].
- [112] M. A. Singer and P. M. Sutcliffe, “Symmetric instantons and Skyrme fields,” *Nonlinearity* **12** (1999) 987–1003, [arXiv:hep-th/9901075](https://arxiv.org/abs/hep-th/9901075) [hep-th].
- [113] P. Sutcliffe, “Instantons and the buckyball,” *Proc.Roy.Soc.Lond.* **A460** (2004) 2903–2912, [arXiv:hep-th/0309157](https://arxiv.org/abs/hep-th/0309157) [hep-th].
- [114] R. Ward, “Two Yang-Mills Higgs monopoles close together,” *Phys.Lett.* **B102** (1981) 136–138.
- [115] P. Forgács, Z. Horváth, and L. Palla, “Exact multi-monopole solutions in the Bogomolny-Prasad-Sommerfield limit,” *Phys.Lett.* **B99** (1981) 232.
- [116] P. Forgács, Z. Horváth, and L. Palla, “Solution-generating technique for selfdual monopoles,” *Nucl.Phys.* **B229** (1983) 77.

- [117] M. Prasad and P. Rossi, “Construction of exact Yang-Mills Higgs multi-monopoles of arbitrary charge,” *Phys.Rev.Lett.* **46** (1981) 806.
- [118] W. Nahm, “The construction of all self-dual multimonopoles by the ADHM method,” in *Monopoles in quantum field theory: proceedings of the Monopole Meeting, Trieste, Italy, December, 1981.* 1982.